

COMPRESSIVE STRENGTH AND MICROSTRUCTURE OF RIGID
POLYURETHANE FOAM AND ITS APPLICATION IN
ROAD MAINTENANCE



A Thesis Submitted in Partial Fulfillment of the Requirements for the
Degree of Doctor of Philosophy in Civil Engineering
and Construction Management
Suranaree University of Technology
Academic Year 2023

กำลังอัดและโครงสร้างจุลภาคของโพลียูรีเทนโฟมแบบแข็งเกร็ง
และการประยุกต์ใช้ในงานซ่อมบำรุงถนน



นายอรุณเดช บุญสูง

วิทยานิพนธ์นี้เป็นส่วนหนึ่งของการศึกษาตามหลักสูตรปริญญาปรัชญาดุษฎีบัณฑิต
สาขาวิชาวิศวกรรมโยธาและการบริหารงานก่อสร้าง
มหาวิทยาลัยเทคโนโลยีสุรนารี
ปีการศึกษา 2566

COMPRESSIVE STRENGTH AND MICROSTRUCTURE OF RIGID POLYURETHANE
FOAM AND ITS APPLICATION IN ROAD MAINTENANCE

Suranaree University of Technology has approved this thesis submitted in partial fulfillment of the requirements for the Degree of Doctor of Philosophy.

Thesis Examining Committee


.....

(Prof. Dr. Panich Voottipruex)

Chairperson


.....

(Prof. Dr. Suksun Horpibulsuk)

Member (Thesis Advisor)


.....

(Asst. Prof. Dr. Menglim Hoy)

Member


.....

(Dr. Apichat Suddeepong)

Member


.....

(Dr. Teerasak Yaowarat)

Member


.....
(Assoc. Prof. Dr. Yupaporn Ruksakulpiwat)

Vice Rector for Academic Affairs
and Quality Assurance


.....

(Assoc. Prof. Dr. Pornsiri Jongkol)

Dean of institute of Engineering

อรุณเดช บุญสูง : กำลังอัดและโครงสร้างจุลภาคของโพลียูรีเทนโฟมแบบแข็งเกร็ง
และการประยุกต์ใช้ในงานซ่อมบำรุงถนน (COMPRESSIVE STRENGTH AND
MICROSTRUCTURE OF RIGID POLYURETHANE FOAM AND ITS APPLICATION IN
ROAD MAINTENANCE)

อาจารย์ที่ปรึกษา : ศาสตราจารย์ ดร.สุขสันต์ หอพิบูลสุข, 166 หน้า

คำสำคัญ: โพลียูรีเทนโฟมแบบแข็งเกร็ง/กำลังรับแรงอัด/โครงสร้างทางจุลภาค/กรณีศึกษาของ
ผิวทาง/การฉีต โพลียูรีเทนโฟม

การก่อสร้างถนนนับได้ว่าเป็นการพัฒนาโครงสร้างพื้นฐานที่สำคัญต่อการคมนาคมและ
ขับเคลื่อนเศรษฐกิจของประเทศ ถนนในประเทศไทยมีการขยายโครงข่ายเพิ่มมากขึ้นในทุก ๆ ปี โดย
ถนนส่วนใหญ่ถูกออกแบบเพื่อรองรับปริมาณการจราจรที่เพิ่มขึ้นเพื่อให้มีอายุการใช้งาน 15-20 ปี
อย่างไรก็ตาม ปริมาณการจราจรที่เพิ่มขึ้นอย่างรวดเร็วก่อการบรทุกน้ำหนักเกินกว่าที่กฎหมาย
กำหนดของรถบรรทุกขนาดใหญ่ ทำให้ถนนเกิดความเสียหายเนื่องจากการหลุดตัวของโครงสร้างทาง
โดยเฉพาะอย่างยิ่ง บริเวณส่วนเชื่อมต่อระหว่างสะพานกับถนน การแก้ไขปัญหาแบบดั้งเดิมในประเทศ
ไทยทำโดยการรื้อโครงสร้างทางเดิมทิ้งและก่อสร้างใหม่ ซึ่งต้องปิดการใช้งานถนนเป็นเวลานานและ
ใช้งบประมาณซ่อมบำรุงที่สูง ส่งผลกระทบอย่างมากต่อระบบการคมนาคมและก่อให้เกิดการสูญเสีย
ประโยชน์ด้านธุรกิจการขนส่ง เทคโนโลยีการฉีตโฟม PU เป็นอีกหนึ่งทางเลือกที่สามารถแก้ปัญหา
การหลุดตัวของผิวทางและเริ่มได้รับความนิยมในประเทศ เนื่องจากสามารถแก้ไขปัญหการปิดถนน
และลดงบประมาณในการซ่อมแซม อย่างไรก็ตาม การประยุกต์ใช้เทคโนโลยีการฉีตโฟม PU นี้ ยังขาด
มาตรฐานในการควบคุมคุณภาพการผลิตและติดตามผลการดำเนินงานตามหลักการทางวิศวกรรม

วิทยานิพนธ์นี้เป็นการศึกษากำลังอัดและโครงสร้างจุลภาคของโฟม PU ในห้องปฏิบัติการ
และการประยุกต์ใช้งานเพื่อซ่อมแซมโครงสร้างชั้นทางที่เกิดการหลุดตัวจากการใช้งานทั้งในกรณี
ผิวทางแบบยึดหยุ่นและแบบแข็งเกร็ง งานวิจัยส่วนแรกศึกษาอิทธิพลของปริมาณ polyol
อัตราส่วนระหว่าง polyol ต่อ isocyanate (p/d ratio) และอุณหภูมิระหว่างผสมของ polyol และ
isocyanate ที่มีต่อกำลังอัดและโครงสร้างจุลภาค งานวิจัยส่วนที่สองเป็นการนำเสนอกรณีศึกษาการ
เสริมความแข็งแรงของโครงสร้างชั้นทางด้วยเทคนิคการฉีตโฟมทั้งในระดับต้นและลึก เพื่อซ่อมแซมผิว
ทางคอนกรีตเสริมเหล็กและผิวทางแอสฟัลต์

จากผลการศึกษาทั้งสองส่วน ผู้วิจัยได้เสนอแนวปฏิบัติสำหรับเทคนิคการฉีตโฟม PU เพื่อ
แก้ไขปัญหการหลุดตัวของถนนตามหลักการทางวิศวกรรม ซึ่งประกอบด้วยวิธีการสำรวจลักษณะ
ทางกายภาพ การวางแผน มาตรการความปลอดภัย การควบคุมคุณภาพ การติดตามตรวจสอบ และ

การจัดทำรายงานผลการปฏิบัติ แนวปฏิบัตินี้สามารถใช้เป็นพื้นฐานในจัดทำเป็นมาตรฐานการทำงาน สำหรับหน่วยงานที่เกี่ยวข้อง เช่น กรมทางหลวง กรมทางหลวงชนบท และกรมการปกครอง ส่วนท้องถิ่น เพื่อแก้ปัญหาคาการหลุดตัวของถนน อันจะสนับสนุนการพัฒนาระบบขนส่งของประเทศ อย่างยั่งยืน



สาขาวิชา วิศวกรรมโยธาและการบริหารงานก่อสร้าง
ปีการศึกษา 2566

ลายมือชื่อนักศึกษา.....

ลายมือชื่ออาจารย์ที่ปรึกษา.....

AROONDET BOONSUNG : COMPRESSIVE STRENGTH AND MICROSTRUCTURE OF RIGID POLYURETHANE FOAM AND ITS APPLICATION IN ROAD MAINTENANCE.

THESIS ADVISOR : PROF. SUKSUN HORPIBULSUK, Ph.D., 166 PP.

Keywords: Rigid Polyurethane Foam/Compressive Strength/Microstructure/Pavement Geotechnical/Polyurethane Foam Injection

Road construction is an essential infrastructure development for transportation and driving the country's economy. The road network in Thailand is expanding annually. Most roads are designed to accommodate increased traffic volumes for 15-20 years of service. However, the rapid increase in traffic volumes combined with the heavy truck loads exceeding legal limits has caused road damages due to the settlement of road structures, especially at the bridge approach slabs. The traditional solution in Thailand is to demolish the existing road structure and build a new one, which requires long periods of road closure and high maintenance costs, significantly impacting the transportation system and causing a loss of benefits in the transportation business. PU foam injection technology is an alternative technique that can solve the problem of pavement settlement. It has become trendy in the country because it can solve road closure problems and reduce repair budgets. However, applying this PU foam injection technology still needs to improve standards for controlling production quality and monitoring performance based on engineering principles.

This thesis consists of a laboratory study of PU foam's compressive strength and microstructure and its applications to repair pavement structures that have collapsed from use, both in the case of flexible and rigid pavement surfaces. The first part presents the influence of the amount of polyol, the ratio of polyol to isocyanate (p/d ratio), and the mixing temperature of polyol and isocyanate on the compressive strength and the microstructure. The second part of the thesis presents case studies of the road maintenance using shallow and deep PU foam injection techniques for both concrete and asphalt concrete pavements.

From the results of both parts of the study, the research has proposed a guideline for applying the PU foam injection technique to solve the problem of road

settlement based on engineering principles. The guideline included methods for surveying physical characteristics, planning, safety measures, quality control, and preparing performance reports. This guideline can be extended to develop a working standard for relevant agencies such as the Department of Highways, the Department of Rural Roads, and the Department of Local Administration for repairing road settlements that will support the sustainable development of the country's transportation system.



School of Civil Engineering and Construction Management
Academic Year 2023

Student's Signature.....

Advisor's Signature.....

ACKNOWLEDGMENT

I would like to express my sincere gratitude to my advisor, Professor Dr. Suksun Horpibulsuk, who has always supported me while I was doing my doctorate. He made me learn new things about education and research. It taught me patience, motivation, enthusiasm, and excellent knowledge I had never experienced before. Moreover, he has also been a role model in my personal development to have excellent academic skills. Without his guidance and diligence, this dissertation would not have been possible until now. It gives me great confidence that studying for a PhD in civil engineering and construction management at Suranaree University of Technology was one of the best decisions I have made in my life.

In addition, I would like to thank the examination committee that played an essential role in my thesis, including Professor Dr. Panich Wuttipruk, chairman of the thesis examination committee; Assist Prof Dr.Menglim Hoy; Dr. Apichat Suddeepong; and Dr. Teerasak Yaowarat.

I would like to thank the scholarship throughout the Ph.D. program in Civil Engineering and Construction Management. from Uttaradit Rajabhat University, and officials who facilitate financial documents in all sectors are also here.

Finally, I would like to thank my beloved family for their constant spiritual support, even when I was tired, discouraged, and drowning in sadness. My family pushed me to overcome many problems and obstacles throughout my Ph.D. studies, making me the strong person I am today.

Aroondet Boonsung

TABLE OF CONTENTS

	Page
ABSTRACT (THAI).....	I
ABSTRACT (ENGLISH).....	III
ACKNOWLEDGMENT.....	V
TABLE OF CONTENT.....	VI
LIST OF TABLE.....	X
LIST OF FIGURES.....	XI
SYMBOLS AND ABBREVIATIONS.....	XIV
CHAPTER	
I INTRODUCTION.....	1
1.1 Statement of the problem.....	1
1.2 Objectives of the study.....	6
1.3 Organization of the dissertation.....	6
1.4 Reference.....	8
II LITERATURE REVIEW.....	15
2.1 Introduction.....	15
2.2 Light Weight Material for Road Construction.....	15
2.2.1 Air Foam Mixed Stabilized Soil (AMS).....	17
2.2.2 Expanded Polystyrene Block (EPS).....	18
2.3 Polyurethane.....	22
2.4 Polyurethane Synthesis Process.....	27
2.4.1 Polyurethane Foam Synthesis Reaction.....	28
2.4.2 Polymerization Reaction.....	29
2.5 Enhancement of Properties and Use of Polyurethane Foams.....	30
2.5.1 Mechanical Properties.....	30
2.5.2 Thermal Regulation.....	32

TABLE OF CONTENTS (Continued)

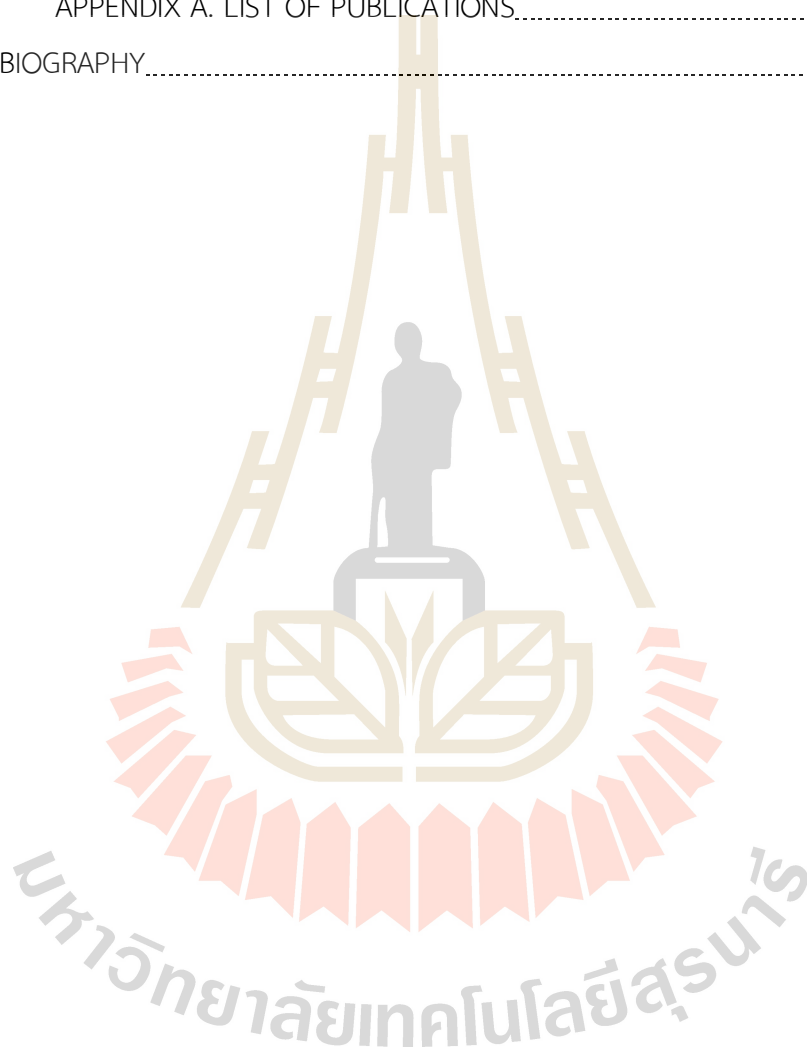
	Page
2.5.3 Reaction to Fire.....	33
2.5.4 Sound Absorption Properties.....	35
2.5.5 Other Properties and Applications.....	36
2.6 Mechanicals Behavior of polyurethane foam.....	37
2.7 Microstructural Analysis Techniques.....	47
2.7.1 Scanning electron microscopy (SEM).....	47
2.7.2 Energy Dispersive X-Ray Spectroscopy (EDS).....	48
2.8 Use of polyurethane foam for soil improvement.....	53
2.9 References.....	61
III COMPRESSIVE STRENGTH AND MORPHOLOGY OF RIGID POLYURETHANE FOAM FOR ROAD APPICATIONS.....	77
3.1 Introduction.....	77
3.2 Materials and Methods.....	81
3.2.1 Materials.....	81
3.2.2 Preparation of specimens.....	81
3.2.3 Experimental Program.....	82
3.3 Results.....	85
3.3.1 Compressive Strength for Ambient Mixing Temperature.....	85
3.3.2 Stress-Strain Relationship.....	87
3.3.3 Influence of Mixing Temperature.....	88
3.4 Microstructural Analysis.....	92
3.5 Conclusions.....	98
3.6 References.....	99
IV PERFORMANCE OF THE POLYURETHANE FOAM INJECTION TECHNIQUE FOR ROAD MAINTENANCE APPLICATIONS.....	106
4.1 Introduction.....	106
4.2 Polyurethanes.....	109

TABLE OF CONTENTS (Continued)

	Page
4.2.1 Chemical Composition.....	109
4.2.2 Characteristics of Polyurethane.....	111
4.3 PU Foam Injection Technique.....	113
4.4 Application of PU Foam for Road Maintenance.....	115
4.4.1 Flexible Pavement.....	116
4.4.2 Rigid Pavement.....	120
4.4.3 Bridge Approach Slab.....	125
4.5 Compressive Strength of PU Foam Samples.....	131
4.6 Guidelines for Repairing the Pavement Structure Using PU Foam Injection.....	136
4.6.1 Survey of Physical Characteristics.....	136
4.6.2 Planning.....	136
4.6.3 Safety Measures.....	137
4.6.4 Quality Control.....	137
4.6.5 Monitoring.....	139
4.6.6 Performance Report.....	139
4.7 Conclusions.....	141
4.8 References.....	142
V CONCLUSION AND RECOMMENDATION.....	149
5.1 Summary and conclusion.....	149
5.1.1 Compressive strength and morphology of rigid polyurethane foam for road applications.....	149
5.1.2 Performance of the polyurethane foam injection technique for road maintenance applications.....	150
5.1.3 Guidelines for repairing the pavement structure using PU Foam Injection.....	151
5.2 Recommendations for future work.....	151

TABLE OF CONTENTS (Continued)

	Page
APPENDIX	
APPENDIX A. LIST OF PUBLICATIONS.....	153
BIOGRAPHY.....	166



LIST OF TABLES

Table	Page
2.1	Properties of Air Foam Mixed Stabilized Soil Improved with Cement.....18
2.2	Physical Property of Geofoam according to ASTM D6817.....20
2.3	Classification of different types of polyurethane foam.....25
2.4	Polyol specification.....27
2.5	Physical and chemical properties of TDI and MDI.....27
3.1	RPUF mixing proportion.....83
4.1	Specific properties of polyols (Szycher, 2013).....111
4.2	Physical and chemical properties of TDI and MDI (Szycher, 2013).....111
4.3	Classification of polyurethane foam (Ashida, 2006).....112
4.4	Pressure range of PU foam injection sequence for soil improvement (Mohamed Jais, 2017).....137

LIST OF FIGURES

Figure	Page
2.1	Area distribution and thickness of Bangkok soft clay.....16
2.2	EPS-geofoam manufacturing process.....21
2.3	Three important forms of EPS.....21
2.4	General structural characteristics of polyurethane.....22
2.5	Polyurethane synthesis reaction.....23
2.6	soft segment and hard segment in polyurethane chemical structure.....23
2.7	Thermoset polyurethane synthesis reaction.....24
2.8	Molecular structure of diphenylmethane diisocyanate.....27
2.9	Compressive stress-strain curves of PUFs-EG foams.....31
2.10	SEM images of PUF-EG-0.00 (a), PUF-EG-0.25 (b), PUF-EG-0.50 (c), PUF-EG-0.75 (d), PUF-EG-1.00 (e), PUF-EG-1.25 (f), PUF-EG-1.50 (g), PUF-EG-2.00 and (h), PUF-EG-2.50.....32
2.11	Mechanism of heat transfer of polymer foam.....33
2.12	Typical compressive stress-strain response of a polymer foam.....38
2.13	Tensile and compressive responses of foam specimens of different densities.....39
2.14	Equipment used in compression tests of foams.....39
2.15	Results of compression tests of the polyurethane foam (a) 16 kg/m ³ and (b) 62 kg/m ³40
2.16	True stress–strain curves of H130 foam at various strain rates.....41
2.17	(a) Moduli, (b) yield strengths, and (c) ultimate tensile strengths of H130 and H200 foams at various strain rates.....42
2.18	A comparison of stress-strain curves for rigid polyurethane foam subjected to quasi-static and dynamic compression.....43

LIST OF FIGURES (Continued)

Figure	Page
2.19 Dynamic response of polyurethane foam subjected to different strain Rates.....	44
2.20 SEM micrographs of PUR foams with different density: (a) PUR240 and (b) PUR320.....	45
2.21 Relationship between strain rate and peak stress and absorbed energy of PUR with different densities.....	45
2.22 Cell structure of WF51. (Reprinted with permission of Röhm GmbH).....	46
2.23 Fatigue stress-life diagrams for (a) WF51, (b) WF110 and (c) WF200.....	46
2.24 Scanning Electron Microscopy (SEM) Device.....	47
2.25 Components of Scanning Electron Microscopy (SEM).....	48
2.26 EDS Device and Mechanism (a) Scintillator detector for both secondary And backscattered electrons (b) Different penetration level of electron through the sample.....	49
2.27 Results of chemical composition analysis by EDS technique.....	50
2.28 SEM micrographs of the composites PU/VMT: (a) 0%, (b) 5%, (c) 10%, (d) 15%, and (e) 20%.....	51
2.29 EDS profile of the composites PU/VMT: (a) 0%, (b) 5%, (c) 10%, (d) 15%, and (e) 20%.....	52
2.30 FE-SEM image and EDS analysis of Ag-coated Polyurethane foam C%:92.32; O%:1.39; Ag%:6.29.....	52
2.31 UCS test result of marine clay at varying dose of Polyurethane.....	54
2.32 Compressive Strength of Modified Sand with PU Foam.....	55
2.33 Schematic layout of shallow PU foam injection.....	56
2.34 Axial displacement against time of the concrete slab uplifting work at Kota Damansara toll plaza, Malaysia.....	57
2.35 PU injection illustration.....	58
2.36 Points identified for PU injection.....	59

LIST OF FIGURES (Continued)

Figure	Page
2.37 Image of the free expanded polyurethane foam obtained by Scanning Electron Microscope. (a) Magnification x 100. (b) Magnification x 200.....	60
2.38 (a) Magnification of the foam specimen. (b) Microstructure of Polyurethane foam at Magnification x 45.....	61
3.1 Reaction of urethane product.....	79
3.2 Temperature control bath and device.....	85
3.3 Compressive Strength of RPUF for ambient mixing temperature.....	86
3.4 Compressive stress-strain relationship of RPUF prepared at ambient temperature.....	87
3.5 Effect of P content and mixing temperature on compressive strength.....	89
3.6 RPUF specimens with various mixing temperatures and p/d ratios at P content = 23 kg/m ³	91
3.7 EDS analysis results of RPUF specimens at P content of 23 kg/m ³ and p/d ratio of 1.0.....	93
3.8 Foam cells of RPUF specimens at P content of 28 kg/m ³	93
3.9 Distribution of foam cell diameters of RPUF specimens at P content of 28 kg/m ³	94
3.10 Distribution of foam cell for different ranges of cell size of RPUF specimens at P content of 28 kg/m ³	95
3.11 Closed cell structure of RPUF at different p/d ratios at 40°C mixing temperature and P content of 28 kg/m ³ for p/d ratios a) 1.0, b) 0.9 and c) 0.8.....	96
3.12 Closed cell structure of RPUF at P content of 28 kg/m ³ for a) mixing temperature of 25°C and p/d ratios of 1.0, 0.9 and 0.8 and b) mixing temperature of 40, 50 and 60°C and p/d ratios of 1.0, 0.9 and 0.80.....	97
4.1 General structural characteristics of polyurethane.....	110
4.2 Polyurethane synthesis reaction.....	110

LIST OF FIGURES (Continued)

Figure	Page
4.3	Characteristics of deep injection of PU Foam (modified after Rao et al., 2019).....113
4.4	Characteristics of shallow injection of PU Foam (modified after Rao et al., 2019).....114
4.5	Characteristics of Highway No. 9 (Bang Na-Bang Pa-in) and road structure.....116
4.6	Settlement location of the asphalt-covered pavement.....117
4.7	Results of the Kunzelstab Penetration Test (KPT) and the pavement structure.....118
4.8	Steps for deep PU foam injection.....119
4.9	Location and spacing of drill holes (red dots) for foam injection.....119
4.10	Physical characteristics of the road (a) pavement damage (b) settlement surface.....121
4.11	PU foam injection location to raise the pavement surface.....122
4.12	Shallow PU injection process.....123
4.13	Post-injection inspection of PU foam (a) repaired pavement, (b) data collection location.....124
4.14	Level values of the pavement before and after PU foam injection.....125
4.15	Opening due to soil flew out of the bridge approach slab.....126
4.16	(a) Pavement crack line (b) Injection to seal the opening.....127
4.17	Work steps (a) Drilling holes to install foam injection equipment (b) Measuring the level of surface movement.....127
4.18	Subsoil and road information (a) Arrangement of the Bangkok Soft Clay (Eide, 1977) (b) Road structure.....129
4.19	(a) Pavement damage (b) Cavities under the pavement.....130
4.20	Preparing Lightweight concrete for pouring to fill a cavity.....130

LIST OF FIGURES (Continued)

Figure	Page
4.21 PU foam texture of the specimen obtained by injection into the mold.....	132
4.22 Compressive strength test results of PU foam samples prepared by injection pressures (a) 10.4 MPa (b) 13.8 MPa.....	133
4.23 Failure characteristics of the PU foam samples (a) brittle behavior (b) three-phase behavior.....	134
4.24 Unit weight of PU foam injected at different pressures.....	135
4.25 Schematic of the steps for pavement repair by injecting PU foam into the pavement structure layer.....	140

SYMBOLS AND ABBREVIATIONS

EPS	=	expanded polystyrene foam
PUF	=	polyurethane foam
C ₄ H ₁₀	=	butane gas
C ₅ H ₁₂	=	pentane gas
CO ₂	=	carbon dioxide
C	=	carbon
O	=	oxygen
R _{iso}	=	an isocyanate monomer
R _{polyol}	=	a polyol component
MDI	=	4,4-methylene diphenyl diisocyanate
D	=	diisocyanate
P	=	polyol
p/d	=	polyol to diisocyanate ratios
RPUF	=	rigid polyurethane foam
°C	=	degree Celsius
KPT	=	kunzelstab penetration test

CHAPTER I

INTRODUCTION

1.1 Statement of the problem

The road structure consists of a base and a sub-base. The materials used in construction must be of high quality and follow construction standards, which can be examined from the laboratory test results. Settlement problems often occur with structures located on soft soils due to the consolidation of the soil mass. Excessive groundwater pumping is also a cause of subsidence (Peduto et al., 2020). Solving the settlement problem can be done in several ways, including cement or chemical injections to improve stiffness of clay layers. The use of lightweight materials as a substitute for soft soil and surface improvement with asphaltic concrete is an alternative means (Tanchaisawat et al., 2008; Youwai et al., 2011; Vardhanabhuti et al., 2015; Wonglert et al., 2018; Lenart & Kaynia, 2019). Each method has complex workflows and different budgets.

Expanded polystyrene foam (EPS) is a lightweight material often used to solve the settlement problem because it is very light compared to the soil. The weight unit is in the range of 11.2 to 45.7 kg/m³ in accordance with ASTM D6817-07 (ASTM). A lightweight material decreased stress distribution within the soil mass. The applied stress lower than the yield stress of the material causes low deformation with less consolidation time (Youwai et al., 2011). Although expanded polystyrene foam is a powerful geomaterial, it is necessary to use butane (C₄H₁₀), flammable gas, in the

production process. Polystyrene (PS) expands with complex production procedures, causing the production process to be hazardous. Therefore, there is an attempt to develop an alternative safer lightweight material for geotechnical and pavement applications (Sinnathamby et al., 2019).

Polymeric foam, such as foam plastic, cellular plastic, or polymer foam, is a material that consists of solid and gaseous stages. The polymer foam can be manufactured from many polymers, such as polyurethane (PU), polystyrene (PS), polyisocyanate (PIR), polyethylene (PE), polypropylene (PP), ethylene-vinyl acetate (EVA), nitrile rubber (NBR), polyvinyl chloride (PVC), or other polyolefins. Polyurethane foam (PUF) dominates the world market, followed by PS and PVC foam (Titow, 2001; Eaves, 2004; Lee, 2004). Polyurethane foam is widely used in various industries, including lightweight construction materials. The first synthetic urethane was made in 1849 by Wurtz. Otto Bayer developed polyurethane foams in 1937 based on Wurtz's discovery of the reaction between polyester and isocyanate (Ionescu, 2005; Szycher, 2006; Prisacariu, 2011; Sharmin & Zafar, 2012) from the reaction between the OH of the polyol and the NO group isocyanate, designated as "polymerization." (Ionescu, 2005; Prisacariu, 2011). During the reaction, heat is also released. However, it is necessary to add more chemicals to improve the properties of PU foam for it to be appropriate according to the objectives of each type of work (Kausar, 2018), such as improving its mechanical properties by adding cellulose and lignocellulose fibers (Coelho et al., 2010; Otto & Moisés, 2017), micro glass or fiber (Yakushin et al., 2012; Marhoon & Rasheed, 2015; Serban et al., 2016), waste from egg shell, walnuts and hazelnuts and esparto fur (Antunes et al., 2011; Bry et al., 2016; Zieleniewska et al., 2016; Oushabi et al., 2017). The insulation improvement to control the heat can be done by adding carbon nanotube (Yan et al., 2011; you et al., 2011; he et al., 2013; Espadas-Escalante et al., 2017), graphene, carbon fibers (CNFS) or Fe₃O₄, TiO₂, and Iron Oxide (Dolomanova et al., 2011; Hodlur & Rabinal, 2012; Mussatti et al., 2013; Zhang et al., 2013; Yufei et al., 2015; Liu et al., 2016; Strankowski et al., 2016; Kim et al., 2017).

In 2016, it was found that PU foam accounted for approximately 9% of the plastic used worldwide. In 2017, the amount of PU foam sold worldwide was worth up to 60.5 billion US dollars. In 2021, it was expected that PU foam in the polymer

foam market would be up to 29,357 thousand tons, worth 79 billion US dollars, and grow to 37,254 thousand tons in 2026, with a growth rate of 4.9% (Ionescu, 2005; Palm & Svensson Myrin, 2018; Statista Research Department, 2023). In 2020, polyurethane foam was expected to have the largest market share of all polymer foams, with a market share of approximately 51 percent. Currently, polyurethane foam has been used for a variety of purposes, including construction and automotive. Polystyrene foam had a 37% market share in 2020, most of which is used for packaging (Smithers, 2023). Technological growth in many countries significantly contributes to the economic growth of many foam polymer industries such as automotive, building and construction, packaging, bedding, and furniture, for example, in building and construction areas. All of these things are contributing to the increasing demand for foam polymers. For the construction industry, there are 2 types of PU foam used: insulation and lightweight structure (sandwich panels). So far, many studies on engineering qualifications and behavior of PU foam has been reported, leading to its effective use.

Witkiewicz and Zieliński (2006) studied the tensile strength and shear force of PU foam, which has two densities (16 kg/m^3 and 62 kg/m^3). The test results showed that both types of PU foam exhibited anisotropic behavior. Considering compressive, tensile, and shear strength, the PU foam, with a density of 62 kg/m^3 , is suitable for using as a lightweight rowing boat in shallow water, which is consistent with the study of Stirna et al. (2011), investigating the tensile and compressive strengths of the PU foam with $65\text{--}70 \text{ kg/m}^3$ density. It was found that the tensile and compressive strengths increased when the PU foam density increased. In some cases, PU foam is used as a compound absorbing material for packaging to prevent product damage during transportation. The density is an essential factor for the mechanical properties and behaviors of rigid polyurethane foam because, under dynamic compression, modulus, and plateau stress increase according to the increased density. It can be said that these values are a function of foam density (Walter et al., 2009). The load frequency, the material's orientation, and the temperature during the test also significantly influence behavior under compression. It was found that the foam cells stretched and exhibited anisotropic behavior. The bending of the strut that determines the edge of the foam

cells is the primary mechanism that controls the deformation and damage of the foam cells (Ridha & Shim, 2008; Linul et al., 2013; Wiyono et al., 2016). PU foam has been added to create new materials or improve properties according to the purpose. Komurlu and Kesimal (2015) examined the compressive strength of artificial stone made from PU foam and mixed sand sediment in the ratios of 1/7, 1/8, and 1/9 to replace the lighter natural stone. The study found that all the ingredients provided compressive strength of more than 3 MPa with satisfactory impact resistance. Linul et al. (2018) studied on the compressive strength behavior of semi-rigid polyurethane foam reinforced by aluminum microfiber at 0, 0.5, 1.0, 1.5, and 2.0 percent of liquid foam weight. It was found that the compressive strength increased with the content of aluminum microfibers. Energy absorption increased by 61.81% and 71.29%, respectively, compared to the unreinforced case. Václavík et al. (2012) applied PU foam from demolished building to be used as aggregate in producing lightweight concrete to produce prefabricated parts. PU foam is digested by spinning with a high-speed blade so that the PU foam size is not over 6 mm. It was found that lightweight concrete in its fresh state with $1,100 \text{ kg/m}^3$ density had compression strengths of 2.9 MPa and 5.1 MPa after 24 hours and 28 days.

Nowadays, PU foam is also used as a grouting material for geotechnical applications to stabilize the soil by improving its essential properties, including shear strength, compressibility, water permeability. The basis of this method is similar to general cement grouting, but it uses two different chemicals: polyol and isocyanate.. Natural Soils with high organic matter content, such as peat soil, are greatly compressible. Using PU foam with a polyol and isocyanate ratio of 1:1 injected into the soil mass was found to decrease voids in the mass and resulted in reduced settlement (Mohamed Jais et al., 2019). Expansive soils that expand and cause swelling pressure can cause cracks within the soil mass. The PU foam could reduce the permeability of water through the soil mass and hence reduced their swelling (Buzzi et al., 2007, 2008). For the sandy soil layer, Sidek et al. (2015) studied the influence of injected PU foam by varying the amount of PU foam in the range of 0–95% compared to the amount of sand in the samples. It was found that the compressive strength of sand increased with the amount of PU foam, which varied in the range of 20 kPa–500

kPa (10%–95%). Saleh et al. (2018) used polyurethane to improve the strength of marine soil in the laboratory by varying the amount of PU foam equal to 0%, 1%, 2%, 3%, 4%, and 5% of clay weight. The uniaxial compressive strength test results showed that polyurethane could improve the shear strength of marine clay from 75 kPa to 250 kPa (a 230% increase). It also reduces the accumulated stress on the soil from 5.18% to 2.92% (77% decrease).

In addition, it was found that using PU Foam in soil nailing can increase the friction between the nail and the ground, reducing the subsidence of the ground before and after reinforcement from 5.33 mm to 2.002 mm and from 4.71 mm to 1.818 mm, respectively (Chun et al., 1997). For micro-pile applications, high-pressure injection of PU foam improved the response to ambient vibration, which affected the system's fundamental frequency and foundation behavior at small strains (Capatti et al., 2016; Valentino & Stevanoni, 2016). PU foam could improve bearing capacity and reduce compressibility of the pavement structure, which enhance the service life (Priddy et al., 2010; Vennapusa et al., 2016; Bagus, 2017; Mohamed Jais, 2017).

The above information shows that PU foam will have a higher market growth trend in the future due to its wide range of applications. It has been used in various manufacturing industries and has started to play a role in the construction industry. It can be used as lightweight materials in buildings, heat insulating material and injection material for repair work.

In this study, polyol and liquid diisocyanate were used for PU foam production under various influence factors: polyol content, polyol to diisocyanate ratio, temperature of mixing polyol and diisocyanate. The role of these factors on the compressive strength development was illustrated. The microstructural study via scanning electron microscopy (SEM) and energy dispersive X-Ray spectroscopy (EDS) was performed on the PU foam samples to investigate the structural changes with the influence factors. This study would yield the optimum ingredient to produce the cost-effective PU foam. Finally, field investigation of the two studied road remedy projects using PU foam injection technique would be performed and the field measurement data would be recorded and compared with simulated finite element results. All the studied results would be analyzed to develop a guideline for PU foam injection

technique in Thailand, which will promote this technique as an effective solution alternative to conventional technique.

1.2 Objectives of the study

This research has been undertaken with the following objectives:

1.2.1 To investigate the effect of polyol content, polyol to isocyanate ratio, and mixing temperature of polyol and diisocyanate on the compressive strength and microstructure of rigid polyurethane foam (RPUF).

1.2.2 To measure the performance of two road repaired projects using PU foam injection technique .

1.2.3 To develop a guideline and code of practice for PU foam injection technique in geotechnical applications

1.3 Organization of the thesis

This thesis consists of five chapters and outlines of each chapter are presented as follows:

Chapter I presents the introduction part, describing the statement of the problems, the objectives of the study and the organization of the thesis.

Chapter II presents a literature review related to PU Foam, chemical development in production, applications in construction projects in the past, present and future trends.

Chapter III presents the study results of the compressive strength of rigid PU foam (RPUF). Samples used in the study were prepared by mixing diisocyanate (d) and liquid polyol (p) and poured them into a PVC mold with a diameter of 7.5 cm and a height of 20 cm. During the reaction, the mold was closed to create a confinement-limited state, resulting in a closed-cell structure of PU foam, a feature of rigid PU foam (RPUF). The study variables consisted of P contents of 23, 28, 34, 40, 45, 51, and 87 kg per 1 m³, p/d ratios of 0.8, 0.9, and 1.0, and p and d temperatures of 25 °C, 40 °C, 50 °C, and 60 °C. The obtained RPUFs were trimmed to a size of 5 cm x 5 cm x 5 cm for compressive strength test using a universal testing machine (UTM). SEM and Energy EDS

were performed on the PU foam samples to examine the effect of p content, p/d ratio, and temperature of p and d on compressive strength and microstructure.

Chapter IV presents the case studies data of solving the problem of road settlement and the connection point between approach slab and bridge using the PU foam injection technique in 2 patterns: shallow PU foam injection and deep PU foam injection. The case study of shallow PU foam injection included the settlement problem solving of the reinforced concrete pavement surface at the U-turn on rural highway number 3026, Sing Buri Province. The case studies of deep PU foam injection included 1) the settlement problem solving of connection between the road and bridge on Rural Road 4012, Chanthaburi Province. The holes that formed in the bridge neck were small but quite deep; 2) the settlement problem solving of the asphalt pavement on Highway 9 (Motorway), Bangkok Province. The soil beneath the pavement surface was found to be a loose sand layer with 2.7 meters thickness; and 3) the settlement problem solving of a pavement surface heading to Suvarnabhumi Airport. Cavities were found under the slab approach. For cost-effective construction, the remedy was the combined usage of PU foam and cellular lightweight concrete. The lightweight concrete was poured into the cavities to reduce the volume of the cavities-filling material and then allowed it to harden before PU foam injection to completely fill the cavities. The current study results showed that the PU foam injection technique can effectively repair settled pavement surfaces at various damage levels.

In addition, the researcher has proposed a code of practice (CoP) for applying the PU foam injection technique to solve the problem of road settlement based on engineering principles to be used as a minimum operating guideline. The guideline included methods for surveying physical characteristics, planning, safety measures, quality control, and preparing performance reports. This CoP can be extended to develop a working standard for relevant agencies such as the Department of Highways, the Department of Rural Roads, and the Department of Local Administration for repairing road settlement that will support the sustainable development of the country's transportation system.

Chapter V presents the conclusion of each chapter and the overall conclusion. The suggestion for further study is also included in this chapter.

1.4 References

- Antunes, M., Cano, Á., Haurie, L., & Velasco, J. (2011). Esparto wool as reinforcement in hybrid polyurethane composite foams. *Industrial Crops and Products*, *34*, 1641–1648. <https://doi.org/10.1016/j.indcrop.2011.06.016>
- ASTM. (2017). *Standard Specification for rigid cellular polystyrene geofoam*. ASTM D6817-07, West Conshohocken, PA.
- Bagus, M. J. I. (2017). Rapid remediation using polyurethane foam/resin grout in Malaysia. *Geotechnical Research*, *4*(2), 107-117. <https://doi.org/10.1680/jgere.17.00003>
- Bryśkiewicz, A., Zieleniewska, M., Przyjemska, K., Chojnacki, P., & Ryszkowska, J. (2016). Modification of flexible polyurethane foams by the addition of natural origin fillers. *Polymer Degradation and Stability*, *132*. <https://doi.org/10.1016/j.polymdegradstab.2016.05.002>
- Buzzi, O., Fityus, S., Sasaki, Y., & Sloan, S. (2008). Structure and properties of expanding polyurethane foam in the context of foundation remediation in expansive soil. *Mechanics of Materials*, *40*(12), 1012-1021. <https://doi.org/10.1016/j.mechmat.2008.07.002>
- Buzzi, O., Fityus, S., Sasaki, Y., 2007. Influence of polyurethane resin injection on hydraulic properties of expansive soils. In: *Proceedings of the Third Asian Conference on Unsaturated Soils*, Nanjing, China, pp. 539–544.
- Capatti, M. C., Dezi, F., & Morici, M. (2016). Field tests on micropiles under dynamic lateral loading. *Procedia Engineering*, *158*, 236-241.
- Chun, B.-S., Ryu, D.-S., Shin, C.-B., Im, G.-S., Choi, J.-K., Lim, H.-S., & Son, J.-Y. (1997). The performance of polyurethane injection method with soil nailing system for ground reinforcement. *Ground improvement geosystems Densification and reinforcement: Proceedings of the Third International Conference on Ground Improvement Geosystems London*, 3-5 June 1997,
- Coelho Da Silva, M., Takahashi, J., Chaussy, D., Belgacem, N., & Silva, G. (2010). Composites of Rigid Polyurethane Foam and Cellulose Fiber Residue. *Journal of Applied Polymer Science*, *117*, 3665-3672. <https://doi.org/10.1002/app.32281>

- Dolomanova, V., Jcm, R., Jensen, L., Pyrz, R., & Barros-Timmons, A. (2011). Mechanical properties and morphology of nano-reinforced rigid PU foam. *Journal of Cellular Plastics - J CELL PLAST*, 47, 81-93. <https://doi.org/10.1177/0021955X10392200>
- Eaves, D. Handbook of Polymer Foams; Rapra Technology Ltd.: Shawbury, UK, 2004; p. 289.
- Espadas Escalante, J. J., Aviles, F., Gonzalez-Chi, P. I., & Oliva, A. (2016). Thermal conductivity and flammability of multiwall carbon nanotube/polyurethane foam composites. *Journal of Cellular Plastics*, 53. <https://doi.org/10.1177/0021955X16644893>
- Fakhar, A. M. M., & Asmaniza, A. (2016). Road Maintenance Experience Using Polyurethane (PU) Foam Injection System and Geocrete Soil Stabilization as Ground Rehabilitation. *IOP Conference Series: Materials Science and Engineering*, 136(1), 012004. <https://doi.org/10.1088/1757-899X/136/1/012004>
- He, T., Liao, X., He, Y., & Li, G. (2013). Novel electric conductive polylactide/ carbon nanotubes foams prepared by supercritical CO₂. *Progress in Natural Science: Materials International*, 23, 395–401. <https://doi.org/10.1016/j.pnsc.2013.06.006>
- Hodlur, R., & Rabinal, M. (2012). Graphene based Polyurethane Material: As Highly Pressure Sensitive Composite. 1447, 1279- 1280. <https://doi.org/10.1063/1.4710479>
- Ionescu, M. Chemistry and Technology of Polyols for Polyurethanes; Rapra Technology Limited: Shawbury, UK, 2005; ISBN 1859574912.
- Kausar, A. (2017). Polyurethane Composite Foams in High Performance Applications: A Review. *Polymer-Plastics Technology and Engineering*, 57. <https://doi.org/10.1080/03602559.2017.1329433>
- Kim, J. M., Lee, Y., Jang, M., Han, C., & Kim, W. (2016). Electrical conductivity and EMI shielding effectiveness of polyurethane foam– conductive filler composites. *Journal of Applied Polymer Science*, 134. <https://doi.org/10.1002/app.44373>
- Komurlu, E., & Kesimal, A. (2015). Experimental study of polyurethane foam reinforced soil used as a rock-like material. *Journal of Rock Mechanics and Geotechnical Engineering*, 7(5), 566-572. <https://doi.org/10.1016/j.jrmge.2015.05.004>

- Lee, S.-T.; Ramesh, N.S. *Polymeric Foams: Mechanisms and Materials*; CRC Press: New York, NY, USA, 2004.
- Lenart, S., & Kaynia, A. (2019). Dynamic properties of lightweight foamed glass and their effect on railway vibration. *Transportation Geotechnics*, 21, 100276. <https://doi.org/10.1016/j.trgeo.2019.100276>
- Linul, E., Marsavina, L., Voiconi, T., & Sadowski, T. (2013). Study of factors influencing the mechanical properties of polyurethane foams under dynamic compression. *Journal of Physics: Conference Series*, 451(1), 012002. <https://doi.org/10.1088/1742-6596/451/1/012002>
- Linul, E., Vălean, C., & Linul, P.-A. (2018). Compressive behavior of aluminum microfibers reinforced semi-rigid polyurethane foams. *Polymers*, 10(12), 1298.
- Liu, Z., Shen, D., Yu, J., Dai, W., Li, C., Du, S., Jiang, N., Li, H., & Lin, C.-T. (2016). Exceptionally high thermal and electrical conductivity of three dimensional graphene foam based polymer composites. *RSC Adv.*, 6. <https://doi.org/10.1039/C5RA27223H>
- Marhoon, I., & Rasheed, A. (2015). Mechanical and Physical Properties of Glass Wool-Rigid Polyurethane Foam Composites. 18, 41-49.
- Marhoon, I., & Rasheed, A. (2015). Mechanical and Physical Properties of Glass Wool-Rigid Polyurethane Foam Composites. 18, 41-49.
- Mohamed Jais, I. B. (2017). Rapid remediation using polyurethane foam/resin grout in Malaysia. *Geotechnical Research*, 4(2), 107-117.
- Mohamed Jais, I., Che Lat, D., & Endut, T. (2019). COMPRESSIBILITY OF PEAT SOIL IMPROVED WITH POLYURETHANE. *Malaysian Journal of Civil Engineering*, 31. <https://doi.org/10.11113/mjce.v31n1.545>
- Mussatti, E., Merlini, C., Barra, G. M. O., Güths, S., Oliveira, A. P. N. d., & Siligardi, C. (2012). Evaluation of the properties of iron oxide-filled castor oil polyurethane. *Materials Research-ibero-american Journal of Materials*, 16, 65-70.
- Otto, G.P.; Moisés, M.P.; Carvalho, G.; Rinaldi, A.W.; Garcia, J.C.; Radovanovic, E.; Fávaro, S.L. (2017). Mechanical properties of a polyurethane hybrid composite with natural lignocellulosic fibers. *Compos. Part B Eng.* 2017, 110, 459– 465. <https://doi.org/10.1016/j.compositesb.2016.11.035>

- Oushabi, A., Sair, S., Abboud, Y., Tanane, O., & Abdeslam, E. B. (2017). An experimental investigation on morphological, mechanical and thermal properties of date palm particles reinforced polyurethane composites as new ecological insulating materials in building. *Case Studies in Construction Materials*, 7. <https://doi.org/10.1016/j.cscm.2017.06.002>
- Palm, E.; Svensson Myrin, E. Mapping the Plastics System and Its Sustainability Challenges; Lund University: Lund, Sweden, 2018; p. 37.
- Peduto, D., Giangreco, C., & Venmans, A. (2020). Differential settlements affecting transition zones between bridges and road embankments on soft soils: Numerical analysis of maintenance scenarios by multi-source monitoring data assimilation. *Transportation Geotechnics*, 24, 100369. <https://doi.org/10.1016/j.trgeo.2020.100369>
- Priddy, L. P., Jersey, S. R., & Reese, C. M. (2010). Full-Scale Field Testing for Injected Foam Stabilization of Portland Cement Concrete Repairs. *Transportation Research Record*, 2155(1), 24-33. <https://doi.org/10.3141/2155-03>
- Prisacariu, C. Polyurethane Elastomers from Morphology to Mechanical Aspects; Springer: New York, NY, USA, 2011; ISBN 9783709105139
- Ridha, M., & Shim, V. P. W. (2008). Microstructure and Tensile Mechanical Properties of Anisotropic Rigid Polyurethane Foam. *Experimental Mechanics*, 48(6), 763-776. <https://doi.org/10.1007/s11340-008-9146-0>
- Saleh, S., Yunus, N. Z. M., Ahmad, K., & Ali, N. (2018). Stabilization of Marine Clay Soil Using Polyurethane. *MATEC Web Conf.*, 250, 01004. <https://doi.org/10.1051/mateconf/201825001004>
- Şerban, D., Weißenborn, O., Geller, S., Marsavina, L., & Gude, M. (2015). Evaluation of the mechanical and morphological properties of long fibre reinforced polyurethane rigid foams. *Polymer Testing*, 49. <https://doi.org/10.1016/j.polymertesting.2015.11.007>
- Sharmin, E.; Zafar, F. Polyurethane: An Introduction; InTech: London, UK, 2012.
- Sidek, N., Mohamed, K., Jais, I., & Abu Bakar, I. (2015). Strength characteristics of polyurethane (PU) with modified sand. *Applied Mechanics and Materials*,

- Sinnathamby G, Korkiala-Tanttu L, Gustavsson H. (2019). Post-use examination of EPS block characteristics: finnish case histories BT - 5th international conference on geofoam blocks in construction applications. In: Arellano D, Ozer AT, Bartlett SF, Vaslestad J, editors., Cham: Springer International Publishing. p. 99–109.
- Smithers. (2023). The Future of Polymer Foams to 2026. <https://www.smithers.com/services/market-reports/materials/the-future-of-polymer-foams-to-2025>
- Statista Research Department. (2023). Global Polyurethane Market Volume 2015-2029. <https://www.statista.com/statistics/720341/global-polyurethane-market-size-forecast>
- Stirna, U., Beverte, I., Yakushin, V., & Cabulis, U. (2011). Mechanical properties of rigid polyurethane foams at room and cryogenic temperatures. *Journal of Cellular Plastics - J CELL PLAST*, 47, 337-355. <https://doi.org/10.1177/0021955X11398381>
- Strankowski, M., Włodarczyk, D., Piszczyk, Ł., & Strankowska, J. (2016). Thermal and Mechanical Properties of Microporous Polyurethanes Modified with Reduced Graphene Oxide. *International Journal of Polymer Science*, 2016, 1- 8. <https://doi.org/10.1155/2016/8070327>
- Szycher, M. Szycher's Handbook of Polyurethanes, 2nd ed.; CRC Press: New York, NY, USA, 2006
- Tanchaisawat, T., Bergado, D. T., & Voottipruex, P. (2008). Numerical simulation and sensitivity analyses of full-scale test embankment with reinforced lightweight geomaterials on soft Bangkok clay. *Geotextiles and Geomembranes*, 26(6), 498-511. <https://doi.org/https://doi.org/10.1016/j.geotexmem.2008.05.005>
- Titow, W.V. PVC Technology; Rapra Technology Ltd.: Shawbury, UK, 2001; p. 146, ISBN 1859572405.
- Václavík, V., Dvorský, T., Dirner, V., Jaromír, D., & Martin, Š. (2012). Polyurethane foam as aggregate for thermal insulating mortars and lightweight concrete. *Tehnicki Vjesnik*, 19, 665-672.
- Valentino, R., & Stevanoni, D. (2016). Behaviour of reinforced polyurethane resin micropiles. *Proceedings of the Institution of Civil Engineers - Geotechnical Engineering*, 169(2), 187-200. <https://doi.org/10.1680/jgeen.14.00185>

- Vardhanabhuti B, Chantawarangul K, Seawsirikul S. Utilization of EPS Geofom for Bridge Approach Structure on Soft Bangkok Clay. *Geotech Saf Risk V* 2015: 602–7. doi:10.3233/978-1-61499-580-7-602
- Vennapusa, P. K., Zhang, Y., & White, D. J. (2016). Comparison of pavement slab stabilization using cementitious grout and injected polyurethane foam. *Journal of Performance of Constructed Facilities*, 30(6), 04016056.
- Walter, T. R., Richards, A. W., & Subhash, G. (2009). A unified phenomenological model for tensile and compressive response of polymeric foams.
- Witkiewicz, W., and Zieliński, A. (2006). Properties of the Polyurethane (PU) Light Foam. *Advances in Materials Science* 6(2): 35-51.
- Wiyono, P., Faimun, P., and Kristijanto, H. (2016). “Charaterization of Physical and Mechanical Properties of rigid Polyurethane.” *ARPN Journal of Engineering and Applied Sciences* 11(24): 14398-14405.
- Wonglert, A., Jongpradist, P., Jamsawang, P., & Larsson, S. (2018). Bearing capacity and failure behaviors of floating stiffened deep cement mixing columns under axial load. *Soils and Foundations*, 58. <https://doi.org/10.1016/j.sandf.2018.02.012>
- Yakushin, V., Bel'kova, L., & Sevastyanova, I. (2012). Properties of Rigid Polyurethane Foams Filled with Glass Microspheres. *Mechanics of Composite Materials*, 48. <https://doi.org/10.1007/s11029-012-9302-6>
- Yan, D.-X., Dai, K., Xiang, Z.-D., Zhong, G., Ji, X., & Zhang, W.-Q. (2011). Electrical Conductivity and Major Mechanical and Thermal Properties of Carbon Nanotube-Filled Polyurethane Foams. *Journal of Applied Polymer Science*, 120, 3014-3019. <https://doi.org/10.1002/app.33437>
- You, K., Park, S., Lee, C., Kim, J. M., Park, G., & Kim, W. (2011). Preparation and characterization of conductive carbon nanotube-polyurethane foam composites. *Journal of Materials Science - J MATER SCI*, 46. <https://doi.org/10.1007/s10853-011-5645-y>
- Youwai S, Kongkitkul W, Sripobink T, Meesamuth N. Application of EPS for remedial work of bridge bearing unit on Bangkok Soft Clay: A case study. In: 4th Ed int conf geofoam blocks constr appl, Lillestrøm, Norway: 6–8 June 2011; 2011, p. 294–302

- Yufei, C., Zhichao, L., Junyan, T., Qingyu, Z., & Yang, H. (2015). Characteristics and Properties of TiO₂ /EP-PU Composite. *Journal of Nanomaterials*, 2015, 1-7. <https://doi.org/10.1155/2015/167150>
- Zhang, S., Li, Y., Peng, L., Li, Q., Chen, S., & Hou, K. (2013). Synthesis and characterization of novel waterborne polyurethane nanocomposites with magnetic and electrical properties. *Composites Part A: Applied Science and Manufacturing*, 55, 94-101. <https://doi.org/10.1016/j.compositesa.2013.05.018>
- Zieleniewska, M., Leszczyński, M., Szczepkowski, L., Bryśkiewicz, A., Bień, K., & Ryszkowska, J. (2016). Development and applicational evaluation of the rigid Polyurethane foam composites with egg shell waste. *Polymer Degradation and Stability*, 132. <https://doi.org/10.1016/j.polymdegradstab.2016.02.030>



CHAPTER II

LITERATURE REVIEW

2.1 Introduction

Thailand is one of the fastest-growing developing countries among ASEAN countries. There has been a great deal of economic expansion and progress. Therefore, road infrastructure is essential to economic growth (Nikomborirak, 2004; DOH, 2012). Road construction is, therefore, a type of construction project that has continuously developed materials to reduce some limitations of traditional materials, such as increasing their bearing capacity, and reducing the weight of the material, etc. Road construction on soft soils with a high risk of subsidence of foundation soils resulting from the consolidation settlement caused by the heavy weight of traditional construction materials (Peduto et al., 2020). Therefore, using materials with high load-bearing capacity and lightweight in construction for geotechnical engineering is necessary to overcome the above mentioned problems.

2.2 Light Weight Material for Road Construction

The issue of embankment failure is typically brought on by the foundation's poor bearing capability, which results in significant subsidence or movement of the embankment. The soft clay soil beneath the embankment generally causes this issue. Thailand has an area of soft clay covering up to 14,000 km² around Bangkok and metropolitan area. The width of the estuary of the Gulf of Thailand from Ratchaburi Province to Chonburi Province is a distance of 140 kilometers, and the length extends north to Phra Nakhon Si Ayutthaya Province for a distance of 100 kilometers (Department of Rural Roads, 2009) as shown in Figure 2.1.

This layer of soft clay is known as "Bangkok Clay". The precipitation of this soft clay layer is approximately 10–18 m thick and shaped like a basin (Moh et al., 1969). In general, soft clays are composed mainly of silty soil, clayey soil, or soils that contain organic matter (peat) and a high amount of moisture in the soil mass (Kamon &

Bergado, 1991). The undrained shear strength test results from the vane shear test at the same depth, even in different areas, differed by at most 10% (Eide, 1968; 1977).

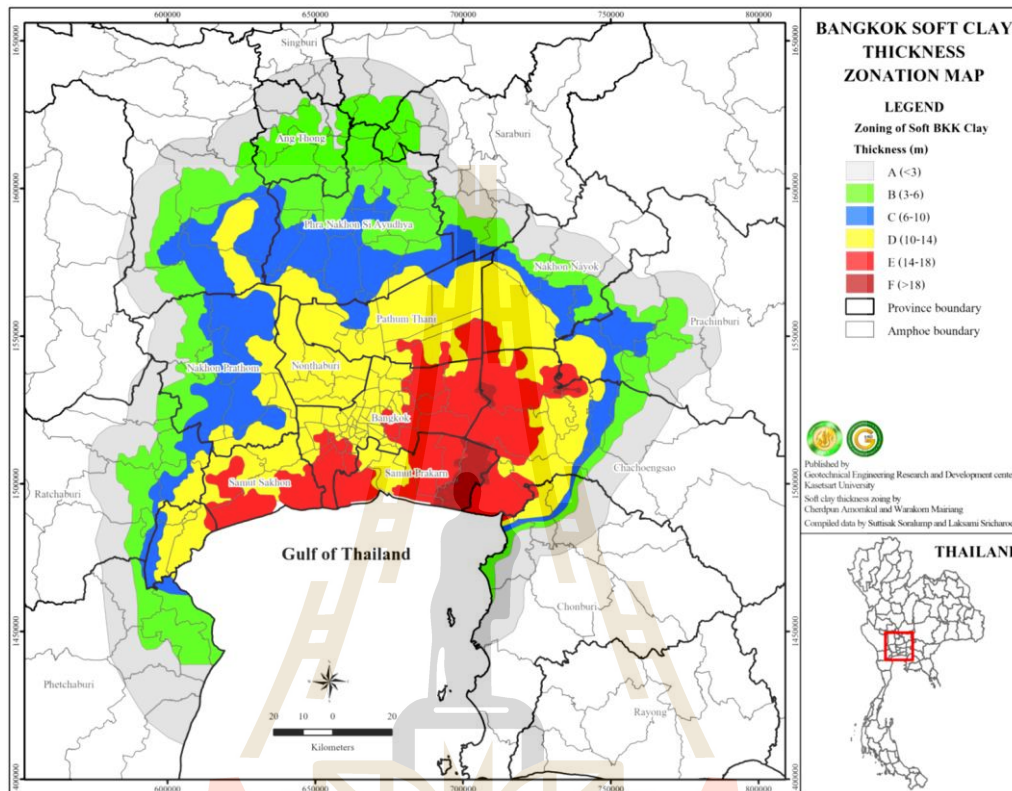


Figure 2.1 Area distribution and thickness of Bangkok soft clay (GERD, 2018).

Thailand has many highway construction projects on soft clay deposit. Stability issues arise when an embankment is too heavy for the soil beneath the foundation to support during road construction on this soft soil layer. Improvement methods may be implemented in several ways. In Thailand, popular methods are preloading with prefabricated vertical drains (PVD), geosynthetics reinforcement, pile, and soil-cement columns. Some may take a long time, and complex construction techniques with required specialized operators.

In the 18th and 19th centuries, the only basic materials used in the building were wood, stone, brick, mortar, iron, and steel. Later in the 20th century, lightweight materials such as aluminum, magnesium, beryllium, titanium, titanium-aluminide, plastics, ceramics, and composites containing polymers, metals, and ceramics were

developed. The transportation, electronics, chemicals, and ceramics industries are the top four industries in terms of manufacturing in the US. (Campbell, 2012). Another method for resolving construction issues on soft soils has emerged due to the evolution of material development. This method reduces the load on soft soils rather than enhancing the foundation soils' bearing capabilities. This idea focuses on replacing traditional soil and stone construction materials with lightweight materials to build pavement structures. The foundation soil is also subjected to less vertical pressure when using lightweight materials. Additionally, it lessens the lateral pressure put on bridge approaches or retaining walls. Lightweight materials generally have a unit weight of less than 10 kN/m^3 or slightly more.

2.2.1 Air Foam Mixed Stabilized Soil (AMS)

Japan has a concept for promoting soil utilization in construction. Therefore, research has been conducted to improve the properties of low-quality soils so that they can be used continuously. Until the 1990s, Japan successfully enhanced the soil quality into a lightweight material called Air Foam Mixed Stabilized Soil, which may also be called "Air Foam Mortar." This can be achieved by mixing soil, cement, water, and chemicals that cause foaming (foam agents) to form a lightweight material weighing $6\text{--}12 \text{ kN/m}^3$. Its compressive strength was in the range of $100\text{--}1,000 \text{ kPa}$, depending on the amount of cement or other cementing agent used. In addition, this technique can also be used on sandy soil (Chen & Wang, 2003; Jamnonpipatkul et al., 2009; Yang & Chen, 2016; Lim et al., 2017; She et al., 2018), such as embankment material and backfill material. AMS properties can be shown in Table 2.1. In a past study on AMS, Yajima et al. (1995) found that AMS with a cement mix ratio of 100 kN/m^3 had a compressive strength (q_u) between 105 and 247 MPa. Hayashi (2000) found that AMS with a cement mix ratio of 200 kN/m^3 had a compressive strength of 570 to 2,240 kPa, showing that the compressive strength was proportional to the amount of cement used. Moreover, the development of compressive strength depends on curing time, where the modulus of deformation (E_{50}) is about 150–300 times the compressive strength.

Table 2.1 Properties of Air Foam Mixed Stabilized Soil Improved with Cement
(Mori, 2005)

Properties	value
Unit Weight	6 – 12 kN/m ³
Compressive Strength	100 – 1,000 kN/m ²
Flowability	16 – 20 cm
Permeability	10x10 ⁻⁵ – 10x10 ⁻⁶ cm/sec.

Hayashi (2002) studied the relationship between void ratio and consolidation pressure (p) under the 1D consolidation test on AMS samples incubated for 28 days and found that the yield stress was $1.19 q_u$ ($p_c = 1.19 q_u$). This relationship was consistent with Tanaka and Terashi (1986)'s study ($p_c = 1.20-1.5q_u$). Hayashi et al. (2005) studied the relationship between the compressive strength and the California Bearing Ratio (CBR) of unsoaked and soaked AMS at 28 days of curing. Soaked and unsoaked had a significant relationship with uniaxial compressive strength.

Mori (2005) studied the settlement behavior of embankments built from AMS on soft soil layers constructed in Fukuoka, Japan. The AMS had a unit weight of 8 kN/m³, and its compressive strength at 28 days was 400 kN/m². After 13 months of construction, it was found that the subsidence of the embankment constructed from AMS was only 5–10 cm, while the embankment built from conventional material had a value of up to 123.5 cm.

2.2.2 Expanded Polystyrene Block (EPS)

Foam block, or Expanded Polystyrene Block, also known as Geofoam, was developed by the Norwegian Road Research Laboratory (NRRL). In the 1960s, it was used as a lightweight material for construction and began to be used in 1972 as a lightweight material in road works around the bridge sections connecting roads in many projects. The settlement was satisfactorily reduced by replacing the 1 m-thick soft soil layer. By 1985, EPS foam became widely known, and approximately 10 years later, it was widely used, with 50% of EPS foam usage occurring in construction projects in Japan (Miki, 1996; Giuliani, 2020). In addition, Hotta et al. (1996) reported the performance of EPS foam under the magnitude of the earthquake of 6.6 to 8.1 on the

Richter scale and found no damage to EPS Foam in construction embankments. In Thailand, EPS foam has been used to repair the bridge approach due to the settlement of the road connecting Intercity Motorway No. 7 and the Bangna-Trad Highway. It is 42 km southeast of Bangkok, which receives annual heavy traffic of about 9,300 vehicles per day (Malai et al., 2022).

Generally, EPS foam is 1 m wide, 2 m long, and 0.5 m thick. Its unit weight ranges from 0.1 to 0.3 kN/m³ (Miki, 2001). Its compressive strength ranges from 70 to 180 kPa, depending on the unit weight. The American Society for Testing and Materials (ASTM) defines the minimum physical properties of the materials listed in Table 2.2. Figure 2.2 shows the production process of EPS foam by softening the polystyrene resin by continuously heating it in the form of steam at 90–100°C and then adding a blowing agent, pentane gas (C₅H₁₂) for polystyrene plastic pellets to expand. After that, the inflated foam beads are kept in an airtight silo to allow the pentane inside to release both the internal pressure and the atmospheric pressure simultaneously. Only 2% of the volume comprises polystyrene; the remaining 98% is air. Then the foam beads are injected into the mold and compressed with a steam pressure of 100–110°C to melt and compact the foam. Figure 2.3 shows polystyrene and polystyrene expansion due to blowing agents and EPS foam from the production process.

Table 2.2 Physical Property of Geofoam according to ASTM D6817 (ASTM, 2017)

Property		EPS12	EPS15	EPS19	EPS22	EPS29	EPS39	EPS46
Density	pcf	0.70	0.90	1.15	1.35	1.80	2.40	2.85
	kg/m ³	11.2	14.4	18.4	21.6	28.8	38.4	45.7
Compressive Resistance at 1% deformation	Psi	2.2	3.6	5.8	7.3	10.9	15	18.6
	kPa	15	25	40	50	75	103	128
Compressive Resistance at 5% deformation	Psi	5.1	8.0	13.1	16.7	24.7	35.0	43.5
	kPa	35	55	90	115	170	241	300
Compressive Resistance at 10% deformation	Psi	5.8	10.2	16.0	19.6	29.0	40.0	50.0
	kPa	40	70	110	135	200	276	345
Elastic Modulus	Psi	220	360	580	730	1090	1500	1860
	kPa	1500	2500	4000	5000	7500	10300	12800
Flexural Strength	Psi	10.0	25.0	30.0	40.0	50.0	60.0	75.0
	kPa	69	172	207	276	345	414	517
Water Absorption by total immersion	Volume %	4.0	4.0	3.0	3.0	2.0	2.0	2.0
Oxygen Index	Volume %	24.0	24.0	24.0	24.0	24.0	24.0	24.0
Buoyancy Force	Pcf	61.7	61.5	61.3	61.1	60.6	60.0	59.5
	Kg/m ³	990	980	980	980	970	960	950

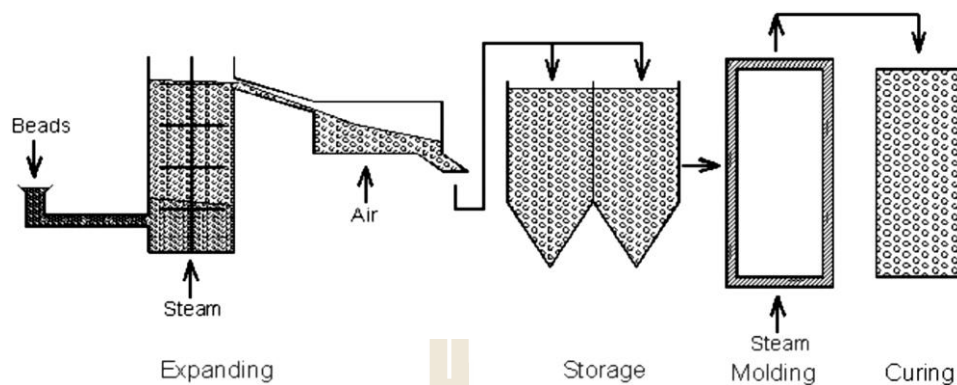


Figure 2.2 EPS-geofoam manufacturing process (Elragi 2000)

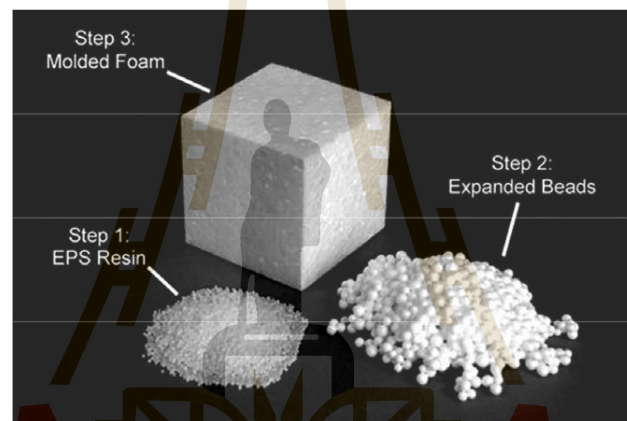


Figure 2.3 Three important forms of EPS (Hangzhou Fuyang Longwell Industry, 2018)

Choo et al. (2007) studied the use of EPS foam as a filling material over pipes and found that EPS could reduce lateral force by up to 90% and vertical force by 17–30%. Bartlett and Lingwall (2014) studied the protection of underground pipes and structures by using EPS foam to solve the problem of ground settlement, using soil as fill material four times. Sayadi et al. (2016) studied the effect of EPS particles on fire resistance, thermal conductivity, and the compressive strength of lightweight concrete foam (LWC). They found that foam concrete with a large amount of EPS had low thermal conductivity with high fire resistance and compressive strength. In addition, applying LWC helps reduce the load on the structure, thereby reducing the impact of earthquakes.

However, despite its lightweight nature, EPS foam can be used in various applications. But with a production process that requires pentane (C₅H₁₂) or, in some cases, butane (C₄H₁₀), which is the same gas group as LPG, as a blowing agent and has a highly complex production process, EPS production is hazardous without suitable precautions. When exposed to sunlight for an extended period, EPS blocks are easily burt and may shatter, not able to withstand some substances, including saturated aliphatic hydrocarbons, fuel water (hydrocarbon), oxidizing solid acids, fuming sulfuric acid organic solvents, etc. (Department of Rural Roads, 2009). If there is an accident on a road where EPS foam is used for construction and a vehicle fuel leakage occurs, there is a high chance that the road structure will be damaged. Therefore, the use of EPS foam for pavement construction is limited and must be used cautiously.

2.3 Polyurethane

A polyurethane-containing polymer (-NHCOOH) in a molecular chain was first found in the 1930s by Otto Bayer et al. It is sometimes referred to as polycarbonate (Komurlu & Kesimal, 2012, 2014). Polyols and diisocyanates with equal weights, functionally acceptable values, and additional substances containing reactive hydrogen atoms in the molecular structure make up the polyurethane structure. Figure 2.4 displays the overall chemical structure of polyurethane. Figure 2.5 depicts the reaction between the dioxide and the diisocyanate. Later, in the 1950s, they began to use more polyurethane by preparing polyurethane from toluene diisocyanate (TDI) and polyester polyol, which was used to make flexible foam and later invented to use polyether polyol instead. Polyester polyol, from which the invention of polyurethane came, has a wide range of properties and is widely used today (Walker & Rader, 1988; Pimpan, 2004; Ionescu, 2005).

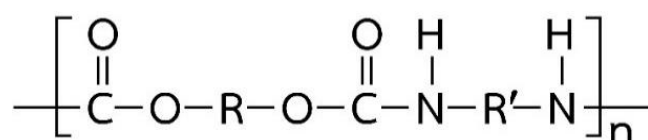


Figure 2.4 General structural characteristics of polyurethane (Herrington and Hock, 1997)

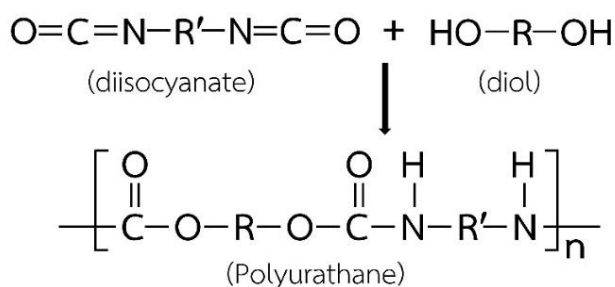


Figure 2.5 Polyurethane synthesis reaction (Ashida, 2005)

The general structure and differentiation of polyurethane species depend on the nature of the alkyl groups (R and R'). In addition, the alkyl group is the differentiating unit of each polyurethane. In addition, the structure of the alkyl group can be used as a trend indicator for polyurethane properties. Based on the general structure of the repeat unit, it can be divided into two segments: the soft segment (containing the diol group) and the hard segment (containing the diisocyanate group). As shown in Figure 2.6, polyurethane exhibits this behavior because the -C-O-C- in the diol portion is flexible, while the -NH-CO- from the diisocyanate has high stiffness. Then, in addition, the lower elastic bond angle also results in the formation of hydrogen bonds from the functional groups of this segment.

However, the two alkyl groups' chemical structures affect softness and hardness differently. However, more than two functional groups have been added. Then, as depicted in Fig. 2.7, thermoset polyurethane will be created. This plastic can be worked into a sticky solid and then softened until it resembles a sponge in texture. It can be employed in different applications, from fibers to artificial rubber to adhesives or coatings (Herrington & Hock, 1997; Ashida, 2005).

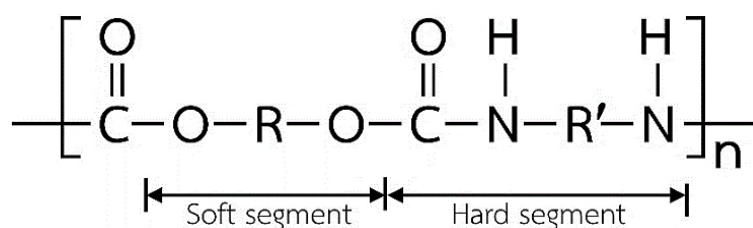


Figure 2.6 soft segment and hard segment in polyurethane chemical structure (Herrington and Hock, 1997).

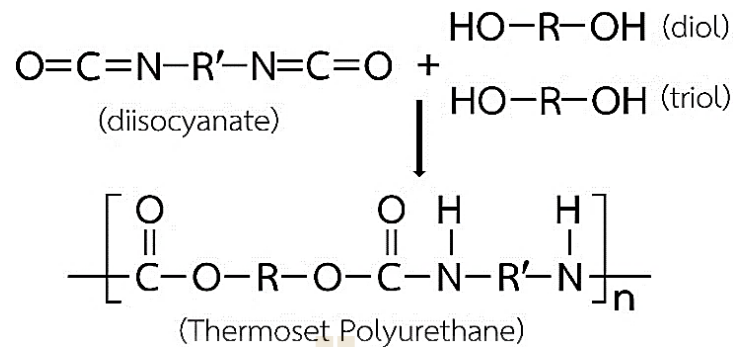


Figure 2.7 Thermoset polyurethane synthesis reaction (Ashida, 2005).

Polyurethane, often called PU, can achieve a wide range of properties due to the molecule's ratio between diol and diisocyanate. The high content of the diisocyanate groups gives polyurethane high strength, so polyurethane with such a structure can be said that, at high temperatures, it is a thermosetting plastic. At low temperatures, it is artificial thermosetting plastic with very high strength, chemical resistance, and abrasion resistance. Therefore, it is used in many applications, such as car seats, furniture, insulators, and heat and cool containers. Furthermore, as a component of ships to reduce weight, etc.,

In addition, polyurethane can be prepared as an elastomer, commonly used as solid tires, shoe soles, and oil-resistant rubber because it can withstand much friction, has good flexibility, and has good resistance to solvents and oils. PU foams can be classified into two main categories: flexible polyurethane foam and rigid polyurethane foam (in some cases, it can also be produced as a semi-rigid foam), with the properties shown in Table 2.3 (Herrington & Hock, 1997; Ashida, 2005; Szycher, 2013; Gama et al., 2018).

1) Flexible Polyurethane Foam

Flexible PU foam has a molecular structure. Its density ranges from 10–80 kg/m³. The foam has an open-cell structure. This allows air to flow easily through the structure. This flexible polyurethane foam has high tensile strength and resistance to many solvents. PU foam in a dry state can withstand heat up to 150 degrees Celsius. It is commonly used in the light industry, furniture, car seats, car headrest pillows, car steering wheels, car spoilers, various cushioning materials, etc.

2) Rigid Polyurethane Foam

Rigid PU foam has a large amount of reticular molecular structure. The cell is a closed cell type. The walls of the gas bubbles within the foam remain structured. Therefore, the movement of gas bubbles cannot occur. This type of foam has chemical properties similar to flexible PU foam. It has good heat-insulating properties and can also withstand the corrosion of oil and gasoline, with a foam density of more than 30 kg/m³. Rigid PU foam is mainly used as insulation (insulator) in refrigerators and the construction of cold storage walls. Hot and cold storage containers are also used as ship components to reduce ship weight and improve buoyancy.

Table 2.3 Classification of different types of polyurethane foam (Ashida, 2005).

polyol	Rigid foam	Semi-rigid foam	Flexible foam
OH No.	350-560	100-200	5.6-70
OH Equivalent No.	100-160	280-560	800-10,000
Functionally	3.0-8.0	3.0-3.5	2.0-3.1
Elastic Modulus at 23 °c			
MPa	>700	>70-700	<70
lb/in ²	>100,000	>10,000-100,00	<10,000

Chemicals or raw materials used in the production of PU foam can be classified into two main groups:

1) Polyol

Ninety percent of the polyols used in industrial production are polyether-type polyols, an essential raw material in polyurethane structures. There are three hydroxyl groups. Polyurethane products with unique properties can be produced by using polyester-based polyols. However, polyester is more expensive than polyether. Therefore, the selection of polyols must consider the size and flexibility of the structure. Quality function (functionality) is the amount of isocyanate and the number of hydroxyl groups per polyol and the degree of reticular formation in molecules. Functionality value controls the stiffness and flexibility of the polymer; the stable foam requires a rigid molecular structure, requiring a polyol with a high level of net structure.

Nevertheless, polyols with a low degree of mesh formation are required for flexible foams. Polyols have been developed that can completely react with isocyanate and produce polyurethane with good properties. Characteristics of polyols needed for the polyurethane production industry are summarized as shown in Table 2.4.

2) Isocyanate

The type of isocyanate can determine the physical and chemical properties of polyurethane. Two types of isocyanates are commonly used: toluene diisocyanate (TDI) and diphenylmethane diisocyanate (MDI). Approximately 90 percent of the isocyanate used in industry is MDI.

(1) Toluene Diisocyanate : TDI at room temperature is available in the liquid or crystalline state. It has a melting point of 22 degrees Celsius, reacts with water at temperatures above 50 degrees Celsius, and reacts violently with acid bases and alcohol, which poses a fire and explosion risk. Upon decomposition by combustion, the 2,4-toluenediamine is formed which is a dangerous substance for humans

(2) Diphenyl Methane Diisocyanate : MDI at room temperature has a solid-state melting point of 37°C. It reacts violently with acids, bases, and alcohols, making it vulnerable to fire and explosion. When decomposition occurs in combustion, hydrogen cyanide, nitrous vapors, and carbon monoxide are produced, which affect human health. Produced from precursors such as aniline and formaldehyde, the product is polymeric MDI, which is used in producing polyurethane foam. In addition, in the production process of polymeric MDI, purified MDI can be isolated and used as a base chemical for further improvement of properties.

The most common isomer in polyurethane foam production is a 4,4-diphenylmethane diisocyanate. Figure 2.8 and Table 2.5 show the molecular structure of polyurethane foam. Diphenylmethane diisocyanate and the physical and chemical properties of TDI and MDI, respectively.

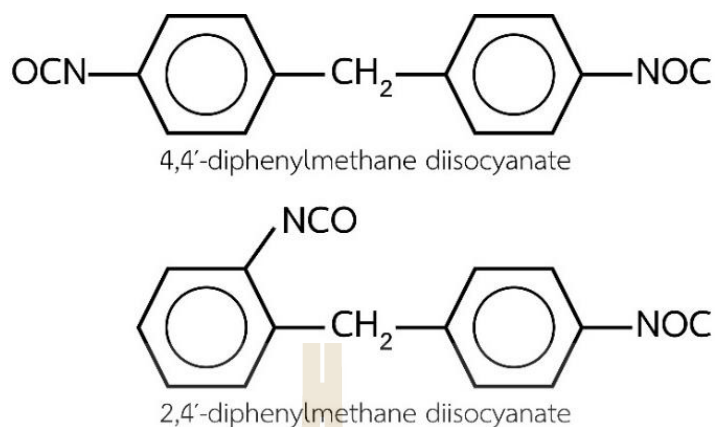


Figure 2.8 Molecular structure of diphenylmethane diisocyanate (Ashida, 2005).

Table 2.4 Polyol specification (Szycher, 2013).

Characteristic	Elastomer Foam and Flexible foam	Solid Foam and Rigid foam
Molecular Weight Range	1,000 to 6,500	100 to 1,200
Functionality	2 to 3	3 to 8
Hydroxyl Value Range	28 to 160	250 to 1,000

Table 2.5 Physical and chemical properties of TDI and MDI (Szycher, 2013).

Properties	TDI	MDI
State	liquid, crystalline	solid, sheet
Color	white to light yellow	white light yellow
Smell	fruity	no smell
Molecular Weight	174.16	250.3
Boiling Point, °C	251	314
Melting Point, °C	22	37
specific gravity	1.22	1.2

2.4 Polyurethane Synthesis Process

The polymerization is the process of creating substances with large molecules from substances with small molecules (monomers). Polymerization reactions will

occur under various conditions, such as catalysts, temperature, pressure, etc., resulting in different polymers. Both natural polymers and polymers synthesized by polymerization reactions can be classified into two types:

1) Addition polymerization : This reaction occurs with unsaturated monomers such as ethylene, propylene, acrylonitrile, and styrene, with the suitable catalyst and temperature to break the double bonds. Then neighboring molecules are bonded until larger molecules have longer polymer chains. The reaction continues until the monomer is gone. This type of reaction takes place in which the carbon double bond is lost without any loss of atoms, so no other byproducts are formed.

2) Condensation polymerization : This reaction takes place with a monomer with two functional groups on the left and right sides to condense with neighboring molecules on both sides and extend the chain length. Small molecules, such as H_2O , NH_3 , HCl , and CH_3OH , are removed from the reaction. Examples of polymers produced by this reaction are polyester, polyurethane, and polyamide.

2.4.1 Polyurethane Foam Synthesis Reaction

The idea behind the creation of PU foam is that when a prepolymer with a $N=C=O$ group at the end of the molecule is exposed to moisture (H_2O), it can react to create a material with the $N=C=O$ group. It produces urea ($-NH(C=O)OH$). The urea-bound polymer occurs simultaneously with the presence of air bubbles in the workpiece as it decomposes to carbon dioxide (CO_2). The prepolymer self-condensation from carbon dioxide gas breakdown occurs simultaneously with the carbon dioxide (CO_2) foaming process.

Therefore, these two reactions compete, with the condensation reaction yielding urea bonds. This can cause linking reactions next to the isocyanate group remaining at the end of the prepolymer, resulting in the polyurethane foam that hardens before carbon dioxide forces the polymer to break down until it cannot maintain its shape. The key to controlling the appearance of the foam that occurs as rigid foam (or flexible foam) will depend on the diol substrate structure used.

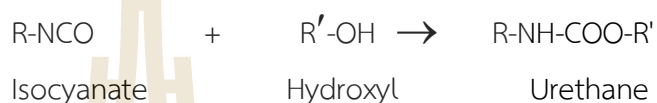
If using polyether polyol, it tends to have soft foam. In addition, if a prepolymer with a high isocyanate group content is used (e.g., one molecule contains more than two isocyanate groups), there will be a chance to obtain cross-bonds or

high levels of intermolecular linkage. In addition, the number of hydroxy groups in the polyol has the same effect. A polyol with large hydroxyl groups, such as a polyhydroxy polyol, will produce a solid foam.

2.4.2 Polymerization Reaction

2.4.2.1 The first (1st) reaction of an isocyanate is divided into three parts:

(1) Reaction of isocyanates with polyols



The reaction between diisocyanates and polyols is an exothermic polymerization. The polymerization rate depends on the molecular structure of isocyanates and polyols, especially aliphatic polyols with hydroxyl groups. Primary polyols reacted with isocyanates about ten times faster than polyols with secondary hydroxyl groups.

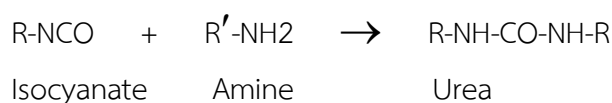
The reaction rate of phenol with isocyanate is prolonged and the resulting polyurethane will decompose back to the substrate quickly. When heated, this reverse reaction is called “blocked isocyanate”.

(2) Reaction of isocyanates with water



The reaction between diisocyanate and water yields the resulting product: Urea, and carbon dioxide, which are the immediate reactions of gas foaming in manufacturing flexible polyurethane foam. The initial product forms carbamic acid and breaks it into amines and carbon dioxide

(3) Reaction of isocyanates with amines



Diisocyanates react with primary and secondary amine compounds, especially diamines. The reactivity of amines increases with base activity, and aliphatic amines are more active than aromatic amines.

2.4.2.2 The Second (2nd) reaction of isocyanate

Under optimal conditions, isocyanates may react with hydrogen atoms. Biuret and allophanic bonds are formed in urea and urethane molecules, respectively. The urea group will develop more quickly and at lower temperatures than the urethane group.



2.5 Enhancement of Properties and Use of Polyurethane Foams

Although polyurethane foams (PUFs) have good properties, they can be used in various applications. However, PUFs must be improved and developed following current operating conditions, including mechanical properties, thermal insulation, and thermal stability. Reaction to fire and sound-absorbing properties, susceptibility to mold in wet environments, and electrical conductivity can be improved by using fillers in the mixture, thereby increasing the range of applications of conventional PUFs.

Beyond the building, construction, and automotive industries are radar absorbers, electromagnetic interference (EMI) suppression, oil absorbers, sensors, fire protection, shape memory or biomedical materials (Kausar, 2017).

2.5.1 Mechanical Properties

The mechanical properties of PUFs are often the first to be considered in deciding applications. When considering strength, PUFs are suitable for almost all applications, which can be customized to meet the purpose of use as appropriate. The use of different types of fillers and nano-fillers, such as cellulose and lignocellulose fibers (Silva et al., 2010; Otto et al., 2017), glass fibers, glass microspheres, or glass fibers (Yakushin et al., 2012; Ibrahim Marhoon & Kais Rasheed, 2015; Serban et al., 2016), eggshell waste (Zieleniewska et al., 2016), dates particles (Oushabi et al., 2017),

Walnut and Hazelnut Shells (Bryśkiewicz et al., 2016) and Esparto wool (Antunes et al., 2011) can be used to improve the structural and mechanical properties of PUFs. However, it will affect the thermal and electrical properties.

The use of carbon-based nanoparticle fillers, such as expanded graphite (EG), carbon nanotubes (CNTs), graphene, and carbon black, can be used to improve mechanical properties and reduce weight, power, and production costs (Kausar, 2018). Incorporating these particles into PUFs is known to enhance the mechanical efficiency of the particles (Athanasopoulos et al., 2012; Gama et al., 2017; Kim et al., 2017; Gama et al., 2018). However, the mechanical performance of these composite PUFs also depends on the amount used. Particle size and whether fillers are included in the cell wall

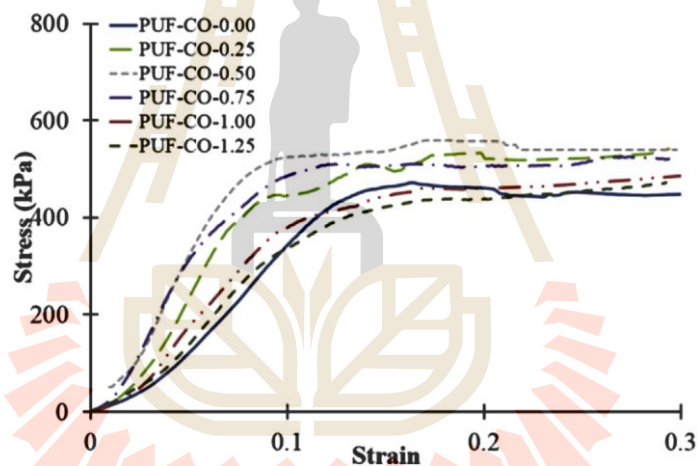


Figure 2.9 Compressive stress-strain curves of PUFs-EG foams (Gama et al., 2017).

Gama et al. (2017)'s findings on the physical characteristics of bio-PUF/EG composites revealed that there is no linear link between the increase in EG and the composite material's Young modulus (E), toughness, or compressive stress (10%). Figure 2.9, which depicts the relationship between stress and strain, demonstrates how decreasing the compressive strength by 0.75 Mpa while increasing the EG content is possible. This results from the foam's microstructure being altered by EG during the foaming process, as seen in Figure 2.10. The matrix fillers' alignment and the cross-linking density of the matrix polymer decreased.

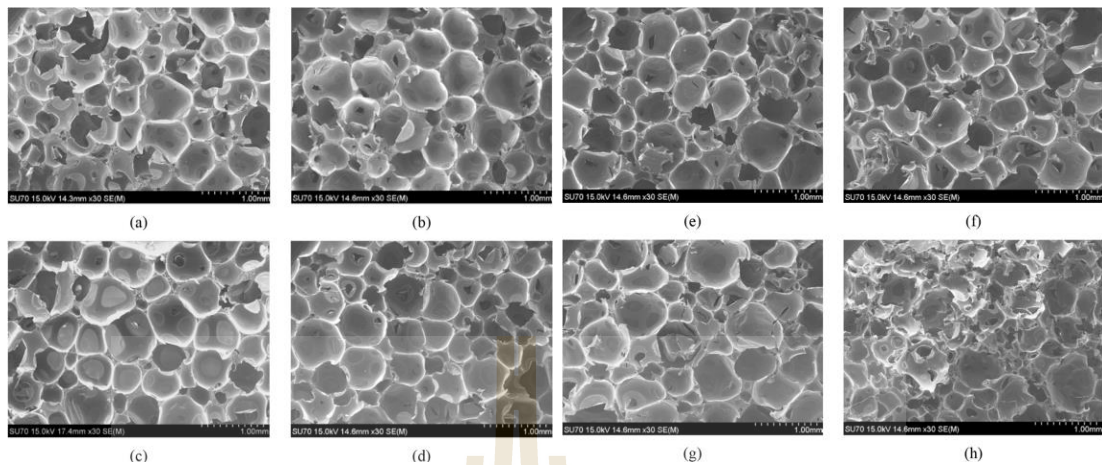


Figure 2.10 SEM images of PUF-EG-0.00 (a), PUF-EG-0.25 (b), PUF-EG-0.50 (c), PUF-EG-0.75 (d), PUF-EG-1.00 (e), PUF-EG-1.25 (f), PUF-EG-1.50 (g), PUF-EG-2.00 and (h), PUF-EG-2.50 (Gama et al., 2017).

2.5.2 Thermal Regulation

The insulating capacity of PUFs depends on the cell structure, with closed-cell foams having thermal insulation properties. At the same time, open-cell foam is ideal for acoustic insulation applications. Due to the different sizes of foam cell aggregation and morphological ridges, PUFs with an average cell size of less than 0.5 mm have a slight heat transfer capacity (Boetes, 1984; Diamant, 1986). Closed cells can trap heat and store it in the cell and are, therefore, often used in industrial refrigeration and sandwich panels for building walls (Lee & Ramesh, 2004). Hard and soft segments In PUFs, the thermal conductivity coefficient (or k) ranges from approximately 0.1–0.3 W.m⁻¹.K⁻¹ and 0.0146 W.m⁻¹.K⁻¹ (Clemitson, 2008; Thermal Conductivity of Common Materials and Gases, 2023). The heat transfer mechanism is caused by three parts: conduction, convection, and radiation (Cunningham & Hilyard, 1994), as shown in Equation 2.1 and Figure 2.11.

$$k = k_{\text{conduction}} + k_{\text{convection}} + k_{\text{radiation}} \quad (2.1)$$

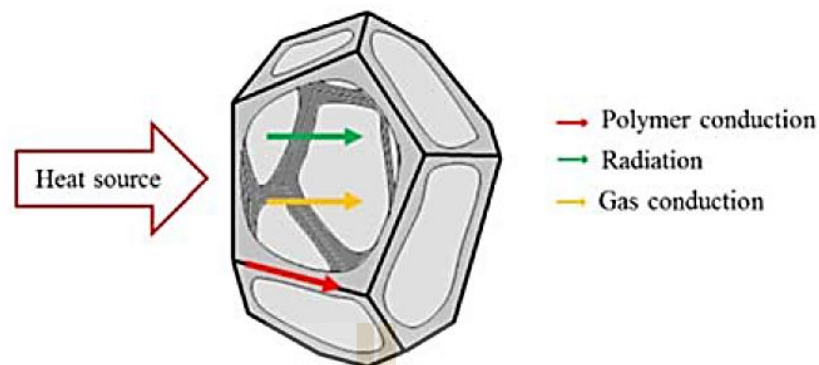


Figure 2.11 Mechanism of heat transfer of polymer foam (Jang et al., 2008).

However, properly managing the foaming process could enhance PUF's thermal insulation qualities. Additionally, the amount of heat gained or lost from or to the environment decreases, and energy savings are more effective if a heat-retaining substance is added to the PUF (Sarier & Onder, 2007; Sarier & Onder, 2008; You et al., 2008; Alkan et al., 2012; Rostamizadeh, 2012; Tinti et al., 2014; Yang, 2015). For instance, expanded graphite (EG) increases carbon-based materials' properties, such as corrosion resistance, flame retardancy, machinability, and cost competitiveness with metalloid fillers (Meng & Hu, 2008).

2.5.3 Reaction to Fire

Evaluation of the ability of materials to exhibit fire resistance behavior can be classified as either fire resistance, which refers to how well a material can maintain its properties when exposed to fire, or fire reactivity, which refers to the development and spread of fire. During a fire, PUFs produce toxic fumes, namely carbon monoxide (CO) and hydrogen cyanide. Inhaling these gases can cause serious health problems or even death (Chattopadhyay & Webster, 2009).

When a material ignites, heat is generated. One important parameter used to assess the reactivity of material further is the heat release rate (HRR), expressed in terms of the amount of heat generated per unit area and time, with the adequate heat of combustion being the ratio of the amount of heat generated per unit area and time. Released to the measured mass loss rate at a point and is related to volatile

gases generated during combustion (Chung, 2009; Qian et al., 2014; Zhou et al., 2018;). PUFs have been developed to resist continuous reactions to fire for safe use.

Wen-Hui Rao et al. (2018) studied the synthesis of novel polyester polyols from dimethyl methylphosphonate and diethanolamine via transesterification. Significant unit flammability was found to be used as a flame retardant in flexible PUFs. Renata Lubczak et al. (2018) studied the production of boron-containing PUFs using oligoetherol as a retarder. The results showed a high oxygen index (24.7%) and high heat resistance. In addition, these materials showed good mechanical resistance before and after annealing at 175 °C. Xu et al. (2018) studied the production of rigid PUFs using a nanostructured additive mixture (zinc oxide (ZnO), zeolite, and montmorillonite (MMT)) and phosphorus flame retardants (ammonium phosphate (APP) and dimethyl methyl phosphate (DMMP)). It was found that the thermal release rate (HRR) of PUF added with zeolite, DMMP, or APP was 91 kW.m⁻², which is lower than 56% of smooth foam and below 26% of foam filled with DMMP/APP.

Expanded graphite (EG) is widely used as a flame retardant in PUFs. When exposed to heat, EG forms low-density "worm"-like structures on the surface of PUFs that prevent heat transfer and oxygen consumption. It is a heat barrier and impedes the diffusion of oxygen. It prevents further material degradation, which provides good fireproof performance (Huang et al., 2017). The presence of EG can thus reduce the mass loss rate and increase the residual mass of PUFs after combustion. Moreover, this filler expansion causes the flame to suffocate, and the tiny carbon layer that forms there limits the heat and mass transfer from the polymer to the heat source. This expansion is caused by a redox process between H₂SO₄ (inside the graphite layer) and the gas-forming inner graphite surface. According to the reaction in Equation 2 (Modesti, 2002).



According to Lorenzetti et al. (2017) the HRR caused by the heat shield generated by the expansion of the EG due to the gas attributable to EG was reduced by the influence of the expansion volume and the interfering agent on the EG flame

retardant in PUFs. The combustible gas, produced by the redox reaction of EG, is diluted. In addition, due to its chemical and structural characteristics, breakdown, an endothermic process, absorbs the heat produced during burning. EG can decrease the EHC value, stop combustion, and release heat when the matrix breaks down into a gaseous product. According to Jarosinski et al. (2009) some of the byproducts produced by flame retardants are to blame for this. This could remove the radicals formed from the matrix and stop the original combustible components from igniting.

2.5.4 Sound Absorption Properties

In addition to excellent physical properties, PUFs have good sound absorption properties. It is often used in theaters, offices, sound studios, and many other applications due to the cavity, opening, or joints inherent in the structure (Diamant, 1986). When sound waves flow through the porous cells of the flexible foam, the friction between the airflow and the cell wall converts sound energy into thermal energy (Najib et al., 2011; Del Rey et al., 2012; Zhang et al., 2012). Determine the energy absorbed when a sound wave strikes a material in terms of the ratio of the sound absorbed (W_{abs}) to the sound incident (W_{inc}) (Kleiner & Tichy, 2004; Jahani et al., 2014).

The effectiveness of sound absorbers is also a result of a balance between the reflection of a small amount of sound and a large amount of sound dispersion. Foams with open and closed cell structures have different sound absorption mechanisms. The open-cell foam acts as a porous absorbent. In closed-cell foam, it acts as a membrane absorber. In addition, in rigid polyurethane foam, the sound-absorbing behavior is related to the mechanical properties of the pore structure (Li & Crocker, 2006; Benkreira et al., 2011; Del Rey et al., 2012; Jahani et al., 2014;).

Producing PUFs with sound-absorbing performance can be achieved by adding certain materials to alter the cell structure; for example, studies have identified the possibility of using liquid coffee grounds and CG-derived foam as sound-absorbing materials. Tiuc et al. (2016) and Gama et al. (2017) studied improving the sound-absorbing properties of rigid PU foam by incorporating textile waste. The homogeneity of the material is challenging to achieve. The influence of mechanical properties on the cell structure on the sound absorption coefficient was not discussed. The role of

fillers is essential for good absorption properties. Moreover, it does not have to be a PU network. Celebi and Kucuk (2012) used leaf fibers to prepare rigid and flexible foams. Although this filler significantly impacts the sound-absorbing properties of flexible foams, it has little effect in the case of solid PUFs.

2.5.5 Other Properties and Applications

In addition to using PUFs as insulators for sound absorption or as lightweight parts such as building walls, the properties of PUFs in biological applications were also improved. Because the material is biocompatible and has biological stability and mechanical properties, PUFs can be used in biomedical applications. For example, composite breast implants covered with polyester and rigid PUFs are used for bone fixation. The elastomeric material used in cardiovascular applications is used as a central venous catheter. Vascular grafts, heart valves, breast prostheses, eyeball transplants, or drug delivery systems (Johnson, 1977; Motokucho et al., 2018) However, for biomedical applications, the material must have excellent biocompatibility.

Johnson (1977) and Davim (2012) have reported that the biostability of polyester-based PU is unstable in water and an oxygen environment; even polyether-based PU is unstable in vivo but can improve its stability. Biodegradation of PU by using polysiloxane and polyolefins. In addition, the surface modification of PUs by adding nanoparticles such as graphene, graphene oxide (GO), and carbon nanotubes (CNTs) enables PUs to be widely used in biomedical applications such as structures in soft tissue engineering. Bio-fluid adsorption or bio-catalytic air filters with high pH resistance, solvent resistance, or high temperature (Sivak et al., 2009; Singhal, 2013; Kausar, 2017; Alves et al., 2022).

PUFs are also used in electrical engineering as conductive or insulating materials (Apyari et al., 2012; Mittal, 2014). Argin and Karady (2008) studied the dielectric strength of broken foams. Using three different AC voltages and lightning impulses under different humidity and temperature conditions, PUFs were found to have two- to three-times better dielectric strength than air. Conductivity in electronic devices such as communications, computing, or automation has increased. Electromagnetic interferences (EMI) lead to pollution; to reduce this pollution,

composite PUFs proved to be one of the best options for EMI shielding (Khatoun & Ahmad, 2017).

Kim et al. (2017) studied electrical conductivity and shielding performance. Electromagnetic interferences (EMI) of a solid PUF containing nickel-coated carbon fiber (3.0 php) The composite material has been found to have higher conductivity and electromagnetic interference shielding performance for improved electrical properties. Efficient fillers such as carbon nanotubes (CNTs) may be used to produce PUFs. Jatin Sethi et al. studied the effect of the morphology of multi-walled CNTs on the electrical and mechanical properties of PU nanocomposites. They found that longer carbon nanotubes conduct electricity better, and this conductivity depends on length and aspect ratio (Kim et al., 2017). Moreover, graphene was the most efficient filler to enhance the electrical and thermal conductivity of PUF composites. Xinzhao et al. (2018) reported that high electrical conductivity is due to graphene-induced 3D networks on the inner surface of PUFs. Graphene oxide (GO) is known to be used in applications like graphene "EMI" (Xinzhao et al., 2018; Sawai et al., 2018).

2.6 Mechanicals Behavior of polyurethane foam

There are several mechanical properties of foam materials. Determining the importance of a treasure depends on its intended use. However, the outstanding property of this material is its load-bearing capacity, which is the most critical parameter as it is necessary for its design. This section reviews past research findings on the behavior of PUFs.

Walter et al. (2005) studied the behavior of polymeric foams under compression and tension. They found that the stress-strain response of porous polymeric materials under compression had three distinct zones. It is the I elastic region, ii plateau region, and iii densification region, as shown in Figure 2.12. The densification region is subject to cell foam structure failure. Under compression, the total compressive strain of these three regions maybe 40-80. % and, in the case of tensile strength, may not occur at 10% (Throne, 1982; Gibson & Ashby, 1999), as shown in Figure 2.13. The material deforms under compression more than under

tension, indicating that polymeric foams are more susceptible to damage under compression than under tension.

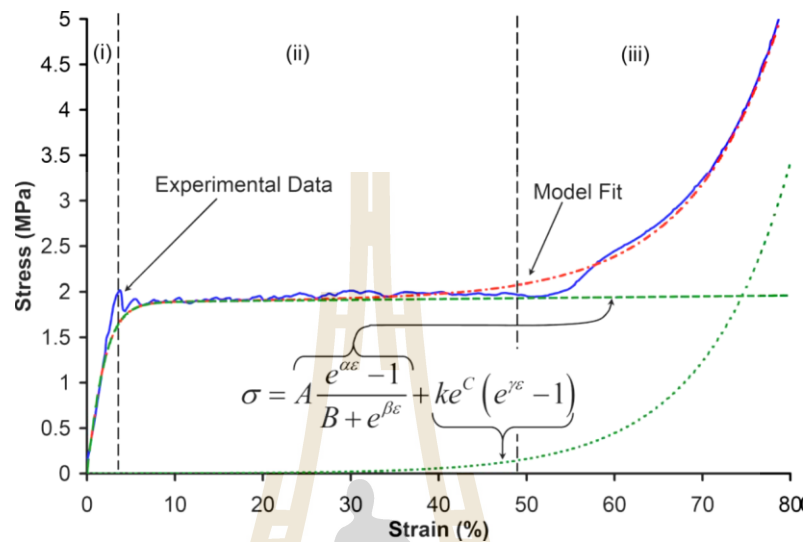


Figure 2.12 Typical compressive stress-strain response of a polymer foam (Subhash et al., 2005).

Additionally, it was discovered that, when subjected to the same load, the material deformed more in compression than in tension. This result supports Kraatz et al. (2006) who used a CCD camera to record size changes during the test to study polymeric foams' behavior under long-term tension and compression. It was discovered that the stress under compression is higher than that under tension for the same amount of stress. The results confirmed that polymeric foams are easily damaged under compression.

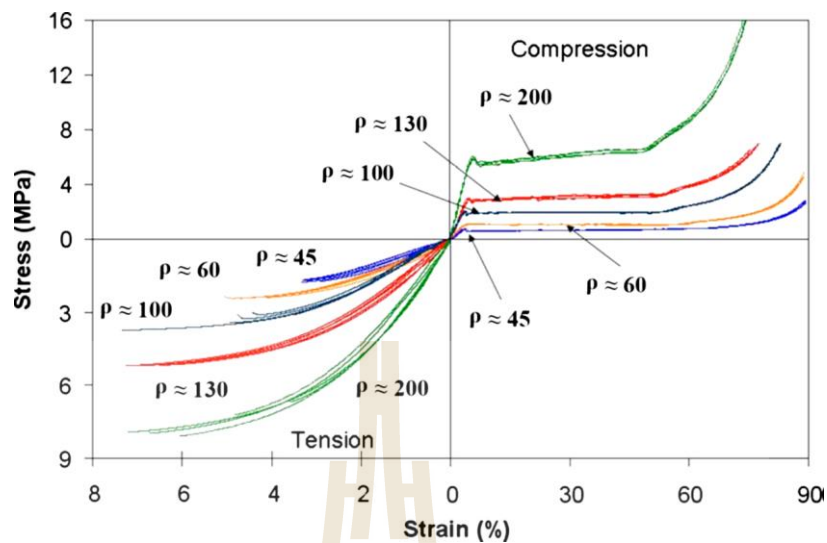


Figure 2.13 Tensile and compressive responses of foam specimens of different densities (Subhash et al., 2005).

Miyase et al. (2016) investigated variations in foam density and cell rise ratio in polymeric foams. Foam density was linearly correlated with stiffness and strength. It was determined that the foam's density impacted its strength when compressed. Additionally, it was shown that the failure of foam cells was caused by cell bulking and the development of shear stress throughout the test sample's cross-sectional surface. Improving a foam's internal microstructure and mechanism is precious to enhance its mechanical qualities.

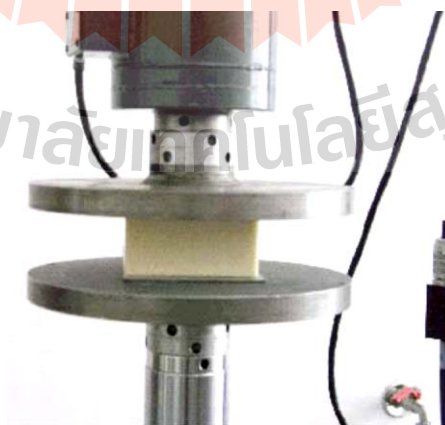


Figure 2.14 Equipment used in compression tests of foams (Witkiewicz and Zieliński, 2006).

Witkiewicz and Zielinski (2006) studied the compressive, tensile, and shear strengths of PU foam with two different densities (16 kg/m^3 and 62 kg/m^3) on MTS 810.12 No. 1012 as shown in Figure 2.14. The force-to-deformation relationship was recorded by computer and processed using the ExMTS software developed by the Naval Design and Research Center. Figure 2.15 shows the compressive strength test results of PU foams of different densities.

Compression test results show that foam with 16 kg/m^3 has lower compressive, tensile, and shear strengths than foam with 62 kg/m^3 . Water absorption and buoyancy reduction are present. At high levels, which indicates a large number of open pores. At the same time, the foam with a density of 62 kg/m^3 has mechanical properties consistent with the reference data for PU foam type EW 045-45-20-K polyurethane foam, which is an anisotropic material. The strength properties of the foam will increase as it moves upward. Especially for compressive and tensile resilient modules, where the internal structure results in compressive strength, tensile strength, and shear strength, PU foam with a density of 62 kg/m^3 is suitable for use in construction lightweight pram for shallow water.

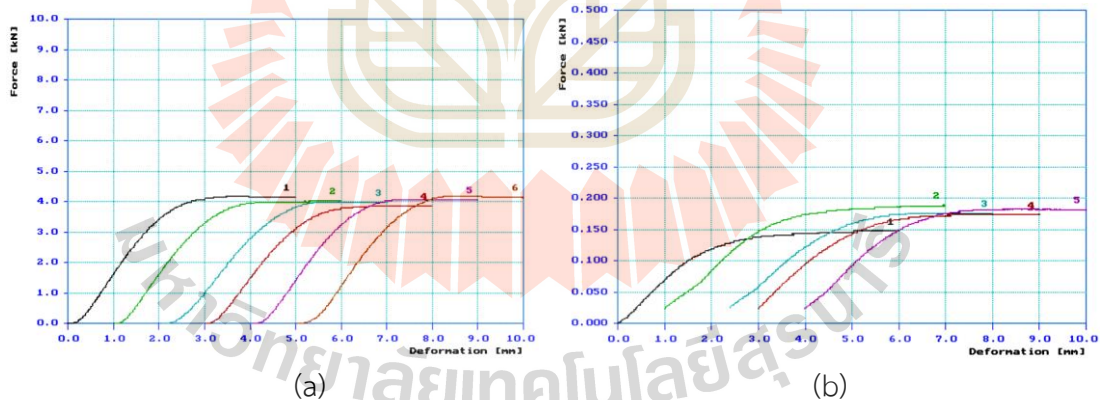


Figure 2.15 Results of compression tests of the polyurethane foam (a) 16 kg/m^3 and (b) 62 kg/m^3 (Witkiewicz and Zielinski, 2006).

This is consistent with a study by Stirna et al. (2011) that tested the tensile and compressive strength of PU foam with a density of $65\text{--}70\text{ kg/m}^3$. It was found that the compressive and tensile strengths increased as the density of PU foam increased. In

some cases, PU foam is used as a shock-absorbing material for packaging applications to protect the product from damage during transportation. Density is an essential factor affecting rigid polyurethane foam's mechanical properties and behavior under dynamic compression. The modulus, yield stress, and plateau stress increase with density. It can be said that these values are a function of foam density. Lung et al., 60–250 kg/m³. Under compressive strength, the peak stress and plateau stress properties were found to depend on the density and the rate of failure of this material due to the buckling of cell walls. The strain rate relationship for each foam density is expressed as a power equation.

Poapongsakorn and Kanchanomai (2011) studied the effects of time on tensile behavior, fracture strength, and fatigue crack propagation. Tensile creep tests were also performed on PVC foams of densities 113 and 176 kg/m³ (H130 and H200). The microstructure is shown in Figure 2.16. The tensile test was performed using a servo-hydraulic testing machine. The strain rate during the test was 10^{-5} – 10^{-1} s⁻¹ (load rate 0.1–1000 mm/min), and the strain rate was 10^{-5} s⁻¹, indicating a low strain rate application (such as pressure vessels), while a strain rate of 10^{-1} s⁻¹ indicates a high strain rate application (such as the structure of an airplane's wing.). The results shown in Figure 2.17 shows the relationship between stress and real strain in H130 foam at various strain rates.

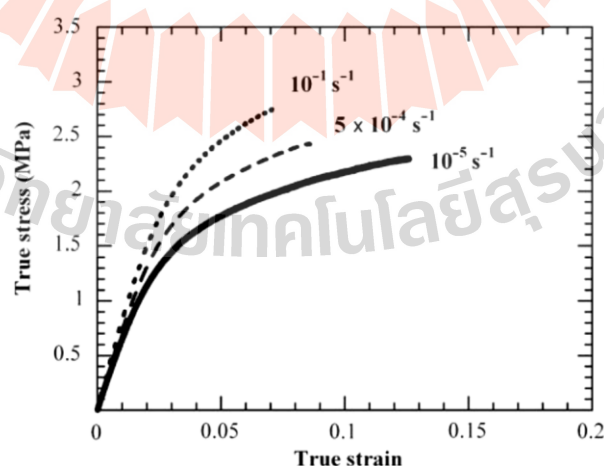


Figure 2.16 True stress–strain curves of H130 foam at various strain rates (Poapongsakorn & Kanchanomai, 2011).

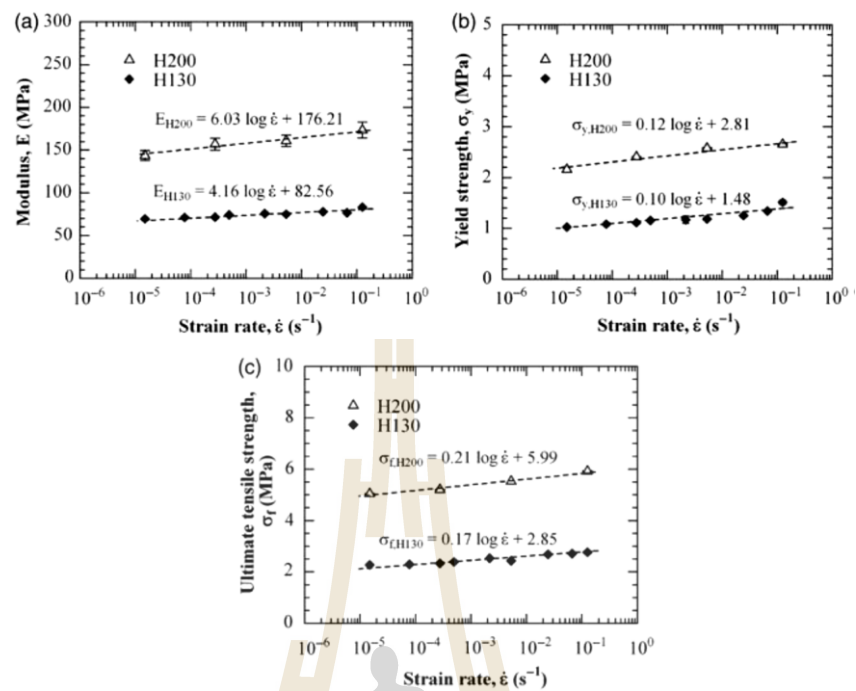


Figure 2.17 (a) Moduli, (b) yield strengths, and (c) ultimate tensile strengths of H130 and H200 foams at various strain rates (Poapongsakorn & Kanchanomai, 2011).

The effect of strain rate on the deformation of PVC foam can be observed. In other words, an increase in strain rate leads to an increase in strain and a decrease in strain with a ratio between true stress and true strain at small deformations (<0.1 y). The moduli of H130 and H200 foams at various strain rates are shown in Figure 2.17(a) while yielding. (obtained from the offset method, 0.2%), Furthermore, Figures 2.17 (b) and (c) show the maximum tensile stress at various strain rates.

For both H130 and H200 foams, similar behavior was observed for the modulus. Yield strength and tensile stress, i.e., they increase with strain rate; on the other hand, fracture strain decreases with increasing strain rate. In addition, the study's results showed that at room temperature, PVC foam exhibited time-dependent behavior, i.e., creep and/or stress. When considering the mechanical properties of PVC foam, the loading rate must always be considered.

Mane et al. (2017) used uniaxial planar compression testing at quasi-static, static, and dynamic strain rates to investigate the responsiveness and deformation effect of PU foam. With the help of UTM and the Drop Weight Tower (DWT), the performance under quasi-static testing was assessed for PU samples. It is a high-density polyurethane foam composite material with dimensions of 50 mm x 50 mm x 50 mm and a density of 288 kg/m³. Figure 2.18 shows the study's findings. Polyurethane foam's plateau stress and density strain under dynamic loading (80 s⁻¹) were discovered to be larger than in the quasi-static loading situation. (0.0033 s⁻¹).

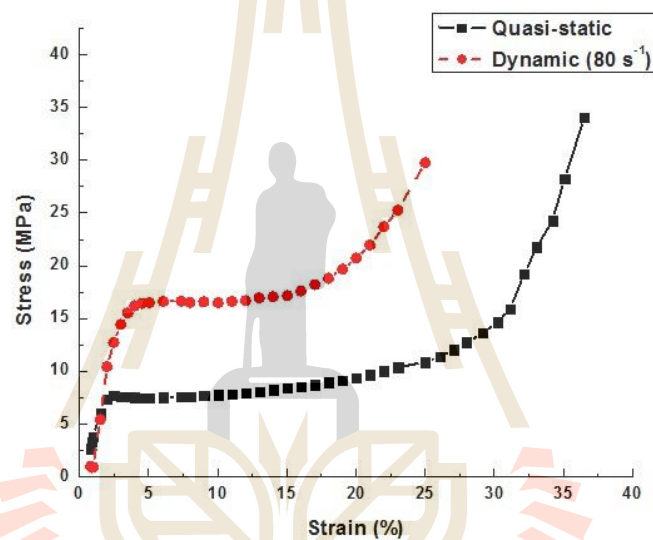


Figure 2.18 A comparison of stress- strain curves for rigid polyurethane foam subjected to quasi-static and dynamic compression (Mane et al., 2017).

When increasing the strain rate under dynamic loading, it was found that the mechanical behavior of the foam was affected by the strain rate, as shown in Figure 2.19 and plateaued with longer spans and higher densification. This resulted in a higher strain compared to the dynamically obtained behavior. Locking occurred at about 44% strain in the deformed quasi-static foam, while at 20%, 18%, and 14% lower strain for the deformed quasi-static foam at the transformed 80 s⁻¹, 120 s⁻¹, and 160 s⁻¹, respectively. Although the curve characteristics were similar in both cases, lockup behavior in the loading case was observed. Dynamic action (at a stress of 33%) occurs

at a lower stress than the stress at the point of cell wall collapse (lockup) in the case of quasi-static loading (at 44% strain).

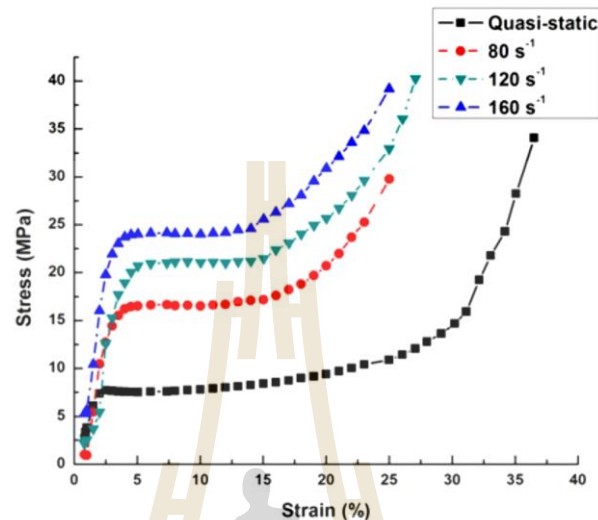


Figure 2.19 Dynamic response of polyurethane foam subjected to different strain rates (Mane et al., 2017).

The results also showed significant changes in mechanical properties, and densification occurred at low loading rates under quasi-static loading. In addition, energy absorption depends on the stress value, length of the compression period, and strain rate, which means that PU foam exhibits different mechanical response behaviors depending on the direction of force action (rise direction and transverse direction), strain rate, and temperature during the test.

Saha et al. (2009) studied the behavior of quasi-static rigid PU foam with two densities of 240 and 320 kg/m³ (PUR240 and PUR320) with microstructure as shown in Fig. 2.20. Under pressure at strain rates of 0.001 s⁻¹, 0.01 s⁻¹, and 0.1 s⁻¹, the peak stress and energy were found to depend on density, foam structure, and strain rate. In addition, the relationship between maximum stress and density is a power equation constant at each loading rate. The structure shows that spherical polyurethane foam (PUR) was completely damaged at 1600 s⁻¹. Figures 2.21 (a) and (b) show the relationship between strain rate and peak stress and strain rate and absorbed energy, respectively.

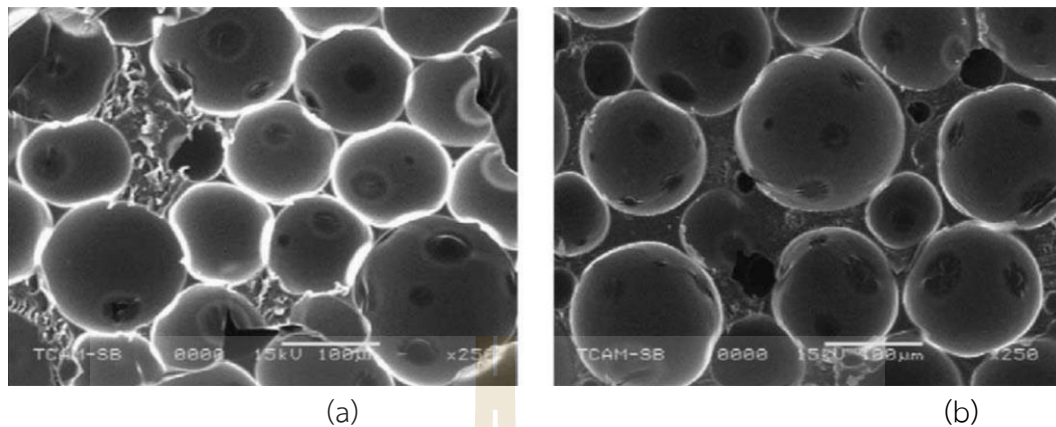


Figure 2.20 SEM micrographs of PUR foams with different density: (a) PUR240 and (b) PUR320 (Saha et al., 2009).

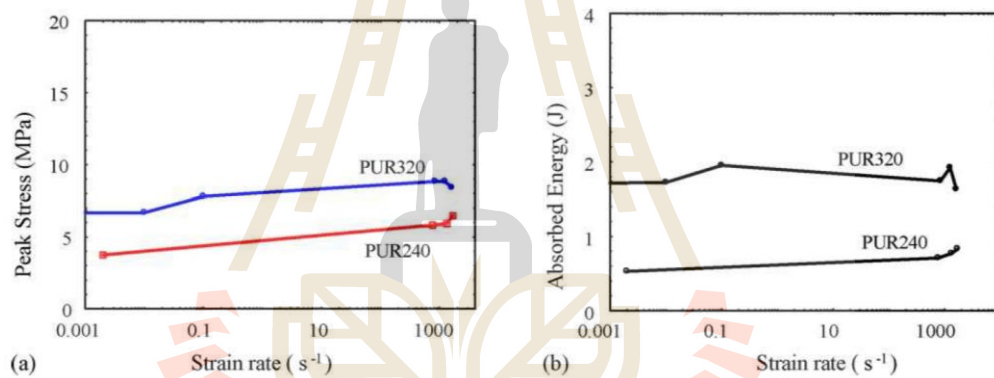


Figure 2.21 Relationship between strain rate and peak stress and absorbed energy of PUR with different densities (Saha et al., 2009).

Zenkert and Burman (2007) studied the fatigue behavior of closed-cell foams under tensile, compressive, and shear stresses with testing frequencies of 5 Hz (tension and compression) and 2 Hz (shear). The foam used in the study is a high-performance closed-cell rigid polymer, Rohacell WF grade. The cell structure of this foam is shown in Figure 2.22. Rohacell is a predominantly closed-cell polymetacrylimide (PMI) foam, which is relatively brittle and tensile with a yield stress of approximately 2–3%. Three different densities were used for the test: WF51, WF110, and WF200, with 52, 110, and 205 kg/m³, respectively; the test results are shown in Figure 2.23. It was found that shear fatigue was similar to that of compression, with compression fatigue being lower

than tensile stress due to how the cell bends during compression. However, if the density is increased, the results will be different. For WF110, the correlation between stress (S) and the number of cycles (N) for compression is higher than SN for both loads in the case of shear and tensile.

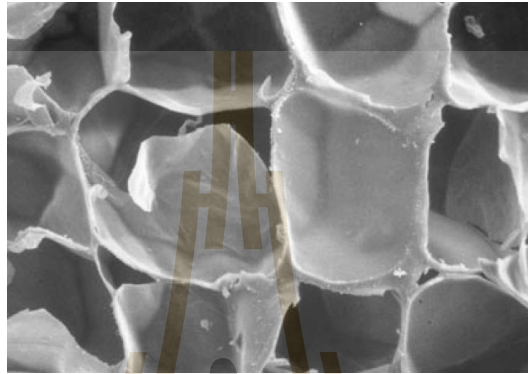


Figure 2.22 Cell structure of WF51. (Reprinted with permission of Röhm GmbH) (Zenkert & Burman, 2007)

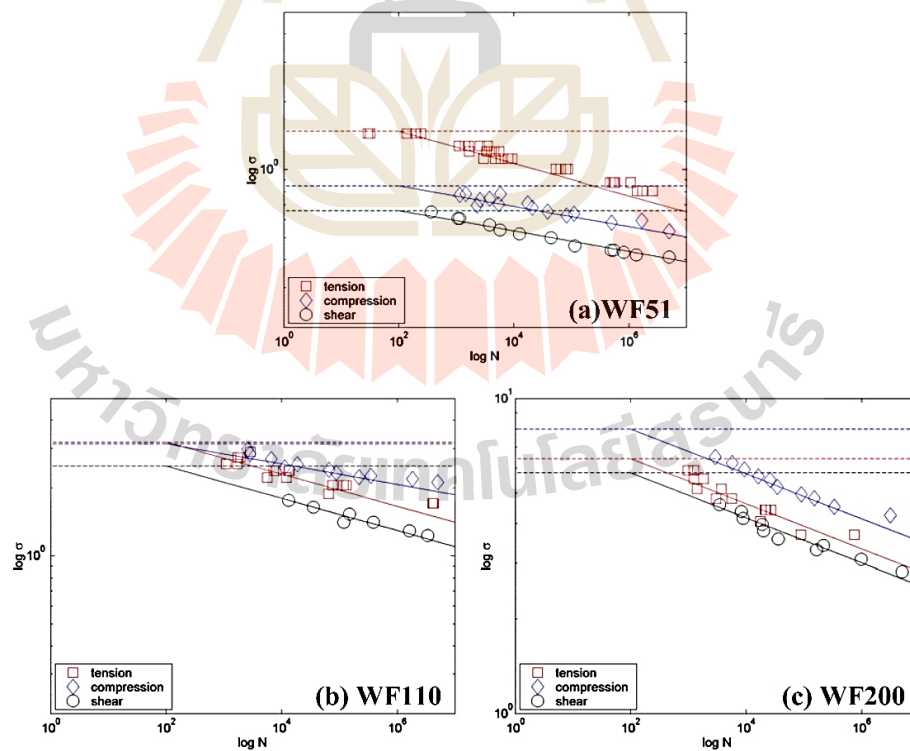


Figure 2.23 Fatigue stress-life diagrams for (a) WF51, (b) WF110 and (c) WF200 (Zenkert & Burman, 2007).

2.7 Microstructural Analysis Techniques

Microstructural and mechanical characteristics control the mechanical properties of materials. Miyase et al. (2016) studied the microstructure and chemical composition, and therefore it is necessary to study the mechanical response behavior of materials. Here are the tools used to analyze this study's microstructure and chemical composition.

2.7.1 Scanning electron microscopy (SEM)

There are two types of microscopes: optical microscopy (OM) and scanning electron microscopy (SEM), with their respective magnification ranges. 400–1,000 and 300,000 times the original size, respectively. Duxson et al. (2006) stated that scanning electron microscopy (SEM) allows the viewing products from millimeters to micrometers, providing clear microstructure information for crystalline and amorphous materials. It can explain mechanical behavior that other techniques may not detect.



Figure 2.24 Scanning Electron Microscopy (SEM) Device
(Thermo Fisher Scientific Inc, 2023).

Figure 2.24 shows a scanning electron microscope (SEM) based on the principle of scattering electrons onto the sample surface by a high-energy electron beam emitted from an electron beam gun when such electrons hit the surface. Tasks

containing atoms emit signals that can be processed and provide information on the object's surface, composition, and other properties, such as electrical conductivity.

The components of SEM can be seen in Figure 2.25, which consists of the topmost part, which is a source of electrons called electrons. The electron gun from the source is accelerated down the vacuum column. Accelerating voltage in the range of 0–30 kV (some machines up to 50 kV) with the direction of movement is controlled by electromagnetics; two or more lenses are used, and the amount of electrons is controlled by different apertures (Goldstein et al., 2003; Zhang & Ulerý, 2018).

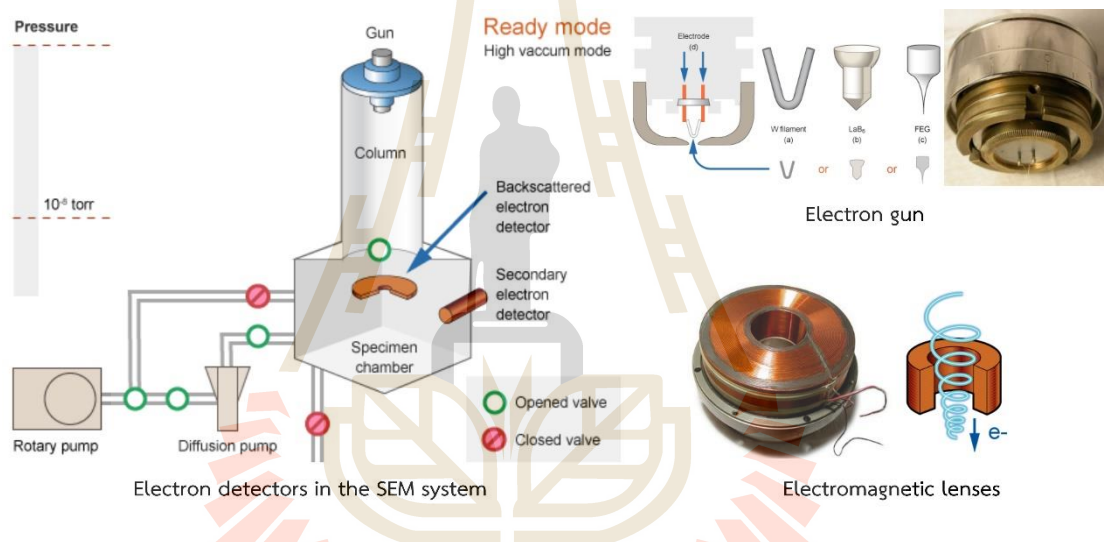


Figure 2.25 Components of Scanning Electron Microscopy (SEM) (Australian Microscopy and Microanalysis Research Facility, 2023)

2.7.2 Energy Dispersive X-Ray Spectroscopy (EDS)

Energy-Dispersive X-ray Spectroscopy (EDS) is an analysis of chemical composition by energy-dispersive X-ray spectrometry used in conjunction with scanning electron microscopy. It comes from a penetrating gun and interacts with the subsurface volume of the sample (Mohammed & Abdullah, 2018). The analysis sample splits when the electron beam strikes it. To produce ionization, the sample's electrons must be pushed away from the atoms to keep them stable. The electrons in the subsequent orbital layer will take their place and release energy in the form of

characteristic X-rays, which are X-rays with a characteristic frequency. (X-ray) When this form of X-ray reaches silicon drift detectors (SSD), as shown in Figure 2.26, the energy is particular to the element type.

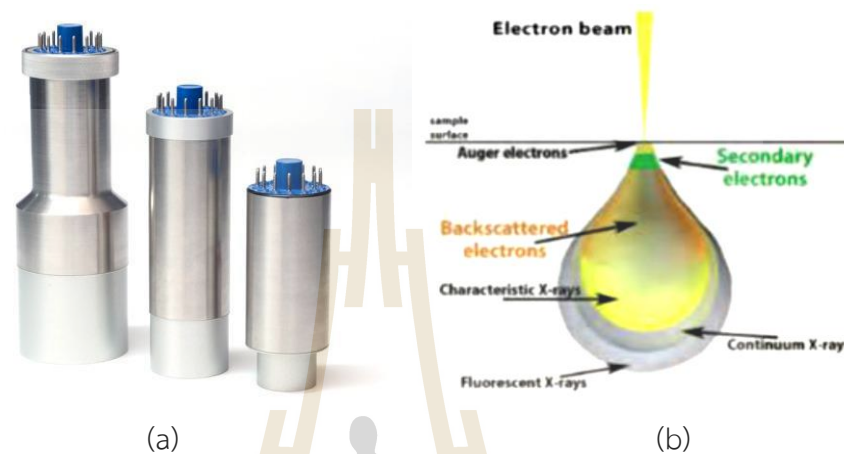


Figure 2.26 EDS Device and Mechanism (a) Scintillator detector for both secondary and backscattered electrons (b) Different penetration level of electron through the sample (A Caen group company, 2023; Zhang and Uler, 2018)

The probe generates an electrical signal directly proportional to the energy of the incident radiation. It will analyze the signal for its height and send it to the computer system to evaluate and report the spectral value of further X-rays (Goldstein et al., 1992, 2003). The advantage of using EDS is that it can perform qualitative analysis quickly and detect many elements simultaneously. The sample object has lost its original state and can be used with sample objects in a solid state.

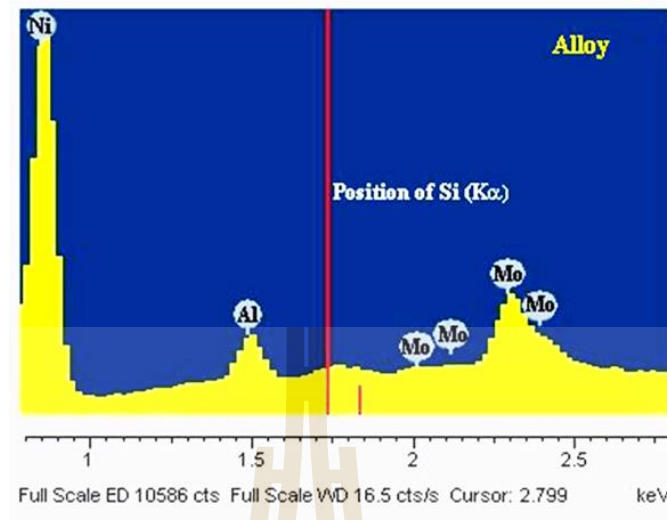


Figure 2.27 Results of chemical composition analysis by EDS technique
(Integrating Research and Education, 2016)

Rachan (2009) states that elemental analysis can be tested with scanning electron microscopy tests by installing an optional accessory called an analytical electron microscope. Elemental analysis is spot analysis. Spot Electron Probe Microanalysis (EPMA) uses elemental analysis using characteristic X-ray measurements, which are both Wavelength Dispersive X-Ray Spectrophotometry (WDS) and Energy Dispersive X-Ray Spectrophotometry. Tometry (Energy Dispersive X-Ray Spectrophotometry, EDS) The difference between the above elemental analyses is different. The radiation separation principle for the energy order measured by the electron detector can be obtained from Figure 2.27. Demonstrates an example of the results of the analysis of elemental content in metal alloys by EDS technique.

Alves et al. (2022) studied the microstructures of polyurethane composites containing vermiculite clay at ratios of 0%, 5%, 10%, 15%, and 20% for use. It is a material for vertical flame retardants. Scanning electron microscopy (SEM/EDS) analysis techniques were used to observe the microstructures under the vertical combustion test principle. Figure 2.28 presents an analysis showing that clay addition controls the particle size of the polyurethane foam and gives the structure a spherical structure with relatively uniformly distributed closed cells. Figure 2.29 shows the results of the chemical composition analysis by EDS. It was found that the

composition of the PU/VMT non-clay composites in the PU foam substrate presented typical constituents such as carbon (53.3%), oxygen (20.4%), and gold (26.3%), which come from the device sample holder. Other composite materials containing boron, aluminum, silicon, and magnesium are formed by the decomposition of aluminosilicate clays containing many chemical elements by Containing residual chlorine and bromine in 5% PU/VMT and 10% PU/VMT, respectively.

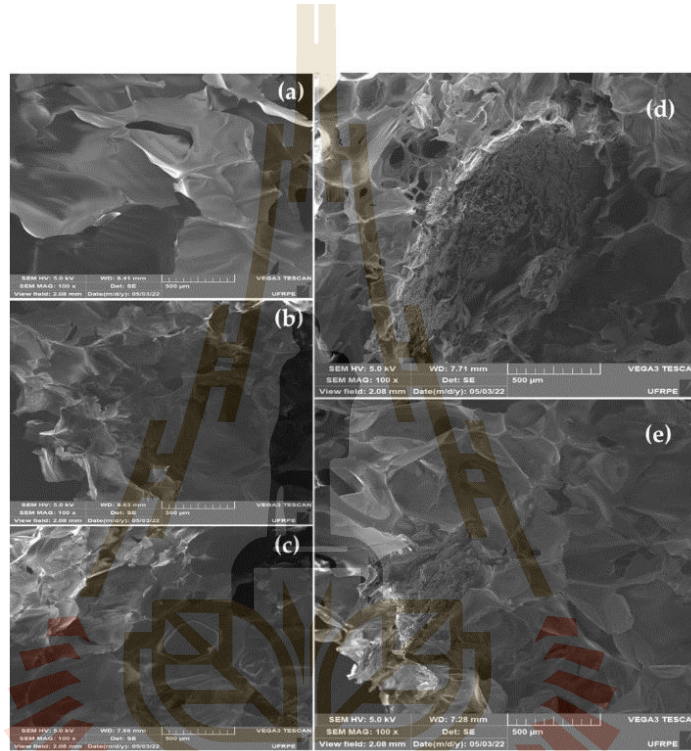


Figure 2.28 SEM micrographs of the composites PU/VMT: (a) 0%, (b) 5%, (c) 10%, (d) 15%, and (e) 20% (Alves et al., 2022).

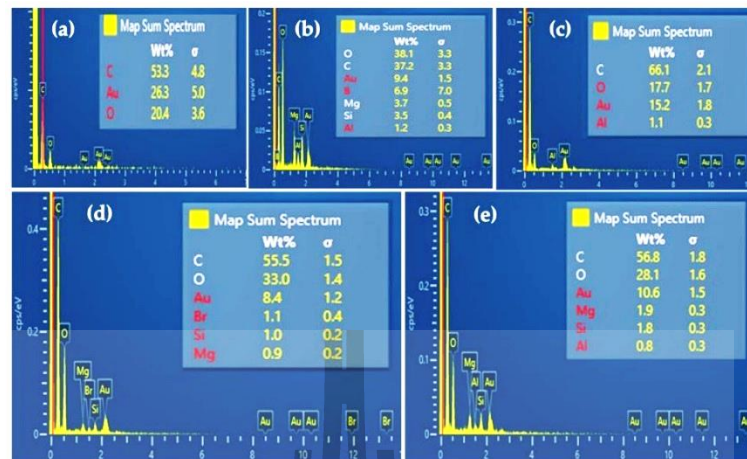


Figure 2.29 EDS profile of the composites PU/VMT: (a) 0%, (b) 5%, (c) 10%, (d) 15%, and (e) 20% (Alves et al., 2022).

Phuong et al. (2009) used a field emission scanning electron microscope (FESEM) and EDS to analyze surface characteristics, particle shape, and phase distribution characteristics in the microstructure to construct antibacterial water filters by coating silver nanoparticles (Ag) and silver type nitrate (AgNO_3) on flexible polyurethane foam. FE-SEM/EDS analysis results are shown in the figure. 2.30 clearly showed the presence of Ag nanoparticles in polyurethane foam sheets. Furthermore, it can show interactions between nitrogen (bonds N-H), oxygen (C-O or N-C-O bonds), and silver nanoparticles obtained from EDS analysis results.

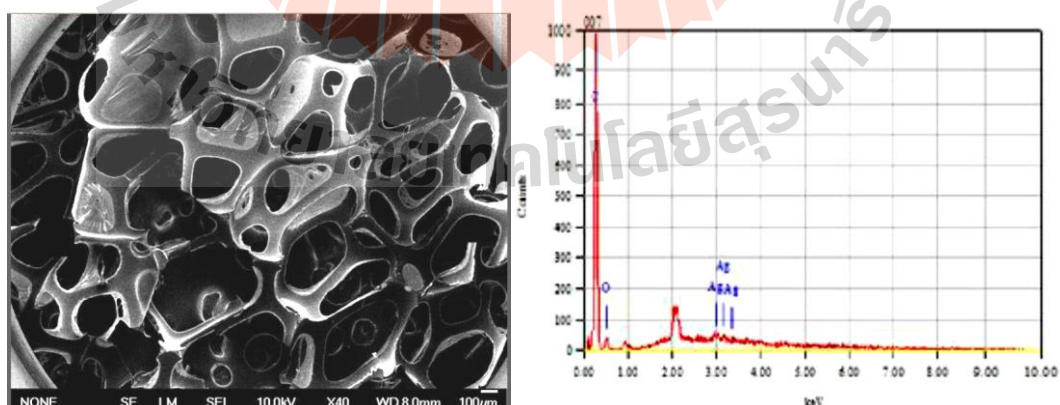


Figure 2.30 FE-SEM image and EDS analysis of Ag-coated Polyurethane foam C%:92.32; O%:1.39; Ag%:6.29 (Phuong et al., 2009).

2.8 Use of polyurethane foam for soil improvement

Soil improvement techniques mainly aim to improve soil engineering properties by focusing on increasing strength or bearing capacity, reducing compaction, reducing seepage, etc. The soil property improvement method selection must consider suitability in various aspects. The admixture technique is widely used due to its low improvement cost and uncomplicated operation method. Popular materials include cement, pozzolanic materials, and chemicals injected into the soil mass, known as the grouting technique (Weaver & Bruce, 2007). The foam continuously improves soil properties in various ways (Che Lat et al., 2020).

Injecting polyurethane foam in soil nailing can increase the friction between nails and soil mass and reduce ground subsidence before and after reinforcement (Chun et al., 1997) and horizontal impact force polyurethane injection. The foam can modify the dynamic response at small strains, influencing the system's fundamental frequency and directional behavior (Capatti et al., 2016; Valentino & Stevanoni, 2016). In addition, polyurethane injection foam is injected into the pavement layer to strengthen strength, stiffness, and bearing capacity, which decreases volume change. In addition, during the injection process, the pavement concrete slab can be lifted to the required level (Mohamed Jais, 2017), avoiding high uplift levels above the level needed (Vennapusa & Zhang, 2016). Foam injected into rock crevices for tunnel construction can also block water entering the construction system and reduce the pressure exerted on the tunnel structure.

Mohamed Jais et al. (2019) studied the compressibility of polyurethane-enhanced peat soil with a 1:1 ratio of polyol and isocyanate by oedometer test with compressive units between 10 kPa and 640 kPa. The peat soil used in the study had a very high moisture content of about 345%, 92% organic matter, and a very low dry density. The test results showed that polyurethane foam fills the gaps within the soil mass, resulting in a decrease in the compression index (C_c) and swelling index (C_s) while the pre-consolidated pressure (P_c') increases.

The use of polyurethane to improve the strength of marine clay has been studied in the laboratory with rigid polyurethane foam (RPU), with PU foam content variations of 0%, 1%, 2%, 3%, 4%, and 5% of soil weight. The marine clay samples

used in the study were disturbed by backhoe excavations at a depth of 1.5 m at the University Tun Hussein Onn Malaysia (UTHM), Batu Pahat campus. Untreated marine clay has a natural moisture content of 67%, the liquid limit. And plastic limits of 65% and 26%, respectively.

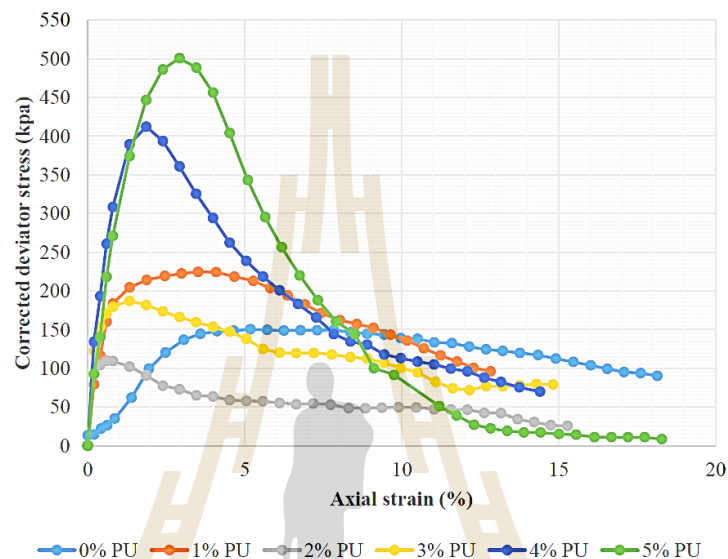


Figure 2.31 UCS test result of marine clay at varying dose of Polyurethane (Saleh et al., 2018).

Figure 2.31 presents the UCS test results of modified marine clays with different amounts of RPU, showing that RPU can improve the marine shear strength of clay by using RPU 5% to improve the shear strength of untreated marine clay from 75 kPa (more than 230%) and make the cumulative stress decrease from 5.18% to 2.92% (reduce 77%) compared to the cumulative stress of untreated marine clay. Untreated marine clay in its natural state, unsuitable for subgrade material or as foundation materials, can improve its strength properties with RPU (Saleh et al., 2018).

In sandy soil, Sidek et al. (2015) studied the effect of injecting PU foam to improve the shear strength of different amounts by varying the amount of PU foam in the range of 0–95 percent. The UCS test obtained the shear strength; the test results are presented as a stress-strain relationship. Figure 2.32 shows the relationship between the uniaxial compressive strength and the amount of PU. Foam test results

show that the compressive strength gradually increased with increasing PU content, with a variation of 20 kPa – 500 kPa (10%–95% of PU in sand).

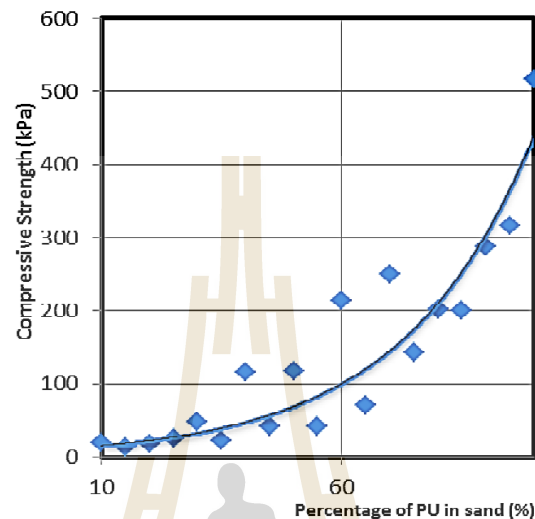


Figure 2.32 Compressive Strength of Modified Sand with PU Foam (Sidek et al., 2015).

It is well known that infrastructure is an essential element in any country's overall economic and social development. The largest infrastructure network is a road (high-speed highway or corridor) serving public road users. Over long periods of use, it tends to deteriorate, especially on soft ground and weak road bases. Therefore, it must be maintained to be used safely by using a method that should be stable, reduce the frequency of repair and correction, and reduce working time. Pavement structure can be improved for sufficient strength and smoothness to ensure safe use (Mounanga & Gbongdon, 2008; Jong-Pil et al., 2010).

Saleh et al. (2019) noted that polyurethane could improve weak soil types for infrastructure development. Foam for solving soil subsidence problems by elevating the road surface by injecting PUR into the subsoil mass in the road ridge repair work in Malaysia, namely FT31, Jalan Banting Semenyih, Petronas MTBE, Km 88.78 Ayer Hitam, and Km 48.7 Kuala Lumpur-Karak Expressway The injection pattern is shown in Figure 2.33.

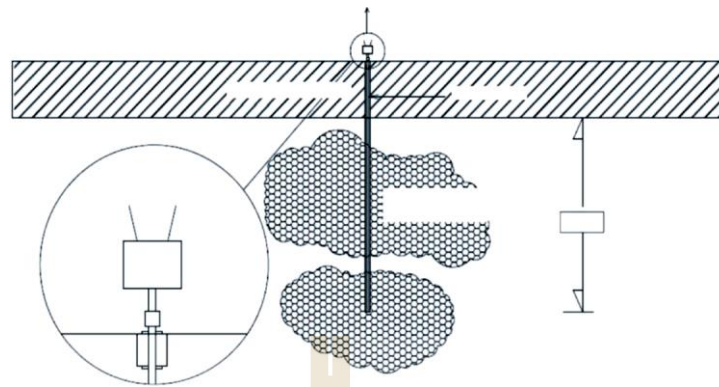


Figure 2.33 Schematic layout of shallow PU foam injection (courtesy of Progrout Injection Sdn. Bhd., Malaysia) (Mohamed Jais, 2017).

Figure 2.34 shows an example of axial displacement versus time between the grouting and slab-raising processes of the secondary concrete road at the Kota toll gate. Damansara, Selangor, Malaysia, can be divided into several stages.

- stage 1 – injection of PU foam at point 1 (furthest from the toll plaza).
- stage 2 – demobilisation and mobilisation of the injector and generator to point 2.
- stage 3 – injection of PU foam at point 2 (inset of point 1).
- stage 4 – demobilisation and mobilisation of the injector and generator to point 3.
- stage 5 – injection of PU foam at point 3 (inset of point 1).
- stage 6 – demobilisation of the injector and generator.

In step 1, during PUR injection, the concrete pavement near the injection site is lifted with a drop of approximately 1.2 mm where the tool is located. It starts to lift by about 6.4 mm. In phase 2, the value decreases slightly to 5.5 mm as the PU foam expands and loosens. In step 3, PUR was injected for approximately 8 minutes, and the expansion caused the concrete to be raised substantially to 30 mm. In stage 4, the PU foam was allowed to expand freely, but extreme subsidence occurred due to the movement of heavy vehicles on the concrete pavement. Immediately causes the pavement to press about 26 mm. In step 5, the injection continues, and the concrete pavement is raised to the required level of approximately 46.8 mm, thus completing the slab process (step 6) (Mohamed Jais, 2017).

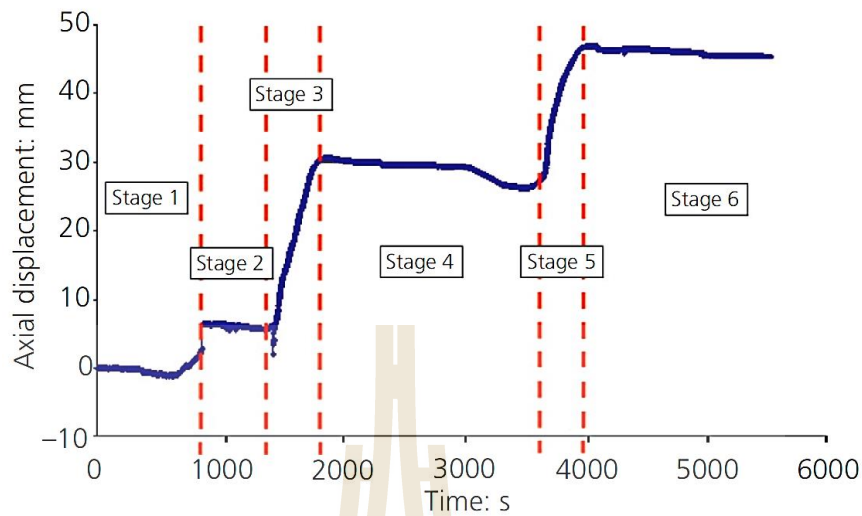


Figure 2.34 Axial displacement against time of the concrete slab uplifting work at Kota Damansara toll plaza, Malaysia (Mohamed Jais, 2017).

Fakhar and Asmaniza (2016) presented a road maintenance experience using a polyurethane (PU) injection foam system and a patented chemical grout process using liquid isocyanate and polyol. Both chemicals are environmentally friendly, non-toxic products. PU foam is based on a high-strength, three-dimensionally networked, rigid polymer produced by heating and volumizing when mixing liquid isocyanates and polyol (Wolf, 1956; Ulrich, 1982; Wood, 1982).

Therefore, the product obtained by mixing isocyanate and polyol can enhance, level, seal, fill gaps, and strengthen the soil structure (Soltész, 2002; Gaspard & Morvant, 2004). The compressive strength is about 90% of the maximum (minimum compressive strength 0.276 N/mm^2) within 15 minutes (Puppala et al., 2009) and the bridge can be opened for traffic the next day.

The PU grouting method is the same as cement grouting. General grouting By injecting isocyanate and polyol through boreholes inserted into the soil, efficiency needs to be improved, as shown in Figure 2.35. It helps to level the soil surface. In addition, the lightweight nature of PU also reduces the settlement rate (Sidek et al., 2015).

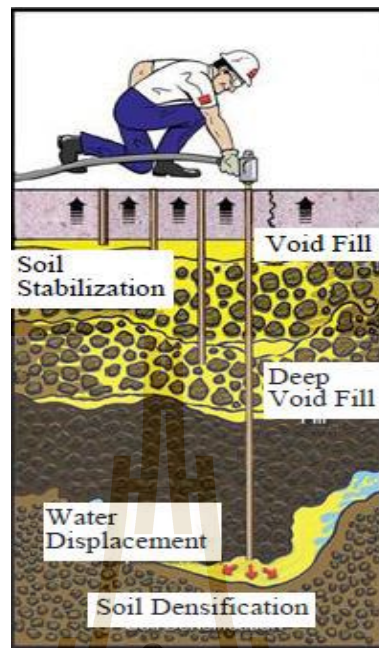


Figure 2.35 PU injection illustration (Fakhar and Asmaniza, 2015).

The case study presented here is at the KLIA Toll Plaza, the North-South Central Link of Malaysia, which faces the problem of undulating roads on concrete sidewalks. Therefore, 2 types of polyurethane chemicals have been proposed: rapid polyurethane (for soil conditioning and compaction) and dense polyurethane (to increase density and lift concrete structures). Using a mixture of isocyanate and polyol in the ratio of 1.1:1.0, respectively, with additional chemicals to catalyze the reaction that uses nitrogen to improve foam expansion, the operation area is 51 m x 45 m, which covers 4 smart tag slots, 3 touch-and-go slots, and 2 cash slots, as shown in Figure 2.36. There is a PU injection point of 621 with a hole diameter of 16 mm for fast polyurethane injection and 32 mm diameter holes for dense polyurethane injection, respectively. Under the concrete structure, polyurethane is injected into each site twice: once quickly, at a depth of 2.0 m, and once densely, at a depth of 1.0 m. Soil samples are drilled before and after injection to assess the soil's strength, stiffness, and compressibility using the unconfined and one-dimensional consolidation tests.

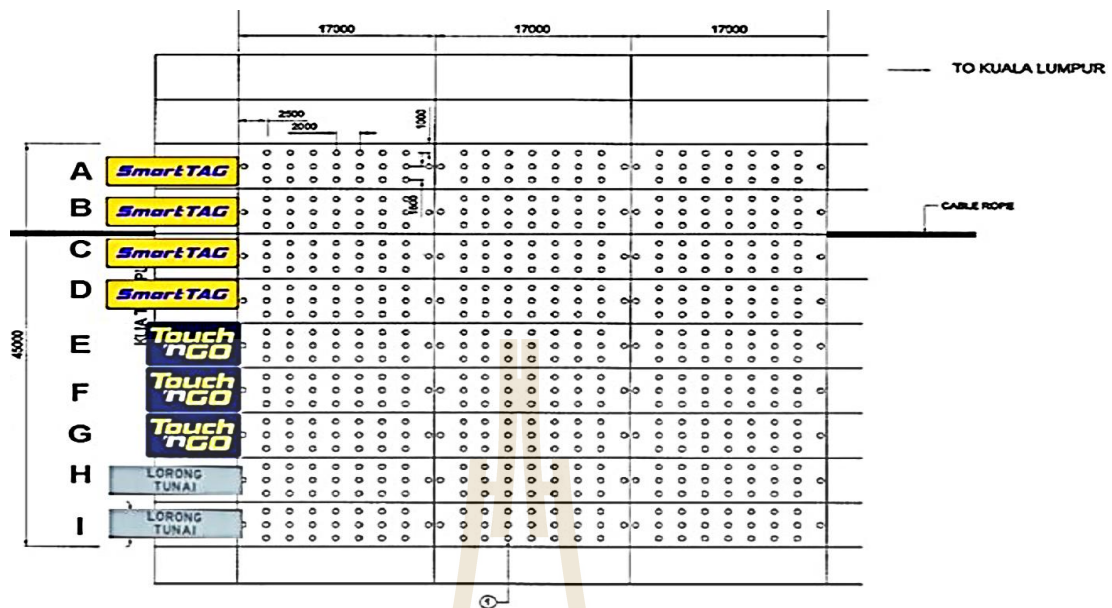


Figure 2.36 Points identified for PU injection (Fakhar and Asmaniza, 2015).

Table 3 shows the testing results of the strength properties of the soil mass in natural conditions and the mass of PU-treated soil nature 1–3 times (62.10–145.00 kPa), and hardness increases about 5–6 times. In terms of compressibility, it was found that the PU-treated soil mass had an initial void ratio (e_o) of 0.435, which decreased by about 31.5% compared to In the natural soil ($e_o = 0.635$), PU expansion fills most of the gaps, and together with the expansion pressure, the water or moisture trapped in the soil is expelled, resulting in The inflation index also declined. 60.9% (0.009) compared to soil in its natural state (0.023), indicating that volumetric changes in the settlement rate and plastic deformation are infrequent.

However, although there are studies on the properties of polyurethane, foam is widely accepted in various applications. However, most of them are the results of laboratory studies with precise production control, resulting in products with high homogeneity properties of the material.

Buzzi et al. (2008) studied the structure and properties of polyurethane foam for foundation rehabilitation injected into the expansive. Soil using scanning electron microscopy and physical testing. It was found that when applied to modified polyurethane foundations, foam quality control during the manufacturing process is

difficult compared to in the lab, causing macro-voids and affecting the integrity of the interface. As a result, the foam material is non-uniform. Figure 2.37 shows the foam's closed cell structure at 37 kg/m^3 . From the scanning electron microscopy images obtained in the laboratory, the basal cells range in size from 0.1 mm to 0.4 mm, and the cell has an irregular polyhedron. Figure 2.38 shows the closed-cell structure of foam of the same density injected to improve the foundation. There is a big difference in the size of the closed-cell foam, which can be divided into 2 zones, with zone 2 being different. Zone 1 is more extensive and longer, with the longer axis likely indicating the direction of foam diffusion from Figures 2.37 and 2.38. It can be confirmed that the production or use conditions affect the microstructure of the foam cell, which in turn affects its physical properties.

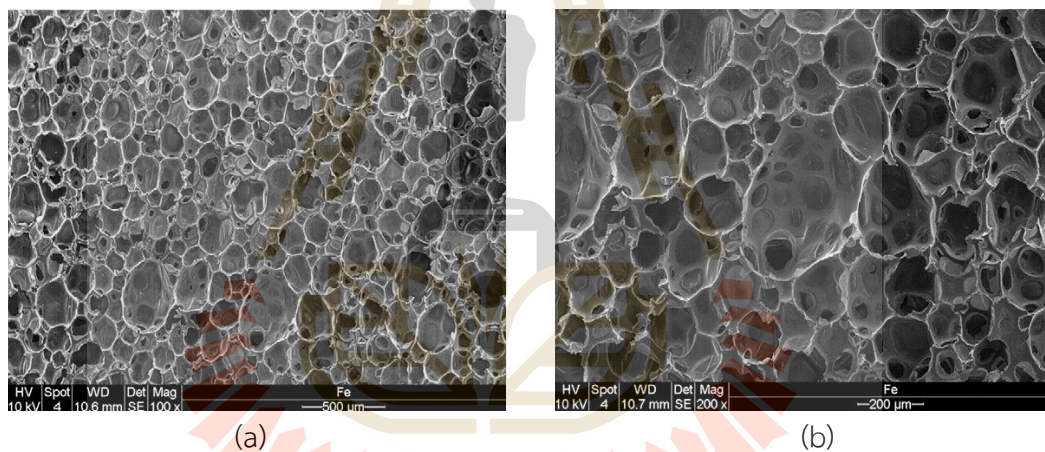


Figure 2.37 Image of the free expanded polyurethane foam obtained by Scanning Electron Microscope. (a) Magnification x 100. (b) Magnification x 200 (Buzzi et al., 2008).

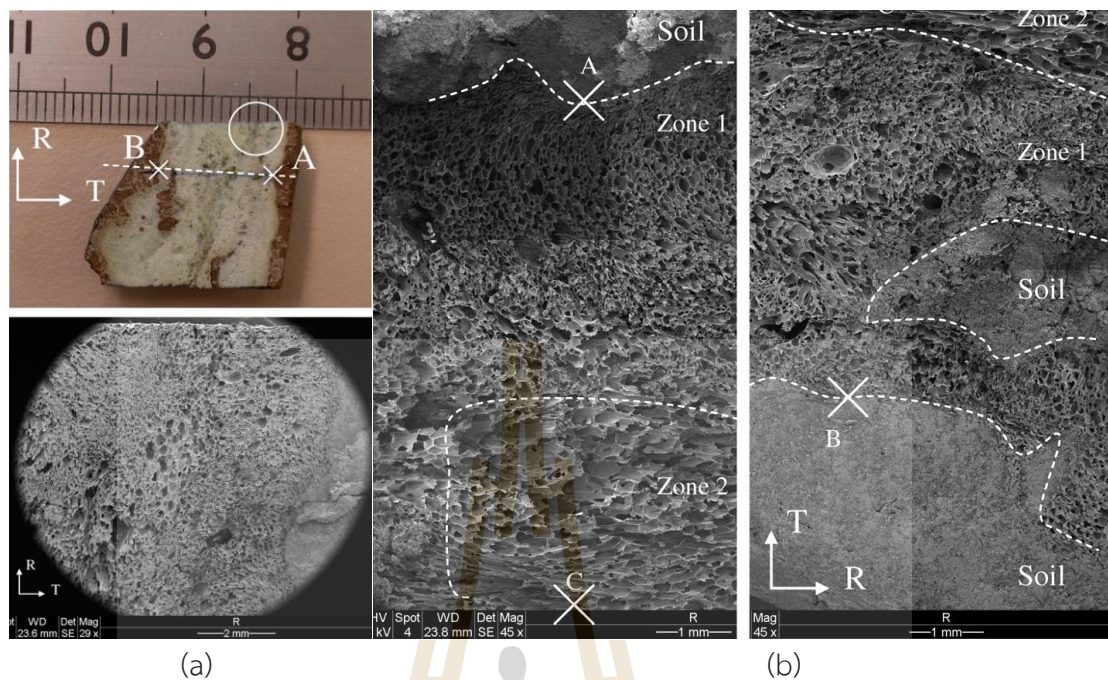


Figure 2.38 (a) Magnification of the foam specimen. (b) Microstructure of Polyurethane foam at Magnification x 45 (Buzzi et al., 2008).

The compressive strength test results of the homogeneous foam obtained in the laboratory compared with the foam injected into the soil for foundation improvement clearly show that the foam injected into the soil is stressed. Yields range from 250 to 500 kPa, 40% to 80% lower than homogeneous materials. In addition, the permeability test revealed almost no water permeability in the homogeneous foam due to its relatively complete closed-cell structure, whereas in the soil-injected foam test, which had a cellular structure, due to local cell structure damage resulting from multiple injections and expansion, a small amount of water is allowed to pass (approximately 10^{-10} m/s) (Buzzi et al., 2008).

2.9 References

A Caen group company, Inorganic Scintillator Detectors. (2023). https://caensys.com/inorganic_sd/

- Alkan, C., Günther, E., Hiebler, S., Ensari, Ö., & Kahraman, D. (2012). Polyurethanes as solid-solid phase change materials for thermal energy storage. *Solar Energy*, *86*, 1761. <https://doi.org/10.1016/j.solener.2012.03.012>
- Alves, L. R. P. S. T., Alves, M. D. T. C., Honorio, L. M. C., Moraes, A. I., Silva-Filho, E. C., Peña-Garcia, R., Furtini, M. B., da Silva, D. A., & Osajima, J. A. (2022). Polyurethane/Vermiculite Foam Composite as Sustainable Material for Vertical Flame Retardant. *Polymers*, *14*(18), 3777. <https://www.mdpi.com/2073-4360/14/18/3777>
- Alves, P., Coelho, J. F. J., Haack, J., Rota, A., Bruinink, A., & Gil, M. H. (2009). Surface modification and characterization of thermoplastic polyurethane. *European Polymer Journal*, *45*(5), 1412-1419. <https://doi.org/https://doi.org/10.1016/j.eurpolymj.2009.02.011>
- Antunes, M., Cano, Á., Haurie, L., & Velasco, J. (2011). Esparto wool as reinforcement in hybrid polyurethane composite foams. *Industrial Crops and Products*, *34*, 1641-1648. <https://doi.org/10.1016/j.indcrop.2011.06.016>
- Apyari, V., Volkov, P., & Dmitrienko, S. (2012). Synthesis and optical properties of polyurethane foam modified with silver nanoparticles Synthesis and optical properties of polyurethane foam modified with silver nanoparticles. *Adv. Nat. Sci.: Nanosci. Nanotechnol.*, *3*, 15001-15007. <https://doi.org/10.1088/2043-6262/3/1/015001>
- Argin, M., & Karady, G. G. (2008). Characterization of Polyurethane Foam Dielectric Strength. *Dielectrics and Electrical Insulation, IEEE Transactions on*, *15*, 350-356. <https://doi.org/10.1109/TDEI.2008.4483452>
- Ashida, K. 2006. *Polyurethane and Related Form: Chemistry and Technology*. Boca Raton, USA: CRC Press.
- ASTM. (2017). *Standard Specification for rigid cellular polystyrene geofoam*. ASTM D6817-07, West Conshohocken, PA.
- Athanasopoulos, N., Baltopoulos, A., Matzakou, M., Vavouliotis, A., & Kostopoulos, V. (2012). Electrical Conductivity of Polyurethane/MWCNT Nanocomposite Foams. *Polymer Composites*, *33*, 1302-1312. <https://doi.org/10.1002/pc.22256>

- Australian Microscopy and Microanalysis Research Facility, “*My Scope-training for advanced research*” <http://www.ammrf.org.au/myscope/sem/background/>
- Bartlett, S., Asce, M., & Lingwall, B. (2014). *Protection of Pipelines and Buried Structures Using EPS Geofoam*. <https://doi.org/10.1061/9780784413401.054>
- Bayati, M., & Hamidii, J. (2017). A case study on TBM tunnelling in fault zones and lessons learned from ground improvement. *Tunnelling and Underground Space Technology*, *63*, 162-170. <https://doi.org/10.1016/j.tust.2016.12.006>
- Benkreira, H., Khan, A., & Horoshenkov, K. (2011). Sustainable acoustic and thermal insulation materials from elastomeric waste residues. *Chemical Engineering Science*, *66*, 4157-4171. <https://doi.org/10.1016/j.ces.2011.05.047>
- Boetes, R. (1984). Heat transfer reduction in closed cell polyurethane foams.
- Bryśkiewicz, A., Zieleniewska, M., Przyjemka, K., Chojnacki, P., & Ryszkowska, J. (2016). Modification of flexible polyurethane foams by the addition of natural origin fillers. *Polymer Degradation and Stability*, *132*. <https://doi.org/10.1016/j.polymdegradstab.2016.05.002>
- Buzzi, O., Fityus, S., Sasaki, Y., & Sloan, S. (2008). Structure and properties of expanding polyurethane foam in the context of foundation remediation in expansive soil. *Mechanics of Materials*, *40*(12), 1012-1021. <https://doi.org/10.1016/j.mechmat.2008.07.002>
- Campbell, F. C. (Ed.). (2012). *Lightweight materials: understanding the basics*. ASM international.
- Capatti, M. C., Dezi, F., & Morici, M. (2016). Field Tests on Micropiles Under Dynamic Lateral Loading. *Procedia Engineering*, *158*, 236-241. <https://doi.org/10.1016/j.proeng.2016.08.435>
- Celebi, S., & Kucuk, H. (2012). Acoustic Properties of Tea-Leaf Fiber Mixed Polyurethane Composites. *Cellular Polymers*, *31*, 241-255. <https://doi.org/10.1177/026248931203100501>
- Chattopadhyay, D. K., & Webster, D. C. (2009). Thermal stability and flame retardancy of polyurethanes. *Progress in Polymer Science*, *34*(10), 1068-1133. <https://doi.org/10.1016/j.progpolymsci.2009.06.002>

- Che Lat, D., Ali, N., Bagus, I., Mohamed Jais, I., Zurairahetty, N., Yunus, M., Razali, R., Rosseira, A., & Abu Talip, A. (2020). A review of polyurethane as a ground improvement method. 70-74. <https://doi.org/10.11113/mjfas.v16n1.1235>
- Choo, Y. W., Abdoun, T., O'Rourke, M., & Ha, D. (2007). Remediation for buried pipeline systems under permanent ground deformation. *Soil Dynamics and Earthquake Engineering*, 27, 1043-1055. <https://doi.org/10.1016/j.soildyn.2007.04.002>
- Chun, B.-S., Ryu, D.-S., Shin, C.-B., Im, G.-S., Choi, J.-K., Lim, H.-S., & Son, J.-Y. (1997). The performance of polyurethane injection method with soil nailing system for ground reinforcement. Ground improvement geosystems Densification and reinforcement: Proceedings of the Third International Conference on Ground Improvement Geosystems London, 3-5 June 1997,
- Chung, Y.-j., Kim, Y., & Kim, S. (2009). Flame retardant properties of polyurethane produced by the addition of phosphorous containing polyurethane oligomers (II). *Journal of Industrial and Engineering Chemistry*, 15(6), 888-893.
- Clemiston, I.R. Castable Polyurethane Elastomers; CRC Press: New York, NY, USA, 2008; p. 272.
- Cunningham, A., & Hilyard, N. (1994). Physical behaviour of polymeric foams-An overview. *Low density cellular plastics: Physical basis of behaviour*, 1-21.
- Del Rey, R., Alba, J., Arenas, J. P., & Sanchis, V. J. (2012). An empirical modelling of porous sound absorbing materials made of recycled foam. *Applied Acoustics*, 73(6-7), 604-609.
- Department of Rural Roads. (2009). Guide to road construction on soft ground, Team Group and Geotechnical Co., Ltd. & Foundation Engineering Co., Ltd. (GFE)
- Diamant, R. M. E. Thermal and Acoustic Insulation; Elsevier: Amsterdam, The Netherlands, 1986.
- DOH. (2012). Privatization of highway infrastructure in Thailand.
- Eide, O. (1968). Geotechnical engineering problems with soft Bangkok clay on the Nakhon Sawan highway project, Pub. No 78, Norwegian Geotechnical Institute, Norway.
- Eide, O. (1977). Exploration, sampling and in-situ testing of soft clay in the Bangkok area, Proc. of International Symposium on Soft Clay, Thailand, pp122-137.

- Elragi, A., Negussey, D., & Kyanka, G. (2001). *Sample Size Effects on the Behavior of EPS Geofoam* (Vol. 112). [https://doi.org/10.1061/40552\(301\)22](https://doi.org/10.1061/40552(301)22)
- Fakhar, A., & Asmaniza, A. (2016). Road Maintenance Experience Using Polyurethane (PU) Foam Injection System and Geocrete Soil Stabilization as Ground Rehabilitation. *IOP Conference Series: Materials Science and Engineering*, 136, 012004. <https://doi.org/10.1088/1757-899X/136/1/012004>
- Gama, N. V., Ferreira, A., & Barros-Timmons, A. (2018). Polyurethane Foams: Past, Present, and Future. *Materials*, 11(10), 1841. <https://www.mdpi.com/1996-1944/11/10/1841>
- Gama, N., Costa, L., Amaral, V., Ferreira, A., & Barros-Timmons, A. (2016). Insights into the physical properties of biobased polyurethane/ expanded graphite composite foams. *Composites Science and Technology*, 138. <https://doi.org/10.1016/j.compscitech.2016.11.007>
- Gama, N., Silva, R., Carvalho, A., Ferreira, A., & Barros-Timmons, A. (2017). Sound absorption properties of polyurethane foams derived from crude glycerol and liquefied coffee grounds polyol. *Polymer Testing*, 62, 13-22. <https://doi.org/10.1016/j.polymertesting.2017.05.042>
- Gama, N., Silva, R., Mohseni, F., Davarpanah, A., Amaral, V., Ferreira, A., & Barros-Timmons, A. (2018). Enhancement of physical and reaction to fire properties of crude glycerol polyurethane foams filled with expanded graphite. *Polymer Testing*, 69. <https://doi.org/10.1016/j.polymertesting.2018.05.012>
- Gaspard K and Morvant M 2004 Assessment of the Uretek Process on Continuously Reinforced Concrete Pavement, Jointed Concrete Pavement and Bridge Approach Slabs. Technical Assistance Report Number 03- 2TA, Louisiana Transportation Research Center.
- Geotechnical Engineering Research and Development Center (GERD). (2018). Bangkok soft clay layer thickness map. Kasetsart University.
- Gibson, L. J., and Ashby, M. F., 1999, *Cellular Solids: Structure and Properties*, Cambridge University Press, Cambridge.

- Giuliani, F., Autelitano, F., Garilli, E., & Montepara, A. (2020). Expanded polystyrene (EPS) in road construction: Twenty years of Italian experiences. *Transportation Research Procedia*, 45, 410-417. <https://doi.org/10.1016/j.trpro.2020.03.033>
- Goldstein, J.I., D.E. Newbury, P. Echlin, D.C. Joy, C.E. Lyman, E. Lifshin, L. Sawyer, and J.R. Michael. "Scanning Electron Microscopy and X-Ray Microanalysis", Kluwer Academic, New York. (2003).
- Goldstein, J.I.; Newbury, D.E.; Echlin, P., David C.; Romig Jr, A.D.; Charles E.L.; Fiori, C.; and Lifshin, E. 1992. Scanning Electron Microscopy and X-ray Microanalysis. 2nd ed. New York: Plenum Press.
- Hangzhou Fuyang Longwell Industry. (2023). EPS Foam Making Machine Factory. <http://m.lweps.com/eps-machine/eps-preexpander/eps-foam-making-machine-factory.html/>
- Hayashi, Y., Suzuki, A., & Matsuo, A. (2002). Mechanical properties of air-cement-treated soils. *Proceedings of the Institution of Civil Engineers-Ground Improvement*, 6(2), 69-78.
- Herrington, R., and Hock, K. 1997. Flexible Polyurethane Foams. 2nd Ed., Midland, USA: Dow Chemical Co.
- Hotta, H., Nishi, T., & Kuroda, S. (1996). Report of Results of Assessments of Damage to EPS Embankments Caused by Earthquakes. PROCEEDINGS OF INTERNATIONAL SYMPOSIUM ON EPS (EXPANDED POLY-STYROL) CONSTRUCTION METHOD (EPS TOKYO'96),
- Huang, J., Tang, Q., Liao, W., Wang, G., Wei, W., & Li, C. (2017). Green Preparation of Expandable Graphite and Its Application in Flame-Resistance Polymer Elastomer. *Industrial & Engineering Chemistry Research*, 56. <https://doi.org/10.1021/acs.iecr.6b04860>
- Integrating Research and Education. (2016). Geochemical Instrumentation and Analysis. https://serc.carleton.edu/research_education/geochemsheets/wds.html/
- Ionescu, M. 2005. Chemistry and Technology of Polyols for Polyurethanes. Shawbury, UK: Rapra Technology.

- Jahani, D., Ameli, A., Jung, P. U., Park, C. B., & Naguib, H. (2014). Open-cell cavity-integrated injection-molded acoustic polypropylene foams. *Materials and Design*, 53, 20-28. <https://doi.org/10.1016/j.matdes.2013.06.063>
- Jamnongpipatkul, P., Dechasakulsom, M., & Sukolrat, J. (2009). Application of air foam stabilized soil for bridge-embankment transition zone in Thailand. *Asphalt Material Characterization, Accelerated Testing, and Highway Management: Selected Papers from the 2009 GeoHunan International Conference*,
- Jang, W.-Y., Kraynik, A. M., & Kyriakides, S. (2008). On the microstructure of open-cell foams and its effect on elastic properties. *International Journal of Solids and Structures*, 45(7), 1845-1875. <https://doi.org/10.1016/j.ijsolstr.2007.10.008>
- Jarosinski, J.; Veyssiere, B. *Combustion Phenomena: Selected Mechanisms of Flame Formation, Propagation, and Extinction*; CRC Press: New York, NY, USA 2009.
- Johnson, O. B. (1977). Method for continuous hydrolysis of polyurethane foam in restricted tubular reaction zone and recovery. In: Google Patents.
- Kamon, M. and Bergado, D.T. (1991). Ground improvement techniques. *Proceedings of 9th Asian Regional Conference on Soil Mechanics and Foundation Engineering*, Bangkok, 2: 526-546.
- Kausar, A. (2017). Polyurethane Composite Foams in High Performance Applications: A Review. *Polymer-Plastics Technology and Engineering*, 57. <https://doi.org/10.1080/03602559.2017.1329433>
- Khaton, H., & Ahmad, S. (2017). A review on conducting polymer reinforced polyurethane composites. *Journal of Industrial and Engineering Chemistry*, 53. <https://doi.org/10.1016/j.jiec.2017.03.036>
- Kim, J. M., Lee, Y., Jang, M., Han, C., & Kim, W. (2016). Electrical conductivity and EMI shielding effectiveness of polyurethane foam-conductive filler composites. *Journal of Applied Polymer Science*, 134. <https://doi.org/10.1002/app.44373>
- Kleiner, M.; Tichy, J. *Acoustics of Small Rooms*; CRC Press: New York, NY, USA, 2014; ISBN 9780415779302.
- H. Kohashi, H., 2000, Influence of the void ratio in soil treated with air foam and cement, *Proceeding of the International symposium on coast geotechnical engineering in practice*, Yokohama, pp. 453-458.

- H. Kohashi, H., 2005, Technology using soil high grade soil – foam mixed stabilization soil method technical document, Public Work Research Institute.
- Komurlu, E., & Kesimal, A. (2012). *Investigation of polyurethane reinforced soil strength*.
- Komurlu, E., & Kesimal, A. (2014). Improved Performance of Rock Bolts using Sprayed Polyurea Coating. *Rock Mechanics and Rock Engineering*, 48. <https://doi.org/10.1007/s00603-014-0696-4>
- Kraatz, A., Moneke, M., & Kolupaev, V. (2006). Long-term Tensile and Compressive Behavior of Polymer Foams. *Journal of Cellular Plastics - J CELL PLAST*, 42, 221-228. <https://doi.org/10.1177/0021955X06063511>
- Lee, S.-T.; Ramesh, N.S. *Polymeric Foams: Mechanisms and Materials*; CRC Press: New York, NY, USA, 2004.
- Li, S., Liu, R., Zhang, Q., & Zhang, X. (2016). Protection against water or mud inrush in tunnels by grouting: A review. *Journal of Rock Mechanics and Geotechnical Engineering*, 8(5), 753-766. <https://doi.org/10.1016/j.jrmge.2016.05.002>
- Li, Z., & Crocker, M. J. (2006). Effects of thickness and delamination on the damping in honeycomb-foam sandwich beams. *Journal of Sound and Vibration*, 294(3), 473-485. <https://doi.org/10.1016/j.jsv.2005.11.024>
- Lim, S. K., Tan, C. S., Li, B., Ling, T.-C., Hossain, M., & Poon, C. S. (2017). Utilizing high volumes quarry wastes in the production of lightweight foamed concrete. *Construction and Building Materials*, 151, 441-448. <https://doi.org/10.1016/j.conbuildmat.2017.06.091>
- Lorenzetti, A., Dittrich, B., Schartel, B., Roso, M., & Modesti, M. (2017). Expandable graphite in polyurethane foams: The effect of expansion volume and intercalants on flame retardancy. *Journal of Applied Polymer Science*, 134. <https://doi.org/10.1002/app.45173>
- Lubczak, R., Szczęch, D., Broda, D., Szymańska, A., Wojnarowska-Nowak, R., Kusliński, M., & Lubczak, J. (2018). Preparation and characterization of boron-containing polyurethane foams with carbazole. *Polymer Testing*, 70. <https://doi.org/10.1016/j.polymertesting.2018.07.027>

- Luong, D., Pinisetty, D., & Gupta, N. (2013). Compressive properties of closed-cell polyvinyl chloride foams at low and high strain rates: Experimental investigation and critical review of state of the art. *Composites Part B: Engineering*, 44, 403–416. <https://doi.org/10.1016/j.compositesb.2012.04.060>
- Mairaing, W and Amonkul, C. (2010). Soft Bangkok Clay Zoning. EIT-Japan Symposium on Engineering for Geo-Hazards : Earthquakes and Landslides- Surface and Subsurface Structures, Imperial Queen' s Park Hotel, Bangkok, Thailand, September 6-7.
- Malai, A., Youwai, S., Watcharasawe, K., & Jongpradist, P. (2022). Bridge approach settlement mitigation using expanded polystyrene foam as light backfill: Case study and 3D simulation. *Transportation Geotechnics*, 35, 100794. <https://doi.org/https://doi.org/10.1016/j.trgeo.2022.100794>
- Mane, J. V., Chandra, S., Sharma, S., Ali, H., Chavan, V. M., Manjunath, B. S., & Patel, R. J. (2017). Mechanical Property Evaluation of Polyurethane Foam under Quasi-static and Dynamic Strain Rates- An Experimental Study. *Procedia Engineering*, 173, 726-731. <https://doi.org/https://doi.org/10.1016/j.proeng.2016.12.160>
- Marhoon, I., & Rasheed, A. (2015). Mechanical and Physical Properties of Glass Wool-Rigid Polyurethane Foam Composites. *18*, 41-49.
- Meng, Q., & Hu, J. (2008). A poly(ethylene glycol)-based smart phase change material. *Solar Energy Materials and Solar Cells*, 92, 1260- 1268. <https://doi.org/10.1016/j.solmat.2008.04.026>
- Miki, H. (1996). An overview of lightweight banking technology in Japan. In Proceedings of International Symposium ROCEEDINGS OF INTERNATIONAL SYMPOSIUM ON EPS (Expanded XPANDED PolyOLYstyrol-STYROL) Construction Method ONSTRUCTION METHOD (EPS TOKYO'96).
- Miki, H., 2001, "An overview of lightweight banking technology," First IRST Semina on EMINAR ON Highway Engineering IGHWAY ENGINEERING Volume OLUME 1, 16-17 July 2001, Miracle Grand Convention Hotel IRACLA GRAND CONVENTION HOTEL Bangkok BANGKOK, pp. 65-76.
- Mittal, V. Polymer Nanocomposite Foams; CRC Press: London, UK; New York, NY, USA, 2014; ISBN 9781466558120.

- Miyase, A., Lo, K. H., & Wang, S. S. (2016). Effects of density and cell rise ratio on compressive stiffness and strength of PVC structural foam. Proceedings of the American Society for Composites: Thirty-First Technical Conference,
- Modesti, M., & Lorenzetti, A. (2002). Halogen-free flame retardants for polymeric foams. *Polymer Degradation and Stability*, 78(1), 167-173.
- Moh, Z.-C., Nelson, J., & Brand, E. (1969). *Strength and deformation behaviour of Bangkok clay*. Asian Institute of Technology.
- Mohamed Jais, I. (2017). Rapid remediation using polyurethane foam/resin grout in Malaysia. *Geotechnical Research*, 4, 1-11. <https://doi.org/10.1680/jgere.17.00003>
- Mohamed Jais, I., Che Lat, D., & Endut, T. (2019). COMPRESSIBILITY OF PEAT SOIL IMPROVED WITH POLYURETHANE. *Malaysian Journal of Civil Engineering*, 31. <https://doi.org/10.11113/mjce.v31n1.545>
- H. Mori, H., Y. Kon., Y., & H. Kohashi, H., 2005, Lightweight embankment on soft ground to reduce settlement. 15th International Road Federation World Meeting 2005, 14-15 June 2005, BITEC, Bangkok, pp. 67.
- Motokucho, S., Nakayama, Y., Morikawa, H., & Nakatani, H. (2017). Environment-friendly chemical recycling of aliphatic polyurethanes by hydrolysis in a CO₂-water system: ARTICLE. *Journal of Applied Polymer Science*, 135, 45897. <https://doi.org/10.1002/app.45897>
- Mounanga, P., Gbongbon, W., Poullain, P., & Turcry, P. (2008). Proportioning and characterization of lightweight concrete mixtures made with rigid polyurethane foam wastes. *Cement and Concrete Composites*, 30, 806-814. <https://doi.org/10.1016/j.cemconcomp.2008.06.007>
- Najib, N. N., Ariff, Z., Bakar, A., & Sipaut, C. (2011). Correlation between the acoustic and dynamic mechanical properties of natural rubber foam: Effect of foaming temperature. *Materials & Design*, 32, 505-511. <https://doi.org/10.1016/j.matdes.2010.08.030>
- Nikomborirak, D. (2004). *Private sector participation in infrastructure: The case of Thailand. on the Nakhon Sawan highway project*”, Pub. No 78, Norwegian

- Otto, G. P., Moisés, M. P., Carvalho, G., Rinaldi, A. W., Garcia, J. C., Radovanovic, E., & Fávoro, S. L. (2017). Mechanical properties of a polyurethane hybrid composite with natural lignocellulosic fibers. *Composites Part B: Engineering*, 110, 459-465. <https://doi.org/https://doi.org/10.1016/j.compositesb.2016.11.035>
- Oushabi, A., Sair, S., Abboud, Y., Tanane, O., & Bouari, A. E. (2017). An experimental investigation on morphological, mechanical and thermal properties of date palm particles reinforced polyurethane composites as new ecological insulating materials in building. *Case Studies in Construction Materials*, 7, 128-137. <https://doi.org/https://doi.org/10.1016/j.cscm.2017.06.002>
- Peduto, D., Giangreco, C., & Venmans, A. (2020). Differential settlements affecting transition zones between bridges and road embankments on soft soils: Numerical analysis of maintenance scenarios by multi-source monitoring data assimilation. *Transportation Geotechnics*, 24, 100369. <https://doi.org/10.1016/j.trgeo.2020.100369>
- Phong, N., Thanh, N., & Phuong, P. (2009). Fabrication of antibacterial water filter by coating silver nanoparticles on flexible polyurethane foams. *Journal of Physics: Conference Series*, 187, 012079. <https://doi.org/10.1088/1742-6596/187/1/012079>
- Pimpan, V. 2004. Plastic Recycling. Department of Materials Science Faculty of Science Chulalongkorn University, Bangkok.
- Poapongsakorn, P., & Kanchanomai, C. (2011). Time-dependent deformation of closed-cell PVC foam. *Journal of Cellular Plastics - J CELL PLAST*, 47, 323-336. <https://doi.org/10.1177/0021955X11401014>
- Puppala, A., Archeewa, E., Saride, S., Nazarian, S., & Lr, H. (2012). *Recommendations for Design, Construction, and Maintenance of Bridge approach Slabs*.
- Qian, L., Feng, F., & Tang, S. (2013). Bi-phase flame-retardant effect of hexa-phenoxy-cyclotriphosphazene on rigid polyurethane foams containing expandable graphite. *Polymer*, 55. <https://doi.org/10.1016/j.polymer.2013.12.015>
- Rachan, R. (2009). Strength Development and Microstructural Characteristics of Soft Bangkok Clay Admixed with Cement and Biomass Ash. Doctoral Thesis. Civil Engineering. Thammasat University.

- Rao, W.-H., Xu, H.-X., Xu, Y.-J., Qi, M., Liao, W., Xu, S., & Wang, Y.-Z. (2018). Persistently flame-retardant flexible polyurethane foams by a novel phosphorus-containing polyol. *Chemical Engineering Journal*, 343, 198-206. <https://doi.org/10.1016/j.cej.2018.03.013>
- Rostamizadeh, M., Khanlarkhani, M., & Sadrameli, S. M. (2012). Simulation of energy storage system with phase change material (PCM). *Energy and Buildings*, 49, 419–422. <https://doi.org/10.1016/j.enbuild.2012.02.037>
- Saha, M. C., Mahfuz, H., Chakravarty, U. K., Uddin, M., Kabir, M. E., & Jeelani, S. (2005). Effect of density, microstructure, and strain rate on compression behavior of polymeric foams. *Materials Science and Engineering: A*, 406(1), 328-336. <https://doi.org/https://doi.org/10.1016/j.msea.2005.07.006>
- Saleh, S., Mohd yunus, N. Z., Ahmad, K., & Ali, N. (2019). Improving the strength of weak soil using polyurethane grouts: A review. *Construction and Building Materials*, 202, 738-752. <https://doi.org/10.1016/j.conbuildmat.2019.01.048>
- Saleh, S., Yunus, N., Ahmad, K., & Ali, N. (2018). Stabilization of Marine Clay Soil Using Polyurethane. *MATEC Web of Conferences*, 250, 01004. <https://doi.org/10.1051/mateconf/201825001004>
- Sarier, N., & Onder, E. (2007). Thermal characteristics of polyurethane foams incorporated with phase change materials. *Thermochimica Acta*, 454(2), 90-98. <https://doi.org/10.1016/j.tca.2006.12.024>
- Sarier, N., & Onder, E. (2008). Thermal insulation capability of PEG-containing polyurethane foams. *Thermochimica Acta*, 475, 15-21. <https://doi.org/10.1016/j.tca.2008.06.006>
- Sawai, P., Chattopadhyaya, P. P., & Banerjee, S. (2018). Synthesized reduce Graphene Oxide (rGO) filled Polyetherimide based nanocomposites for EMI Shielding applications. *Materials Today: Proceedings*, 5(3, Part 3), 9989-9999. [/https://doi.org/10.1016/j.matpr.2017.10.197](https://doi.org/10.1016/j.matpr.2017.10.197)
- Sayadi, A. A., Tapia, J. V., Neitzert, T. R., & Clifton, G. C. (2016). Effects of expanded polystyrene (EPS) particles on fire resistance, thermal conductivity and compressive strength of foamed concrete. *Construction and Building Materials*, 112, 716-724. <https://doi.org/10.1016/j.conbuildmat.2016.02.218>

- Şerban, D.-A., Weissenborn, O., Geller, S., Marşavina, L., & Gude, M. (2016). Evaluation of the mechanical and morphological properties of long fibre reinforced polyurethane rigid foams. *Polymer Testing*, *49*, 121-127. <https://doi.org/10.1016/j.polymertesting.2015.11.007>
- She, W., Du, Y., Zhao, G., Feng, P., Zhang, Y., & Cao, X. (2018). Influence of coarse fly ash on the performance of foam concrete and its application in high-speed railway roadbeds. *Construction and Building Materials*, *170*, 153- 166. [/https://doi.org/10.1016/j.conbuildmat.2018.02.207](https://doi.org/10.1016/j.conbuildmat.2018.02.207)
- Sidek, N., Mohamed, K., Mohamed Jais, I., & abu bakar, I. (2015). Strength Characteristics of Polyurethane (PU) With Modified Sand. *Applied Mechanics and Materials*, *773- 774*, 1508- 1512. <https://doi.org/10.4028/www.scientific.net/AMM.773-774.1508>
- Silva, M., Takahashi, J., Chaussy, D., Belgacem, M., & Silva, G. (2010). Composites of rigid polyurethane foam and cellulose fiber residue. *Journal of Applied Polymer Science*, *117(6)*, 3665-3672.
- Singhal, P., Small, W., Cosgriff-Hernandez, E., Maitland, D., & Wilson, T. (2013). Low density biodegradable shape memory polyurethane foams for embolic biomedical applications. *Acta biomaterialia*, *10*. <https://doi.org/10.1016/j.actbio.2013.09.027>
- Sivak, W., Zhang, J., Petoud, S., & Beckman, E. (2009). Simultaneous drug release at different rates from biodegradable polyurethane foams. *Acta biomaterialia*, *5*, 2398-2408. <https://doi.org/10.1016/j.actbio.2009.03.036>
- Soltész, S. (2002). Injected polyurethane slab jacking : final report [Tech Report]. <https://rosap.nsl.bts.gov/view/dot/22955>
- Stirna, U., Beverte, I., Yakushin, V., & Cabulis, U. (2011). Mechanical properties of rigid polyurethane foams at room and cryogenic temperatures. *Journal of Cellular Plastics - J CELL PLAST*, *47*, 337- 355. <https://doi.org/10.1177/0021955X11398381>
- Szycher, M. 2013. Szycher's Handbook of Polyurethanes. 2nd Ed. Boca Raton, USA: CRC Press.

- Thermal Conductivity of Common Materials and Gases.(2023). Solids, Liquids and Gases - Thermal Conductivities. https://www.engineeringtoolbox.com/thermal-conductivity-d_429.html/
- Thermo Fisher Scientific Inc.(2018). Electron Microscopy Solutions. <https://www.fei.com/products/sem/quanta-sem/>
- Throne, J. L., 1982, "Structural Foams," *Mechanics of Cellular Plastics*, N. C.Hilyard, ed., Macmillan, New York, pp. 236–322.
- Tinti, A., Tarzia, A., Passaro, A., & Angiuli, R. (2014). Thermographic analysis of polyurethane foams integrated with phase change materials designed for dynamic thermal insulation in refrigerated transport. *Applied Thermal Engineering*, 70, 201–210. <https://doi.org/10.1016/j.applthermaleng.2014.05.003>
- Tiuc, A. E., Vermesan, H., Gabor, T., & Vasile, O. (2016). Improved Sound Absorption Properties of Polyurethane Foam Mixed with Textile Waste. *Energy Procedia*, 85, 559-565. <https://doi.org/10.1016/j.egypro.2015.12.245>
- Ulrich, H. (1982). Introduction to industrial Polymers. 56 – 79.
- Valentino, R., & Stevanoni, D. (2016). Behaviour of reinforced polyurethane resin micropiles. *Proceedings of the Institution of Civil Engineers - Geotechnical Engineering*, 169, 187-200. <https://doi.org/10.1680/jgeen.14.00185>
- Vennapusa, P. K., Zhang, Y., & White, D. J. (2016). Comparison of pavement slab stabilization using cementitious grout and injected polyurethane foam. *Journal of Performance of Constructed Facilities*, 30(6), 04016056.
- Walker, B.M., and Rader, C.P. 1988. Handbook of Thermoplastic Elastomers. 2nd Ed., New York, USA: Van Nostrand Reinhold.
- Walter, T. R., Richards, A., & Subhash, G. (2009). A Unified Phenomenological Model for Tensile and Compressive Response of Polymeric Foams. *Journal of Engineering Materials and Technology, Transactions of the ASME*, 131. <https://doi.org/10.1115/1.3026556>
- Weaver, K.D. and Bruce, D.A. (2007). Dam Foundation Grouting, 2007, pp. 87–136.
- Witkiewicz, W., & Zieliński, A. (2006). Properties of the polyurethane (PU) light foams. *Advances in Materials Science*, 6(2), 35-51.

- Wolf, H. (1956). Catalyst activity in one-shot urethane foam. *Technical Bulletin, Dupont, Wilmington*, 30-65.
- Won, J.-P., Kim, J.-M., Lee, S.-J., Lee, S.-W., & Park, S.-K. (2011). Mix proportion of high-strength, roller-compacted, latex-modified rapid-set concrete for rapid road repair. *Construction and Building Materials - CONSTR BUILD MATER*, 25, 1796-1800. <https://doi.org/10.1016/j.conbuildmat.2010.11.085>
- Wood G 1982 Flexible Polyurethane Foams, Chemistry and Technology. Applied Science Publishers, London. 120 – 160.
- Xu, W., Wang, G., & Zheng, X. (2015). Research on highly flame-retardant rigid PU foams by combination of nanostructured additives and phosphorus flame retardants. *Polymer Degradation and Stability*, 111, 142-150. <https://doi.org/10.1016/j.polymdegradstab.2014.11.008>
- Xu, X., Lin, G., Liu, D., Sui, G., & Yang, R. (2017). Electrically conductive graphene-coated polyurethane foam and its epoxy composites. *Composites Communications*, 7, 1-6. <https://doi.org/10.1016/j.coco.2017.11.003>
- Yajima, J., Maruo, S., & Ogawa, S. (1995). Influence of foam volume ratio on mechanical properties in light-weight soil. *Doboku Gakkai Ronbunshu*, 1995(511), 173-180.
- Yakushin, V., Bel'kova, L., & Sevastyanova, I. (2012). Properties of Rigid Polyurethane Foams Filled with Glass Microspheres. *Mechanics of Composite Materials*, 48. <https://doi.org/10.1007/s11029-012-9302-6>
- Yang, C., Fischer, L., Maranda, S., & Worlitschek, J. (2015). Rigid polyurethane foams incorporated with phase change materials: A state-of-the-art review and future research pathways. *Energy and Buildings*, 87, 25-36. <https://doi.org/10.1016/j.enbuild.2014.10.075>
- Yang, Y., & Chen, B. (2016). Potential use of soil in lightweight foamed concrete. *KSCE Journal of Civil Engineering*, 20(6), 2420-2427. <https://doi.org/10.1007/s12205-016-0140-2>
- You, M., Zhang, X. X., Li, W., & Wang, X. C. (2008). Effects of MicroPCMs on the fabrication of MicroPCMs/polyurethane composite foams. *Thermochimica Acta*, 472(1), 20-24. <https://doi.org/10.1016/j.tca.2008.03.006>

- Yuan, X., Lu, Z., Yao, H., Tan, X., Zhao, Y., Tang, C., Cheng, M., & Gao, Y. (2022). Engineering Properties and Applications of Air- Foamed Lightweight Soil. *Advances in Materials Science and Engineering*, 2022, 4967037. <https://doi.org/10.1155/2022/4967037>
- Zenkert, D., & Burman, M. (2009). Tension, Compression and Shear Fatigue of a Closed Cell Polymer Foam. *Composites Science and Technology*, 69, 785- 792. <https://doi.org/10.1016/j.compscitech.2008.04.017>
- Zhang, C., Li, J., Hu, Z., Zhu, F., & Huang, Y. (2012). Correlation between the acoustic and porous cell morphology of polyurethane foam: Effect of interconnected porosity. *Materials & Design*, 41, 319- 325. <https://doi.org/10.1016/j.matdes.2012.04.031>
- Zhang, R., & Ulery, B. (2018). Synthetic Vaccine Characterization and Design. *Journal of Bionanoscience*, 12, 1-11. <https://doi.org/10.1166/jbns.2018.1498>
- Zhou, Y., Gong, J., Jiang, L., & Chen, C. (2018). Orientation effect on upward flame propagation over rigid polyurethane foam. *International Journal of Thermal Sciences*, 132, 86-95. <https://doi.org/10.1016/j.ijthermalsci.2018.04.037>
- Zieleniewska, M., Leszczyński, M. K., Szczepkowski, L., Bryśkiewicz, A., Krzyżowska, M., Bień, K., & Ryszkowska, J. (2016). Development and applicational evaluation of the rigid polyurethane foam composites with egg shell waste. *Polymer Degradation and Stability*, 132, 78-86.

CHAPTER III

COMPRESSIVE STRENGTH AND MORPHOLOGY OF RIGID POLYURETHANE FOAM FOR ROAD APPLICATIONS

3.1 Introduction

Road construction is the leading utility that drives national and global economies. For convenient transportation, road construction often occurs in areas where soil conditions are unsuitable for supporting the load of the road structure. But it is necessary to take action to drive the economy in the area. Engineering soil improvement techniques are often used to make the soil layer suitable for carrying loads. One popular method is the deep mixing and jet grouting technique with cement paste as the binder, often called Soil Cement Column (SCC). With much expertise, it's convenient and fast. However, in the working process, it is necessary to use high pressure to inject the binder. The soil mass structure is disturbed by changes in stress and strain conditions the vertical movement of the soil mass. The ground surface is elevating. And lateral displacement throughout the depth results in a varying diameter of the SCC (Wang et al., 2013), which directly affects the load-bearing capacity. Shen et al. (2013) presented a generalized approach for the prediction of jet grout column diameter based on the theoretical framework of turbulent kinematic flow and soil erosion. Flora et al. (2013) The kinetic energy at the nozzle position versus the field experiment results. In addition,

computer processing by an artificial neural network (ANN) model is also optimized using differential evolution (DE) and a network model. bidirectional long short-term memory (Bi-LSTM) (Ochmaski et al., 2015; Atangana Njock et al., 2021; Shen et al., 2021). Despite attempts to resolve unevenness by forecasting on-field conditions, implementing it is still challenging. In addition, because many other factors affect the diameter consistency of SCC, lightweight materials are used to replace conventional materials in the construction process.

The development of lightweight materials for the construction industry has been continuing for a long time to improve their engineering properties at reasonable production costs. Lightweight materials are continually manufactured under various concepts with the main objective of reducing the load on the structural system (Lee & Ramesh, 2004; Sulong et al., 2019). Due to the superior properties of foam when compared to other similar lightweight materials, the foam is often considered as the first priority. Foam applications may also be found in other forms, such as electronic and automotive equipment, food packaging, and thermal insulation in aerospace industries (Eaves, 2004; Ashida, 2006; Wellnitz, 2007; Das et al., 2017). In the construction industry, it is often used as the core of the structural insulated panel, principal exterior wall, framing, partition wall, roof, floor, and structural framing (Manalo, 2013; Chen & Hao, 2014; Chen et al., 2015).

In addition to being used as a component of building structures, foam materials can be used in the construction of roads and highways to overcome the settlement problem. In 1965, expanded polystyrene (EPS) foam was used as insulation in road construction in Norway. In 1972, the Norwegian Public Roads Authority developed a standard for the use of EPS foam as a lightweight material to replace the traditional backfill material in road construction projects. It was found that the EPS foam successfully minimized the settlement of the road structure (Frydenlund, 1991; Frydenlund & Aabøe, 2001; Norwegian Public Roads Administration (NPRA), 2002; Aabøe & Frydenlund, 2011). Norway is therefore the pioneering country in the use of foam in construction projects. In the early 1980s, the EPS foam was used in construction projects in Europe, the USA, and Japan and has become more popular since then (Sanders, 1996; National Cooperative Highway Research Program (NCHRP), 2004).

The EPS foam has been widely applied to geotechnical engineering applications such as improved slope stability, retaining wall structures, and fill material for road and bridge approaches (Refsdal, 1985; Duskov, 1991; Duskov, 1997; Jutkofsky et al., 2000; Negussey, 2002; Riad et al., 2003; Stark et al., 2004; Meguid et al., 2017).

Polyurethane foam (PUF) is a plastic foam in the same group of polymer foam group as EPS foam but it is manufactured more safely because the manufacturing process of PUF is simple and does not require flammable gasses such as Butane (C_4H_{10}) or Pentane (C_5H_{12}). PUF was first synthesized in 1937 by Otto Bayer through a reaction between polyester diol and diisocyanate (Ionescu, 2005; Prisacariu, 2011; Sharmin & Zafar, 2012; Szycher, 2013). PUF is produced by polymerizing two organic compounds : isocyanates in the NCO group and hydroxyl alcohol, resulting in a urethane group with polymerization. When the urethane decomposes, it produces carbon dioxide (CO_2), which causes bubbles inside the foam. At the same time, heat will be released (Herrington & Hock, 1997; Król, 2008). Figure 3.1 shows the urethane reaction diagram where R_{iso} is an isocyanate monomer and R_{polyol} is a polyol component (Ionescu, 2005). PUF is classified according to its structure into two types: flexible and rigid PU foams . The flexible PUF structure is connected by a strut network without wall cells (membrane) that rises under atmospheric pressure, called "open-cell". Because of its flexibility, low density, and lightweight, it is often used in furniture production as a cushioning material. The structure of the rigid PUF (RPUF) is similar to that of flexible PUF, but its cell walls are connected by the struts under pressure from the closed cells. It has a higher density than the flexible PUF, with a compressive strength in a range of 100–500 kPa (Padopoulos, 2005; Villasmil et al., 2009).

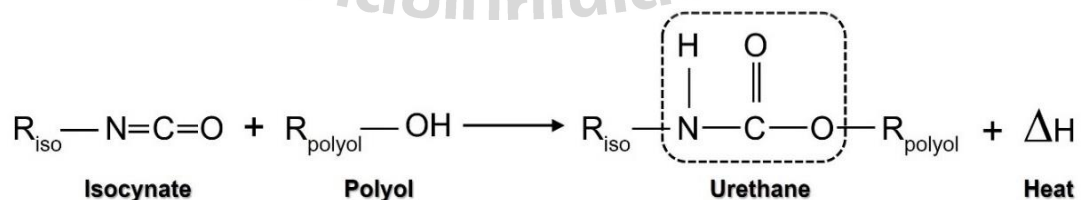


Figure 3.1 Reaction of urethane product (Ionescu, 2005).

In 2017, global use of PU foam was reported to have reached US\$60.5 billion. With a continued upward trend, it was estimated that by 2021, PU foam usage would be more than US\$79 billion. With advanced manufacturing technology and superior properties compared to other lightweight materials, PUF has gained a wide application popularity. Berardi and Madzarevic (2020) investigated the effect of microstructure and concentration of the foaming agent in PUF on the insulating properties over time. The results showed that the cell wall thickness increased over time, resulting in the reduced heat transfer. Stirna et al. (2011) investigated the mechanical properties of RPUFs. The test foam samples were obtained by drilling a sheet of RPUF produced by a pouring process under $22 \pm 2^\circ\text{C}$. Their density was in a range of $65\text{--}70 \text{ kg/m}^3$. Its mechanical properties, such as the compressive strength, depend on two factors working together: one is the covalent bonds of the polymer network. The other is polymer matrix and compaction energy of the foam, which are independent of covalent bonds.

Wiyono et al. (2016) studied physical and mechanical properties of RPUF made from a polyol and diisocyanate mixture at a 1:1 ratio. It was found that the cell structure was anisotropic and the compressive strength and elastic modulus linearly increased with foam density. Witkiewicz and Zieliński (2006) studied the mechanical properties of RPUFs at densities of 16 kg/m^3 and 62 kg/m^3 . The compressive strength depended on the structure of closed-cell foam, density, and temperature. Ridha and Shim (2008) investigated tensile strength, compressive strength, and the microstructure of RPUFs with three different densities. The authors reported that the cell foam was stretched when RPUF was under tensile force, indicating its anisotropic property; the strut was deformed under compression, shrunk from bending, and eventually failed. In other words, the deformation of the strut under load causes a loss of RPUF's capability due to the reduction in the force acting on the foam cell's longitudinal orientation.

Koyama et al. (2022) studied the dynamic uniaxial compressive properties of RPUF under seismic load using the stress control method with 0.1 Hz. The results reported showed that the dynamic properties depended on the RPUF's confining pressure direction and deformation direction. Linul et al. (2013) studied the factors

influencing the dynamic compressive strength of RPUFs with densities of 100 kg/m^3 , 160 kg/m^3 , and 300 kg/m^3 . The modulus, yield stress, and plateau stress increased with the increased density of RPUFs and the speed of loading, and material orientation under loading. To the authors' best knowledge, there has been no complete research undertaken on the effect of production factors on the compressive behavior and microstructure of RPUF, which is the focus of this research. The studied production factors included polymer content, polyol to isocyanate ratio, and mixing temperature of polyol and diisocyanate. The scanning electron microscope (SEM) technique was utilized to explain the compressive behavior of RPUF under the various production factors. The outcome of this study will facilitate the road engineers and manufacturers to select the suitable production factors to develop RPUF with a target compressive strength at a reasonable cost. This promotes the usage of the RPUF as a lightweight material for retaining structure and road applications, which has the simpler and safer production process with comparable properties than the traditional lightweight EPS foams.

3.2 Materials and Methods

3.2.1 Materials

The RPUF specimens in this study were made from various combinations of two liquid components: polyol and diisocyanate, at various temperatures. The diisocyanate was a combination of diphenylmethane diisocyanate, isomer, and homologs (4,4-methylene diphenyl diisocyanate (MDI)) (POLYONE-200), while the polyol was polyether polyol (POLY-225).

3.2.2 Preparation of Specimens

The RPUF specimen was prepared by mixing diisocyanate (D) and liquid polyol (P) at various ingredients. To prevent foam expansion due to the chemical interaction, the RPUF was prepared in a confined PVC mold with dimensions of 75 mm diameter and 200 mm height. As a result, the liquid foam underwent pressured compression, forming an interlocking closed-cell foam structure with a high cell density. The studied P contents were 23, 28, 34, 40, 45, 51 and 87 kg per 1 m^3 of the specimen and the difference mixture content of the two chemicals in terms of the

polyol to diisocyanate (p/d) ratios were 0.8, 0.9 and 1 to determine the effect of the mixture on the compressive strength and microstructure. The prepared RPUF specimen, along with the mold, was left in the laboratory for three hours. This was to make sure that the foaming process had fully taken place and allowed the reaction heat to be decreased to room temperature. Subsequently, the RPUF specimen was demolded and trimmed to have a dimension of cubic 50 mm x 50 mm x 50 mm for compressive tests (Public Roads Administration, 1992). The ingredient of each RPUF mixture is summarized in Table 1.

3.2.3 Experimental Program

The tests were performed on RPUF specimens after 1 day of curing. For each test condition, test reports were based on the mean compressive strength values of five specimens to ensure the consistency of test results. In all tests, the deviation, SD, was found with $SD/x < 10\%$, in which x is the mean value of the test result.

3.2.3.1 Compressive Test

Compressive strength tests were performed in accordance with the Norwegian Directorate of Public Roads (Public Roads Administration, 1992). Cubic 50 mm x 50 mm x 50 mm specimens were tested by a universal testing machine (UTM), and the compressive strength was determined at 1% strain. Presently, there is no clear definition for the compressive strength of PUF material. It is dependent upon the purpose of users. However, ASTM (2017) has established a standard for extended polystyrene (EPS) geofoam materials. where the compressive strength at 1% strain is recommended as the typical design load limit of foam for general work.

Table 3.1 RPUF mixing proportion

Mix	Total Weight of p and d per Volume (kg/m ³)	Mixing Proportion (kg/m ³)		p/d ratio	Specimen Unit Weight (kg/m ³)
		Polyol (P)	Diisocyanate (D)		
P23p/d1.0	46	23	23	1.0	70
P28p/d1.0	56	28	28	1.0	73
P34p/d1.0	68	34	34	1.0	75
P40p/d1.0	80	40	40	1.0	78
P45p/d1.0	90	45	45	1.0	80
P51p/d1.0	102	51	51	1.0	82
P57p/d1.0	114	57	57	1.0	84
P23p/d0.9	48	23	25	0.9	72
P28p/d0.9	59	28	31	0.9	74
P34p/d0.9	71	34	38	0.9	77
P40p/d0.9	84	40	45	0.9	79
P45p/d0.9	95	45	50	0.9	81
P51p/d0.9	108	51	57	0.9	83
P57p/d0.9	119	57	63	0.9	86
P23p/d0.8	52	23	29	0.8	77

Table 3.1 RPUF mixing proportion (Continued)

Mix	Total Weight of p and d per Volume (kg/m ³)	Mixing Proportion (kg/m ³)		p/d ratio	Specimen Unit Weight (kg/m ³)
		Polyol (P)	Diisocyanate (D)		
P28p/d0.8	65	28	36	0.8	79
P34p/d0.8	77	34	42	0.8	83
P40p/d0.8	89	40	49	0.8	85
P45p/d0.8	102	45	56	0.8	89
P51p/d0.8	114	51	63	0.8	92
P57p/d0.8	127	57	70	0.8	94

Since the RPUF is a manufactured temperature-dependent material, the mixing temperatures of P and D were varied at 25°C, 40°C, 50°C, and 60°C to determine the effect of temperature on compressive strength as well as the microstructural characteristics of RPUF at different p/d ratios and P contents. The P and D were heated in a basin at the target temperatures, as shown in Figure 3.2, for 1.5 hours. The temperatures of heated P and D were measured using an infrared thermometer, which is commonly used in the manufacturing sectors and capable of measuring temperatures from -50 °C to 400 °C with a resolution of 0.1 °C and a measurement error of only 1.0 °C.



Figure 3.2 Temperature control bath and device

3.2.3.2 Scanning Electron Microscopy (SEM)

The microstructural investigation on RPUF was performed via scanning electron microscopy (SEM). The specimens were prepared at various P contents, p/d ratios, and mixing temperatures of P and D. The SEM specimens were gold-coated (Sukmak et al., 2013). The SEM analysis was based on the X-ray energy dissipation theory using the Tescan brand (model MIRA), manufactured from the Czech Republic. This testing machine meets world-class standards. In addition, the tests were performed by experienced material microstructural analysis scientists. Over ten years of work have made SEM data analysis results highly reliable. The SEM images were analyzed to evaluate the role of P content, p/d ratio, and temperature on the microstructural changes.

3.3 Results

3.3.1 Compressive Strength for Ambient Mixing Temperature

The compressive strength at 1% strain of the RPUF specimens at various P contents with p/d ratios of 1.0, 0.9, and 0.8 at ambient mixing temperature (25 °C) is presented in Figure 3.3. The higher P content resulted in a greater compressive strength for the same p/d ratio. For instance, specimens with $P = 57 \text{ kg/m}^3$ exhibited the highest compressive strength for all p/d ratios tested when compared to the specimens with other lower P contents. Specimens P57p/d1.0, P57p/d0.9 and P57p/d0.8 (P content = 57 kg/m^3) had the highest compressive strengths of 0.22, 0.24, and 0.26 MPa, respectively while specimens P23p/d1.0, P23p/d0.9 and P23p/d0.8 ($P = 23 \text{ kg/m}^3$) had

the lowest compressive strengths of 0.11, 0.11, and 0.11 MPa, respectively. The lower p/d ratio resulted in the higher compressive strength for the same P content. The compressive strength of RPUF with P23 and P28 was between the lower and upper limits (0.015 MPa and 0.128 MPa) of EPS gefoams according to ASTM D6817 (ASTM., 2017). However, the RPUF with higher P contents was found to have greater compressive strength than the upper limit for all p/d ratios studied.

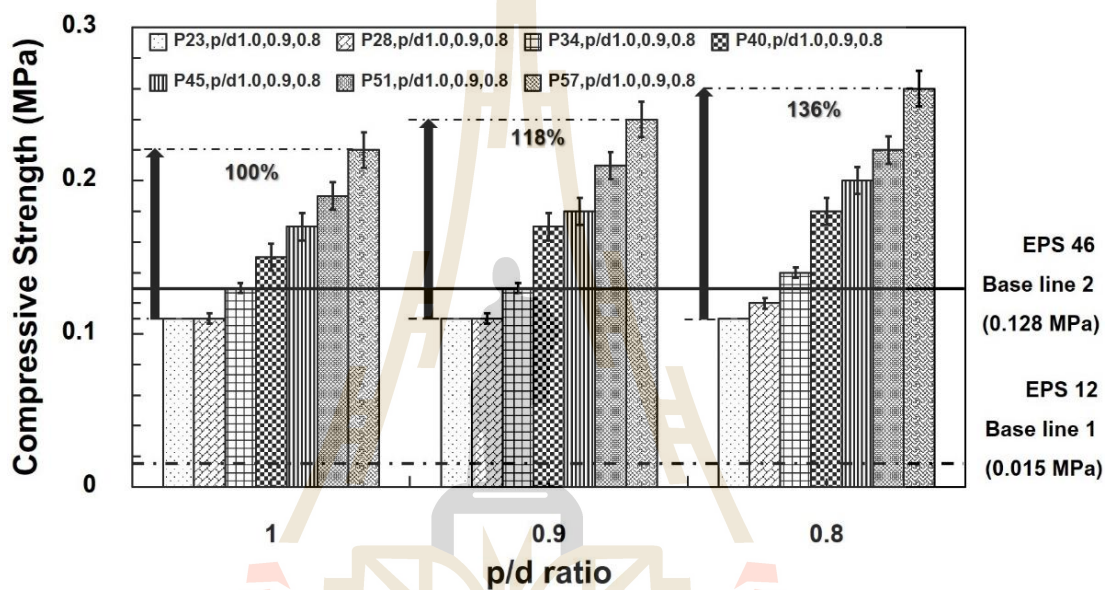


Figure 3.3 Compressive Strength of RPUF for ambient mixing temperature

The increase in P content from 23 to 57 kg/m³ increased compressive strength by 100%, 118%, and 136% for p/d ratios of 1.0, 0.9, and 0.8, respectively. For a given P content at ambient mixing temperature, increasing the D content (decreasing the p/d ratio) results in a higher amount of chemically reactive urethane and urea, which leads to the stronger hydrogen bonds in the hard segments, to strengthen the foam structure network. The high D content causes a large amount of urea and when the urea decomposes, only CO₂ is left while the pressure inside the cell is retained (Ashida, 2006; Shufen et al., 2006; Wellnitz, 2007; Prisacariu, 2011; Szycher, 2013). This CO₂ results in a high cell-contact pressure and hence the higher strength was evident at a lower p/d ratio.

3.3.2 Stress-Strain Relationship

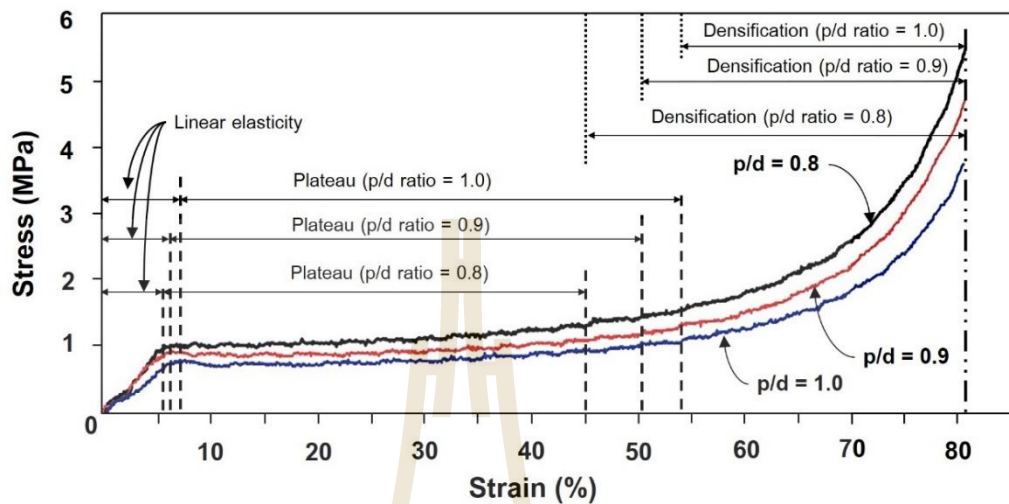


Figure 3.4 Compressive stress-strain relationship of RPUF prepared at ambient temperature

Figure 3.4 shows the stress-strain relationship under the compression strength test on RPUF specimens P28 series prepared at ambient mixing temperature and different p/d ratios. The stress-strain relationships at all p/d ratios were similar. Walter et al. (2005) reported that although the strength of the RPUF was different, the relationship between stress and strain was similar under the compression and tensile tests. The stress-strain relationship of RPUF consisted of three regions: the elastic, plateau, and densification regions. The elastic behavior started from the position where the stress was equal to zero and increased to the first yield stress, during which elastic bending stress occurs at the cell edge. The plateau behavior occurred later when the stress was increased sufficiently to cause the cell edge to deform until it is unable to recover into the plastic bending of the edge state. The strain increased while the stress remained almost constant. Densification occurs after a cell collapses due to deflection of the cell wall. The deflection of the cell wall results in the compression of the intracellular space, resulting in a sharp increase in the compressive stress with increasing the strain. The strain at the start of this densification state is called the densification strain (Ashby & Lu, 2003; Outlet et al., 2006).

Figure 3.4 depicts the effect of the p/d ratio on stress-strain behavior. The results showed that at lower p/d ratios of 0.9 and 0.8, linear elastic, plateau, and densification zones started at lower strain with higher yield stress and compressive strength when compared to the case where the p/d ratio was 1.0. Densification strains of RPUF specimens were 45%, 50%, and 54% for p/d ratios of 1.0, 0.9, and 0.8, respectively. The longer densification zone was found for the lower p/d ratio.

However, the stress-strain relationship of the semi-rigid PUF structure has a smooth transition from the elastic to the plateau ranges; without a clear traction point due to no drop in stress (Linul et al., 2013; Leng et al., 2017; Movahedi & Linuk 2017; Serrano et al., 2017; Gunther et al., 2018). The energy absorption capacity of RPUF per unit volume can be illustrated by the area under the stress-strain diagram. When considering the area under the diagram in Figure 3.4, the RPUF absorbed more energy when the p/d ratio was lower. The energy absorbed by the RPUF decays continuously as the foam progresses from the plateau region to densification (Lu and Yu. 2003). The compressive test results at the ambient mixing temperature revealed that the lower p/d ratio and the higher P content yielded the higher compressive strength and toughness (energy absorbability).

3.3.3 Influence of Mixing Temperature

Figure 3.5 shows the compressive strength at 1% strain versus mixing temperature of RPUF specimens at different P contents (P23, P28 and P34) and p/d ratios. The specimens P23 and P28 seires at ambient mixing temperature had compressive strengths lower than the upper limit of 0.128 MPa for EPS foam specified by ASTM D6817. However, the elevated mixing temperature could booth up the compressive strength.

The role of p/d ratio on the compressive strength of the RPUF at high temperatures ($> 40^{\circ}\text{C}$) was different from that at ambient temperature. For all P contents studied, the compressive strength of RPUF prepared at $> 40^{\circ}\text{C}$ mixing temperature decreased with the decrease in p/d ratio. For low P contents of 23 and 28 kg/m³, an increase of mixing temperature from 25°C to 40°C increased the compressive strength of the specimen for a given p/d ratio (Figure 3.5(a) and (b)).

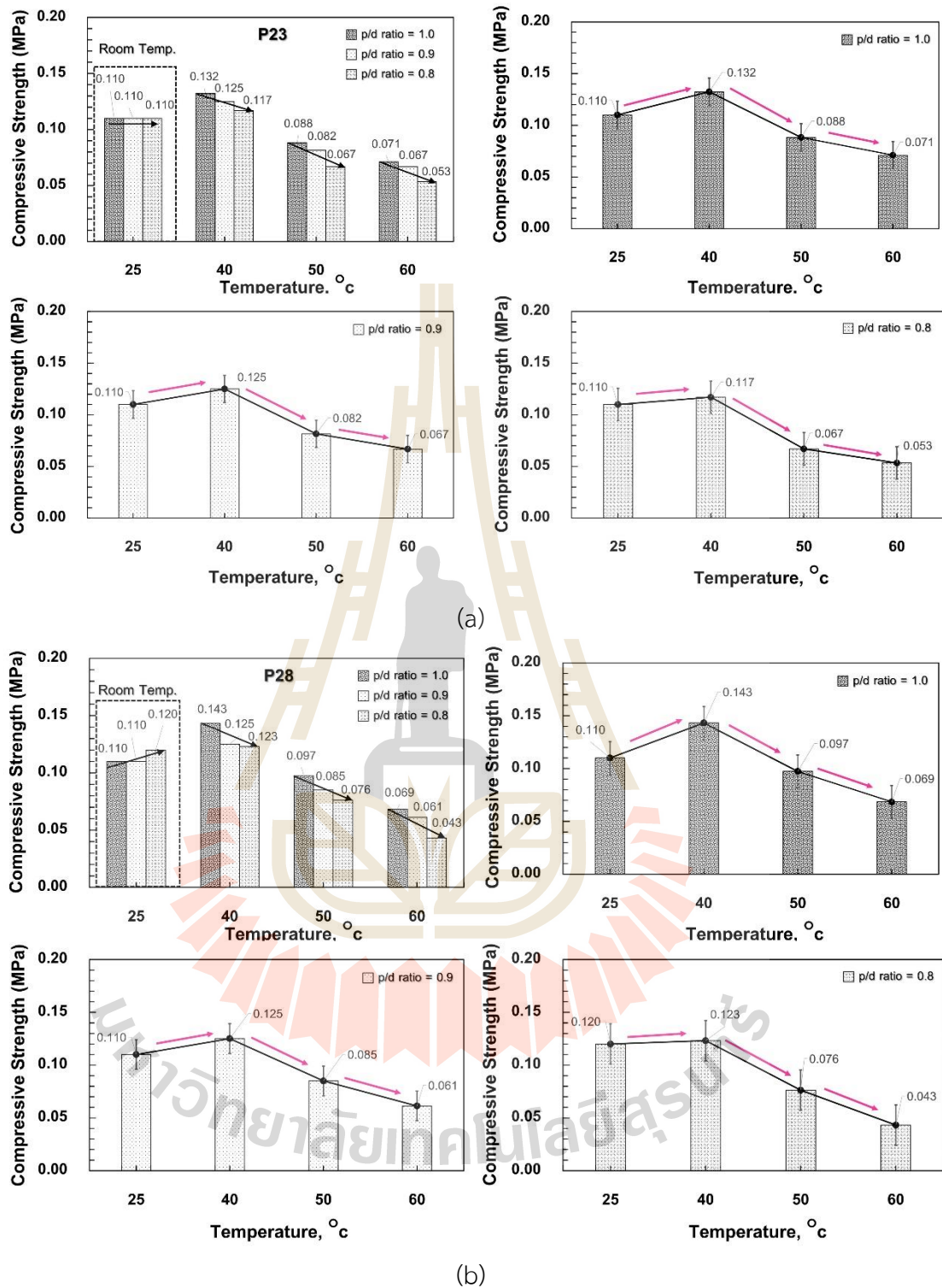


Figure 3.5 Effect of P content and mixing temperature on compressive strength

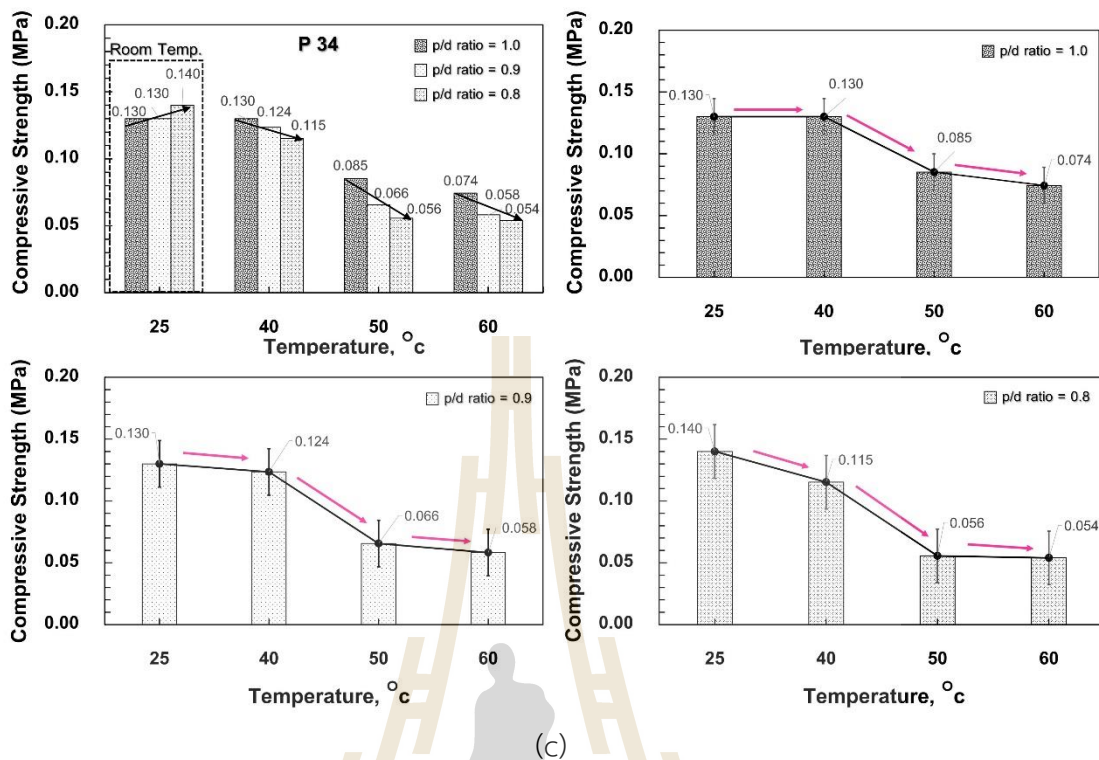


Figure 3.5 Effect of P content and mixing temperature on compressive strength
(Continued)

The same is not true for high P content of 34 kg/m^3 . For all p/d ratios, the increased mixing temperature from 25°C to 40°C caused the reduction in compressive strength. The compressive strengths of RPUF at mixing temperatures $\geq 40^\circ\text{C}$ were found to be lower than the compressive strength of RPUF at 25°C mixing temperature for all p/d ratios (Figure 3.5(c)). In other words, the ambient mixing temperatures was the most suitable for high P content of 34 kg/m^3 . To meet the upper limit of 0.128 MPa for EPS foam, the increased temperature could improve compressive strength at low P contents of 23 and 28 kg/m^3 ; the 40°C and $p/d = 1$ were considered as the best ingredient. Figure 3.6 shows the damage characteristics of the RPUF specimens due to the elevated temperature (40°C to 60°C) and the decreased p/d ratios at P content = 23 kg/m^3 . The most serious damage was found at a mixing temperature of 60°C and p/d ratio of 0.8 (Figure 3.6(c)). This indicated that the macro-

cracks and pore space were larger with a higher mixing temperature and lower p/d ratio.

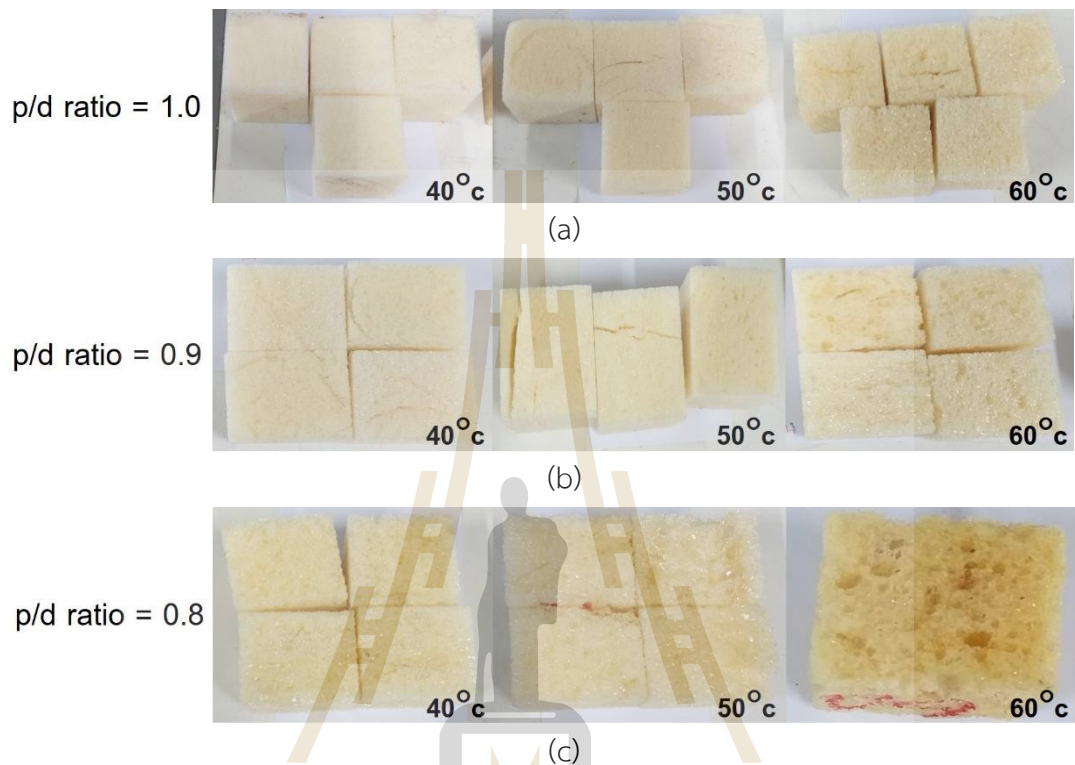


Figure 3.6 RPUF specimens with various mixing temperatures and p/d ratios at P content = 23 kg/m^3

At a mixing temperature of 40°C , the specimen with p/d ratio = 1.0 had a relatively complete structure compared to the specimens with higher temperatures and lower p/d ratios. As such, the specimen with p/d ratio = 1.0 and 40°C mixing temperature exhibited the highest compressive strength. Comparing Figure 3.6(a) with Figure 3.6(c) at the same mixing temperature, a decrease in p/d ratio increased foam cell-contact pressure as seen by more micro-cracks in the RPUF. In addition, with excess amount of D (p/d = 0.8), some parts of the D did not react with the monomer link (Jiao et al. 2013), causing liquid isocyanate residual in the test specimen.

It is therefore evident from Figure 3.6 that for low P contents of 23 and 28 kg/m^3 , the elevated mixing temperature of P and D to 40°C resulted in the rapid

gasification reaction and high cell-contact pressure, hence high compressive strength. However, the excessive mixing temperatures ($> 40^{\circ}\text{C}$) and very low p/d ratio led to the extremely large cell-contact pressure; and eventually the large macro-cracks generated within the foam. This led to the reduced compressive strength. It was noted that the higher mixing temperature of P and D resulted in more cracks than the decreased p/d ratios. For high P content of 34 kg/m^3 , both the increased mixing temperature and reduced p/d ratio caused the excessive large cell-contact pressure and hence the reduction in compressive strength. The data showed a tendency that if using higher amounts of polyol than diisocyanate (p/d ratio > 1.0), it may result in lower compressive strength due to incomplete reaction. On the other hand, using a very high amount of diisocyanate (p/d ratio < 0.8) will decrease the compressive strength due to foam cell wall damage. Increasing the content of chemicals in both cases increases the production cost.

3.4 Microstructural Analysis

Figure 3.7 shows the chemical composition analysis of the RPUF specimens at P content of 23 kg/m^3 and p/d ratio of 1.0 with mixing temperatures in the range of 40°C to 60°C using Energy Dispersive X-Ray Spectroscopy (EDS). The cell wall and the monomer link were mainly composed of carbon (C) and oxygen (O), forming covalent bonds, strengthening the hard segment through urethane linkage, and increasing the compressive strength (Thirumal et al., 2008). The EDS result showed that the change in mixing temperature did not alter the chemical compositions of the RPUF structure as seen by the similar amount of C and O. In other words, the compressive strength development with mixing temperature and p/d ratio did not result from the change in chemical compositions.

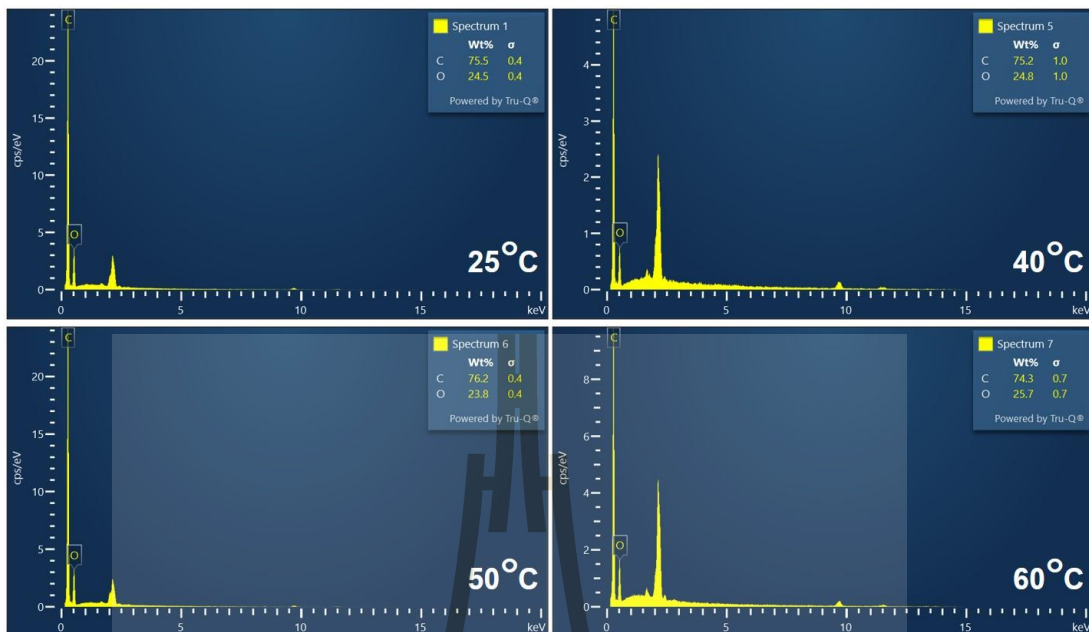


Figure 3.7 EDS analysis results of RPUF specimens at P content of 23 kg/m^3 and p/d ratio of 1.0

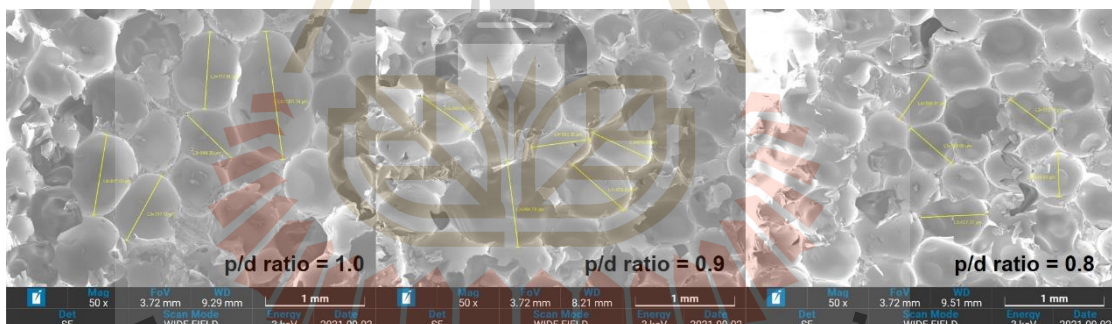


Figure 3.8 Foam cells of RPUF specimens at P content of 28 kg/m^3

The microstructure and cellular structure morphology of the RPUF specimens at $P = 28 \text{ kg/m}^3$ with different p/d ratios were studied via SEM analysis as illustrated in Figure 3.8. The specimens were prepared at the mixing temperature of 40°C , which exhibited the highest compressive strength, to investigate the role of the decreased p/d ratio on compressive strength. The equivalent diameter per SEM image frame ($3,700 \mu\text{m} \times 2,800 \mu\text{m}$) of each specimen was measured. The SEM image showed that

the foam cells were polygonal in shape and the cell diameters varied across the specimen's section.

The data from the SEM images were statistically analyzed in the form of a frequency-distribution diagram of the mean cell foam diameter in the SEM image frame, as shown in Figure 3.9. The mean diameters of RPUF specimens were $691 \pm 116 \mu\text{m}$, $622 \pm 122 \mu\text{m}$, and $681 \pm 25 \mu\text{m}$ for p/d ratios of 1.0, 0.9, and 0.8, respectively. This indicates that foam cell size varied with the p/d ratio. Figure 3.10 shows the percent distribution of foam cells with various ranges of foam cell size for the p/d ratios of 1.0, 0.9 and 0.8 in the SEM image frame. It is worthwhile mentioning that the majority of the cells in specimens was greater than $400 \mu\text{m}$, $300 \mu\text{m}$ and $200 \mu\text{m}$ for p/d ratios of 1.0, 0.9 and 0.8, respectively. The specimens with the lowest p/d ratio of 0.8 possessed the lowest volume of $> 800 \text{ mm}$ foam cells while the specimens with the highest p/d ratio of 1.0 possessed the highest volume of $> 800 \text{ mm}$ foam cells. This implied that the lower p/d ratio was associated with the more small sized foam cells.

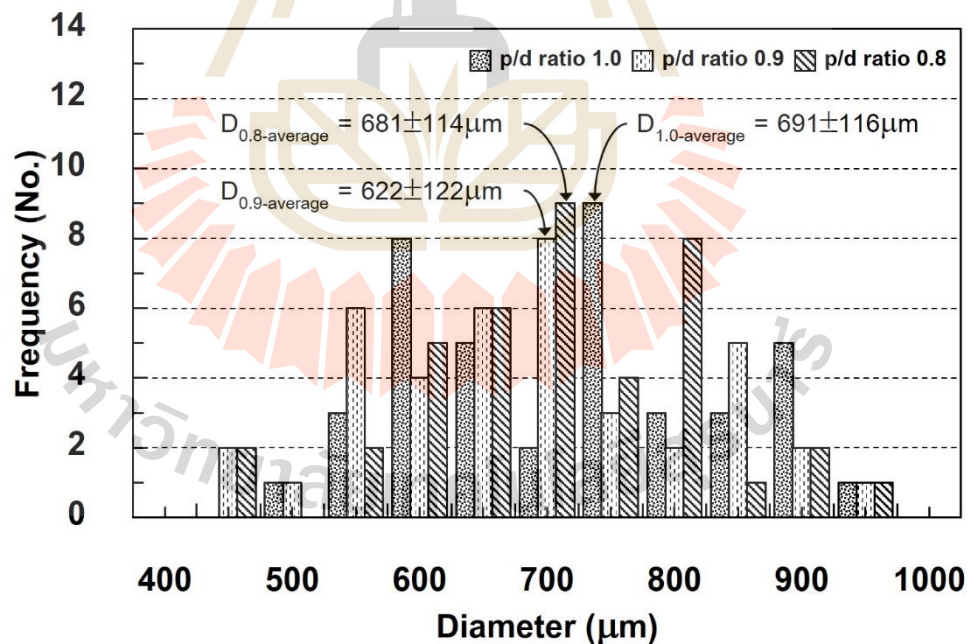


Figure 3.9 Distribution of foam cell diameters of RPUF specimens at P content of 28 kg/m^3

Hejna et al. (2017) investigated the cell size of RPUF at p/d ratios of 1.5, 2.0, and 2.5 and reported that an increase in D content (decrease in p/d ratio) tended to decrease the foam cell size, which was associated with an increase in crosslink density due to the rise in allophanate and biuret groups. Consequently, a decrease in the p/d ratio increased the specimen's density, as shown in Table 3.1. In other words, the low-density specimen has larger cell size than the high-density specimen. Considering the minimum energy principle of thermodynamics, the increased contact area between the cells results in more energy at the contact surfaces.

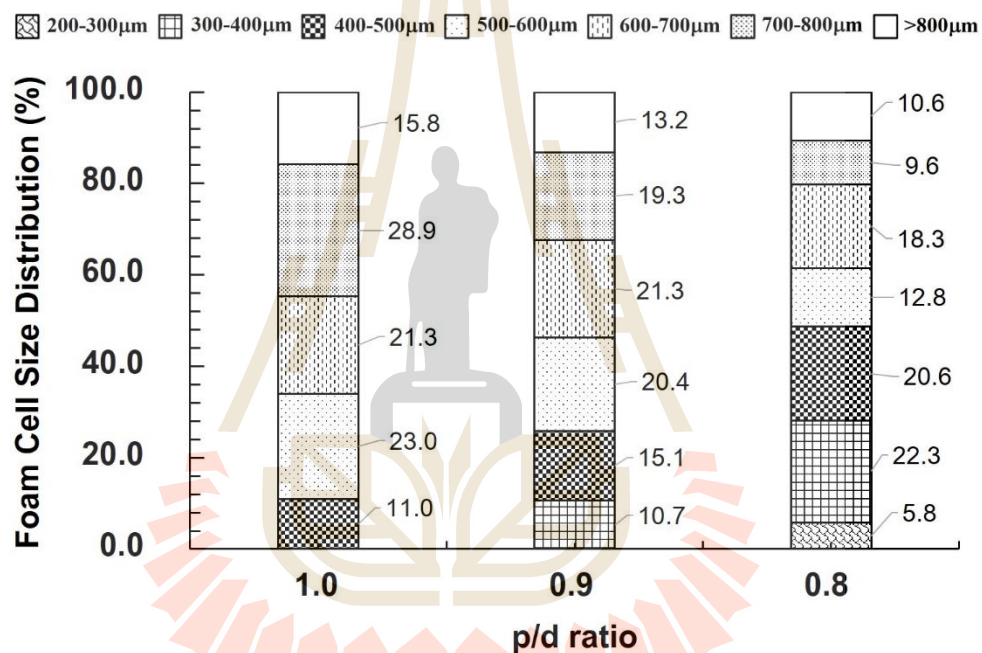


Figure 3.10 Distribution of foam cell for different ranges of cell size of RPUF specimens at P content of 28 kg/m³

Figure 3.11 shows the closed foam cell structure of specimens at P = 28 kg/m³ with different p/d ratios at the mixing temperature of 40°C. The cell wall deformation due to the cell-contact pressure can be observed for different p/d ratios. The cell structure with a p/d ratio of 1.0 was subjected to less deformation (less pressure) than the cell structures with p/d ratios of 0.9 and 0.8, respectively, which is associated with the relatively complete specimen (Figure 3.6). The very high D (very low p/d ratio)

caused an excessive amount of urea and CO_2 . When CO_2 decomposed the extremely large cell-contact pressure developed and resulted in large damage (macro-cracks).

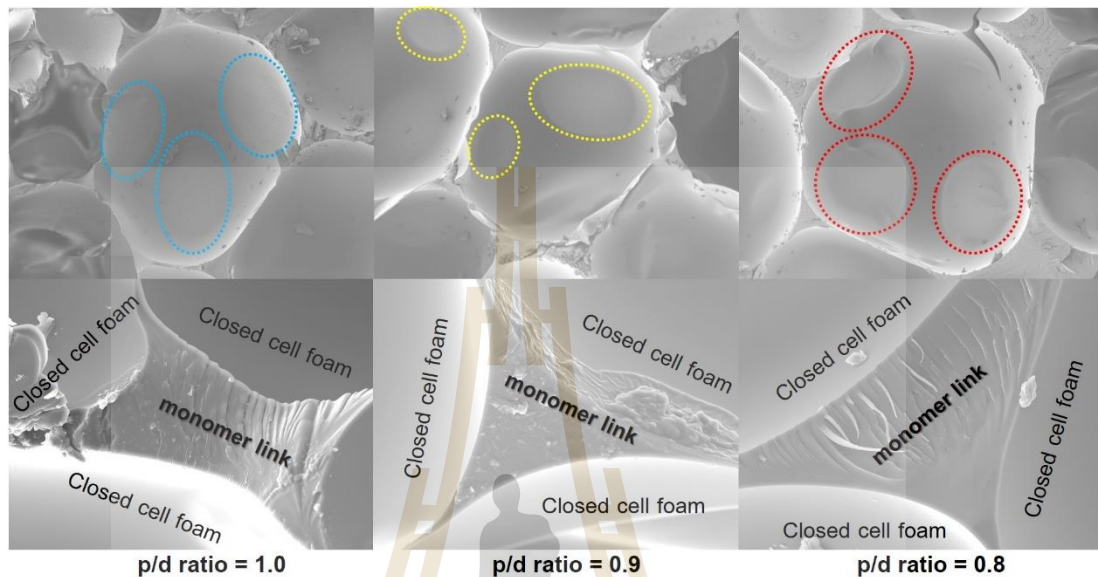


Figure 3.11 Closed cell structure of RPUF at different p/d ratios at 40°C mixing temperature and P content of 28 kg/m^3 for p/d ratios a) 1.0, b) 0.9 and c) 0.8.

Figure 3.12 shows the results of SEM analysis at 50 times magnification of RPUF specimens at P content = 28 kg/m^3 with different mixing temperatures and p/d ratios. At a mixing temperature of 25°C, as shown in Figure 3.12(a), the cell wall damage (indicated by the dotted circle) increased with decreasing the p/d ratio, which is approximately 8%, 15%, and 27% of the total cell for the p/d ratios of 1.0, 0.9, and 0.8, respectively, compared to the total number of cells in each image. However, even with larger damage, the higher cell-contact pressure resulted in higher compressive as seen by the highest strength at p/d ratio of 0.8.

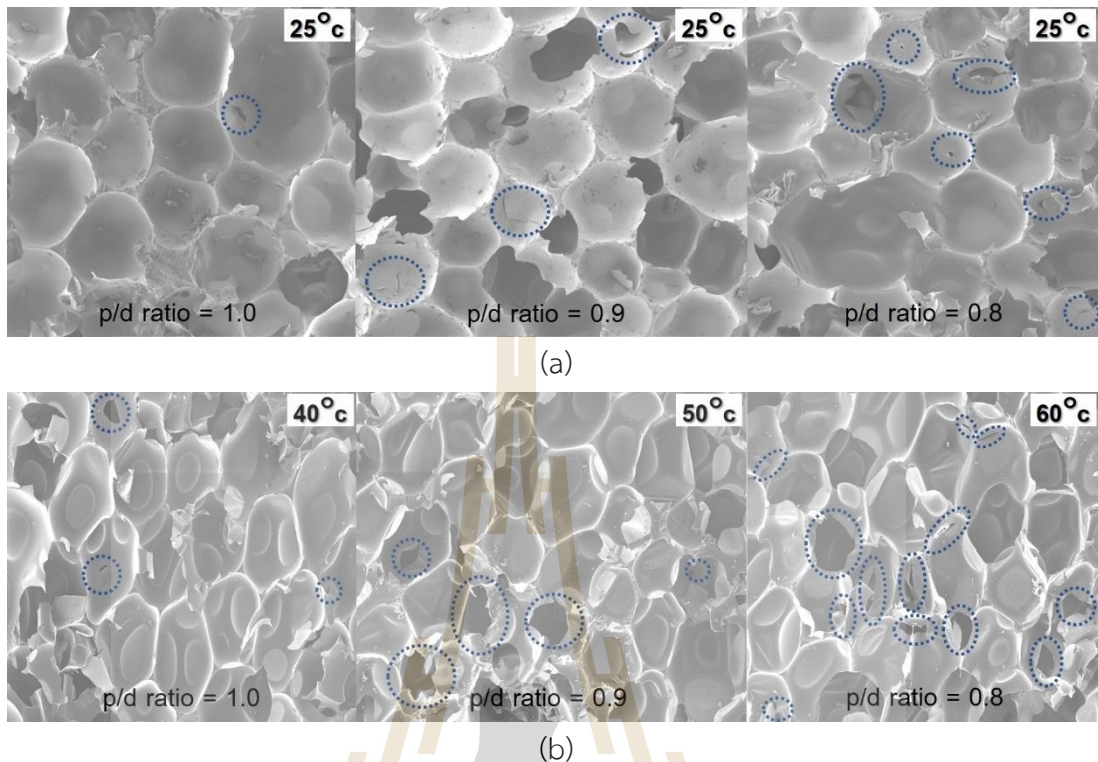


Figure 3.12 Closed cell structure of RPUF at P content of 28 kg/m^3 for a) mixing temperature of 25°C and p/d ratios of 1.0, 0.9 and 0.8 and b) mixing temperature of 40, 50 and 60°C and p/d ratios of 1.0, 0.9 and 0.80

Comparing Figure 3.12(a) to Figure 3.12(b), it was evident that the cell size was dependent upon both the mixing temperature and p/d ratio. The higher mixing temperature and the lower p/d ratio resulted in the smaller cell size and the higher cell-contact pressure. At a mixing temperature of 40°C with p/d ratio of 1.0, the cell foam damage was less than that with lower p/d ratios, as shown in Figure 3.12(b). At p/d of 0.9, when the mixing temperature was raised from 25°C to 50°C , the cell damage increased to 19%, while at p/d ratio of 0.8, when the temperature was raised from 25°C to 60°C , the cell damage increased to 34% compared to the total number of cells.

From the critical analysis of the test results, it was evident that the cell-contact pressure controlled the strength development. With the increase in mixing temperature and the reduction in p/d ratio, the sufficient cell-contact pressure

enhanced the strength and toughness improvement whereas the extremely high cell-contact pressure damaged the foam cell and caused the strength and toughness reduction.

3.5 Conclusions

This research investigated the role of production factors on the compressive strength development of rigid polyurethane foam (RPUF). The production factors included polyol (P) content, polyol to diisocyanate (p/d) ratio and mixing temperature of polyol to diisocyanate (D). The microstructure and morphology of RPUF were investigated to understand the mechanism controlling the compressive strength development with various production factors and to suggest the optimal production factors. The following conclusions can be drawn from this research study:

1) The stress-strain relationship of RPUF was found to have three zones: linear, plateau and densification. At ambient mixing temperature, for a given P content, the lower p/d ratio resulted in the lower strains at the start of each zone and higher yield stress, toughness and compressive strength.

2) Unlike at the ambient mixing temperature (25°C), for a particular P content, the compressive strength of RPUF prepared at high temperatures (> 40°C) decreased with the decrease in p/d ratio. For low P contents of 23 and 28, an increase of mixing temperature from 25°C to 40°C increased the compressive strength of RPUF for a given p/d ratio. However, for high P content of 34 kg/m³, the increased mixing temperature from 25°C to 40°C caused the reduction in compressive strength. In other words, the ambient mixing temperatures were the most suitable for high P content of 34 kg/m³.

3) The EDS results showed the unchanged compositions in the RPUF structure with the elevated mixing temperatures as seen by the similar amount of C and O for all the mixing temperatures tested. The compressive strength development with mixing temperature did not result from the chemical bonding development but was due to the increased cell-contact pressures.

4) The microstructural analysis results showed that both the elevated the mixing temperature and reduced p/d ratio stimulated gasification, resulting in the small-sized cells with high cell-contact pressures. The sufficient cell-contact pressure

increased the compressive strength of RPUF and toughness while the extremely large cell-contact pressure caused the cell damage and the reduction in strength and toughness. At low P content, both the elevated mixing temperature to 40°C and the reduced p/d ratio improved compressive strength of RPUF. However, at high P content, the elevated mixing temperature resulted in the cell damage; the reduced p/d ratio was recommended to enhance the compressive strength.

5) To meet the upper limit of 0.128 MPa for EPS foam, the increased mixing temperature from ambient to 40°C could improve compressive strength at low P contents of 23 and 28 kg/m³; the 40°C and p/d ratio of 1 were the best ingredient. The ambient mixing temperature and p/d = 0.8 were however the best for high P content. With high cost of P and D, the usage of low P content of < 28 kg/m³ with 40°C mixing temperature is therefore recommended in practice.

6) The outcome of this research will promote the usage of the RPUF as a lightweight material in geotechnical structures such as retaining wall and road embankment. It had a comparable compressive strength to EPS but with safer manufacturing process. The RPUF can also be adopted as a filling material under eroded geotechnical structures such as road concrete pavement and bridge approach slab due to its large expansion nature.

3.6 References

- Aabøe, R., and Frydenlund, T.E. 2011. "40 Years of experience with the use of EPS geofom blocks in road construction". In Proc., The Use of Geofom Block in Construction Application 4th Int. Conf., 1-14. Lillestrom, Norway. (2011).
- Ashby, M., & Lu, T. (2003). Metal foams: A survey. *Science in China (B)*, 46, 521-532. <https://doi.org/10.1360/02yb0203>
- Ashida, K. 2006. Polyurethane and Related Form: Chemistry and Technology. Boca Raton, USA: CRC Press.
- ASTM. (2017). Standard Specification for rigid cellular polystyrene geofom. ASTM D6817-07, West Conshohocken, PA.

- Atangana Njock, P. G., Shen, S.-L., Zhou, A., & Modoni, G. (2021). Artificial neural network optimized by differential evolution for predicting diameters of jet grouted columns. *Journal of Rock Mechanics and Geotechnical Engineering*, 13(6), 1500-1512. <https://doi.org/10.1016/j.jrmge.2021.05.009>
- Berardi, U., & Madzarevic, J. (2019). Microstructural analysis and blowing agent concentration in aged polyurethane and polyisocyanurate foams. *Applied Thermal Engineering*, 164, 114440. <https://doi.org/10.1016/j.applthermaleng.2019.114440>
- Chen, W., & Hao, H. (2014). Experimental and numerical study of composite lightweight structural insulated panel with expanded polystyrene core against windborne debris impacts. *Materials & Design*, 60, 409–423. <https://doi.org/10.1016/j.matdes.2014.04.038>
- Chen, W., Hao, H., Hughes, D., Shi, Y., Cui, J., & Li, Z.-X. (2015). Static and dynamic mechanical properties of expanded polystyrene. *Materials & Design*, 69. <https://doi.org/10.1016/j.matdes.2014.12.024>
- Das, S., Heasman, P., Ben, T., & Qiu, S. (2017). Porous Organic Materials: Strategic Design and Structure–Function Correlation. *Chemical Reviews*, 117(3), 1515-1563. <https://doi.org/10.1021/acs.chemrev.6b00439>
- Duškov, M. (1997). Measurements on a flexible pavement structure with an EPS geof foam sub-base. *Geotextiles and Geomembranes*, 15(1), 5-27. [https://doi.org/10.1016/S0266-1144\(97\)00004-6](https://doi.org/10.1016/S0266-1144(97)00004-6)
- Duskov, M. 1991. “Use of expanded polystyrene (EPS) in flexible pavements on poor subgrades.” In Proc., Geotechnical Engineering for Coastal Development Int. Conf., 783-788. Yokohama, Japan.
- Eaves, D. 2004. Handbook of Polymer Foam. Shawbury, UK: Rapra Technology Ltd.
- Flora, A., Modoni, G., Lirer, S., & Croce, P. (2013). The diameter of single, double and triple fluid jet grouting columns: Prediction method and field trial results. *Géotechnique*, 63, 934-945. <https://doi.org/10.1680/geot.12.P.062>
- Frydenlund, T.E. 1991. Expanded Polystyrene: A Lighter Way across Soft Ground. Volume 1502. San Diego, CA.

- Frydenlund, T.E., and Aabøe, R. 2001. "Long Term Performance and Durability of EPS as a Lightweight Filling Material." In Proc., The Use of Geofom Block in Construction Application 3th Int. Conf., 1-15. Salt Lake City, USA.
- Günther, M., Lorenzetti, A., & Schartel, B. (2018). Fire Phenomena of Rigid Polyurethane Foams. *Polymers*, 10, 1166. <https://doi.org/10.3390/polym10101166>
- Hejna, A., Haponiuk, J., Piszczyk, Ł., Klein, M., & Formela, K. (2017). Performance properties of rigid polyurethane-polyisocyanurate/brewers' spent grain foamed composites as function of isocyanate index. *e-Polymers*, 17(5), 427-437. <https://doi.org/doi:10.1515/epoly-2017-0012>
- Herrington, R., and Hock, K. 1997. Flexible Polyurethane Foams. 2nd Ed., Midland, USA: Dow Chemical Co.
- Horvath, J., Ricci, A., Riad, H., & Osborn, P. (2003). *Expanded Polystyrene (EPS) Geofom for Road Embankments and Other Lightweight Fills in Urban Environments*.
- Ionescu, M. 2005. Chemistry and Technology of Polyols for Polyurethanes. Shawbury, UK: Rapra Technology.
- Jiao, L., Xiao, H., Wang, Q., & Sun, J. (2013). Thermal degradation characteristics of rigid polyurethane foam and the volatile products analysis with TG- FTIR- MS. *Polymer Degradation and Stability*, 98(12), 2687-2696. <https://doi.org/10.1016/j.polymdegradstab.2013.09.032>
- Jutkofsky, W. S., Teh Sung, J., & Negusse, D. (2000). Stabilization of Embankment Slope with Geofom. *Transportation Research Record*, 1736(1), 94-102. <https://doi.org/10.3141/1736-12>
- Koyama, A., Suetsugu, D., Fukubayashi, Y., & Mitabe, H. (2022). Experimental study on the dynamic properties of rigid polyurethane foam in stress-controlled cyclic uniaxial tests. *Construction and Building Materials*, 321, 126377. <https://doi.org/10.1016/j.conbuildmat.2022.126377>
- Król, P. 2008. Linear Polyurethane: Synthesis Method, Chemical Structure, Properties and Application. Boca Raton, USA: CRC Press.
- Lee, S-T., and Ramesh, N.S. 2004. Polymeric Foams: Mechanisms and Materials. Boca Raton, USA: CRC Press.

- Leng, W., Li, J., & Cai, Z. (2017). Synthesis and Characterization of Cellulose Nanofibril-Reinforced Polyurethane Foam. *Polymers*, 9, 597. <https://doi.org/10.3390/polym9110597>
- Linul, E., Marsavina, L., Voiconi, T., & Sadowski, T. (2013). *Study of factors influencing the mechanical properties of polyurethane foams under dynamic compression* (Vol. 451). <https://doi.org/10.1088/1742-6596/451/1/012002>
- Lu, G., and Yu, T.X. 2003. Energy absorption of Structure and material. Sawston, UK: Woodhead Publishing.
- Manalo, A. (2013). Structural behaviour of a prefabricated composite wall system made from rigid polyurethane foam and Magnesium Oxide board. *Construction and Building Materials*, 41, 642- 653. / <https://doi.org/10.1016/j.conbuildmat.2012.12.058>
- Meguid, M. A., Hussein, M. G., Ahmed, M. R., Omeman, Z., & Whalen, J. (2017). Investigation of soil-geosynthetic-structure interaction associated with induced trench installation. *Geotextiles and Geomembranes*, 45(4), 320-330. <https://doi.org/10.1016/j.geotexmem.2017.04.004>
- Movahedi, N., & Linul, E. (2017). Quasi-static Compressive Behavior of the Ex-situ Aluminum-alloy Foam-filled Tubes under Elevated Temperature Conditions. *Materials Letters*, 206, 182-184. <https://doi.org/10.1016/j.matlet.2017.07.018>
- National Cooperative Highway Research Program (NCHRP). 2004. Guideline and Recommended Standard for Geofoam Application in Highway Embankment. Project 529, Washington, DC.
- Negussey, D. 2002. Slope stabilization with geofoam. Report to FHWA and the EPS industry. Geofoam Research Center, Syracuse University.
- Norwegian Public Roads Administration (NPRA). 2002. Lightweight filling materials for road construction. Publication no.100, Oslo, Norway: Directory of Public Roads (Road Technology Department)
- Ochmański, M., Modoni, G., & Bzówka, J. (2015). Prediction of the diameter of jet grouting columns with artificial neural networks. *Soils and Foundations*, 55(2), 425-436. <https://doi.org/10.1016/j.sandf.2015.02.016>

- Ouellet, S., Cronin, D., & Worswick, M. (2006). Compressive response of polymeric foams under quasi-static, medium and high strain rate conditions. *Polymer Testing*, 25(6), 731-743. <https://doi.org/10.1016/j.polymeresting.2006.05.005>
- Papadopoulos, A. (2005). State of the Art in Thermal Insulation Materials and Aims for Future Developments. *Energy and Buildings*, 37, 77- 86. <https://doi.org/10.1016/j.enbuild.2004.05.006>
- Prisacariu, C. 2011. Polyurethane Elastomers from Morphology to Mechanical Aspects. New York, USA: Springer.
- Public Roads Administration. 1992. Quality Control of Expanded Polystyrene Used in Road Embankments 484E. Oslo, Norway: Road Research Laboratory.
- Refsdal, G. 1985. Plastic Foam in Road Embankments: Future Trends for EPS Use (Internal report). Oslo, Norway: Road Research Laboratory.
- Ridha, M., & Shim, V. P. W. (2008). Microstructure and Tensile Mechanical Properties of Anisotropic Rigid Polyurethane Foam. *Experimental Mechanics*, 48(6), 763-776. <https://doi.org/10.1007/s11340-008-9146-0>
- Sanders, R. L. (1996). "United Kingdom design and construction experience with EPS." Proceedings of International Symposium on EPS construction method (EPS TOKYO '96), Tokyo, Japan, 236-46.
- Serrano, A., Borreguero, A., Garrido, I., Rodríguez, J., & Carmona, M. (2017). The role of microstructure on the mechanical properties of polyurethane foams containing thermoregulating microcapsules. *Polymer Testing*, 60. <https://doi.org/10.1016/j.polymeresting.2017.04.011>
- Sharmin, E., & Zafar, F. (2012). Polyurethane: An Introduction. doi:10.5772/51663.
- Shen, S.-L., Atangana Njock, P. G., Zhou, A., & Lyu, H.-M. (2021). Dynamic prediction of jet grouted column diameter in soft soil using Bi-LSTM deep learning. *Acta Geotechnica*, 16(1), 303-315. <https://doi.org/10.1007/s11440-020-01005-8>
- Shen, S.-L., Wang, Z.-F., Yang, J., & Ho, C.-E. (2013). Generalized Approach for Prediction of Jet Grout Column Diameter. *Journal of Geotechnical and Geoenvironmental Engineering*, 139, 2060- 2069. [https://doi.org/10.1061/\(ASCE\)GT.1943-5606.0000932](https://doi.org/10.1061/(ASCE)GT.1943-5606.0000932)

- Shufen, L., Jiang, Z., Kaijun, Y., & Shuqin, Y. (2006). Studies on the Thermal Behavior of Polyurethanes. *Polymer-plastics Technology and Engineering - POLYM-PLAST TECHNOL ENG*, 45, 95-108. <https://doi.org/10.1080/03602550500373634>
- Stark, T.D., Arellano, D., Horvath, J.S., and Leshchinskyb, D. 2004. Geofam Applications in the Design and Construction of Highway Embankments, Project 24-11, Lllinois, USA: Transportation Research Board (TRB).
- Stirna, U., Beverte, I., Yakushin, V., & Cabulis, U. (2011). Mechanical properties of rigid polyurethane foams at room and cryogenic temperatures. *Journal of Cellular Plastics - J CELL PLAST*, 47, 337- 355. <https://doi.org/10.1177/0021955X11398381>
- Sukmak, P., Horpibulsuk, S., & Shen, S.-L. (2013). Strength development in clay-fly ash geopolymer. *Construction and Building Materials*, 40, 566-574. <https://doi.org/10.1016/j.conbuildmat.2012.11.015>
- Sulong, H. , Mustapa, S. , & Abdul Rashid, M. K. (2019). Application of expanded polystyrene (EPS) in buildings and constructions: A review. *Journal of Applied Polymer Science*, 136. <https://doi.org/10.1002/app.47529>
- Szycher, M. 2013. Szycher's Handbook of Polyurethanes. 2nd Ed. Boca Raton, USA: CRC Press.
- Thirumal, M., Khastgir, D., Singha, N. K., Manjunath, B., & Naik, Y. (2008). Effect of foam density on the properties of water blown rigid polyurethane foam. *Journal of Applied Polymer Science*, 108(3), 1810-1817.
- Villasmil, W., Fischer, L. J., & Worlitschek, J. (2019). A review and evaluation of thermal insulation materials and methods for thermal energy storage systems. *Renewable and Sustainable Energy Reviews*, 103, 71-84. <https://doi.org/https://doi.org/10.1016/j.rser.2018.12.040>
- Walter, T. R., Richards, A., & Subhash, G. (2009). A Unified Phenomenological Model for Tensile and Compressive Response of Polymeric Foams. *Journal of Engineering Materials and Technology, Transactions of the ASME*, 131. <https://doi.org/10.1115/1.3026556>

- Wang, Z.-F., Shen, S.-L., Ho, C.-E., & Kim, Y.-H. (2013). Investigation of field-installation effects of horizontal twin-jet grouting in Shanghai soft soil deposits. *Canadian Geotechnical Journal*, 50, 288-297. <https://doi.org/10.1139/cgj-2012-0199>
- Wellnitz, C. C. (2007). *Assessment of Extruded Polystyrene Foam for Sandwich Composite Applications* Michigan Technological University].
- Witkiewicz, W., & Zieliński, A. (2006). Properties of the polyurethane (PU) light foams. *Advances in Materials Science*, 6(2), 35-51.
- Wiyono, P., Faimun, Suprobo, P., & Kristijanto, H. (2016). Characterization of Physical and Mechanical Properties of Rigid Polyurethane Foam.



CHAPTER IV

PERFORMANCE OF THE POLYURETHANE FOAM INJECTION TECHNIQUE FOR ROAD MAINTENANCE APPLICATIONS

4.1 Introduction

The population of Thailand has been gradually growing over the years resulting in increased economic development and hence a steady rise in traffic volume (DOH, 2012; Nikomborirak, 2004). Development of road transportation networks are crucial in facilitating the economic development of a nation. Roads are composed of pavement surface and pavement structure, i.e. subgrade, embankment, subbase, and base. The pavement surface is classified into two primary types: asphalt concrete pavement (flexural pavement) and concrete pavement (rigid pavement). Nevertheless, both pavements frequently undergo substantial damages around the country after a certain duration of utilization.

The central region of Thailand is located on a vast soft clay deposit over an area of approximately 14,000 square kilometers. This area includes the Bangkok and its surrounding metropolitan provinces (Department of Rural Roads, 2009). This soft clay deposit is generally known as "Bangkok Clay" and has a basin-like form. It consists mostly of silty or clayey soil with a high moisture content (Moh et al., 1969; Kamon and Bergado, 1991). The soft Bangkok clay layer is uniform with a thickness ranging

from 15 to 20 meters, according to research by the Norwegian Geotechnical Institute (NGI) and the Asian Institute of Technology (AIT). The shear strength at different depths was found to have a low variation which does not exceed 10 percent within the same depth level (Eide, 1968; Eide, 1977).

Roads constructed on soft clay deposits often encounter the surface settlement and subsidence of the road structure. This problem results from the excessive groundwater pumping and consolidation settlement of the soft clay (Peduto et al., 2020). In addition, the quality control of the road construction also plays a crucial role in contributing to the deterioration of the pavement surface and structure. This

includes issues such as material compaction in restricted areas or in the presence of obstacles, leading to subsequent settlement due to the low stiffness of soil foundation and the large voids beneath the pavement, particularly around bridge abutments.

To address the settlement issues resulting from the aforementioned factors, various methods can be employed. These include chemical stabilization and the usage of lightweight materials. The chemical stabilization enhances soil characteristics and fill the voids under the pavement surface. Lightweight materials are utilized as alternatives to replace the damaged pavement structure and then the pavement surface improvement is achieved through the use of asphaltic concrete (Jongpradist et al., 2011; Lenart & Kaynia, 2019; Tanchaisawat et al., 2008; Vardhanabhuti et al., 2015; Wonglert et al., 2018). Each technique has its own operational procedure and financial requirements. The chemical injection approach is favored for its cost-effectiveness and straightforward operation, commonly utilizing substances such as cement. The process of chemicals injection into the soil is referred to as the grouting technique (Weaver & Bruce, 2007). When selecting a maintenance approach, it is crucial to consider the longevity of the repaired road, the time required for remedy and the performance of the repaired road, including its strength and smoothness. This is essential to ensure safety during usage (Mounanga et al., 2008; Patil & Molenaar, 2011).

Currently, there are several ongoing studies exploring the use of polyurethane (PU) foam in various applications to enhance soil properties (Lat et al., 2020). One such application involves injecting PU foam in conjunction with soil nailing, to enhance the adhesion and a slope stability. Another application combines PU foam injection with pile foundations to improve the resistance to vibration and horizontal forces of the piles (Capatti et al., 2016; Valentino & Stevanoni, 2016). The technique of injecting PU foam was initially invented in Italy in 1996 by the Uretek Company and later adapted for high-pressure injection systems (Sabri et al., 2018; Sabri & Shashkin, 2018; Guo et al., 2019). The PU foam is injected to the desired depth; it is formed from two compounds: polyols and isocyanates. These compounds are mixed in a hydraulic system and injected to the soil foundation at high pressure using a spray gun or nozzle through a drilled hole with a diameter of approximately 12–30 mm (Buzzi et al., 2010; Fityus et al., 2011; Sánchez et al., 2017; Sabri et al., 2018; Sabri & Shashkin, 2018; Sabri

& Shashkin, 2020). The ensuing chemical reaction produces a product that can expand up to 30 times its original volume and rapidly harden within seconds. The reaction time is dependent on the specific type of resin injected and the mixing temperature (Buzzi et al., 2008; Sánchez et al., 2017; Sánchez Lavín et al., 2018; Sabri & Shashkin, 2020).

Boonsung et al. (2023) reported the impact of various parameters, including polyol content, the ratio of polyol to diisocyanate (p/d), and the mixing temperature of polyol (P) and diisocyanate (D), on rigid polyurethane (PU) foam's microstructure and compressive strength. At a specific concentration of polyol, an increase in mixing temperature and a decrease in the p/d ratio produced a large number of compact cells with high cell contact pressure. A sufficiently substantial increase in this pressure will result in a corresponding enhancement of the compressive strength and durability of the PU foam. Excessive contact pressure can cause harm to the cell, resulting in a reduction in its strength and resilience. At 1% strain, the minimum compressive strength requirement for geofoam is 0.015 MPa, according to ASTM D6817: 2017. For P contents between 23 and 28 kg/m³, a p/d ratio of 1.0 and a mixing temperature of 40°C are recommended. When the P content is 34 kg/m³, it is recommended to utilize at an ambient mixture temperature and a p/d ratio of 0.8.

The chemical grouting procedure for road maintenance utilizing a PU foam injection system, according to Fakhar and Asmaniza (2016), consists of liquid P and D. This procedure is secure for the environment because the PU foam is non-toxic. PU foam, a three-dimensional network polymer product of exceptional strength, is produced through the thermal combination of liquid P and D (Wolf, 1956; Ulrich, 1982; Wood, 1982). This material has been found to have various beneficial properties, including the ability to elevate, realign, seal leaks, fill voids, and fortify soil structures (Soltész, 2002; Gaspard & Morvant, 2004; Yu et al., 2013; Mohamed Jais, 2017). The molecular weight of the polyester polyols influences the properties of PU; flexible PU foams are produced by polyols with a high molecular weight, whereas rigid PU foams are generated by those with a low molecular weight (Sharmin & Zafar, 2012). Within 15 minutes, PU foam injected into the soil reaches 90 percent of its maximal compressive strength of 0.276 MPa; the road can subsequently be reopened to traffic

the following day (Puppala et al., 2012). Similar to conventional cement grouting, PU grouting involves the injection of P and D via a nozzle inserted through drilled holes in the soil layer that needs to be improved. By expanding and filling the cavities in the soil mass, PU foam increases the load bearing capacity of the composite ground. Moreover, the low unit weight of PU serves to alleviate the rate of settlement in soft clay layer (Sidek et al., 2015).

The use of PU foam injection techniques to address soil settlement problems has become very popular in Thailand. This approach finds extensive application, ranging from fortifying soil layers to support machinery and level industrial manufacturing floors to enhancing road surfaces in various public and private construction projects. This paper includes case studies that demonstrate the utilization of PU foam injection techniques to effectively overcome pavement settlement concerns in Thailand. The method entails using shallow injection to uplift the pavement and deep injection to address soil mass loss beneath the pavement structure. This soil enhancement technique signifies a groundbreaking strategy in the construction industry of Thailand. It is crucial to provide a thorough framework or set of rules in order to inspire trust in the construction quality for engineers and stakeholders participating in the projects.

This research work will provide a detailed and systematic approach for the PU injection technique, doing a complete analysis of its performance and evaluating the behavior of the pavement after the process of restoration. The practical requirements include survey processes, attentive work planning, strict safety measures, effective quality control, precise monitoring, and systematic reporting of practice outcomes. The results of this study are intended to promote the extensive implementation of the PU foam injection technique as an environmentally friendly substitute for treating road surface settlement problems in Thailand.

4.2 Polyurethanes

4.2.1 Chemical Composition

Polyurethane (PU), alternatively known as polycarbonate, constitutes a class of polymers characterized by recurring urethane groups (-NHCOO-) within a

molecular chain, possessing two primary attributes: rigidity and flexibility (Islam et al., 2014; Akindoyo et al., 2016). Otto Bayer first discovered PU in 1930. The molecular structure of PU is comprised of P and D, which share similar chemical characteristics, equal weight, functional values (Komurlu and Kesimal, 2012, 2014), or other compounds. Reactive hydrogen atoms are integral to its molecular structure (Herrington & Hock, 1997; Ashida, 2006). The general chemical structure of PU is depicted in Figure 4.1. The synthetic production of PU involves the condensation reaction between P and D, as illustrated in Figure 4.2.

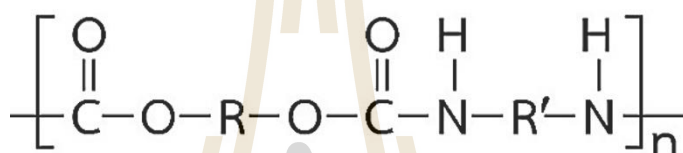


Figure 4.1. General structural characteristics of polyurethane

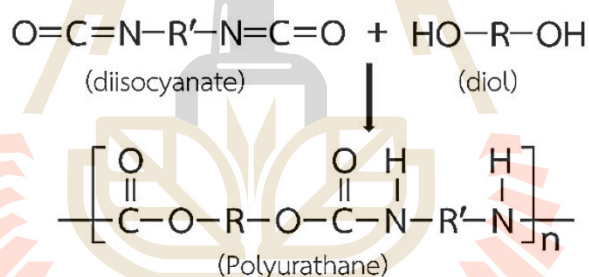


Figure 4.2. Polyurethane synthesis reaction

The key constituents utilized in the production of PU foam consist of two main components:

4.2.1.1 Polyol

Polyol serves as a crucial raw material in the industrial production of PU. It encompasses various related compounds. The polyols utilized for PU production fall into three main categories: 1) polyether polyols 2) polyester polyols and 3) polyester-biological polyols, constituting 90%, 9%, and 1% of the industrial usage volume, respectively, in relation to the overall market share of all polyols. Table 4.1 illustrates the specific properties of polyols.

Table 4.1 Specific properties of polyols (Szycher, 2013).

Characteristic	Elastomer Foam and Flexible foam	Solid Foam and Rigid foam
Molecular Weight Range	1,000 to 6,500	100 to 1,200
Functionality	2 to 3	3 to 8
Hydroxyl Value Range	28 to 160	250 to 1,000

4.2.1.2 Diisocyanate

The properties of polyurethane, including its physical and chemical attributes, depend on the particular type of isocyanate used. Two commonly used forms of diisocyanates are toluene diisocyanate (TDI) and diphenylmethane diisocyanate (MDI). The industry primarily relies on MDI, which accounts for about 90 percent of isocyanate use. Table 4.2 presents a comprehensive overview of the physical and chemical characteristics of both TDI and MDI.

Table 4.2 Physical and chemical properties of TDI and MDI (Szycher, 2013).

Properties	TDI	MDI
State	liquid, crystalline	solid, sheet
Color	white to light yellow	white light yellow
Smell	fruity	no smell
Molecular Weight	174.16	250.3
Boiling Point, °C	251	314
Melting Point, °C	22	37
specific gravity	1.22	1.2

4.2.2 Characteristics of Polyurethane

The molecule characteristics of PU foam depend on the ratio of P to D. PU foam can be classified into two primary types: flexible PU foam and rigid PU foam (often manufactured as semi-rigid foam). Table 4.3 summaries the characteristics of PU

foams, as reported by Herrington and Hock (1997), Ashida (2006), Szycher (2013), and Gama et al. (2018).

4.2.2.1 Flexible polyurethane foam

Flexible PU foam possesses a reticular molecular structure and exhibits a density that varies between 10 and 80 kg/m³. With its open-cell structure, this material allows for efficient airflow. This form of PU foam demonstrates exceptional tensile strength and displays resistance to a wide range of solvents. This PU exhibits thermal stability up to 150 °C when it is in a dry state. Extensively employed in the automobile and furniture upholstery sector, it is used for various purposes like as car headrest pillows, car steering wheels, car spoilers, shock-absorbent materials, and more.

4.2.2.2 Rigid polyurethane foam

Rigid PU foam is distinguished by its extensive reticulated molecular structure, which consists of gas bubble-encircling cells with closed walls. In contrast to flexible PU foam, this rigid PU foam cultivates an enclosed configuration that restricts airflow. With chemical properties resembling those of flexible polyurethane foam, this substance exhibits exceptional thermal insulation capabilities and a high strength-to-weight ratio. Furthermore, it demonstrates remarkable resistance to corrosion caused by petroleum and oil, exhibiting a foam density that covers a range of 30 to 80 kg/m³. As insulation, rigid PU foam is utilized in refrigerators, cold room walls, heated and cold storage containers, and an assortment of other container types. Additionally, it is employed in marine apparatus to decrease mass and improve buoyancy.

Table 4.3 Classification of polyurethane foam (Ashida, 2006)

polyol	Rigid foam	Semi-rigid foam	Flexible foam
OH No.	350-560	100-200	5.6-70
OH Equivalent No.	100-160	280-560	800-10,000
Functionally	3.0-8.0	3.0-3.5	2.0-3.1
Elastic Modulus at 23 °c			
MPa	>700	>70-700	<70
lb/in ²	>100,000	>10,000-100,00	<10,000

4.3 PU Foam Injection Technique

An individualized strategy that focuses on resolving the issue at this point is necessary when repairing the pavement surface with PU foam injection. Determining optimal injection points while minimizing compound usage is an essential aspect of developing efficient work procedures. Area type, injection site placement, and the dimensions of the expansion area are all elements that should be taken into account during operation planning. These factors contribute to the efficient operation of PU foam and assist operators in its evaluation. Moinda (2004, 2008) identified variables such as pressure and injection patterns that influence the expansion capacity of PU foam.

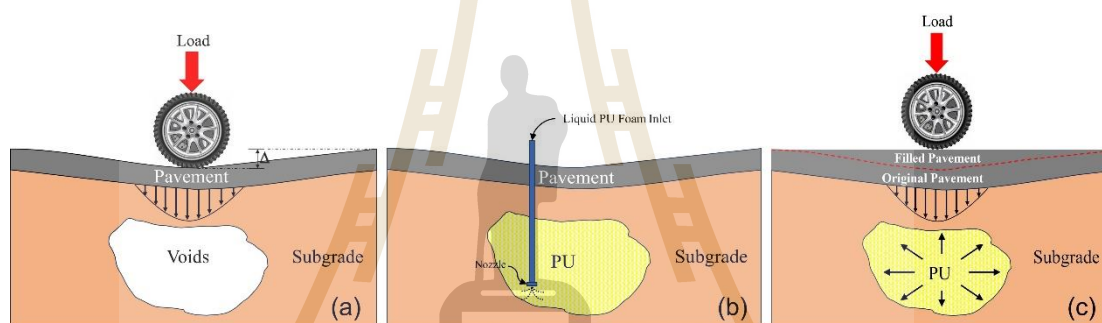


Figure 4.3 Characteristics of deep injection of PU Foam
(modified after Rao et al., 2019)

A simulation diagram illustrating substantial settlement that takes place on flexible surfaces, as is commonly observed in asphalt pavements, is presented in Figure 4.3. Extensive soil mass deficiency beneath the pavement causes the formation of expansive cavities at a considerable depth beneath the surface, which in fact causes this settlement. The expansion of cavities in the pavement is a consequence of dynamic forces generated by the vehicle load. This expansion directly influences surface settlement, as illustrated in Figure 4.3(a). By injecting PU foam into these voids beneath the pavement, compressive stress in the pavement structure is evenly distributed and tensile stress concentrations are reduced, thereby preventing further surface settlement. Following this, the surface is modified through the application of

a overlaying surface material (Figure 4.3(b) and (c)). The process by which PU foam is deeply injected to minimize settlement concerns is called "deep injection."

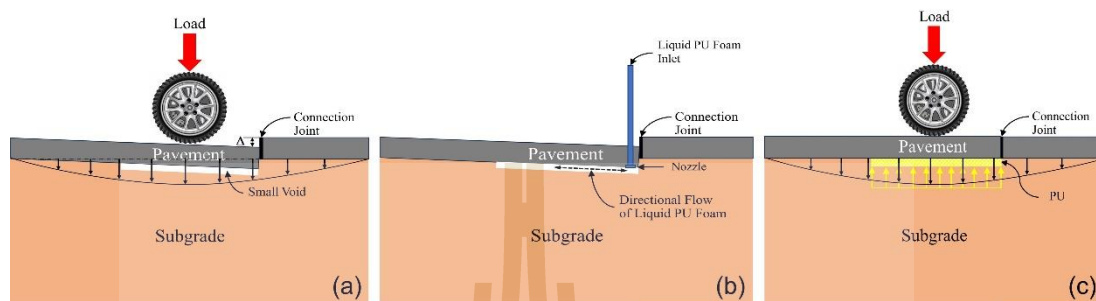


Figure 4.4 Characteristics of shallow injection of PU Foam
(modified after Rao et al., 2019)

Figure 4.4 presents a simulated diagram illustrating minor settlement commonly seen in rigid or concrete pavements. The weight of vehicles induces dynamic stress on the pavement surface, leading to differential settlement within the pavement structure and on the surface. This is particularly noticeable around connection joints, as depicted in Figure 4.4(a). This disruption can result from factors like weakened soil bearing capacity due to water seeping through connection joints, uneven compaction near connection joints, issues with construction quality control, and external factors beyond control, such as variations in the properties from different material sources. Even slight initial settlements can significantly escalate with increased traffic, affecting driving safety.

The injection of PU foam in this case aims to readjust the surface level to a usable state by harnessing the lifting force generated from the chemical reaction of both mixed compounds. This type of PU foam injection is referred to as 'shallow injection' (see Figure 4.4(b) and 4.4(c)). The injected PU foam expands and fills voids rapidly within 30-60 seconds.

The method of introducing PU foam, whether it be for deep or shallow injection, is occasionally referred to as 'Compaction Grout Injection' (Yu et al., 2013). Although the method of injecting PU foam to resolve settlement problems may differ

depending on the unique circumstances, the primary procedures can be outlined as follows:

- 1) Prepare the work area by setting up road barriers to limit the working space and prevent vehicles from entering during operations. This includes arranging safety equipment to protect individuals during work, involving the steps of surveying the area, and during the injection process.

- 2) Verify the settlement values of the area to be addressed using precise measurement tools. Additionally, create a detailed map outlining the scope of work and develop a plan detailing the operational steps (the surveying process).

- 3) In situations involving observable settlement in the work area, the implementation of deep injection techniques becomes imperative. To determine how deeply and in what pattern the PU foam should be injected, the designer must first determine the strength of the soil on-site through the use of techniques such as a light hammer test.

- 4) Determine the injection positions and drill the pavement surface to create holes of sufficient size for the PU foam injection pipes. Inject the PU foam until reaching the desired depth for soil improvement according to the proposed operational plan. While injecting the PU foam, monitor the movement of the surface level to ensure confidence that the foam adequately fills the voids beneath the surface and achieves the desired level of lifting.

After the completion of the PU foam injection, it is recommended to provide a resting period of 15 minutes. Subsequently, seal the drilled holes with cement grout and proceed to reopen the roadway after the expiration of one hour.

4.4 Application of PU Foam for Road Maintenance

The use of PU foam to enhance the stability of road structure in Thailand is gaining popularity and steadily growing. This is due to its advantages in terms of streamlined work processes, avoiding the need for digging or damaging the surface to address soil issues below. Importantly, it can be completed within a relatively short timeframe. To address surface settling problems in Thailand utilizing PU foam injection, three distinct applications are identified, as illustrated in the following case studies.

4.4.1 Flexible Pavement

Motorway Number 9 (Bang Na - Bang Pa-in) is a vital main route that encircles and connects the peripheral regions of Bangkok, including Nonthaburi, Pathum Thani, and Samut Prakan. Additionally, it extends through Phra Nakhon Si Ayutthaya province. The motorway spans 181 km and comprises an eight-lane mainline roadway with a concrete surface, along with two additional asphalt concrete lanes designated for westbound and eastbound traffic, capable of handling a daily traffic volume of 8,000 passenger car unit (PCU). This infrastructure plays a crucial role in connecting the central and eastern areas. Construction was completed in 1998 (B.E. 2541). According to data provided by the Motorway Authority of Thailand (Department of Highways, 2022), the average daily traffic volume in 2022 peaked at 271,860 PCU. Figure 5 displays the attributes of Motorway Number 9 and its road structure.

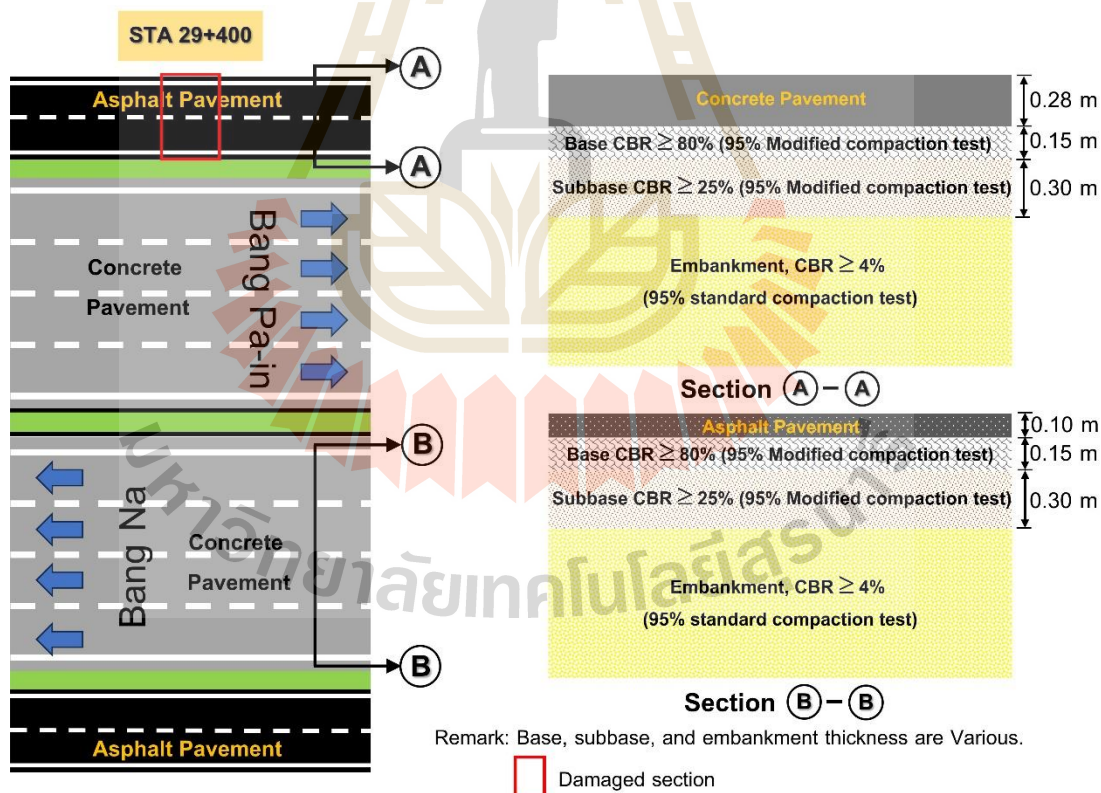


Figure 4.5 Characteristics of Highway No. 9 (Bang Na-Bang Pa-in) and road structure

This motorway is built on the soft Bangkok clay, with a thickness ranging from 15 to 18 meters. The soil has low shear strength and is prone to settling, coupled with a high liquid limit and water content. After its completion in 1998 (B.E. 2541), a significant settling issue emerged on December 25, 2022, affecting the westbound lanes at STA 29+400 and making that section impassable, as shown in Figure 4.5. To address this, the Motorway Authority of Thailand temporarily used asphalt concrete to raise the level, allowing traffic to resume on January 10, 2023, as illustrated in Figure 4.6. However, settlement issues continued until the intervention of the S-Class Engineer Company, which applied PU foam on February 6, 2023. The repair activities were conducted between 2:00 p.m. and 8:00 p.m.



Figure 4.6 Settlement location of the asphalt-covered pavement.

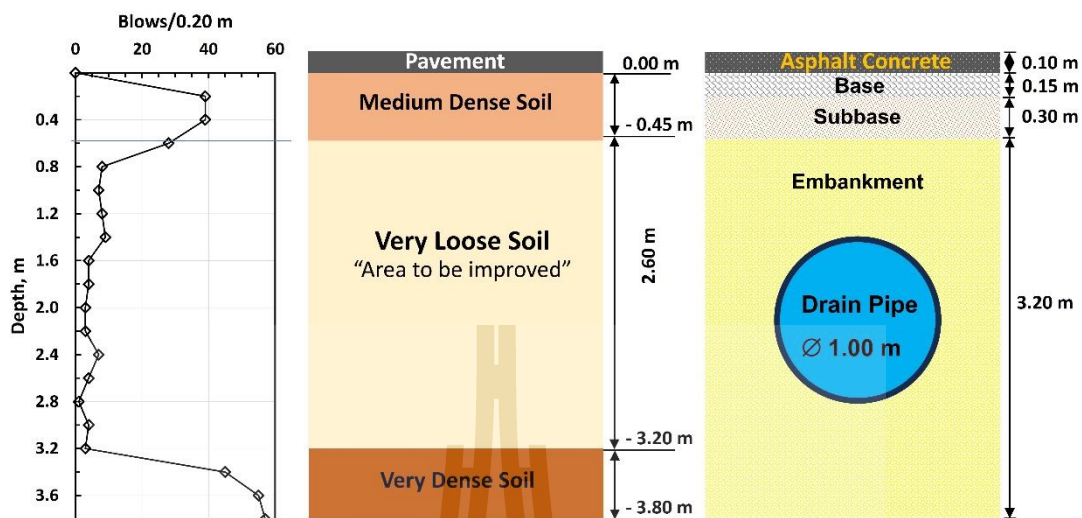


Figure 4.7 Results of the Kunzelstab Penetration Test (KPT) and the pavement structure

Figure 4.7 illustrates the results of the Kunzelstab Penetration Test (KPT) conducted to evaluate the soil's bearing capacity beneath the settled pavement surface. The objective is to determine the depth at which PU foam injection is required for enhancing the soil's engineering properties and to plan the remedial work. The assessment spans from the soil surface level (level 0.00) to a depth of 0.45 meters (level -0.45 meters). The base and subbase are identified as a moderately compacted layer with a KPT number around 40. Next to the subbase, there is an embankment layer susceptible to depressions due to damaged water pipes. This embankment layer has a thickness of 2.75 meters (ranging from level -0.45 meters to level -3.20 meters) and consists of coarse sand with a KPT number less than 8. Beneath the sandy soil layer, there is a dense soil layer with a KPT number exceeding 40. Consequently, the engineering enhancement of the soil involves injecting PU foam to a depth of -3.20 meters.

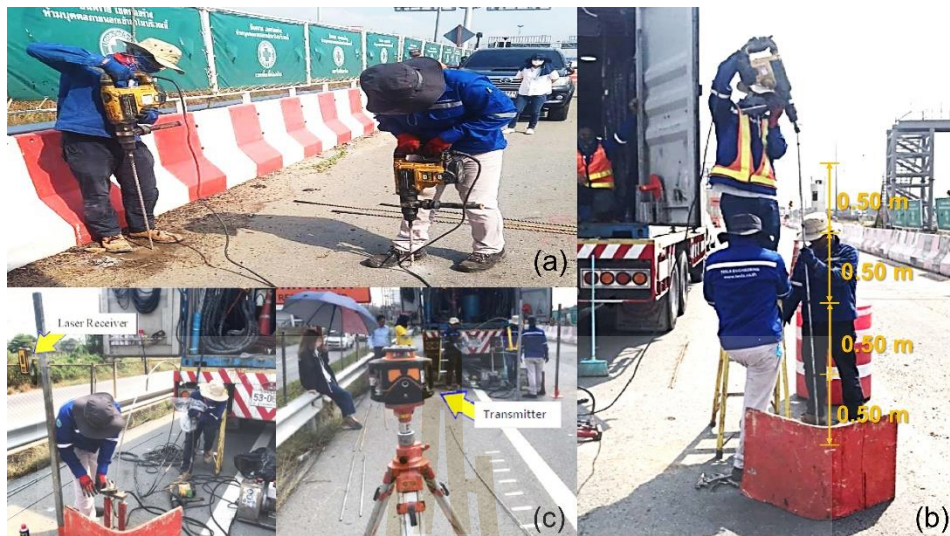


Figure 4.8 Steps for deep PU foam injection.

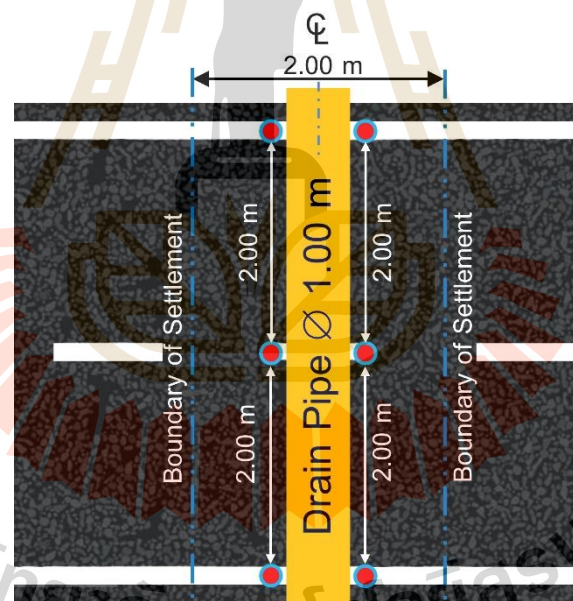


Figure 4.9 Location and spacing of drill holes (red dots) for foam injection.

The PU foam employed for soil improvement is a mixture of P and D at a 1:1 ratio. Diphenylmethane diisocyanate, its isomers, and homologs like 4,4-methylene diphenyl diisocyanate (MDI) (POLYONE-200) are all parts of the diisocyanate part. The P used is polyether polyol (POLY-225). The process of injecting PU foam

began with the calibration of tools, measuring the quantity of foam fluid injected per cycle, commonly known as a "stroke." It was determined that the volume of foam fluid utilized per stroke averaged 0.0939 kg based on three measurements (the quantity of chemical injected per cycle relative to applied pressure). This value was employed to compute the overall amount of liquid foam utilized for the complete repair process once the total number of strokes used for maintenance was established.

Figure 4.8 outlines the steps involved in PU foam injection until the process was complete. In Figure 4.8(a), holes were drilled using an electric drill with a 16-millimeter diameter, slightly beyond the desired depth (level -3.20 meters from the ground), and spaced 2.00 meters apart. There are a total of 6 drill points covering an area of 8 square meters, as shown in Figure 4.9. Following this, aluminium pipes, 12 millimeters in diameter and 4.50 meters in length, were prepared and marked at 500-millimeter intervals to control the PU injection pipe's lifting speed (Figure 4.8(b)). The P and D solvents were heated to 40°C at the injection head position and injected under pressure of approximately 13.8 MPa (2,000 psi). PU foam was injected from the bottom up, and the number of strokes was calculated by dividing the amount of chemical needed per 500 millimeters of depth by the average amount of liquid foam used per stroke. The injection was carried out by gradually moving the conduit upward while injecting PU foam to achieve a chemical quantity of 10 kilograms per 500 millimeters of depth. The final injection depth was set slightly below the surface to ensure complete foam filling. The practitioner measures the surface movement using a transmitter (Figure 4.8(c)). PU foam injection stopped when the pavement surface was lifted by 2.0–3.0 millimeters compared to the adjacent undamaged pavement surface. Following this, the practitioner closed the drill holes with non-shrinkage grout, cleaned the area, and reopened the pavement for use after approximately 1 hour. The total chemical used for this surface repair was 436 kg (P = 218 kg and D = 218 kg).

4.4.2 Rigid Pavement

Rural Road No. 3026 (km. 0+000 to 5+000) is a road that branches off from Rural Road No. 3030, spanning a distance of 5.6 kilometers. It is a four- to six-lane road intersecting at Rural Road No. 3032 (Bypass), which is designed to divert urban traffic. The purpose of constructing Rural Road No. 3026 is to channel the traffic volume

from the urban area to the western side of the central region of Thailand. The pavement surface is reinforced concrete, and the pavement structure consists of a base course with a CBR value $> 80\%$, 15 centimeters thick, and a subgrade with a CBR value $> 4\%$. It was opened on April 24, 2009, and has been in operation for 11 years. Damage started occurring in February 2023, specifically at STA 5+200, due to differential settlement at the concrete pavement near the connection joint in the curve area close to the shoulder of the road. This settlement is believed to result from challenges in compacting the base course in the narrow area, as shown in Figure 4.10(a). The damage to the pavement occurred both longitudinally and transversely to the traffic direction. Additionally, this area serves as a U-turn point, causing vehicles to decelerate significantly while entering the curve and accelerate when exiting the curve. Consequently, this area experiences higher compressive and shear forces beneath the pavement surface than other areas. Figure 4.10(b) illustrates the damage to the pavement in the transverse direction, indicating a settlement of 25 millimeters compared to the original surface.



Figure 4.10 Physical characteristics of the road (a) pavement damage (b) settlement surface

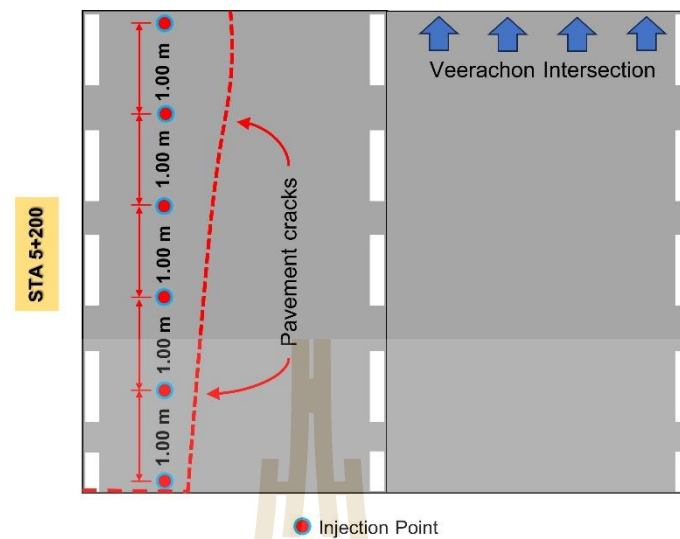


Figure 4.11 PU foam injection location to raise the pavement surface.

The soil investigation demonstrated the stability of the subgrade. However, problems with the concrete surface occurred due to soil settlement at a shallow depth below the pavement surface. The most notable settlements measured 25 mm in width and 15 mm in length. In order to enhance the bearing capacity of the pavement, it was necessary to strengthen the shallow foundation (base course) and raise the concrete surface to a level that can be used. As illustrated in Figure 4.11, this required the implementation of PU injection technique at the particular site.

Since the concrete pavement includes reinforcing steel bars, it was necessary to cut them along the crack line. This enables the original pavement on the settling side to lift during PU foam injection, as shown in Figure 4.12(a). Following the cutting process, holes were drilled on the settlement's pavement surface, reaching a depth 20-30 mm below the pavement surface. These holes, spaced at 1.00 m intervals along the length, served as installation points for a liquid PU foam injection tool. The tool has a volume of 0.0875 kg per stroke and operates within a pressure of approximately 10.4 MPa (1,500 psi), as illustrated in Figure 4.12(b).

Throughout the PU foam injection procedure, careful monitoring was carried out on the raised area of the settled pavement. The injection of PU foam was stopped when a raised concrete surface was 5.0 mm above the level of the adjacent undamaged pavement, as shown in Figure 4.12(c). Figure 4.12(d) clearly depicts the

concrete surface after the uplift and repair process. The total chemical usage for this project was 150 kg, with 75.5 kg of P and 75.5 kg of D.

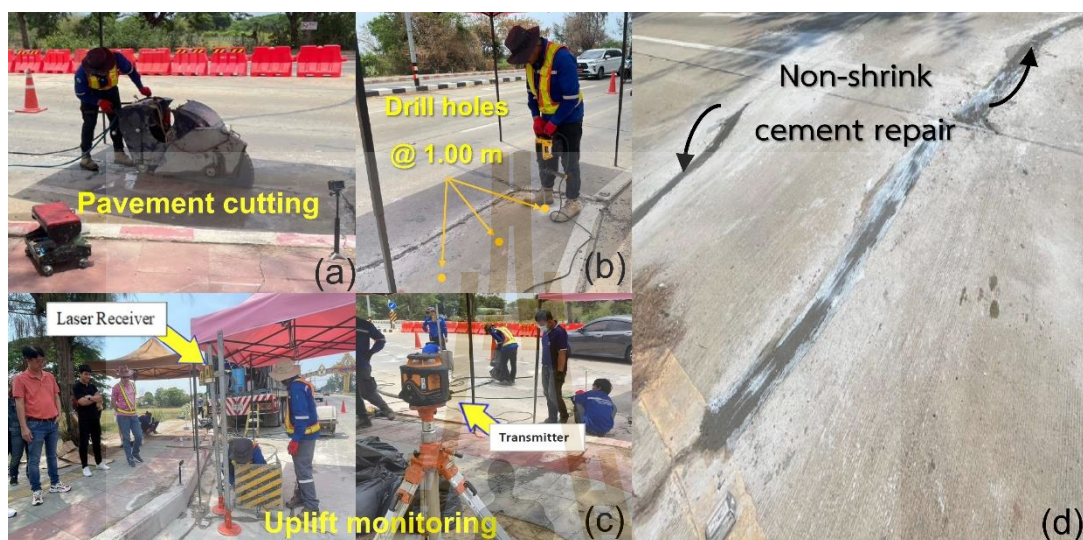


Figure 4.12 Shallow PU injection process.

After the injection of PU foam and the regular operation of the road over a six-month period, the authors conducted an examination of the repair outcomes. This involved a thorough survey of the pavement surface level and a comparative analysis with the levels observed both before and after the PU foam injection. Figure 4.13(a) illustrates the concrete pavement that experienced damage, where the settlement on the left-hand side caused it to descend below the operational level. The repair was executed through PU injection, effectively restoring it to its original position. The pavement surface exhibited a width of 3.0 meters and a length of 6.0 meters, segmented into horizontal intervals of 0.5 meters and longitudinal intervals of 1.5 meters.

The intersection point of the two lines was designated as the reference point for collecting position level data. The level value data were then collected, as illustrated in Figure 4.13(b). Figure 4.14 presents the measurement results of the pavement surface level both before and after the PU foam injection. It indicated that, prior to the injection, the highest longitudinal settlement occurred at grid line 1, a

specific section of the pavement surface, with an average transverse settlement of 25 mm. Following the PU foam injection to improve the shallow foundation (base course) beneath the pavement and elevate the surface level, the road demonstrated the capability to sustain traffic loads without succumbing to settlement-related damages. This was evident from the minimal difference between the level measured immediately after the PU foam injection and the level measured after a six-month period.

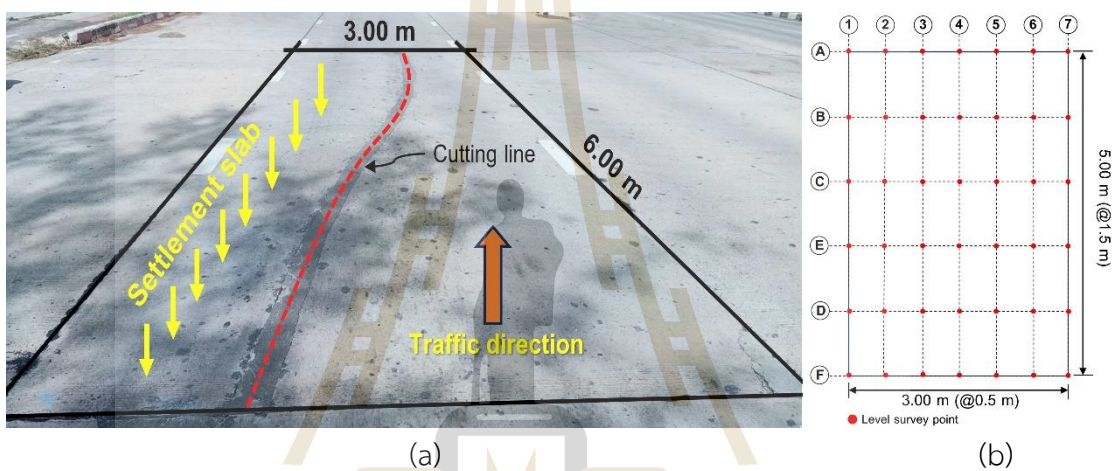


Figure 4.13 Post-injection inspection of PU foam (a) repaired pavement
(b) data collection location.

มหาวิทยาลัยเทคโนโลยีสุรนารี

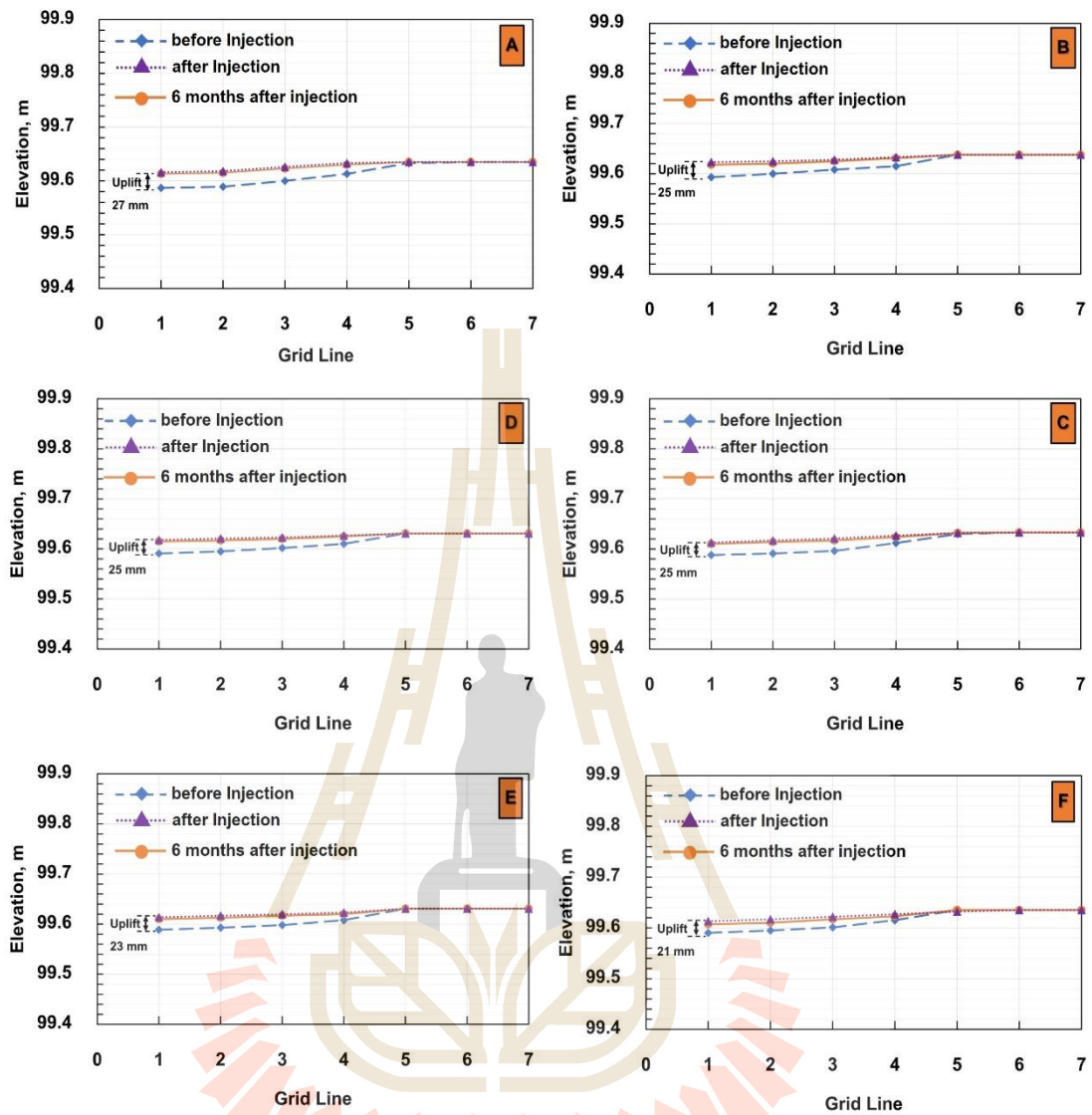


Figure 4.14 Level values of the pavement before and after PU foam injection.

4.4.3 Bridge Approach Slab

Bridges conventionally depend on pile foundations, while bridge approaches are supported on compacted soil. In other words, they are built on supports with varying stiffness. Compacting the pavement structure, particularly near the bridge approach, remains a consistent challenge, requiring more efficient compaction methods than those used in other locations.

Moreover, dynamic forces generated by acceleration in the bridge approach cause the soil mass to flow beneath the concrete pavement, resulting in

different settlements between the bridge abutment and the pavement surface. In Figure 4.15, there was a visible opening on the side of the bridge approach where the soil mass flowed out, measuring approximately 200 millimeters in width and 300 millimeters in length. Such damage is common in Thailand, especially in the central region, where bridge approach slabs are often built on soft clay. One potential solution to this issue involves using lightweight EPS materials instead of traditional compacted soil. A study by Malai et al. (2022) found that EPS foam, when installed for 100 days, significantly reduced stress intensity on the soft clay foundation, resulting in minimal settlement. However, this approach requires the excavation of open areas for construction, which is time-consuming and impacts project costs.



Figure 4.15 Opening due to soil flew out of the bridge approach slab

The Rural Road No. 4012 located in Chanthaburi Province, eastern Thailand, spans 36 kilometers and features a four-lane asphalt pavement with two lanes in each direction. The area is susceptible to monsoons, which leads to frequent flooding and the accumulation of sand at the bridge approach, resulting in a large cavity and settlement issues on the pavement surface. Figure 4.16(a) displays noticeable cracks on the pavement surface at the intersection between the road and the bridge approach, stretching along the entire approach length. Cavity measurements, performed by inserting a small steel rod beneath the pavement surface, revealed a continuous cavity extending across the road and the bridge

approach. Although the depth ranges from 0.5 to 1.0 meters, it was not excessively deep. To address this, deep injection PU foam technique was employed to fill the cavities beneath the pavement surface for maintenance. The process commenced with the injection of PU foam to fill the cavities between the asphalt concrete pavement edge and the shoulder, as depicted in Figure 4.16(b). PU foam filled the left and right cavities along the shoulder of the bridge abutment slab. Following this, PU foam was injected into each asphalt concrete.



Figure 4.16 (a) Pavement crack line (b) Injection to seal the opening.



Figure 4.17 Work steps (a) Drilling holes to install foam injection equipment (b) Measuring the level of surface movement.

Figure 4.17(a) shows the layout of the pavement drill line situated between the pavement surface and the bridge approach. The drill holes are 16 mm in diameter, spaced at intervals of 1.50 m. Afterward, a aluminium pipe with a 12 mm diameter was inserted, extending from 0.5 to 1.0 meters along the road and spanning the bridge connection down to the level of hard soil. The subsequent step involved injecting liquid PU foam at a rate of 0.0851 kg per stroke, employing a working pressure of approximately 13.8 MPa (2,000 psi). The injection process began from the bottom and proceeds upward. The number of injection strokes was calculated based on the required chemical amount per 0.5 meters of depth, divided by the average liquid foam amount per stroke. Following this, the pipe was moved upward to inject the next layer. To ensure thorough distribution beneath the concrete pavement surface, the final injection depth was slightly below the pavement level. The injection process stopped when the asphalt concrete pavement surface rises by 5 mm compared to the adjacent undamaged pavement surface, as shown in Figure 4.17(b). Subsequently, the drilled holes were sealed with non-shrink cement. The total chemical consumption for maintenance in this project was 320 kg (P = 160 kg and D = 160 kg).

Pavement settlement caused by widespread cavities is a frequent issue in the central region of Thailand, characterized by a prevalent soft clay sediment basin with a thickness ranging from 10.0 to 18.0 meters. Exclusively depending on conventional PU foam injection procedures, operational expenses will be elevated. In order to save costs, lightweight materials and PU foam can be utilized together. The utilization of lightweight materials helps reduce both the vertical stress on the foundation and the horizontal stress on the retaining structure or bridge approach. A commonly employed method for producing lightweight materials involves integrating foam agents into the mortar mixture, referred to as air foam mortar (AFM), which leads to the creation of lightweight materials (Neramitkornburi et al., 2015a; Neramitkornburi et al., 2015b). The strength characteristics of this low-density material are contingent upon the amount of cement and additives employed. This method can be applied to several types of fine aggregates, including sandy soil and soft clay (Jamnonpipatkul et al., 2009; Horpibulsuk et al., 2012; Yang & Chen, 2016; Lim et al., 2017; She et al., 2018).

The bridge at km 11+050 in Bangkok, a route to Suvarnabhumi International Airport, is built on Bangkok's soft clay layer, featuring a road structure (Figure 4.18). Settlement problems between the road and the bridge approach have resulted in pavement collapse, forming a notable sinkhole, as observed in Figure 4.19(a), documented through a walkthrough survey and distance measurements. Upon inspection, a sizable void was discovered beneath the pavement, situated between the abutment and the road, approximately 2.0 meters deep from the pavement level. As illustrated in Figure 4.19(b), the repair process began with the injection of PU foam to fill the cavities along the road shoulder, limiting the spread of the foam before further injection beneath the pavement surface.

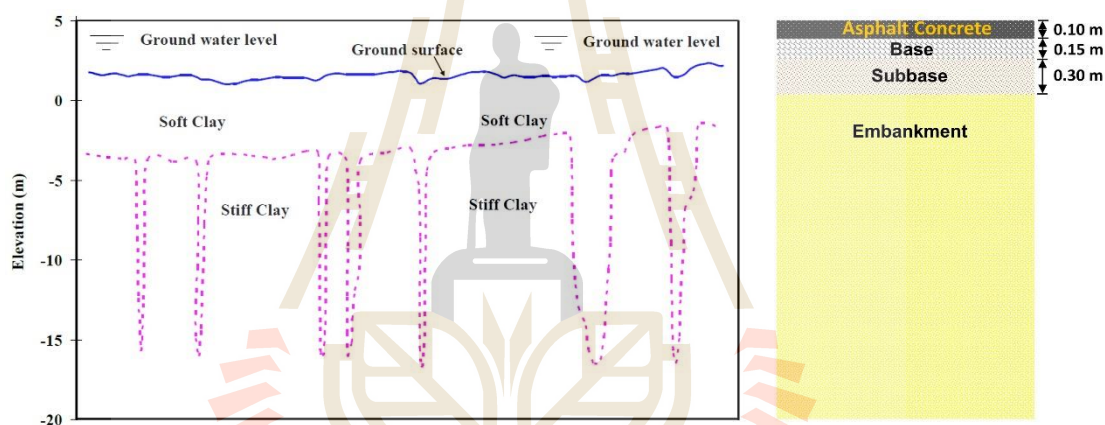


Figure 4.18 Subsoil and road information (a) Arrangement of the Bangkok Soft Clay (Eide, 1977) (b) Road structure

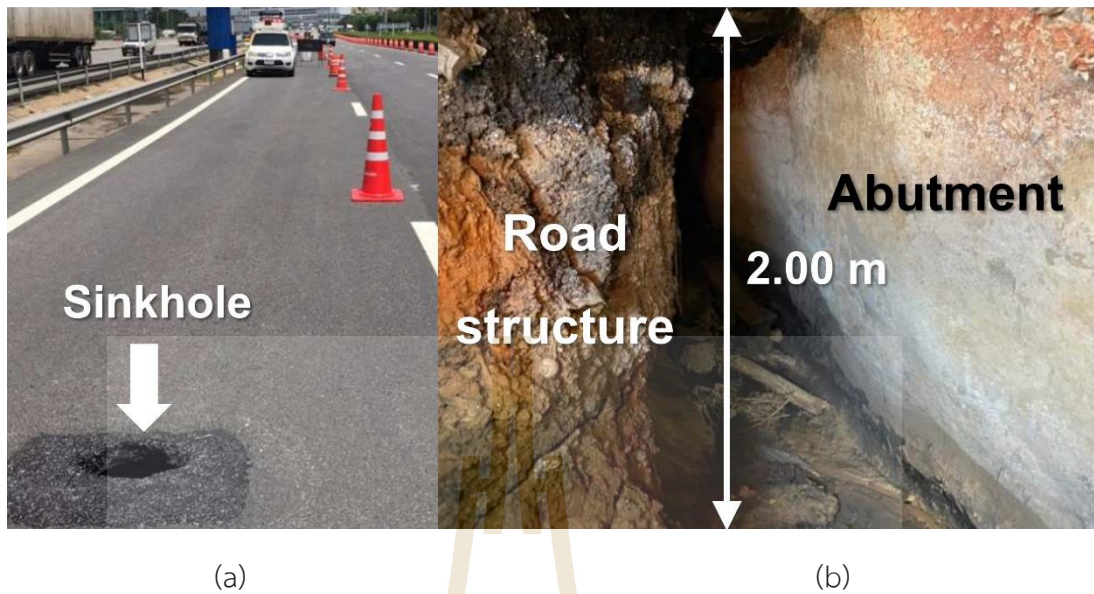


Figure 4.19 (a) Pavement damage (b) Cavities under the pavement



Figure 4.20 Preparing Lightweight concrete for pouring to fill a cavity

Due to the extensive size of the cavity, cellular lightweight concrete, with a volume of 10 cubic meters, was used to fill the space beneath the pavement. It was poured from the roadside, allowing the concrete to flow and fill the cavity. The lightweight concrete was designed to have a unit weight ranging from 800 kg/m^3 to $1,200 \text{ kg/m}^3$ (with a tolerance of $\pm 10\%$) when in a liquid state. On-site checks are conducted to verify the unit weight of the liquid-state lightweight concrete before

filling the bottom of the cavity. As depicted in Figure 4.20, the concrete underwent an 11-day curing process. Subsequently, the PU foam injection process commenced by drilling the pavement with a 16-mm diameter, preparing for the installation of the PU foam injection equipment. The drill holes were strategically placed at intervals of 1.50 m. An aluminum pipe, measuring 12 mm in diameter, was then inserted into the bottom for PU foam injection at a depth of 2.00 m (reaching the hard soil level).

Utilizing lightweight concrete in such cases significantly reduced maintenance costs compared to using PU foam injection alone. The liquid PU foam was injected at a rate of 0.0806 kg/stroke, and the injection progress was monitored by measuring the pavement uplift with a laser level instrument. The injection was stopped when the pavement surface lifted by a minimal 5 millimeters compared to the adjacent undamaged pavement level. The total chemical quantity used for PU foam injection in this maintenance project was 220 kg (P = 110 kg and D = 110 kg).

4.5 Compressive Strength of PU Foam Samples

The compressive strength of PU foam injected in the field could be evaluated by injecting PU foam into a mold under conditions simulating practical applications in terms of chemical composition and pressure. After allowing the molded PU to set for 24 hours, the mold was removed, and the resulting samples were cut to dimensions of 50 x 50 x 50 millimeters, following the standards set by the Norwegian Directorate of Public Roads (Public Road Administration, 1922). These cubic samples then underwent compressive strength testing using a Universal Testing Machine (UTM). Figure 4.21 visually illustrates a PU foam sample obtained through mold injection, highlighting an uneven distribution of the liquid PU foam, leading to a non-uniform solid PU foam product. Buzzi et al.'s study (2010), employing scanning electron microscopy to investigate the microstructure of field-injected PU foam samples for foundation improvement, found that the PU foam samples displayed an incomplete structure. This discovery aligns with the present study's results, indicating a consistent non-uniform distribution observed in field-injected PU foam samples compared to those prepared under laboratory conditions.

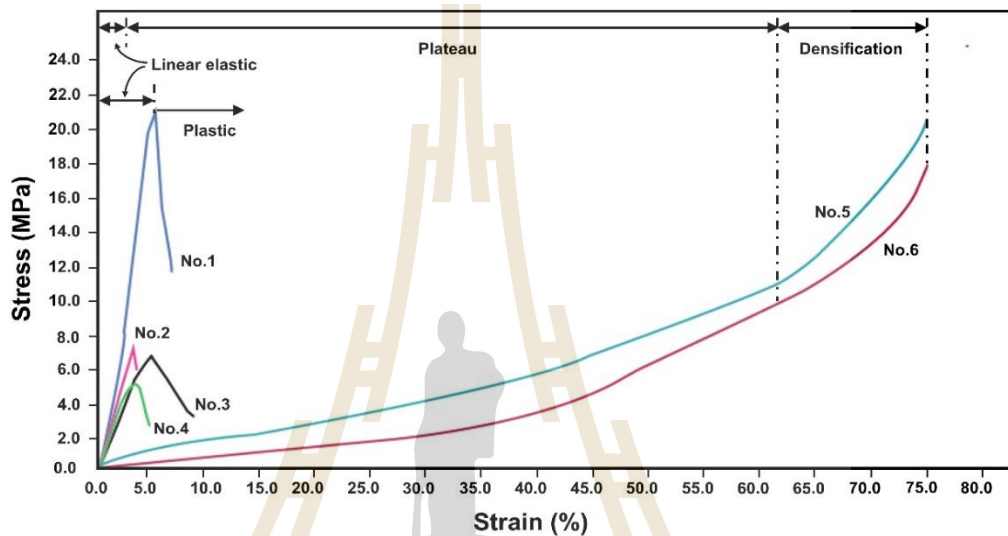


Figure 4.21 PU foam texture of the specimen obtained by injection into the mold.

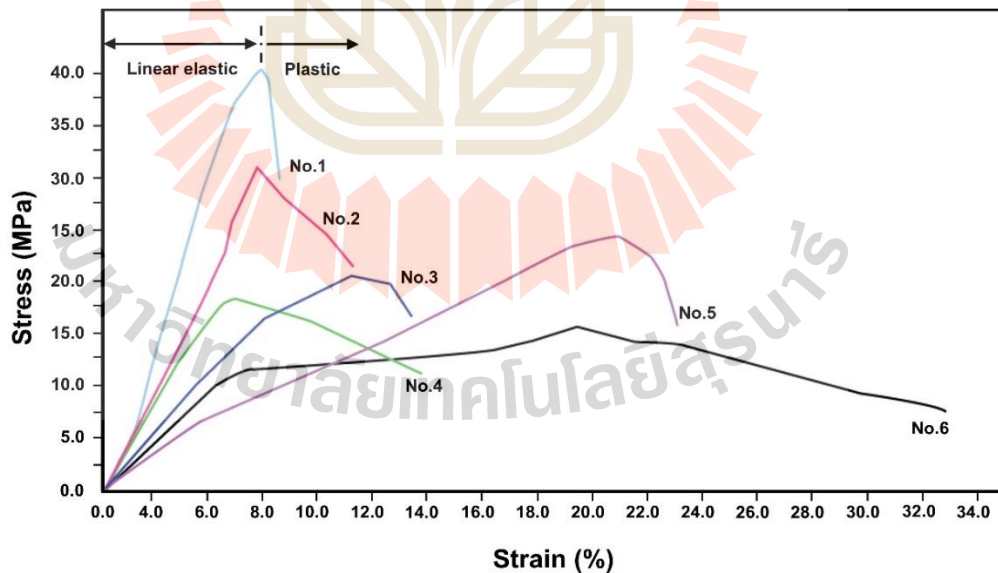
Figures 4.22(a) and (b) show the results of compressive strength tests on PU foam samples prepared under working pressures of 10.4 MPa and 13.8 MPa, used for shallow and deep injection methods, respectively. The average peak compressive strength was found to be 14.3 MPa and 24.7 MPa, respectively. Notably, the compressive strength at 1% strain, a key parameter for designing lightweight foam materials in road construction, was measured at 1.1 MPa and 1.64 MPa, respectively. These values significantly surpassed the recommended threshold (which should not be less than 0.015 MPa) specified by ASTM (ASTM, 2017).

Furthermore, Figure 4.22(a) illustrates the impact of imperfections on the chemical reaction, leading to two types of samples exhibiting distinct behavior in the relationship between stress and strain: 1) PU foam samples that displayed incomplete chemical reactions had a brittle nature, which was characterized by a certain compressive strength value (No. 1-4). The stress-strain relationship exhibited the elastic-plastic properties typically observed in brittle materials and 2) PU foam samples resulting from complete chemical reactions (No. 5-6) exhibited a stress-strain relationship characterized by three phases: elastic, plateau, and densification (Subhash et al., 2005). In the elastic phase, the material yields as the stress increases. When the yield point is exceeded, the sample moves into the plateau phase, undergoing deformation to a degree where it cannot return to its original state and entering the densification period. This results in compaction of the sample, leading to a sudden increase in compressive strength (Ashby & Lu, 2003; Outllet et al., 2006). Figure 4.22(b)

illustrates the sample's behavior following high-pressure injection (13.8 MPa). All samples exhibited brittle material behavior (No. 1–6) with values surpassing the standard values for lightweight foam materials commonly used in road construction. The failure characteristics of both sample types (brittle and three-phase behaviors) are shown in Figure 4.23.



(a)



(b)

Figure 4.2.2 Compressive strength test results of PU foam samples prepared by injection pressures (a) 10.4 MPa (b) 13.8 MPa

Boonsung et al. (2023) conducted a study that investigated the compressive strength and microstructure of PU foam. They created the PU foam samples by combining P with D at different ratios and temperatures inside a PVC mold that had a diameter of 75 mm and a height of 200 mm. The liquid foam generated pressure and expanded inside the mold when its cover was closed, without requiring high-pressure injection. The test results showed that reducing the ratio of p/d was associated with an increase in the compressive strength of PU foam. An examination under a microscope revealed that a decrease in the p/d ratio caused chemical processes to occur more quickly and increased the internal pressure. This resulted in smaller foam cells that were somewhat compressed, ultimately leading to an increase in the unit weight of PU foam. The compressive strength was achieved at a value of 0.132 MPa, with a p/d ratio of 1 and a mixing temperature of 40 °C. Hejna et al. (2017) conducted a separate investigation to examine the sizes of PU foam cells produced with three different p/d ratios: 1.5, 2.0, and 2.5. The results indicated an inverse correlation, whereby an augmentation in D quantity (leading to a diminished p/d ratio) tended to diminish the dimensions of foam cells, consistent with the findings of Boonsung et al.'s research (2023).



Figure 4.23 Failure characteristics of the PU foam samples (a) brittle behavior
(b) three-phase behavior

Figure 4.24 illustrates the relationship between the unit weight and PU foam samples that were generated under different injection pressures. The samples created at a higher pressure of 13.8 MPa had a larger unit weight value than those made at a lower pressure of 10.4 MPa. The average density values for the two groups were 42.1 kg/m³ and 88.8 kg/m³, respectively. The results presented in Figure 4.22 are consistent with these observations regarding compressive strength. Nevertheless, upon comparing the compressive strength measurements of PU foam samples made in the laboratory (Boonsung et al., 2023), it became apparent that the compressive strength of field-injected samples exceeded that of laboratory samples. The difference is attributed to the compression of foam cells caused by pressure in the field, which arises from two main factors: the chemical reaction and the injection pressure. Conversely, the pressure inside the laboratory mold is only produced by the chemical reaction. This comparison highlighted the crucial significance of the pressure exerted during the injection of PU foam in affecting the strength of the foam used to improve pavement structures.

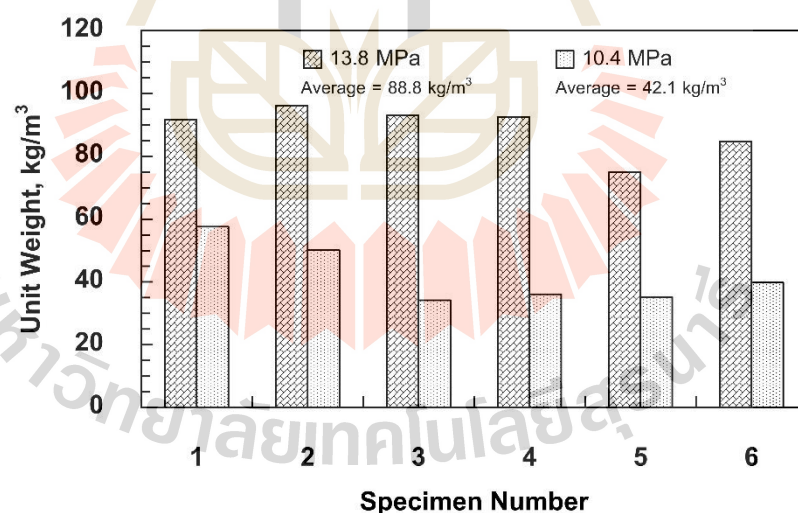


Figure 4.24 Unit weight of PU foam injected at different pressures.

4.6 Guidelines for Repairing the Pavement Structure Using PU Foam Injection

Improving pavement structure in Thailand with settlement issues through PU foam injection techniques can be approached in various ways, depending on the specific problem and the physical characteristics of the work area. While this method effectively deals with pavement settlement, there are currently no established standards for its implementation based on engineering principles. In this paper, the authors have presented a practical step-by-step work guideline. The guideline was designed for use by agencies or service organizations to ensure that the requested service and performance results align with consistent standards.

4.6.1 Survey of Physical Characteristics

The area survey covers several aspects, including geographical features (like the shape of the area and its surroundings), soil properties, water pathways, and essential road information such as location coordinates, road use, and surface type. To understand the damage characteristics, cavity dimensions (measured through resistivity imaging), and pavement settlement values, the accurate measurements are essential, typically obtained with specialized equipment. When dealing with significant settlement issues and deep injection methods, it is crucial to conduct an in-situ soil investigation. This assessment helps determine the required depth, injection pattern, and contributes to creating a diagram outlining the scope of work.

4.6.2 Planning

The planning provides a clear description of the solutions and techniques used for the task, including the specific methodology for injecting PU foam (deep or shallow injection), the precise position and depth of the injection, the mixing temperature, and the ratio of polyol to diisocyanate (p/d ratio). The recommended injection pressure range is 3.45 to 13.80 MPa (500 to 2,000 psi). Table 4.4 suggests the suitable injection pressures according to the repair goal. The comprehensive strategy should also encompass the subsequent inspection procedure following the modification. It is advisable to maintain a mixing temperature of 40°C and a p/d ratio of 1.0 (Boonsung et al., 2023).

Table 4.4 Pressure range of PU foam injection sequence for soil improvement
(Mohamed Jais, 2017)

Description	Pressure, psi	Pressure, kPa
Void/Cavity Filling	500 – 800	3,450 – 5,515
Soil Strengthening and Compaction	800 – 1,200	5,515 – 8,275
Hydrofracturing and Friction Resistance	1,200 – 1,500	8,275 – 10,345
Compensation and Uplifting	1,500 – 2,000	10,345 – 13,790

4.6.3 Safety Measures

In work areas, proper equipment must be prepared to prevent accidents during operations. This involves installing warning signs and setting speed limits for vehicles on the route. Workers are required to wear personal protective equipment consistently while on duty. PU foam injection systems and equipment must be regularly inspected, well-maintained, and prepared for use. Chemicals must be stored in secure containers within confined spaces. In the case of a leak, immediate prevention of the spread and seepage of chemicals into the soil must be implemented. Immediate cleaning should be conducted using appropriate disposal or cleaning equipment at the work site.

4.6.4 Quality Control

Ensure the chemical dosing system's performance by injecting liquid PU foam into a container at atmospheric pressure, allowing the foam to expand freely. Then, weigh the expanded foam to calculate the amount of chemical released per injection (stroke), denoted in units representing the total weight of P and D per stroke. This calculation is crucial for determining the overall amount of liquid PU foam used upon completing the work. Additionally, the operating pressure and the number of injections throughout the pavement repair process until its completion must be documented.

Begin by drilling a hole with a diameter ranging from 12 to 30 mm, adapting the size based on the equipment and PU foam nozzle in use. An injection pipe type is selected to suit the application, such as steel, copper, or aluminum. The selected pipe is inserted into the soil foundation at the desired depth. The compounds

(P and D) are then transported through a hydraulic system and mixed in a temperature-controlled nozzle. The injection is initiated by slowly introducing the liquid PU foam into the soil through a small hole at the end of the injection pipe. For deep PU foam injection, the injection process is divided into 0.5-meter intervals, gradually lifting the injection pipe and allowing PU foam to be injected slowly upward. During each stroke of PU foam injection, the injection is waited for a 10-second period to allow the foam to harden before proceeding to the next stroke. If injecting PU foam at a shallow level with the intention of raising the surface, the injection is continuous and stopped when the pavement surface reaches the desired level.

During injecting PU foam, a high-precision laser level meter (with a resolution of at least 0.01 mm) is recommended to measure the movement of the pavement surface. The expansion of PU foam will gradually raise the pavement surface to the desired level in the final injection stage, slightly below the pavement surface. The injection is continued until the pavement surface raises by at least 5 mm above the desired level, to ensure effective filling of the cavity with liquid PU foam. The complete chemical reaction takes at least 15 minutes for transition from liquid to solid, developing the necessary mechanical properties. Afterward, the drilled holes are sealed with non-shrink cement. The pavement can then be leveled for immediate use, using the same material as the original pavement, and can be opened for regular use after a 2-hour period.

PU foam samples are generated by injecting liquid PU foam into a rigid mold, replicating the field conditions. The collected samples are undergone laboratory testing to evaluate physical and engineering properties, including unit weight and compressive strength. Testing is conducted on cubes with dimensions of 50 mm x 50 mm x 50 mm, following the guidelines set by the Public Roads Administration 484E (1992). The results of the compressive strength test must indicate stress levels at strains equivalent to 1%, 5%, and 10%, along with illustrating the stress-strain relationship up to at least 80% strain. The compressive strength at 1% strain and at failure should not fall below 0.015 MPa and 0.128, respectively, in accordance with the standard specification for rigid cellular polystyrene geofoam (ASTM D6817, 2017).

In situations where the cavity beneath the pavement structure is large, a lightweight material is recommended to fill the space before injecting liquid PU foam over it to manage production costs. However, it is crucial to design the lightweight material with a specific unit weight (8 to 12 kN/m³) and compressive strength (100 to 1,000 kPa). This design can involve various production techniques, such as adding foam, using additives that create air bubbles, and incorporating lightweight composite materials.

4.6.5 Monitoring

The pavement surface-level is immediately recorded after completing the PU foam injection and before opening for operation. The level data and physical characteristics are also recorded one, two, and four weeks after commencement, along with presenting comparative charts.

4.6.6 Performance Report

The post-maintenance work report must include various information, including at least an executive summary, project background and history, project details consisting of location, current situation, repair methods, and work plans. It should also cover the results of testing foam samples and/or lightweight materials, along with the total quantity of PU foam used in the project. The project's outcomes are finally summarized. The pavement repair using the PU foam injection technique can be outlined as steps, as illustrated in Figure 4.25.

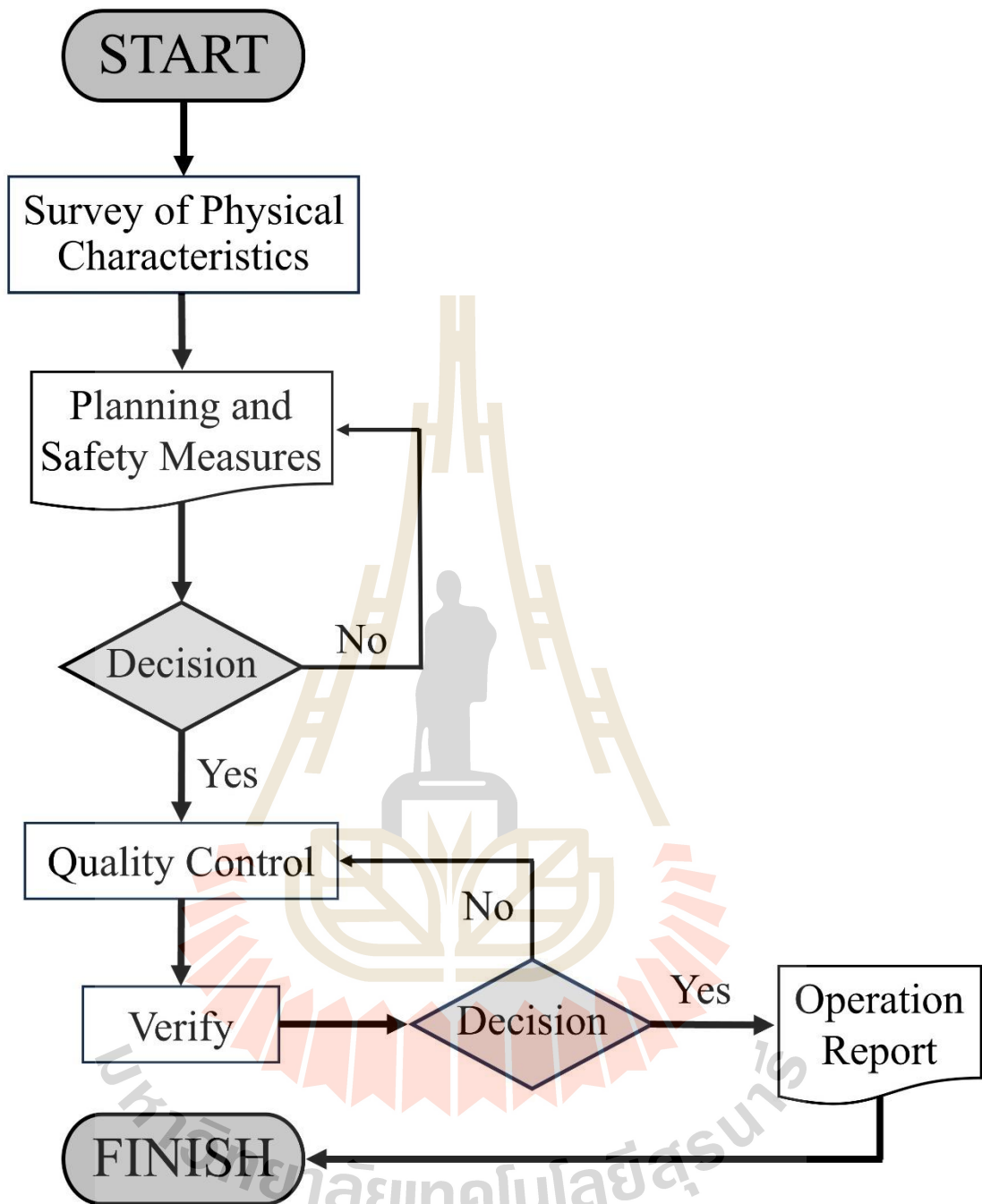


Figure 4.25 Schematic of the steps for pavement repair by injecting PU foam into the pavement structure layer.

4.7 Conclusions

Employing the PU foam injection technique to strengthen the pavement structure proves highly effective and advantageous in terms of budget, time, and environmental considerations compared to traditional methods. However, its implementation requires a thorough understanding of specific issues and constraints. The primary discoveries of the study can be summarized as follows:

1) Polyurethane (PU) foam is created through a chemical reaction between polyol and diisocyanate, which forms the strong molecular chain. In pavement surface maintenance, liquid foam is injected into the pavement structure, filling the gaps in the soil mass and expanding under the ambient pressure exerted by the soil. Upon hardening, PU foam with closed cells exhibited high bearing capacity of soil foundation.

2) Pavement surface settlement manifests in two distinct forms. The first is settlement arising from the compressibility of pavement materials due to inadequate compaction quality control. This settlement type is commonly observed in pavement concretes near connection joints, particularly on the road shoulder at U-turn locations. Employing a shallow PU foam injection technique can effectively rectify this damage, restoring the pavement surface to a normal and usable condition. The second is the loss of soil mass beneath the pavement surface, typically occurring at connection points between bridge approach slab and bridge deck, where compaction is difficult. Soil loss occurs when water infiltrates or a water stream passes through, creating voids beneath the bridge approach slab surface. Addressing this issue involves employing a deep injection technique utilizing a nozzle to convey liquid PU foam to the layer required improvement.

3) In scenarios where the pavement structure contains numerous substantial voids, relying solely on PU foam may pose constraints on the operational budget. The incorporation of a lightweight material as partial backfill, combined with PU foam, proves to be a cost-effective solution, as lightweight materials are more economical than PU foam. Nonetheless, it is essential to ensure that the selected lightweight material is designed with suitable properties concerning compressive strength, unit weight, and working time.

4) While the PU foam injection technique proves effective for pavement repairs in Thailand and is gaining widespread adoption, the absence of a standardized operational framework or quality assessment by government agencies remains a challenge. To address this, the comprehensive step-by-step guideline tailored for this technique is introduced in this paper. This guideline encompasses spatial data collection, data analysis for plan preparation, establishment of safety protocols during work, quality control measures, and the specifics of compiling performance reports to ensure adherence to engineering principles throughout operations.

4.8 References

- Akindoyo, J. O., Beg, M., Ghazali, S., Islam, M. R., Jeyaratnam, N., & Yuvaraj, A. R. (2016). Polyurethane types, synthesis and applications—a review. *Rsc Advances*, 6(115), 114453-114482.
- Ashby, M., and T. Lu. 2003. “Metal foams: A survey.” *Sci. China Ser. B Chem.* 46 (6): 521–532. <https://doi.org/10.1360/02yb0203>.
- Ashida, K. 2006. *Polyurethane and Related Form: Chemistry and Technology*. Boca Raton, USA: CRC Press.
- ASTM. (2017). *Standard Specification for rigid cellular polystyrene geofoam*. ASTM D6817-07, West Conshohocken, PA.
- Boonsung, A., Horpibulsuk, S., Pathompongpaioj, A., Sawatwutichaikul, A., Choenklang, P., & Arulrajah, A. (2023). Compressive Strength and Morphology of Rigid Polyurethane Foam for Road Applications. *Journal of Materials in Civil Engineering*, 35(12), 04023474. <https://doi.org/10.1061/JMCEE7.MTENG-16138>
- Buzzi, O., Fityus, S., & Sloan, S. W. (2010). Use of expanding polyurethane resin to remediate expansive soil foundations. *Canadian Geotechnical Journal*, 47(6), 623-634. <https://doi.org/10.1139/T09-132>
- Buzzi, O., Fityus, S., Sasaki, Y., & Sloan, S. (2008). Structure and properties of expanding polyurethane foam in the context of foundation remediation in expansive soil. *Mechanics of Materials*, 40(12), 1012-1021. <https://doi.org/https://doi.org/10.1016/j.mechmat.2008.07.002>

- Capatti, M. C., Dezi, F., & Morici, M. (2016). Field tests on micropiles under dynamic lateral loading. *Procedia Engineering*, 158, 236-241. <https://doi.org/10.1016/j.proeng.2016.08.435>
- Department of Highways. (2023). Traffic information On the intercity expressway No. 7 and No. 9. <https://www.motorway.go.th/>
- Department of Rural Roads. (2009). Guide to road construction on soft ground, Team Group and Geotechnical Co., Ltd. & Foundation Engineering Co., Ltd. (GFE)
- DOH. (2012). Privatization of highway infrastructure in Thailand.
- Eide, O. (1968). Geotechnical engineering problems with soft Bangkok clay on the Nakhon Sawan highway project, Pub. No 78, Norwegian Geotechnical Institute, Norway.
- Eide, O. (1977). Exploration, sampling and in-situ testing of soft clay in the Bangkok area, Proc. of International Symposium on Soft Clay, Thailand, pp122–137.
- Fakhar, A., & Asmaniza, A. (2016). Road Maintenance Experience Using Polyurethane (PU) Foam Injection System and Geocrete Soil Stabilization as Ground Rehabilitation. *IOP Conference Series: Materials Science and Engineering*, 136, 012004. <https://doi.org/10.1088/1757-899X/136/1/012004>
- Fityus, S. G., Buzzi, O., & Imre, E. (2011). Large scale tests on the expansiveness of resin-injected clay. *Unsaturated Soils: Theory and Practice*, 521-526.
- Gama, N. V., Ferreira, A., & Barros-Timmons, A. (2018). Polyurethane Foams: Past, Present, and Future. *Materials*, 11(10), 1841. <https://www.mdpi.com/1996-1944/11/10/1841>
- Gaspard, K., & Morvant, M. (2004). Assessment of the Uretek process on continuously reinforced concrete pavement, jointed concrete pavement, and bridge approach slabs: technical assistance report (No. 03-2TA). Louisiana Transportation Research Center.
- Guo, C., Sun, B., Hu, D., Wang, F., Shi, M., & Li, X. (2019). A field experimental study on the diffusion behavior of expanding polymer grouting material in soil. *Soil Mechanics and Foundation Engineering*, 56, 171-177. <https://doi.org/10.1007/s11204-019-09586-7>

- Hejna, A., J. Haponiuk, L. Piszczyk, M. Klein, and K. Formela. 2017. "Performance properties of rigid polyurethane-polyisocyanurate/brewers' spent grain foamed composites as function of isocyanate index." *e-Polymers* 17 (5): 427-437. <https://doi.org/10.1515/epoly-2017-0012>.
- Herrington, R., and Hock, K. 1997. *Flexible Polyurethane Foams*. 2nd Ed., Midland, USA: Dow Chemical Co.
- Horpibulsuk, S., Suddeepong, A., Chinkulkijniwat, A., & Liu, M. D. (2012). Strength and compressibility of lightweight cemented clays. *Applied Clay Science*, 69, 11-21.
- Islam, M. R., Beg, M. D. H., & Jamari, S. S. (2014). Development of vegetable-oil-based polymers. *Journal of applied polymer science*, 131(18).
- Jamnongpipatkul, P., Dechasakulsom, M., & Sukolrat, J. (2009). Application of air foam stabilized soil for bridge-embankment transition zone in Thailand. *Asphalt Material Characterization, Accelerated Testing, and Highway Management: Selected Papers from the 2009 GeoHunan International Conference*,
- Jongpradist, P., Youwai, S., & Jaturapitakkul, C. (2011). Effective void ratio for assessing the mechanical properties of cement-clay admixtures at high water content. *Journal of geotechnical and geoenvironmental engineering*, 137(6), 621-627.
- Kamon, M. and Bergado, D.T. (1991). Ground improvement techniques. *Proceedings of 9th Asian Regional Conference on Soil Mechanics and Foundation Engineering*, Bangkok, 2: 526-546.
- Komurlu, E., & Kesimal, A. (2012). Investigation of polyurethane reinforced soil strength.
- Komurlu, E., & Kesimal, A. (2014). Improved Performance of Rock Bolts using Sprayed Polyurea Coating. *Rock Mechanics and Rock Engineering*, 48. <https://doi.org/10.1007/s00603-014-0696-4>
- Lat, D. C., Ali, N., Jais, I. B. M., Yunus, N. Z. M., Razali, R., & Talip, A. R. A. (2020). A review of polyurethane as a ground improvement method. *Malaysian Journal of Fundamental and Applied Sciences*, 16(1), 70-74. <https://doi.org/10.11113/mjfas.v16n1.1235>
- Lenart, S., & Kaynia, A. M. (2019). Dynamic properties of lightweight foamed glass and their effect on railway vibration. *Transportation Geotechnics*, 21, 100276.

- Lim, S. K., Tan, C. S., Li, B., Ling, T.-C., Hossain, M., & Poon, C. S. (2017). Utilizing high volumes quarry wastes in the production of lightweight foamed concrete. *Construction and Building Materials*, 151, 441-448. <https://doi.org/10.1016/j.conbuildmat.2017.06.091>
- Malai, A., Youwai, S., Watcharasawe, K., & Jongpradist, P. (2022). Bridge approach settlement mitigation using expanded polystyrene foam as light backfill: Case study and 3D simulation. *Transportation Geotechnics*, 35, 100794. <https://doi.org/https://doi.org/10.1016/j.trgeo.2022.100794>
- Moh, Z.C., Nelson, J.D. and Brand, E.W. (1969). Strength and Deformation Behavior of Bangkok Clay. *Proceedings, 7th International. Conference on Soil Mechanics and Foundation Engineering, Mexico City, Vol. 1*, pp. 287-295.
- Mohamed Jais, I. (2017). Rapid remediation using polyurethane foam/resin grout in Malaysia. *Geotechnical Research*, 4, 1-11. <https://doi.org/10.1680/jgere.17.00003>
- Molinda G. (2004) Evaluation of polyurethane injection for beltway roof stabilization in a West Virginia coal mine. In: *Proceedings of the 23rd international conference on ground control in mining, Morgantown, WV, 3-5 August 2004*, pp 190-196
- Molinda, G. (2008). Reinforcing coal mine roof with polyurethane injection: 4 case studies. *Geotechnical and Geological Engineering*, 26, 553-566.
- Mounanga, P., Gbongbon, W., Poullain, P., & Turcry, P. (2008). Proportioning and characterization of lightweight concrete mixtures made with rigid polyurethane foam wastes. *Cement and Concrete Composites*, 30, 806-814. <https://doi.org/10.1016/j.cemconcomp.2008.06.007>
- Neramitkornburi, A., Horpibulsuk, S., Shen, S.L., Arulrajah, A. and Disfani, M.M. (2015) (a), "Engineering properties of lightweight cellular cemented clay-fly ash material", *Soils and Foundations*, Vol.55, No.2, pp.471-483
- Neramitkornburi, A., Horpibulsuk, S., Shen, S.L., Chinkulkijniwat, A., Arulrajah, A. and Disfani, M.M. (2015) (b), "Durability against wetting-drying cycles of sustainable lightweight cellular cemented construction material comprising clay and fly ash wastes", *Construction and Building Materials*, Vol.77, pp.41-49

- Nikomborirak, D. (2004). Private sector participation in infrastructure: The case of Thailand.
- Outlet, S., D. Cronin, and M. Worswick. 2006. "Compressive response of polymeric foams under quasi-static medium and high strain rate conditions." *Polym. Test.* 25 (6): 731–743. <https://doi.org/10.1016/j.polymertesting.2006.05.005>.
- Patil, S. S., & Molenaar, K. R. (2011). Risks associated with performance specifications in highway infrastructure procurement. *Journal of Public Procurement*, 11(4), 482-508.
- Peduto, D., Giangreco, C., & Venmans, A. A. (2020). Differential settlements affecting transition zones between bridges and road embankments on soft soils: Numerical analysis of maintenance scenarios by multi-source monitoring data assimilation. *Transportation Geotechnics*, 24, 100369.
- Public Roads Administration. 1992. Quality Control of Expanded Polystyrene Used in Road Embankments 484E. Oslo, Norway: Road Research Laboratory.
- Puppala, A., Archeewa, E., Saride, S., Nazarian, S., & Lr, H. (2012). Recommendations for Design, Construction, and Maintenance of Bridge approach Slabs.
- Rao, S., Abdulla, H., & Yu, T. (2019). Design and Construction of Bases and Subbases for Concrete Pavement Performance. In *Proc., Geo-Structural Aspects of Pavements, Railways, and Airfields (GAP) Conference*, Colorado Springs, CO (pp. 4-7).
- Sabri, M. M., & Shashkin, K. G. (2018). Improvement of the soil deformation modulus using an expandable polyurethane resin. *Magazine of Civil Engineering*, (7 (83)), 222-234. Doi: 10.18720/MCE.83.20
- Sabri, M. M., & Shashkin, K. G. (2020). The mechanical properties of the expandable polyurethane resin based on its volumetric expansion nature. *Magazine of Civil Engineering*, (6 (98)), 9811. doi: 10.18720/MCE.98.11
- Sabri, M. M., Shashkin, K. G., Zakharin, E., & Ulybin, A. V. (2018). Soil stabilization and foundation restoration using an expandable polyurethane resin. *Magazine of Civil Engineering*, (6 (82)), 68-80. doi: 10.18720/MCE.82.7.

- Sánchez Lavín, J. R., Escolano Sánchez, F., & Mazariegos de la Serna, A. (2018). Chemical injections realized with null pressure for underpinning the foundation of an 18th Century Building located in the historical city of Cuenca (Spain). *Applied Sciences*, 8(7), 1117. <https://doi.org/10.3390/app8071117>
- Sánchez, F. E., de la Serna, A. M., Lavín, J. R. S., & del Campo Yagüe, J. M. (2017). Underpinning of shallow foundations by expansive polyurethane resin injections. Case study: Cardinal Diego de Espinosa Palace in Segovia (Spain). *Revista de la Construcción. Journal of Construction*, 16(3), 420-430. <https://doi.org/10.7764/RDLC.16.3.420>
- Sharmin E and Zafar F (2012) Polyurethane: an Introduction. InTech, Rijeka, Croatia.
- She, W., Du, Y., Zhao, G., Feng, P., Zhang, Y., & Cao, X. (2018). Influence of coarse fly ash on the performance of foam concrete and its application in high-speed railway roadbeds. *Construction and Building Materials*, 170, 153-166. <https://doi.org/https://doi.org/10.1016/j.conbuildmat.2018.02.207>
- Sidek, N., Mohamed, K., Mohamed Jais, I., & abu bakar, I. (2015). Strength Characteristics Of Polyurethane (PU) With Modified Sand. *Applied Mechanics and Materials*, 773-774, 1508-1512. <https://doi.org/10.4028/www.scientific.net/AMM.773-774.1508>
- Soltész, S. (2002). Injected polyurethane slab jacking : final report [Tech Report]. <https://rosap.nsl.bts.gov/view/dot/22955>
- Subhash, G., T. R. Walter, and A. W. Richards. 2005. "A unified phenomenological model for tensile and compressive response of polymeric foams." *J. Eng. Mater. Technol.* 131 (1): 1–6. <https://doi.org/10.1115/1.3026556>.
- Szycher, M. 2013. *Szycher's Handbook of Polyurethanes*. 2nd Ed. Boca Raton, USA: CRC Press.
- Tanchaisawat, T., Bergado, D. T., & Voottipruex, P. (2008). Numerical simulation and sensitivity analyses of full-scale test embankment with reinforced lightweight geomaterials on soft Bangkok clay. *Geotextiles and Geomembranes*, 26(6), 498-511.
- Ulrich, H. (1982). *Introduction to industrial Polymers*. 56 – 79.

- Valentino, R., & Stevanoni, D. (2016). Behaviour of reinforced polyurethane resin micropiles. *Proceedings of the Institution of Civil Engineers - Geotechnical Engineering*, 169, 187-200. <https://doi.org/10.1680/jgeen.14.00185>
- Vardhanabhuti, B., Chantawarangul, K., & Seawsirikul, S. (2015). Utilization of EPS Geofoam for Bridge Approach Structure on Soft Bangkok Clay. In *Geotechnical Safety and Risk V* (pp. 602-607). IOS Press.
- Weaver, K.D. and Bruce, D.A. (2007). *Dam Foundation Grouting*, 2007, pp. 87–136.
- Wolf, H. (1956). Catalyst activity in one-shot urethane foam. *Technical Bulletin*, Dupont, Wilmington, 30-65.
- Won, J. P., Kim, J. M., Lee, S. J., Lee, S. W., & Park, S. K. (2011). Mix proportion of high-strength, roller-compacted, latex-modified rapid-set concrete for rapid road repair. *Construction and Building Materials*, 25(4), 1796-1800. <https://doi.org/10.1016/j.conbuildmat.2010.11.085>
- Wonglert, A., Jongpradist, P., Jamsawang, P., & Larsson, S. (2018). Bearing capacity and failure behaviors of floating stiffened deep cement mixing columns under axial load. *Soils and Foundations*, 58(2), 446-461.
- Wood G 1982 *Flexible Polyurethane Foams, Chemistry and Technology*. Applied Science Publishers, London. 120 – 160.
- Yang, Y., & Chen, B. (2016). Potential use of soil in lightweight foamed concrete. *KSCE Journal of Civil Engineering*, 20(6), 2420-2427. <https://doi.org/10.1007/s12205-016-0140-2>
- Yu, L., Wang, R., & Skirrow, R. (2013). The application of polyurethane grout in roadway settlements issues. *Geo Montreal*, 1-7.

CHAPTER V

CONCLUSION AND RECOMMENDATION

5.1 Summary and conclusion

This thesis consists of three main objectives. The first is to investigate the factors influencing compressive strength and microstructure of rigid polyurethane (PU) foam. The second is to present case studies of pavement structure improvement using shallow and deep PU foam injection techniques to remedy the damaged concrete pavements and asphalt concrete pavement. The third is to propose a guideline for applying the PU foam injection technique to solve the problem of road settlement based on engineering principles.

5.1.1 Compressive strength and morphology of rigid PU foam for road applications

This chapter discusses the influence of polyol content, polyol-to-isocyanate ratio (p/d ratio), and temperature when mixing polyol and isocyanate on the compressive strength and microstructure of rigid PU foam. The stress-strain relationship of PU foam was found to have three zones: linear, plateau, and densification. At ambient mixing temperature (25°C), for a given P content, the lower p/d ratio resulted in lower strains at the start of each zone and higher yield stress, toughness, and compressive strength. At the ambient mixing temperature, for a particular P content, the compressive strength of RPUF prepared at high temperatures (> 40°C) decreased with the decrease in p/d ratio. For low P contents of 23 and 28, an increase in mixing temperature from 25°C to 40°C increased the compressive strength of PU foam for a given p/d ratio. However, for a high P content of 34 kg/m³, the increased mixing temperature from 25°C to 40°C caused a reduction in compressive strength. The EDS results showed unchanged chemical compositions in the PU foam structure with the elevated mixing temperatures, as seen by the similar amount of C and O for all the mixing temperatures tested. The compressive strength development with mixing temperature did not result from the chemical bonding development but

was due to the increased cell contact pressures. The microstructural analysis showed that the elevated mixing temperature and reduced p/d ratio stimulated gasification, resulting in small cells with high cell contact pressures. The sufficient cell-contact pressure increased the compressive strength and toughness, while the extremely large cell-contact pressure caused cell damage and reduced the strength and toughness. At low P content, the elevated mixing temperature to 40°C and the reduced p/d ratio improved the compressive strength of RPUF. However, the elevated mixing temperature at high P content resulted in cell damage; the reduced p/d ratio was recommended to enhance the compressive strength. To be economical and to meet the upper limit of 0.128 MPa for EPS foam, the increased mixing temperature from ambient to 40°C could improve compressive strength at low P contents of 23 and 28 kg/m³; the 40°C and p/d ratio of 1 were the best ingredients. The ambient mixing temperature and p/d = 0.8 were the best for high P content. With the high cost of P and D, a low P content of < 28 kg/m³ with a 40°C mixing temperature is recommended.

5.1.2 Performance of the PU foam injection technique for road maintenance applications

This chapter presents the solution to the problem of road settlement with the PU injection technique. PU foam is created through a chemical reaction between polyol and diisocyanate, which forms a strong molecular chain. In pavement surface maintenance, liquid foam is injected into the pavement structure, filling the gaps in the soil mass and expanding under the ambient pressure exerted by the soil. Upon hardening, PU foam with closed cells exhibited a high soil foundation-bearing capacity. Pavement surface settlement manifests in two distinct forms. The first is settlement arising from the compressibility of pavement materials due to inadequate compaction quality control. This settlement type is commonly observed in pavement concrete near connection joints, particularly on the road shoulder at U-turn locations. A shallow PU foam injection technique can effectively rectify this damage, restoring the pavement surface to a normal and usable condition. The second is the loss of soil mass beneath the pavement surface, typically occurring at connection points between the bridge approach slab and the bridge deck, where compaction is difficult. Soil loss occurs when water infiltrates, or a water stream passes through, creating voids beneath

the bridge approach slab surface. Addressing this issue involves employing a deep injection technique utilizing a nozzle to convey liquid PU foam to the layer requiring improvement. In scenarios where the pavement structure contains numerous substantial voids, relying solely on PU foam may constrain the operational budget. Incorporating a lightweight material as a partial backfill, combined with PU foam, proves to be a cost-effective solution, as lightweight materials are more economical than PU foam. Nonetheless, ensuring that the selected lightweight material is designed with suitable properties concerning compressive strength, unit weight, and working time is essential.

5.1.3 Guidelines for repairing the pavement structure using PU Foam Injection

While the PU foam injection technique proves effective for pavement repairs in Thailand and is gaining widespread adoption, the absence of a standardized operational framework or quality assessment by government agencies remains challenging.

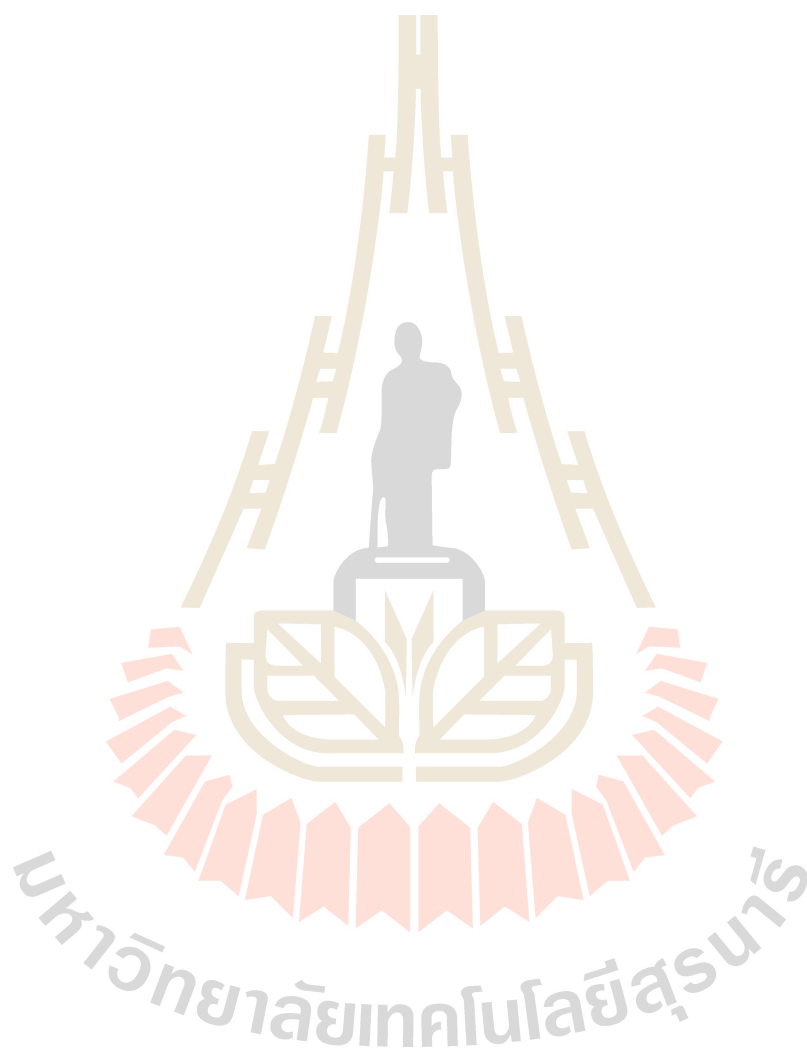
This chapter presented the proposed guideline for applying the PU foam injection technique to solve the problem of road settlement based on engineering principles. The guideline included methods for surveying physical characteristics, planning, safety measures, quality control, and preparing performance reports. This CoP can be extended to develop a working standard for relevant agencies such as the Department of Highways, the Department of Rural Roads, and the Department of Local Administration for repairing road settlements that will support the sustainable development of the country's transportation system.

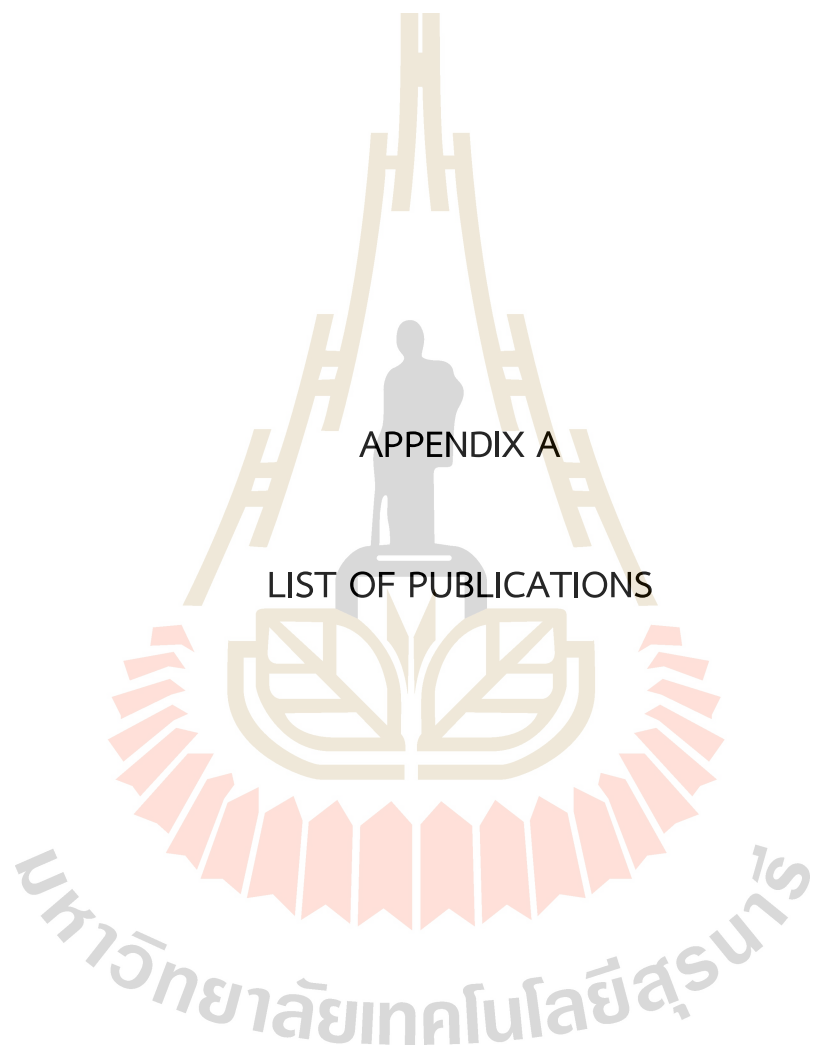
5.2 Recommendations for future work

5.2.1 This study only examined the static compressive strength of PU foam. The flexural strength, compressibility, and behavior of PU foam under repeated loads can be considered for future study.

5.2.2 The stress-strain behavior and load-bearing capacity of PU foam improved soils, such as sand, silt, clay, etc., can be investigated via laboratory test and numerical simulation for future research.

5.2.3 The durability against wetting-drying cycles of PU foam is recommended for future research.





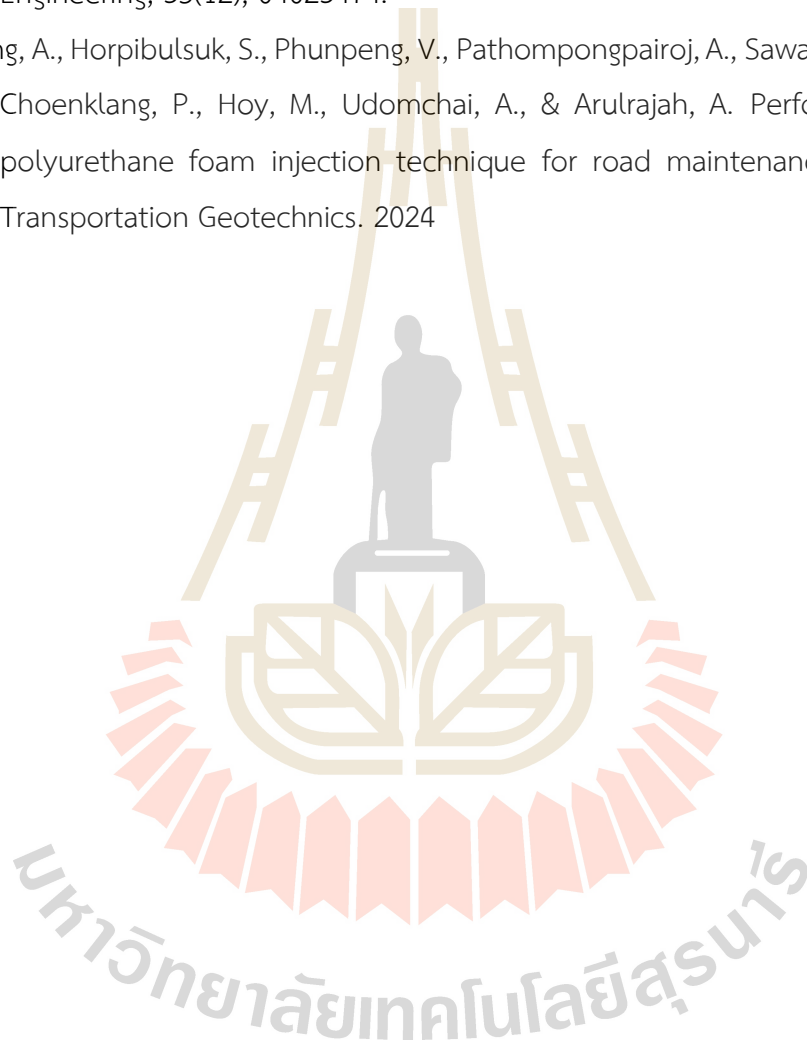
APPENDIX A

LIST OF PUBLICATIONS

List of Publications

Boonsung, A., Horpibulsuk, S., Pathompongpaioj, A., Sawatwutichaikul, A., Choenklang, P., & Arulrajah, A. (2023). Compressive Strength and Morphology of Rigid Polyurethane Foam for Road Applications. *Journal of Materials in Civil Engineering*, 35(12), 04023474.

Boonsung, A., Horpibulsuk, S., Phunpeng, V., Pathompongpaioj, A., Sawatwutichaikul, A., Choenklang, P., Hoy, M., Udomchai, A., & Arulrajah, A. Performance of the polyurethane foam injection technique for road maintenance applications. *Transportation Geotechnics*. 2024




ASCE

Compressive Strength and Morphology of Rigid Polyurethane Foam for Road Applications

Aroondet Boonsung¹; Suksun Horpibulsuk, Ph.D.²; Atthapan Pathompongpaioj³;
Apiwich Sawatwutichaikul⁴; Punvalai Choenklang, Ph.D.⁵; and Arul Arulrajah, Ph.D.⁶

Abstract: Rigid polyurethane foam (RPUF) is a lightweight material similar to expanded polystyrene foam but which has undergone a safer manufacturing process, for instance without flammable gases such as butane (C₄H₁₀) or pentane (C₅H₁₂). RPUF is manufactured from the combination of polyol (P) and diisocyanate (D) and can be used as lightweight and load-bearing materials for pavement applications. This research studied the influence of P content, polyol to diisocyanate ratio (p/d ratio), and mixing temperature of P and D on the compressive strength and microstructure of RPUF. For a particular P content, the increase in mixing temperature and the reduced p/d ratio resulted in a large amount of small-sized cells with high cell-contact pressure. The sufficient cell-contact pressure increased the compressive strength of RPUF and toughness, and extremely large cell-contact pressure caused the cell damage and the reduction in strength and toughness. At low P content, both an elevated mixing temperature to 40°C and reduced p/d ratio improved compressive strength of RPUF. However, at a high P content, the elevated mixing temperature resulted in cell damage, and the ambient mixing temperature of 25°C is recommended. To meet the upper limit of 0.12-MPa compressive strength at 1% strain for geofoam according to current standards the 40°C mixing temperature and p/d ratio of 1.0 are suggested for P content of 23 and 28 kg/m³, and the ambient mixing temperature and p/d ratio of 0.8 are suggested for P content of 34 kg/m³. DOI: 10.1061/JMCEE7.MTENG-16138. © 2023 American Society of Civil Engineers.

Author keywords: Rigid polyurethane foam (RPUF); Microstructure; Strength; Pavement geotechnics.

Introduction

Road infrastructure is the leading utility that drives national and global economics. Road construction is sometimes undertaken on weak soil foundations, whereby ground improvement techniques are often required. Popular methods included deep-mixing and jet-grouting techniques with cement slurry to develop the soil cement column (SCC) due to their convenient and fast execution. The water/cement ratio and diameter of the SCC directly affect its load-bearing capacity (Wang et al. 2013; Sukmak et al. 2022). Shen et al. (2013)

presented a generalized approach for predicting the diameter jet-grouted SCC based on the theoretical framework of turbulent kinematic flow and soil erosion. An artificial neural network (ANN) model can also be applied to approximate the diameter of SCC (Atangana Njock et al. 2021; Ochmański et al. 2015; Shen et al. 2021). In addition to the SCC application, lightweight material is commonly applied on weak soil foundation for road construction (Neramitkornburi et al. 2015).

The development of lightweight materials for the construction industry has been continuing for a long time to improve their engineering properties at reasonable production costs. Lightweight materials are continually manufactured under various concepts with the main objective of reducing the load on the structural system (Lee and Ramesh 2004; Sulong et al. 2019). Due to the superior properties of foam compared with other similar lightweight materials, foam is often considered as the first priority. Foam applications may also be found in other forms, such as electronic and automotive equipment, food packaging, and thermal insulation in aerospace industries (Heaves 2004; Wellnitz 2007; Ashida 2006; Das et al. 2017). In the construction industry, it is often used as the core of the structural insulated panel, principal exterior wall, framing, partition wall, roof, floor, and structural framing (Manalo 2013; Chen and Hao 2014; Chen et al. 2015).

In addition to being used as a component of building structures, foam materials can be used in the construction of roads and highways to overcome the settlement problem. In 1965, expanded polystyrene (EPS) foam was used as insulation in road construction in Norway. In 1972, the Norwegian Public Roads Authority developed a standard for the use of EPS foam as a lightweight material to replace the traditional backfill material in road construction projects. It was found that the EPS foam successfully minimized the settlement of the road structure (Frydenlund 1991; Frydenlund and Aabøe 2001; NPRA 2002; Aabøe and Frydenlund 2011). Norway

¹Ph.D. Scholar, Graduate Program in Civil Engineering and Construction Management, Suranaree Univ. of Technology, Nakhon Ratchasima 30000, Thailand. Email: a.boonsung9@gmail.com

²Professor, School of Civil Engineering, Suranaree Univ. of Technology, Nakhon Ratchasima 30000, Thailand; Director, Center of Excellence in Innovation for Sustainable Infrastructure Development, Suranaree Univ. of Technology, Nakhon Ratchasima 30000, Thailand; Associate Fellow, Academy of Science, Royal Society of Thailand, Bangkok 10300, Thailand (corresponding author). ORCID: <https://orcid.org/0000-0003-1965-8972>. Email: suksun@g.sut.ac.th

³Manager, Tesla Engineering Co. Ltd., 1 Soi. Anamai-ngamjaroen 14, Takham, Bangkoktean, Bangkok 10150, Thailand. Email: atthapanpathompongpaioj@gmail.com

⁴Managing Director, Tesla Engineering Co. Ltd., 1 Soi. Anamai-ngamjaroen 14, Takham, Bangkoktean, Bangkok 10150, Thailand. Email: apiwich@tesla.co.th

⁵Managing Director, S Class Engineer Co. Ltd., 52/200, Moo 2, Nakhon Ratchasima 30000, Thailand. Email: punvalai789@gmail.com

⁶Professor, Dept. of Civil and Construction Engineering, Swinburne Univ. of Technology, Melbourne, VIC 3122, Australia. ORCID: <https://orcid.org/0000-0003-1542-9803>. Email: arulrajah@swin.edu.au

Note. This manuscript was submitted on December 17, 2022; approved on May 5, 2023; published online on September 28, 2023. Discussion period open until February 28, 2024; separate discussions must be submitted for individual papers. This paper is part of the *Journal of Materials in Civil Engineering*, © ASCE, ISSN 0899-1561.

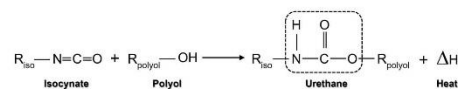


Fig. 1. Reaction of urethane product.

is therefore the pioneering country in the use of foam in construction projects.

In the early 1980s, EPS foam was used in construction projects in Europe, the US, and Japan and has become more popular since then (Sanders 1996; NCHRP 2004). EPS foam has been widely applied to geotechnical engineering applications such as improved slope stability, retaining wall structures, and fill material for road and bridge approaches (Refsdal 1985; Duskov 1991, 1997; Walter et al. 2000; Negussey 2002; Riad et al. 2003; Stark et al. 2004; Meguid et al. 2017).

Polyurethane foam (PUF) is a plastic foam in the same group of polymer foam group as EPS foam, but it is manufactured more safely because the manufacturing process of PUF is simple and does not require flammable gasses such as butane (C_4H_{10}) or pentane (C_5H_{12}). PUF was first synthesized in 1937 by Otto Bayer through a reaction between polyester diol and diisocyanate (Ionescu 2005; Priscacariu 2011; Sharmin and Zafar 2012; Szycher 2013). PUF is produced by polymerizing two organic compounds: isocyanates in the NCO group and hydroxyl alcohol, resulting in a urethane group with polymerization. When the urethane decomposes, it produces carbon dioxide (CO_2), which causes bubbles inside the foam. At the same time, heat will be released (Herrington and Hock 1997; Król 2008).

Fig. 1 shows the urethane reaction diagram where R_{iso} is an isocyanate monomer and R_{polyol} is a polyol component (Ionescu 2005). PUF is classified according to its structure into two types: flexible and rigid PU foams. The flexible PUF structure is connected by a strut network without wall cells (membrane) that rises under atmospheric pressure, called open-cell. Because of its flexibility, low density, and light weight, it is often used in furniture production as a cushioning material. The structure of the rigid PUF (RPUF) is similar to that of flexible PUF, but its cell walls are connected by the struts under pressure from the closed cells. It has a higher density than the flexible PUF, with a compressive strength in a range of 100–500 kPa (Padopoulos 2005; Villasmil et al. 2009). In 2017, global use of PU foam was reported to have reached USD 60.5 billion. With a continued upward trend, it was estimated that by 2021, PU foam usage would be more than USD 79 billion. With advanced manufacturing technology and superior properties compared with other lightweight materials, PUF has gained a wide application popularity.

Berardi and Madzarevic (2020) investigated the effect of microstructure and concentration of the foaming agent in PUF on the insulating properties over time. The results showed that the cell wall thickness increased over time, resulting in the reduced heat transfer. Stina et al. (2011) investigated the mechanical properties of RPUFs. The test foam samples were obtained by drilling a sheet of RPUF produced by a pouring process under $22^\circ\text{C} \pm 2^\circ\text{C}$. Their density was in the range of 65–70 kg/m^3 . Its mechanical properties, such as compressive strength, depend on two factors working together: one is the covalent bonds of the polymer network, and the other is the polymer matrix and compaction energy of the foam, which are independent of covalent bonds.

Wiyono et al. (2016) studied physical and mechanical properties of RPUF made from a polyol and diisocyanate mixture at a 1:1

ratio. It was found that the cell structure was anisotropic and the compressive strength and elastic modulus linearly increased with foam density. Witkiewicz and Zieliński (2006) studied the mechanical properties of RPUFs at densities of 16 and 62 kg/m^3 . The compressive strength depended on the structure of closed-cell foam, density, and temperature. Ridha and Shim (2008) investigated tensile strength, compressive strength, and the microstructure of RPUFs with three different densities. They reported that the cell foam was stretched when RPUF was under tensile force, indicating its anisotropic property; the strut was deformed under compression, shrunk from bending, and eventually failed. In other words, the deformation of the strut under load causes a loss of RPUF's capability due to the reduction in the force acting on the foam cell's longitudinal orientation.

Koyama et al. (2022) studied the dynamic uniaxial compressive properties of RPUF under seismic load using the stress control method with 0.1 Hz. The results reported showed that the dynamic properties depended on the RPUF's confining pressure direction and deformation direction. Linul et al. (2013) studied the factors influencing the dynamic compressive strength of RPUFs with densities of 100, 160, and 300 kg/m^3 . The modulus, yield stress, and plateau stress increased with the increased density of RPUFs, speed of loading, and material orientation under loading.

To the authors' best knowledge, there has been no complete research undertaken on the effect of production factors on the compressive behavior and microstructure of RPUF, which is the focus of this research. The studied production factors included polymer content, polyol to isocyanate ratio, and mixing temperature of polyol and diisocyanate. The scanning electron microscope (SEM) technique was utilized to explain the compressive behavior of RPUF under the various production factors. The outcome of this study will facilitate road engineers' and manufacturers' ability to select the suitable production factors to develop RPUF with a target compressive strength at a reasonable cost. This promotes the usage of the RPUF as a lightweight material for retaining structure and road applications, which has a simpler and safer production process with comparable properties compared with traditional lightweight EPS foams. The RPUF can also be adopted as a filling material under eroded geotechnical structures such as road concrete pavement and bridge approach slabs due to its large expansion nature.

Materials and Methods

Materials

The RPUF specimens in this study were made from various combinations of two liquid components, polyol and diisocyanate, at various temperatures. The diisocyanate was a combination of diphenylmethane diisocyanate, isomer, and homologs [4,4-methylene diphenyl diisocyanate (MDI)] (POLYONE-200), and the polyol was polyether polyol (POLY-225).

Preparation of Specimens

The RPUF specimen was prepared by mixing diisocyanate (D) and liquid polyol (P) at various amounts. To prevent foam expansion due to the chemical interaction, the RPUF was prepared in a confined PVC mold with dimensions of 75-mm diameter and 200-mm height. As a result, the liquid foam underwent pressured compression, forming an interlocking closed-cell foam structure with a high cell density. The studied P contents were 23, 28, 34, 40, 45, 51, and 87 kg per 1 m^3 of the specimen, and the polyol to diisocyanate (p/d) ratios were 0.8, 0.9, and 1. This range of p/d ratios was found to produce the RPUF specimens having compressive strengths within upper and lower requirement of EPS (ASTM 2017).

Table 1. RPUF mixing proportion

Mix	Total weight of P and D per volume (kg/m ³)	Mixing proportion (kg/m ³)		p/d ratio	Specimen unit weight (kg/m ³)
		Polyol, P	Diisocyanate, D		
P23p/d1.0	46	23	23	1.0	70
P28p/d1.0	56	28	28	1.0	73
P34p/d1.0	68	34	34	1.0	75
P40p/d1.0	80	40	40	1.0	78
P45p/d1.0	90	45	45	1.0	80
P51p/d1.0	102	51	51	1.0	82
P57p/d1.0	114	57	57	1.0	84
P23p/d0.9	48	23	25	0.9	72
P28p/d0.9	59	28	31	0.9	74
P34p/d0.9	71	34	38	0.9	77
P40p/d0.9	84	40	45	0.9	79
P45p/d0.9	95	45	50	0.9	81
P51p/d0.9	108	51	57	0.9	83
P57p/d0.9	119	57	63	0.9	86
P23p/d0.8	52	23	29	0.8	77
P28p/d0.8	65	28	36	0.8	79
P34p/d0.8	77	34	42	0.8	83
P40p/d0.8	89	40	49	0.8	85
P45p/d0.8	102	45	56	0.8	89
P51p/d0.8	114	51	63	0.8	92
P57p/d0.8	127	57	70	0.8	94

The prepared RPUF specimen, along with the mold, was left in the laboratory for 3 h. This was to make sure that the foaming process had fully taken place and allowed the reaction heat to be decreased to room temperature. Subsequently, the RPUF specimen was demolded and trimmed to have cubic dimensions of 50 × 50 × 50 mm for the compressive tests (Public Roads Administration 1992). The ingredients of each RPUF mixture are summarized in Table 1.

Experimental Program

The tests were performed on RPUF specimens after 1 day of curing. For each test condition, test reports were based on the mean compressive strength values of five specimens to ensure the consistency of test results. In all tests, the standard deviation (SD) was found with $SD/x < 10\%$, in which x is the mean value of the test result.

Compressive Test

Compressive strength tests were performed in accordance with the Norwegian Directorate of Public Roads (Public Roads Administration 1992). Cubic 50 × 50 × 50-mm specimens were tested by a

universal testing machine (UTM), and the compressive strength was determined at 1% strain. Presently, there is no clear definition for the compressive strength of PUF material. It is dependent upon the purpose of users. However, ASTM (2017) has established a standard for extended polystyrene (EPS) geofoam materials, where the compressive strength at 1% strain is recommended as the typical design load limit of foam for general work.

Because the RPUF is a manufactured temperature-dependent material, the mixing temperatures of P and D were varied at 25°C, 40°C, 50°C, and 60°C to determine the effect of temperature on compressive strength as well as the microstructural characteristics of RPUF at different p/d ratios and P contents. The P and D were heated in a basin at the target temperatures, as shown in Fig. 2, for 1.5 h. The temperatures of heated P and D were measured using an infrared thermometer, which is commonly used in the manufacturing sectors and was capable of measuring temperatures from -50°C to 400°C with a resolution of 0.1°C and a measurement error of only 1.0°C.

Scanning Electron Microscopy

The microstructural investigation on RPUF was performed via SEM. The specimens were prepared at various P contents, p/d ratios, and mixing temperatures of P and D. The SEM specimens were gold-coated (Sukmak et al. 2013). The SEM analysis was based on the X-ray energy dissipation theory using a Tescan brand (model MIRA) SEM analyzer (Brno, Czech Republic). This testing machine is highly reliable and meets world-class standards. The SEM tests were performed by an expert microstructural-analysis scientist. The SEM images were analyzed to evaluate the role of P content, p/d ratio, and temperature on the microstructural changes.

Results

Compressive Strength for Ambient Mixing Temperature

The compressive strength at 1% strain of the RPUF specimens at various P contents with p/d ratios of 1.0, 0.9, and 0.8 at ambient mixing temperature (25°C) is presented in Fig. 3. The higher P content resulted in a greater compressive strength for the same p/d ratio. For instance, specimens with $P = 57 \text{ kg/m}^3$ exhibited the highest compressive strength for all p/d ratios tested when compared with specimens with other lower P contents. Specimens P57p/d1.0, P57p/d0.9, and P57p/d0.8 (P content = 57 kg/m³) had the highest compressive strengths of 0.22, 0.24, and 0.26 MPa, respectively, whereas specimens P23p/d1.0, P23p/d0.9, and P23p/d0.8 ($P = 23 \text{ kg/m}^3$) had the lowest compressive strengths of 0.11, 0.11, and 0.11 MPa, respectively. The lower p/d ratio resulted in the higher

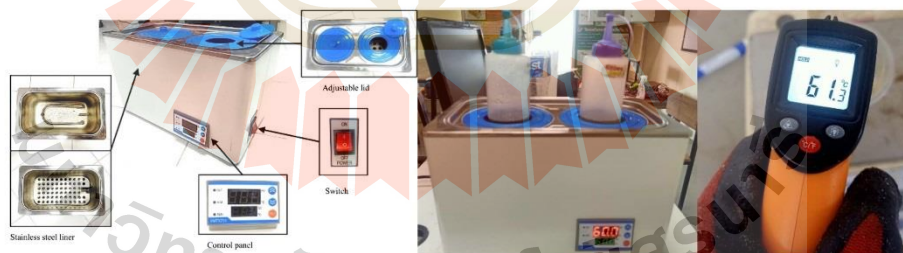


Fig. 2. Temperature control bath and device. (Images by Aroondet Boonsung.)

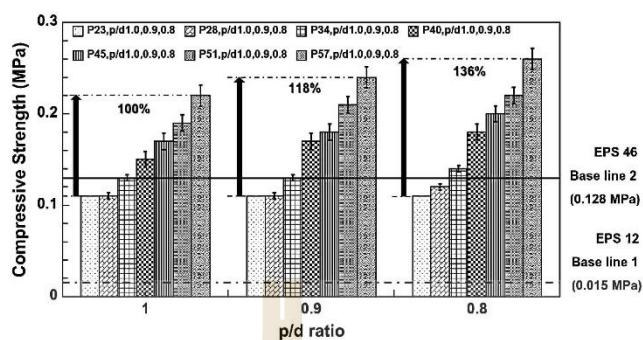


Fig. 3. Compressive strength of RPUF for ambient mixing temperature.

compressive strength for the same P content. The compressive strength of RPUF with P23 and P28 was between the lower and upper limits (0.015 and 0.128 MPa) of EPS geofoams according to ASTM D6817 (ASTM 2017). However, the RPUF with higher P contents was found to have greater compressive strength than the upper limit for all p/d ratios studied.

The increase in P content from 23 to 57 kg/m³ increased compressive strength by 100%, 118%, and 136% for p/d ratios of 1.0, 0.9, and 0.8, respectively. For a given P content at ambient mixing temperature, increasing the D content (decreasing the p/d ratio) resulted in a higher amount of chemically reactive urethane and urea, which led to stronger hydrogen bonds in the hard segments, to strengthen the foam structure network. The high D content caused a large amount of urea, and when the urea decomposes, only CO₂ is left, and the pressure inside the cell is retained (Ashida 2006; Shufen et al. 2006; Wellnitz 2007; Priscaariu 2011; Szycher 2013). This CO₂ results in a high cell-contact pressure, and hence the higher strength was evident at a lower p/d ratio.

Stress–Strain Relationship

Fig. 4 shows the stress–strain relationship under the compression test on the RPUF Specimen P28 series prepared at ambient

mixing temperature and different p/d ratios. The stress–strain relationships at all p/d ratios were similar.

Subhash et al. (2005) reported that although the strengths of the RPUFs were different, the relationship between stress and strain was similar under the compression and tensile tests. The stress–strain relationship of RPUF consisted of three regions: elastic, plateau, and densification regions. The elastic behavior started from the position where the stress was equal to zero and increased to the first yield stress, during which elastic bending stress occurs at the cell edge. The plateau behavior occurred later when the stress was increased sufficiently to cause the cell edge to deform until it was unable to recover into the plastic bending of the edge state. The strain increased, whereas the stress remained almost constant.

Densification occurs after a cell collapses due to deflection of the cell wall. The deflection of the cell wall results in the compression of the intracellular space, resulting in a sharp increase in the compressive stress with increasing the strain. The strain at the start of this densification state is called the densification strain (Ashby and Lu 2003; Outlet et al. 2006).

Fig. 4 depicts the effect of the p/d ratio on stress–strain behavior. The results showed that at lower p/d ratios of 0.9 and 0.8, linear elastic, plateau, and densification zones started at lower strain with higher yield stress and compressive strength compared with the case

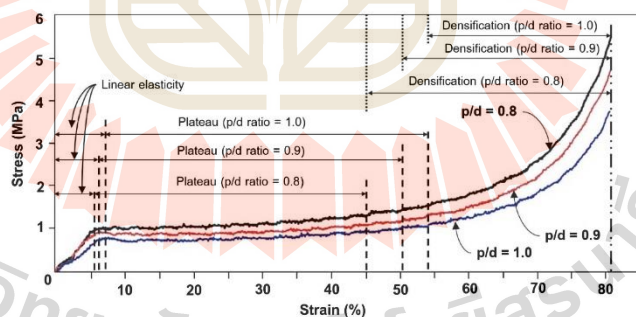


Fig. 4. Compressive stress–strain relationship of RPUF prepared at ambient temperature.

where the p/d ratio was 1.0. Densification strains of RPUF specimens were 45%, 50%, and 54% for p/d ratios of 1.0, 0.9, and 0.8, respectively. The longer densification zone was found for the lower p/d ratio.

However, the stress-strain relationship of the semirigid PUF structure had a smooth transition from the elastic to the plateau ranges, without a clear traction point due to no drop in stress (Linul et al. 2013; Leng et al. 2017; Movahedi and Linul 2017; Serrano et al. 2017; Gunther et al. 2018). The energy absorption capacity of RPUF per unit volume can be illustrated by the area under the stress-strain diagram. When considering the area under the diagram in Fig. 4, the RPUF absorbed more energy when the p/d ratio was lower. The energy absorbed by the RPUF decayed continuously as the foam progressed from the plateau region to densification (Lu and Yu 2003). The compressive test results at the ambient mixing temperature revealed that the lower p/d ratio and the higher P content yielded the higher compressive strength and toughness (energy absorptability).

Influence of Mixing Temperature

Fig. 5 shows the compressive strength at 1% strain versus mixing temperature of RPUF specimens at different P contents (P23, P28, and P34) and p/d ratios. The Specimen P23 and P28 series at ambient mixing temperature had compressive strengths lower than the upper limit of 0.128 MPa for EPS foam specified by ASTM D6817. However, the elevated mixing temperature could boost up the compressive strength.

The role of p/d ratio on the compressive strength of the RPUF at high temperatures ($>40^{\circ}\text{C}$) was different from that at ambient temperature. For all P contents studied, the compressive strength of RPUF prepared at $>40^{\circ}\text{C}$ mixing temperature decreased with the decrease in p/d ratio. For low P contents of 23 and 28 kg/m^3 , an increase of mixing temperature from 25°C to 40°C increased the compressive strength of the specimen for a given p/d ratio [Figs. 5(a and b)].

The same is not true for high P content of 34 kg/m^3 . For all p/d ratios, the increased mixing temperature from 25°C to 40°C caused the reduction in compressive strength. The compressive strengths of RPUF at mixing temperatures $\geq 40^{\circ}\text{C}$ were found to be lower than the compressive strength of RPUF at 25°C mixing temperature for all p/d ratios [Fig. 5(c)]. In other words, the ambient mixing temperatures was the most suitable for high P content of 34 kg/m^3 . To meet the upper limit of 0.128 MPa for EPS foam, the increased temperature could improve compressive strength at low P contents of 23 and 28 kg/m^3 ; 40°C and p/d = 1 were considered as the best ingredient.

Fig. 6 shows the damage characteristics of the RPUF specimens due to the elevated temperature (40°C to 60°C) and the decreased p/d ratios at P content = 23 kg/m^3 . The most serious damage was found at a mixing temperature of 60°C and p/d ratio of 0.8 [Fig. 6(c)]. This indicated that the macrocracks and pore space were larger with a higher mixing temperature and lower p/d ratio.

At a mixing temperature of 40°C , the specimen with p/d ratio = 1.0 had a relatively complete structure compared with specimens with higher temperatures and lower p/d ratios. As such, the specimen with p/d ratio = 1.0 and 40°C mixing temperature exhibited the highest compressive strength. Comparing Fig. 6(a) with Fig. 6(c) at the same mixing temperature, a decrease in p/d ratio increased foam cell-contact pressure as seen by more microcracks in the RPUF. In addition, with excess amount of D (p/d = 0.8), some parts of the D did not react with the monomer link (Jiao et al. 2013), causing liquid isocyanate residual in the test specimen.

It is therefore evident from Fig. 6 that for low P contents of 23 and 28 kg/m^3 , the elevated mixing temperature of P and D to 40°C resulted in a rapid gasification reaction and high cell-contact pressure, and hence high compressive strength. However, the excessive mixing temperatures ($>40^{\circ}\text{C}$) and very low p/d ratio led to the extremely large cell-contact pressure; and eventually the large macrocracks generated within the foam. This led to the reduced compressive strength. The higher mixing temperature of P and D resulted in more cracks than the decreased p/d ratios. For high P content of 34 kg/m^3 , both the increased mixing temperature and reduced p/d ratio caused excessive large cell-contact pressure and hence the reduction in compressive strength.

Microstructural Analysis

Fig. 7 shows the chemical composition analysis of the RPUF specimens at P content of 23 kg/m^3 and p/d ratio of 1.0 with mixing temperatures in the range of 40°C to 60°C using energy dispersive X-ray spectroscopy (EDS). The cell wall and the monomer link were mainly composed of carbon (C) and oxygen (O), forming covalent bonds, strengthening the hard segment through urethane linkage, and increasing the compressive strength (Thirumal et al. 2008). The EDS result showed that the change in mixing temperature did not alter the chemical compositions of the RPUF structure, as seen by the similar amount of C and O. In other words, the compressive strength development with mixing temperature and p/d ratio did not result from the change in chemical compositions.

The microstructure and cellular structure morphology of the RPUF specimens at P = 28 kg/m^3 with different p/d ratios was studied via SEM analysis, as illustrated in Fig. 8. The specimens were prepared at the mixing temperature of 40°C , which exhibited the highest compressive strength, to investigate the role of the decreased p/d ratio on compressive strength. The equivalent diameter per SEM image frame ($3,700 \times 2,800 \mu\text{m}$) of each specimen was measured. The SEM image showed that the foam cells were polygonal in shape, and the cell diameters varied across the specimen's section.

The data from the SEM images were statistically analyzed in the form of a frequency-distribution diagram of the mean cell foam diameter in the SEM image frame, as shown in Fig. 9. Because the foam cells were not perfectly spherical in shape, their mean diameter was measured from edge to edge in the x- and y-directions from their center. The mean diameters of RPUF specimens were 691 ± 116 , 622 ± 122 , and $681 \pm 25 \mu\text{m}$ for p/d ratios of 1.0, 0.9, and 0.8, respectively. This indicates that foam cell size varied with the p/d ratio.

Fig. 10 shows the percent distribution of foam cells with various ranges of foam cell size for the p/d ratios of 1.0, 0.9, and 0.8 in the SEM image frame. Most cells in specimens were greater than 400, 300, and 200 μm for p/d ratios of 1.0, 0.9, and 0.8, respectively. The specimens with the lowest p/d ratio of 0.8 possessed the lowest volume of $>800\text{-nm}$ foam cells, whereas the specimens with the highest p/d ratio of 1.0 possessed the highest volume of $>800\text{-nm}$ foam cells. This implies that a lower p/d ratio was associated with the more small-sized foam cells.

Hejna et al. (2017) investigated the cell size of RPUF at p/d ratios of 1.5, 2.0, and 2.5 and reported that an increase in D content (decrease in p/d ratio) tended to decrease the foam cell size, which was associated with an increase in crosslink density due to the rise in allophanate and biuret groups. Consequently, a decrease in the p/d ratio increased the specimen's density, as indicated in Table 1. In other words, the low-density specimen has a larger cell size than the high-density specimen. Considering the minimum energy

Downloaded from ascelibrary.org by Suksum Llorbolsak on 02/10/24. Copyright ASCE, for personal use only; all rights reserved.

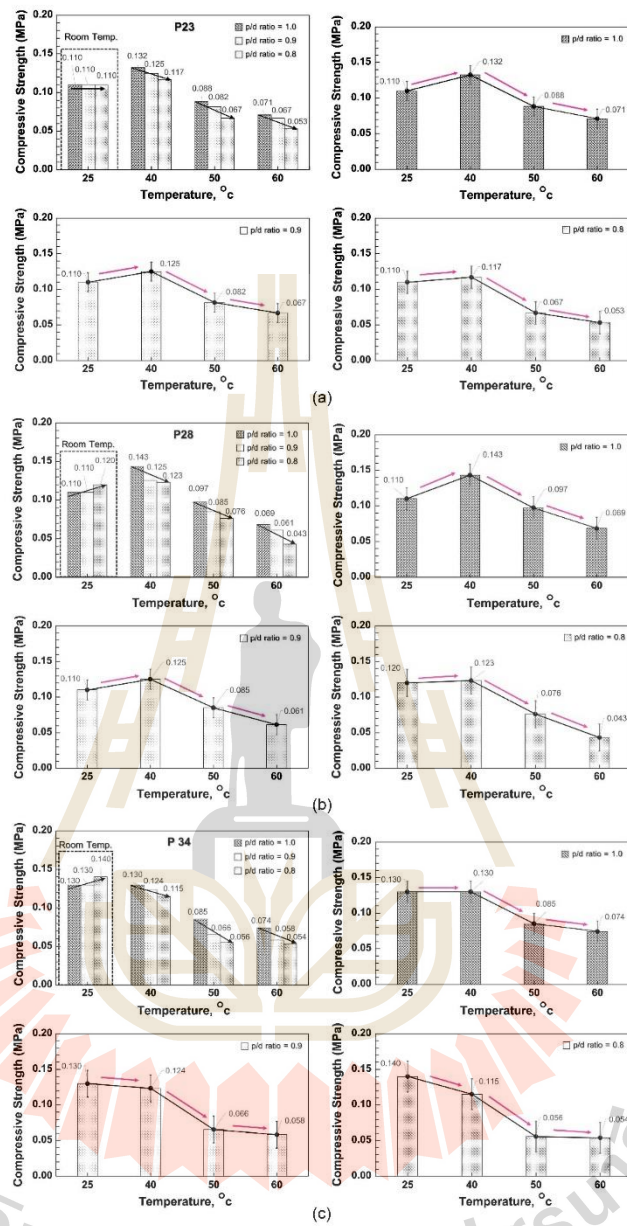


Fig. 5. Effect of P content and mixing temperature on compressive strength.

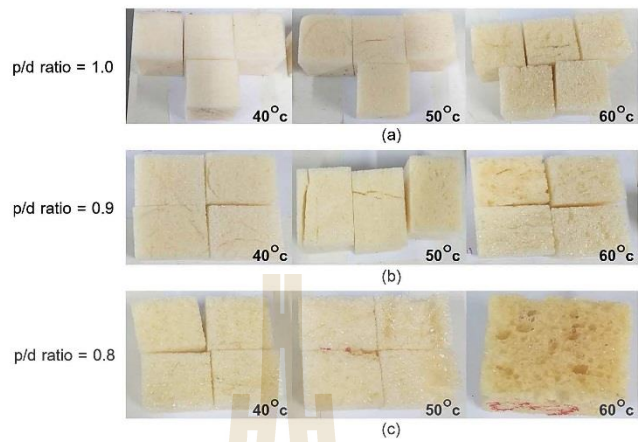


Fig. 6. RPUF specimens with various mixing temperatures and p/d ratios at P content of 23 kg/m³.

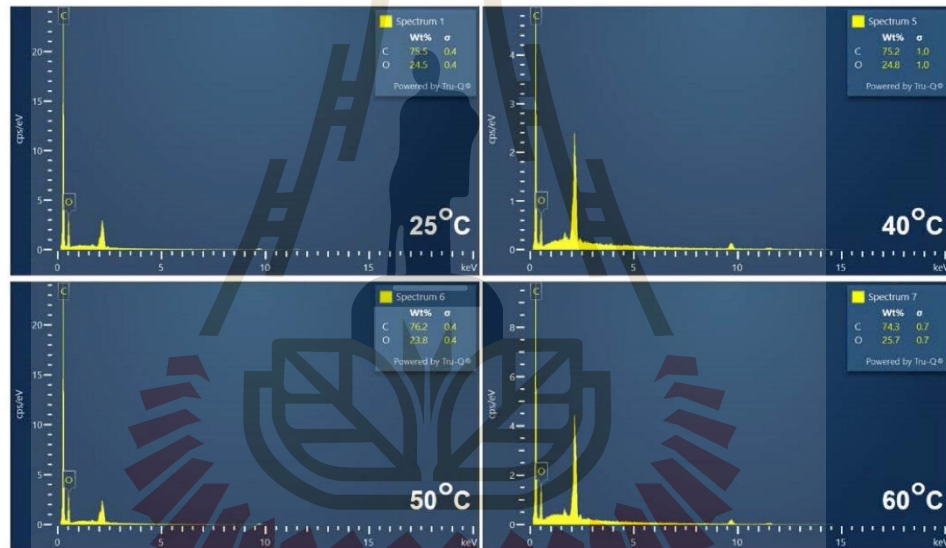


Fig. 7. EDS analysis results of RPUF specimens at P content of 23 kg/m³ and p/d ratio of 1.0.

principle of thermodynamics, the increased contact area between the cells results in more energy at the contact surfaces.

Fig. 11 shows the closed foam cell structure of specimens at P = 28 kg/m³ with different p/d ratios at the mixing temperature of 40°C. The cell wall deformation due to the cell-contact pressure can be observed for different p/d ratios. The cell structure with a p/d

ratio of 1.0 was subjected to less deformation (less pressure) than the cell structures with p/d ratios of 0.9 and 0.8, respectively, which is associated with the relatively complete specimen (Fig. 8). The very high D (very low p/d ratio) caused an excessive amount of urea and CO₂. When CO₂ decomposed, the extremely large cell-contact pressure developed and resulted in large damage (macrocracks).

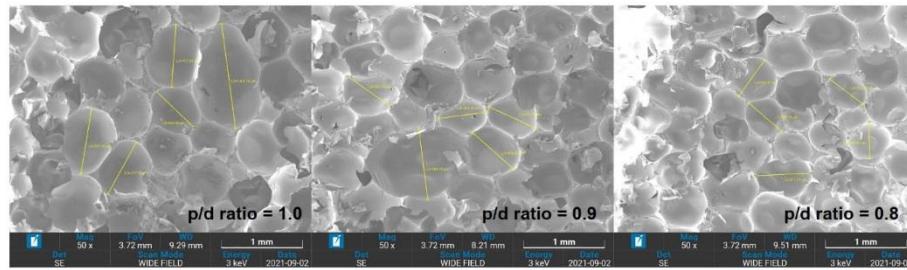


Fig. 8. Foam cells of RPUF specimens at P content of 28 kg/m³.

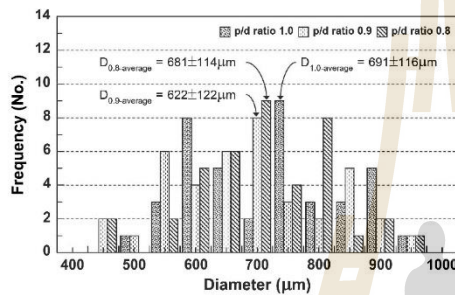


Fig. 9. Distribution of foam cell diameters of RPUF specimens at P content of 28 kg/m³.

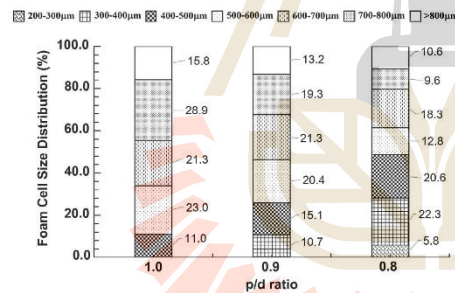


Fig. 10. Distribution of foam cell for different ranges of cell size of RPUF specimens at P content of 28 kg/m³.

Fig. 12 shows the results of SEM analysis at 50 times magnification of RPUF specimens at P content = 28 kg/m³ with different mixing temperatures and p/d ratios. At a mixing temperature of 25°C, as shown in Fig. 12(a), the cell wall damage (indicated by the dotted circle) increased with decreasing the p/d ratio, which was approximately 8%, 15%, and 27% of the total cell for the p/d ratios

of 1.0, 0.9, and 0.8, respectively, compared with the total number of cells in each image. However, even with larger damage, the higher cell-contact pressure resulted in higher compressive strength, as evident by the highest strength attained at p/d ratio of 0.8.

Comparing Figs. 12(a and b), it is evident that the cell size was dependent upon both the mixing temperature and p/d ratio. A higher mixing temperature and lower p/d ratio resulted in the smaller cell size and higher cell-contact pressure. At a mixing temperature of 40°C with p/d ratio of 1.0, the cell foam damage was less than that with lower p/d ratios, as shown in Fig. 12(b). At a p/d of 0.9, when the mixing temperature was raised from 25°C to 50°C, the cell damage increased to 19%, whereas at a p/d ratio of 0.8, when the temperature was raised from 25°C to 60°C, the cell damage increased to 34% compared with the total number of cells.

From the critical analysis of the test results, it is evident that the cell-contact pressure controlled the strength development. With the increase in mixing temperature and the reduction in p/d ratio, the sufficient cell-contact pressure enhanced the strength and toughness improvement, whereas the extremely high cell-contact pressure damaged the foam cell and caused strength and toughness reductions.

Conclusions

This research investigated the role of production factors on the compressive strength development of RPUF. The production factors included polyol content, p/d ratio, and mixing temperature of polyol to diisocyanate. The microstructure and morphology of RPUF were investigated to understand the mechanism controlling the compressive strength development with various production factors and to suggest the optimal production factors. The following conclusions can be drawn from this research study:

- The stress-strain relationship of RPUF was found to have three zones: linear, plateau, and densification. At ambient mixing temperature, for a given P content, the lower p/d ratio resulted in the lower strains at the start of each zone and higher yield stress, toughness, and compressive strength.
- Unlike at the ambient mixing temperature (25°C), for a particular P content, the compressive strength of RPUF prepared at high temperatures (>40°C) decreased with the decrease in p/d ratio. For low P contents of 23 and 28, an increase of mixing temperature from 25°C to 40°C increased the compressive strength of RPUF for a given p/d ratio. However, for high P content of 34 kg/m³, the increased mixing temperature from 25°C to 40°C caused the reduction in compressive strength. In other words, the ambient mixing temperatures was the most suitable for high P content of 34 kg/m³.

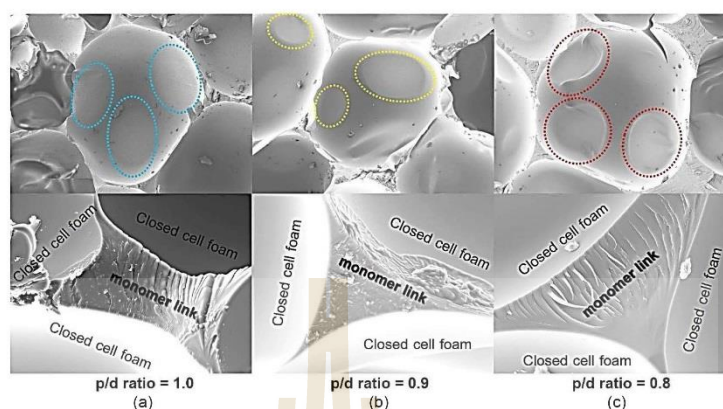


Fig. 11. Closed-cell structure of RPUF at different p/d ratios at 40°C mixing temperature and P content of 28 kg/m³ for p/d ratios of (a) 1.0; (b) 0.9; and (c) 0.8.

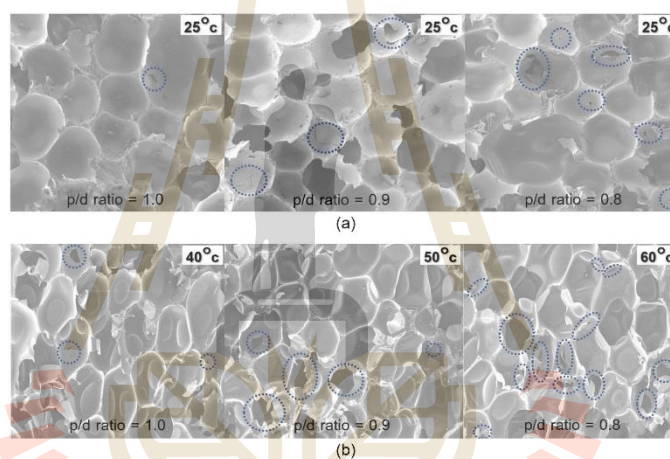


Fig. 12. Closed-cell structure of RPUF at P content of 28 kg/m³ for (a) mixing temperature of 25°C and p/d ratios of 1.0, 0.9, and 0.8; and (b) mixing temperatures of 40°C, 50°C, and 60°C and p/d ratios of 1.0, 0.9, and 0.80.

- The EDS results showed the unchanged in the chemical compositions in the RPUF structure with the elevated mixing temperatures, as seen by the similar amount of C and O for all the mixing temperatures tested. The compressive strength development with mixing temperature did not result from the chemical bonding development but was due to the increased cell-contact pressures.
- The microstructural analysis results showed that both the elevated the mixing temperature and reduced p/d ratio stimulated gasification, resulting in the small-sized cells with high cell-contact

pressures. The sufficient cell-contact pressure increased the compressive strength of RPUF and toughness, whereas the extremely large cell-contact pressure caused the cell damage and the reduction in strength and toughness.

- To meet the upper limit of 0.128 MPa for EPS foam, the increased mixing temperature from ambient to 40°C could improve compressive strength at low P contents of 23 and 28 kg/m³; a temperature of 40°C and p/d ratio of 1 were the best ingredient. The ambient mixing temperature and p/d = 0.8 were however the best for high P content. With high cost of P and D, the usage

of low P content of $< 28 \text{ kg/m}^3$ with 40°C mixing temperature is therefore recommended in practice.

- The outcome of this research will promote the usage of the RPUF as a lightweight material in geotechnical structures such as retaining walls and road embankments. RPUF was found to have a comparable compressive strength to EPS but with a safer manufacturing process. The RPUF can also be adopted as a filling material under eroded geotechnical structures such as road concrete pavement and bridge approach slabs due to its large expansion nature. A durability study, which is essential for long-term application of this material, is recommended for future research.

Data Availability Statement

Some or all data, models, or code that support the finding of this study are available from the corresponding author upon reasonable request. All data shown in figures and tables can be provided on request.

Acknowledgments

The first author appreciate Uttaradit Rajabhat University (URU) for his Ph.D. study scholarship. The authors appreciate the Tesla Engineering Co., Ltd. and S Class Engineer, Co., Ltd. for supplying polyol and isocyanate and financial supports for this research.

References

- Aabøe, R., and T. E. Frydenlund. 2011. "40 Years of experience with the use of EPS geofoam blocks in road construction." In *Proc., Use of Geofoam Block in Construction Application 4th Int. Conf.*, 1–14. Salt Lake City: Unive. of Utah.
- Ashby, M., and T. Lu. 2003. "Metal foams: A survey." *Sci. China Ser. B Chem.* 46 (6): 521–532. <https://doi.org/10.1360/02yb0203>.
- Ashida, K. 2006. *Polyurethane and related form: Chemistry and technology*. Boca Raton, FL: CRC Press.
- ASTM. 2017. *Standard specification for rigid cellular polystyrene geofoam*. ASTM D6817-07. West Conshohocken, PA: ASTM.
- Atangana Njock, P. G., S.-L. Shen, A. Zhou, and G. Modoni. 2021. "Artificial neural network optimized by differential evolution for predicting diameters of jet grouted columns." *J. Rock Mech. Geotech. Eng.* 13 (6): 1500–1512. <https://doi.org/10.1016/j.jmge.2021.05.009>.
- Berardi, U., and J. Madzarevic. 2020. "Microstructural analysis and blowing agent concentration in aged polyurethane and polyisocyanurate foams." *Appl. Therm. Eng.* 164 (Jan): 1–9. <https://doi.org/10.1016/j.applthermaleng.2019.114440>.
- Chen, W., and H. Hao. 2014. "Experimental and Numerical study of composite lightweight structural insulated panel with expanded polystyrene core against windborne debris impacts." *Mater. Des.* 60 (Aug): 409–423. <https://doi.org/10.1016/j.matdes.2014.04.038>.
- Chen, W., H. Hoa, D. Hughes, Y. Shi, J. Cui, and Z. Li. 2015. "Static and dynamic mechanical properties of expanded polystyrene." *J. Mater. Des.* 69 (Mar): 170–180. <https://doi.org/10.1016/j.matdes.2014.12.024>.
- Das, S., P. Heasman, T. Ben, and S. Qiu. 2017. "Porous organic materials Strategic design and structure-function correlation." *Chem. Rev.* 117 (3): 1515–1563. <https://doi.org/10.1021/acs.chemrev.6b00439>.
- Duskov, M. 1991. "Use of expanded polystyrene (EPS) in flexible pavements on poor subgrades." In *Proc., Geotechnical Engineering for Coastal Development Int. Conf.*, 783–788. Tokyo: Coastal Development Institute of Technology.
- Duskov, M. 1997. "Measurements on a flexible pavement structure with an EPS geofoam sub-base." *Geotext. Geomembr.* 15 (1): 5–27. [https://doi.org/10.1016/S0266-1144\(97\)00004-6](https://doi.org/10.1016/S0266-1144(97)00004-6).
- Eaves, D. 2004. *Handbook of polymer foam*. Shawbury, UK: Rapra Technology Ltd.
- Frydenlund, T. E. 1991. Vol. 1502 of *Expanded polystyrene: A lighter way across soft ground*. San Diego: ICON Group International.
- Frydenlund, T. E., and R. Aabøe. 2001. "Long term performance and durability of EPS as a lightweight filling material." In *Proc., Use of Geofoam Block in Construction Application 3th Int. Conf.*, 1–15. Salt Lake City, UT: Unive. of Utah.
- Gunther, M., A. Lorenzatti, and B. Schartel. 2018. "Fire phenomena of rigid polyurethane foam." *Polymers* 10 (10): 1–22. <https://doi.org/10.3390/polym10101166>.
- Hejna, A., J. Haponiuk, L. Piszczyk, M. Klein, and K. Formela. 2017. "Performance properties of rigid polyurethane-polyisocyanurate/brewers' spent grain foamed composites as function of isocyanate index." *e-Polymers* 17 (5): 427–437. <https://doi.org/10.1515/epoly-2017-0012>.
- Herrington, R., and K. Hock. 1997. *Flexible polyurethane foams*. 2nd ed. Midland, TX: Dow Chemical Co.
- Ionescu, M. 2005. *Chemistry and technology of polyols for polyurethanes*. Shawbury: Rapra Technology.
- Jiao, L., H. Xiao, Q. Wang, and J. Sun. 2013. "Thermal degradation characteristics of rigid polyurethane foam and the volatile products analysis with TG-FTIR-MS." *Polym. Degrad. Stab.* 98 (12): 2687–2696. <https://doi.org/10.1016/j.polymdegradstab.2013.09.032>.
- Koyama, A., D. Suetsugu, Y. Fukubayashi, and H. Mitabe. 2022. "Experimental study on the dynamic properties of rigid polyurethane foam in stress-controlled cyclic uniaxial tests." *Constr. Build. Mater.* 321 (Feb): 1–12. <https://doi.org/10.1016/j.conbuildmat.2022.126377>.
- Król, P. 2008. *Linear polyurethane: Synthesis method, chemical structure, properties and application*. Boca Raton, FL: CRC Press.
- Lee, S.-T., and N. S. Ramesh. 2004. *Polymeric foams: Mechanisms and materials*. Boca Raton, FL: CRC Press.
- Leng, W., J. Li, and Z. Cai. 2017. "Synthesis and characterization of cellulose nanofibril-reinforced polyurethane foam." *Polymer* 9 (11): 1–14. <https://doi.org/10.3390/polym9110597>.
- Linul, E., T. Voiconi, L. Marsavia, and T. Sadowski. 2013. "Study of factor influencing the mechanical properties of polyurethane foams under dynamic compression." *J. Phys. Conf. Ser.* 451 (1): 1–6. <https://doi.org/10.1088/1742-6596/451/1/012002>.
- Lu, G., and T. X. Yu. 2003. *Energy absorption of Structure and material*. Sawston, UK: Woodhead Publishing.
- Manalo, A. 2013. "Structural behaviour of a prefabricated composite wall system made from rigid foam polyurethane foam and magnesium oxide board." *Constr. Build. Mater.* 41 (Apr): 642–653. <https://doi.org/10.1016/j.conbuildmat.2012.12.058>.
- Meguid, M., M. Hussein, M. Ahmed, Z. Ozeman, and J. Whalen. 2017. "Investigation of soil-geosynthetic-structure interaction associated with induced trench installation." *Geotext. Geomembr.* 45 (4): 320–330. <https://doi.org/10.1016/j.geotexmem.2017.04.004>.
- Movahedi, N., and E. Lituk. 2017. "Quasi-static compressive behavior of the ex-situ aluminum-alloy foam-filled tube under elevated temperature condition." *Mater. Lett.* 206 (Nov): 182–184. <https://doi.org/10.1016/j.matlet.2017.07.018>.
- NCHRP (National Cooperative Highway Research Program). 2004. *Guideline and Recommended Standard for Geofoam Application in Highway Embankment*. Washington, DC: Transportation Research Board, National Research Council.
- Negussey, D. 2002. *Slope stabilization with geofoam*. Syracuse, NY: Geofoam Research Center, Syracuse Univ.
- Neramitkornburi, A., S. Horphibulsuk, S. L. Shen, A. Arulrajah, and M. M. Disfani. 2015. "Engineering properties of lightweight cellular cemented clay-fly ash material." *Soils Found.* 55 (2): 471–483. <https://doi.org/10.1016/j.sandf.2015.02.020>.
- NPRA (Norwegian Public Roads Administration). 2002. *Lightweight filling materials for road construction*. Oslo, Norway: Road Technology Dept.
- Ochmański, M., G. Modoni, and J. Bzówka. 2015. "Prediction of the diameter of jet grouting columns with artificial neural networks." *Soils Found.* 55 (2): 425–436. <https://doi.org/10.1016/j.sandf.2015.02.016>.

- Outlet, S., D. Cronin, and M. Worswick. 2006. "Compressive response of polymeric foams under quasi-static medium and high strain rate conditions." *Polym. Test.* 25 (6): 731–743. <https://doi.org/10.1016/j.polymer.2006.05.005>.
- Padopoulos, A. M. 2005. "State of the art in thermal insulation materials and aims for future developments." *Energy Build.* 37 (1): 77–86. <https://doi.org/10.1016/j.enbuild.2004.12.011>.
- Prisacariu, C. 2011. *Polyurethane elastomers from morphology to mechanical aspects*. New York: Springer.
- Public Roads Administration. 1992. *Quality control of expanded polystyrene used in road embankments 484E*. Oslo, Norway: Road Research Laboratory.
- Refsdal, G. 1985. *Plastic foam in road embankments: Future trends for EPS Use (Internal report)*. Oslo, Norway: Road Research Laboratory.
- Riad, H. L., A. L. Ricci, P. W. Osborn, and J. S. Horvath. 2003. "Expanded polystyrene (EPS) geofoam for road embankments and other light-weight fills in urban environments." In *Proc., Soil and Rock America 2003-12th Soil Mechanics and Geotechnical Engineering/39th US Rock Mechanics Symp.*, 1–6. West Berlin, NJ: Acer Associates, LLC—Environmental, GPR, Geotechnical.
- Ridha, M., and V. P. W. Shim. 2008. "Microstructure and tensile mechanical properties of anisotropic rigid polyurethane foam." *Exp. Mech.* 48 (6): 763–776. <https://doi.org/10.1007/s11340-008-9146-0>.
- Sanders, R. L. 1996. "United Kingdom design and construction experience with EPS." In *Proc., EPS Construction Method (EPS TOKYO#96) Int. Symp.*, 236–256. Washington, DC: Transportation Research Board.
- Serrano, A., A. M. Borreguero, I. Garrido, J. F. Rodriguez, and M. Carmona. 2017. "The role of microstructure on the mechanical properties of polyurethane foam containing thermoregulating microcapsules." *Polym. Test.* 60 (Jul): 274–282. <https://doi.org/10.1016/j.polymer.2017.04.011>.
- Sharmin, E., and F. Zafar. 2012. *Polyurethane: An introduction*. London: INTECH Open Access Publisher.
- Shen, S.-L., P. G. Atangana Njock, A. Zhou, and H.-M. Lyu. 2021. "Dynamic prediction of jet grouted column diameter in soft soil using Bi-LSTM deep learning." *Acta Geotech.* 16 (1): 303–315. <https://doi.org/10.1007/s11440-020-01005-8>.
- Shen, S.-L., Z.-F. Wang, J. Yang, and C.-E. Ho. 2013. "Generalized approach for prediction of jet grout column diameter." *J. Geotech. Geoenviron. Eng.* 139 (12): 2060–2069. [https://doi.org/10.1061/\(ASCE\)GT.1943-5606.0000932](https://doi.org/10.1061/(ASCE)GT.1943-5606.0000932).
- Shufen, L., J. Zhi, Y. Kajun, Y. Shuqin, and W. K. Chow. 2006. "Studies on the thermal behavior of polyurethanes." *Polym.-Plast. Technol. Eng.* 45 (1): 95–108. <https://doi.org/10.1080/03602550500373634>.
- Stark, T. D., D. Arellano, J. S. Horvath, and D. Leshchinsky. 2004. *Geofoam applications in the design and construction of highway embankments*. Washington, DC: Transportation Research Board.
- Stima, U., I. Beverte, V. Yakushin, and U. Cabulis. 2011. "Mechanical properties of rigid polyurethane foams at room and cryogenic temperatures." *J. Cell. Plast.* 47 (4): 337–355. <https://doi.org/10.1177/0021955X11398381>.
- Subhash, G., T. R. Walter, and A. W. Richards. 2005. "A unified phenomenological model for tensile and compressive response of polymeric foams." *J. Eng. Mater. Technol.* 131 (1): 1–6. <https://doi.org/10.1115/1.3026556>.
- Sukmak, G., P. Sukmak, S. Horpibulsuk, A. Arulrajah, and J. Horpibulsuk. 2022. "Generalized strength prediction equation for cement stabilized clayey soils." *Appl. Clay Sci.* 231 (Jan): 106761. <https://doi.org/10.1016/j.clay.2022.106761>.
- Sukmak, P., S. Horpibulsuk, and S.-L. Shen. 2013. "Strength development in clay-fly ash geopolymer." *Constr. Build. Mater.* 40 (Mar): 566–574. <https://doi.org/10.1016/j.conbuildmat.2012.11.015>.
- Sulong, N. H. R., S. A. S. Mustapa, and M. K. A. Rashid. 2019. "Application of expanded polystyrene (EPS) in building and construction A review." *J. Appl. Polym. Sci.* 136 (20): 1–11. <https://doi.org/10.1002/app.47529>.
- Szycher, M. 2013. *Szycher's handbook of polyurethanes*. 2nd ed. Boca Raton, FL: CRC Press.
- Thirumal, M., D. Khastgir, N. K. Singha, B. S. Manjunath, and Y. P. Naik. 2008. "Effect of foam density on the properties of water blown rigid polyurethane foam." *J. Appl. Polym. Sci.* 108 (3): 1810–1817. <https://doi.org/10.1002/app.27712>.
- Villasmil, W., L. J. Fischer, and J. Worlitschek. 2009. "A review and evaluation of thermal insulation materials and methods for thermal energy storage systems." *Renewable Sustainable Energy Rev.* 103 (Apr): 71–84. <https://doi.org/10.1016/j.rser.2018.12.040>.
- Walter, S. J., J. Teh Sung, and N. Dawit. 2000. "Stabilization of embankment slope with geofoam." *Transp. Res. Rec.* 1736 (1): 94–102. <https://doi.org/10.3141/1736-12>.
- Wang, Z.-F., S.-L. Shen, C.-E. Ho, and Y.-H. Kim. 2013. "Investigation of field-installation effects of horizontal twin-jet grouting in Shanghai soft soil deposits." *Can. Geotech. J.* 50 (3): 288–297. <https://doi.org/10.1139/cgj-2012-0199>.
- Wellnitz, C. C. 2007. *Assessment of extruded polystyrene foam for sandwich composite application*. Houghton: Michigan Technological Univ.
- Witkiewicz, W., and A. Zielinski. 2006. "Properties of the polyurethane (PU) light foam." *Adv. Mater. Sci.* 6 (2): 35–51.
- Wiyono, P., P. Faimun, and H. Kristjanto. 2016. "Characterization of physical and mechanical properties of rigid polyurethane." *ARPJ J. Eng. Appl. Sci.* 11 (24): 14398–14405.

BIOGRAPHY

Mr. Aroondet Boonsung was born in January 1997 in Lampang, Thailand. I received my Bachelor's degree in Civil Engineering (Second-Class Honors) from the Department of Civil Engineering, Mahanakorn University of Technology, in 2002. After graduation, I worked as a civil engineer in the Department of Design and Construction Engineering, L-Thai Clay Tile Co., Ltd., from June 2002 to April 2003; after that, I worked as a lecturer in the Department of Construction Engineering Management, Uttaradit Rajabhat University. I obtained my Master's in Civil Engineering (Geotechnical Engineering) from the Department of Civil Engineering, Chiang Mai University, in 2008.

I was granted a scholarship by Uttaradit Rajabhat University in 2020 to pursue my Ph.D. in civil engineering and construction management at the School of Civil Engineering, Suranaree University of Technology. I currently hold the position of Associate Professor at the Department of Construction Management Engineering. So far, I have published 2 papers in reputed international journals. I am currently interested in ground improvement and geotechnical work.

มหาวิทยาลัยเทคโนโลยีสุรนารี